TOPICS IN ORGANOMETALLIC CHEMISTRY 22

Volume Editors F. Meyer · C. Limberg

Organometallic Oxidation Catalysis

Springer

22
Topics in Organometallic Chemistry

Topics in Organometallic Chemistry

Recently Published and Forthcoming Volumes

Regulated Systems for Multiphase Catalysis
Volume Editors: W. Leitner, M. Hölscher
Vol. 23, 2007

Organometallic Oxidation Catalysis
Volume Editors: F. Meyer, C. Limberg
Vol. 22, 2007

N-Heterocyclic Carbenes in Transition Metal Catalysis
Volume Editor: F. Glorius
Vol. 21, 2006

Dendrimer Catalysis
Volume Editor: L. H. Gade
Vol. 20, 2006

Metal Catalyzed Cascade Reactions
Volume Editor: T. J. J. Müller
Vol. 19, 2006

Catalytic Carbonylation Reactions
Volume Editor: M. Beller
Vol. 18, 2006

Bioorganometallic Chemistry
Volume Editor: G. Simonneaux
Vol. 17, 2006

Surface and Interfacial Organometallic Chemistry and Catalysis
Volume Editors: C. Copéret, B. Chaudret
Vol. 16, 2005

Chiral Diazaligands for Asymmetric Synthesis
Volume Editors: M. Lemaire, P. Mangeney
Vol. 15, 2005

Palladium in Organic Synthesis
Volume Editor: J. Tsuji
Vol. 14, 2005

Metal Carbenes in Organic Synthesis
Volume Editor: K. H. Dötz
Vol. 13, 2004

Theoretical Aspects of Transition Metal Catalysis
Volume Editor: G. Frenking
Vol. 12, 2005

Ruthenium Catalysts and Fine Chemistry
Volume Editors: C. Bruneau, P. H. Dixneuf
Vol. 11, 2004

New Aspects of Zirconium Containing Organic Compounds
Volume Editor: I. Marek
Vol. 10, 2004

Precursor Chemistry of Advanced Materials
CVD, ALD and Nanoparticles
Volume Editor: R. Fischer
Vol. 9, 2005

Metallocenes in Stereoselective Synthesis
Volume Editor: T. Takahashi
Vol. 8, 2004

Transition Metal Arene π-Complexes in Organic Synthesis and Catalysis
Volume Editor: E. P. Kündig
Vol. 7, 2004

Organometallics in Process Chemistry
Volume Editor: R. D. Larsen
Vol. 6, 2004

Organolithiums in Enantioselective Synthesis
Volume Editor: D. M. Hodgson
Vol. 5, 2003

Organometallic Bonding and Reactivity: Fundamental Studies
Volume Editor: J. M. Brown, P. Hofmann
Vol. 4, 1999

Organometallic Oxidation Catalysis

Volume Editors: Franc Meyer · Christian Limberg

With contributions by

M. A. Ciriano · C. Freund · W. A. Herrmann · F. E. Kühn
C. Limberg · F. Meyer · B. V. Popp · D. Schröder · H. Schwarz
S. S. Stahl · T. Strassner · C. Tejel · K. H. Theopold
J. I. van der Vlugt

Springer

The series *Topics in Organometallic Chemistry* presents critical overviews of research results in organometallic chemistry. As our understanding of organometallic structure, properties and mechanisms increases, new ways are opened for the design of organometallic compounds and reactions tailored to the needs of such diverse areas as organic synthesis, medical research, biology and materials science. Thus the scope of coverage includes a broad range of topics of pure and applied organometallic chemistry, where new breakthroughs are being achieved that are of significance to a larger scientific audience.
The individual volumes of *Topics in Organometallic Chemistry* are thematic. Review articles are generally invited by the volume editors.
In references *Topics in Organometallic Chemistry* is abbreviated *Top Organomet Chem* and is cited as a journal.

Springer WWW home page: springer.com
Visit the TOMC content at springerlink.com

Library of Congress Control Number: 2006930270

ISSN 1436-6002
ISBN 978-3-540-37209-7 Springer Berlin Heidelberg New York
DOI 10.1007/11603818

Springer is a part of Springer Science+Business Media

springer.com

Cover design: WMXDesign, Heidelberg
Typesetting and Production: LE-TEX Jelonek, Schmidt & Vöckler GbR, Leipzig

Printed on acid-free paper 02/3100 YL – 5 4 3 2 1 0

Volume Editors

Prof. Dr. Franc Meyer

Universität Göttingen
Institut für Anorganische Chemie
Tammannstr. 4
37077 Göttingen, Germany
franc.meyer@chemie.uni-goettingen.de

Prof. Dr. Christian Limberg

Humboldt-Universität zu Berlin
Institut für Chemie
Brook-Taylor-Str. 2
12489 Berlin, Germany
christian.limberg@chemie.hu-berlin.de

Editorial Board

Topics in Organometallic Chemistry
Also Available Electronically

For all customers who have a standing order to Topics in Organometallic Chemistry, we offer the electronic version via SpringerLink free of charge. Please contact your librarian who can receive a password or free access to the full articles by registering at:

springerlink.com

If you do not have a subscription, you can still view the tables of contents of the volumes and the abstract of each article by going to the SpringerLink Homepage, clicking on "Browse by Online Libraries", then "Chemical Sciences", and finally choose Topics in Organometallic Chemistry.

You will find information about the

- Editorial Board
- Aims and Scope
- Instructions for Authors
- Sample Contribution

at springer.com using the search function.

Preface

For 80% of all compounds produced in chemical and pharmaceutical industry at least one *catalytic* step is essential during their synthesis. At the same time the use of hydrocarbons as feed-stock for commodity and fine chemicals typically requires an *oxidation* step, which is usually mediated by a transition metal compound. Consequently, *oxidation catalysis* is a major research field in chemistry, both in academia and in industry. This volume "Organometallic oxidation catalysis" deals with catalytic oxidation processes where metal-carbon bonds occur in one way or the other, for instance in key intermediates formed as part of the catalytic cycle. This is the case in homogeneous oxidative conversions mediated by palladium complexes, as described by S. S. Stahl et al., or by rhodium and iridium complexes, as outlined by C. Tejel et al. It also applies to the heterogeneous Mo/Bi-based SOHIO process, and C. Limberg describes recent advances with respect to the modelling of crucial organometallic intermediates in this process by molecular compounds. On the other hand, the contribution of D. Schröder et al. highlights the oxidation chemistry of basic organometallic species in the gas phase, as this may reveal fundamental characteristics inherent to oxidation catalysts. A further important aspect that is covered by some of the experts is the use of suitable organic ligands – and their resulting organometallic complex fragments – to achieve efficient oxidation catalysis. Hence, one article by T. Strassner summarises recent developments in the field of N-heterocyclic carbene complexes that proved surprisingly robust under oxidative conditions. It has not been self-evident that organometallic complexes can survive the conditions necessary for polar oxygen-transfer reactions, but research of the last decade concerning oxo and peroxo complexes that are functionalized by organic ligands – as described by K. H. Theopold for organometallics of early transition metals – has clearly shown that relatively non-polar M–C bonds can be quite stable in the presence of oxidants and protic media. They may even be essential for the favourable activity and life-time of a catalyst, so that extensive efforts were made to heterogenise such compounds by linking them to the most different surfaces. The review by F. E. Kühn and W.A. Herrmann outlines results obtained for immobilised organorhenium and organomolybdenum catalysts. In a complementary approach, the active site structures of metal containing oxidase and oxygenase enzymes have provided great inspiration for the development of novel oxidation catalysts. Although

those systems in most cases are not strictly organometallic, selected examples of homogeneous copper-catalyzed oxidations are described in a chapter by J.I. van der Vlugt and F. Meyer to build a bridge to the rapidly expanding field of bioinspired catalysis. We hope that the readers enjoy reading this multi-faceted volume as much as we did.

January 2007

Franc Meyer
Christian Limberg

Contents

Top Organomet Chem (2007) 22: 1–15
DOI 10.1007/3418_056

Published online: 11 August 2006

Intrinsic Mechanisms of Oxidation Reactions as Revealed by Gas-Phase Experiments

Detlef Schröder[1,2] (✉) · Helmut Schwarz[2]

[1]Institute of Organic Chemistry and Biochemistry, Academy of Sciences of the Czech Republic, Flemingovo námesti 2, 16610 Praha 6, Czech Republic
Detlef.Schroeder@uochb.cas.cz

[2]Institut für Chemie der Technischen Universität Berlin, Strasse des 17. Juni 135, 10623 Berlin, Germany

Abstract Oxidation catalysis is of extreme importance in many areas of chemistry. The intrinsic mechanisms of oxidation reactions are, however, quite often understood only rather poorly, and catalyst research is mostly, if not exclusively, based on entirely empirical approaches. In this respect, gas-phase experiments can provide a complementary approach in that they can allow the investigation of the elementary processes in oxidation catalysis step by step. By such, some general insight can be obtained, which may assist in the development of more efficient oxidation catalysts.

Keywords Alkane activation · Mass spectrometry · Oxidation · Transition-metal oxides

1 Introduction

Selective partial oxidation of hydrocarbons poses considerable challenges to contemporary research. While by no means all, most catalytic oxidations are based on transition-metal oxides as active intermediates, and the oxidative dehydrogenation of ethylbenzene to styrene over potassium-promoted iron oxides at a scale of about 20 Mt/year may serve as an example [1]. Despite this

huge interest, detailed knowledge about the molecular mechanisms in oxidation catalysis is still limited, and catalyst improvement is often merely based on trial and error procedures.

Experimental and theoretical studies of ion/molecule reactions of transition-metal oxide ions have uncovered several reactions that permit the oxygenation of methane to methanol on a molecular scale [2]. If it were possible to upscale such a catalytic oxidation of methane from the laboratory to an industrial process, the enormous resources of CH_4 available either as natural gas or from biologic sources could be used more efficiently [3, 4]. In addition to oxygenation, the oxidative coupling of methane to larger hydrocarbons is also of considerable interest. Accordingly, fundamental studies on the mechanistic details in oxidation catalysis and the nature of the elementary steps involved can aid and perhaps even direct catalyst development. One approach to gain more profound insight into the fundamental steps in oxidation catalysis is to study well-designed and properly defined ion/molecule reactions in the idealized gas phase. Among others, one obvious advantage of this approach is the possibility of a direct comparison of experimental data with results obtained using adequate theoretical methods. A first link between small, often only diatomic, model systems to applied catalysis can be provided by the investigation of metal-oxide clusters. Further, inclusion of ligand effects and of the influences of solvent molecules can mimic processes occurring in homogenous catalysis. Likewise, inclusion of adatoms and possible lattice effects may link gas-phase studies and surface science in applied catalysis (Scheme 1).

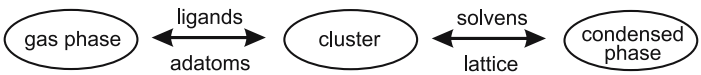

Scheme 1

Despite the promise of gas-phase studies, at the very outset it needs to be clarified that the results obtained in gas-phase experiments (e.g., thermodynamic data, rate constants, selectivities, or isotope effects) cannot be expected

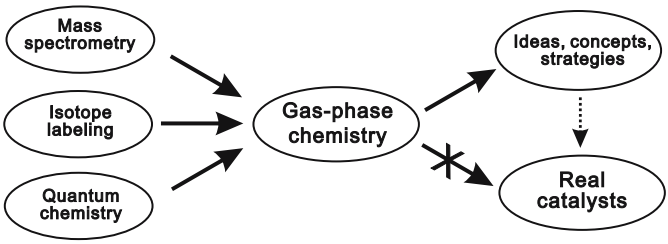

Scheme 2

to be directly transferable to applied catalysis. Instead, the emphasis is on describing the trends, concepts, or strategies (Scheme 2). Factors affecting regioselectivities, understanding the tuning of ligand effects, the role of counter ions, or the order of reduction and re-oxidation steps are all more likely to be comparable in the gas phase and in applied catalysis.

2
General Mechanistic Considerations in Oxidation

2.1
Thermochemical Boundaries

Any catalytic sequence needs to fulfill certain thermochemical boundary conditions as far as the elementary steps are concerned. For illustration, consider the oxygenation of an organic substrate *S* by a transition-metal oxo species [M]O according to reaction 1, where [M] stands for a bare or ligated, neutral or charged metal fragment:

$$[M]O + S \rightarrow [M] + SO \quad (1)$$

In order to render the occurrence of reaction 1 exothermic, the bond strength of the oxidant, $D([M]-O)$ needs to be lower than $D(S-O)$ of the substrate. For most organic reactants, the energies gained upon oxygenation range from 350 to 450 kJ/mol [5–8]. Hydroxylation of methane, for example, liberates 375 kJ/mol ($CH_4 \rightarrow CH_3OH$), and even 428 kJ/mol are released upon hydroxylation of benzene ($C_6H_6 \rightarrow C_6H_5OH$). Similarly, epoxidation of ethene liberates 354 kJ/mol ($C_2H_4 \rightarrow c\text{-}C_2H_4O$), and 472 kJ/mol are released when the O-atom transfer to ethene leads to the more stable acetaldehyde isomer ($C_2H_4 \rightarrow CH_3CHO$). As a consequence, $D([M]-O)$ should not exceed 450 kJ/mol, and even more efficient oxidation sequences are expected for more weakly bounded metal-oxo species.

On the other hand, the re-oxidation step required to convert the reduced form of the catalyst into the active species also sets some thermochemical boundaries, because only stoichiometric oxidation can be expected, if $D([M]-O)$ is too low. With regard to the most conceivable terminal oxidants, O_2, N_2O, or H_2O_2, a bond strength in the order of $D([M]-O) \approx 250$ kJ/mol appears as a minimum for successful re-oxidation [7]. Hence, promising candidates for oxidation catalysis should have bond strengths that meet both boundaries, i.e., $D([M]-O)$ should lie between 250 and 450 kJ/mol, where values closer to the lower limit are required in the particularly challenging case of alkane hydroxylation. Reviewing the existing data for metal-oxo bond strengths of gaseous transition-metal compounds, the most promising candidates appear to be either monoxides of late 3d transition metals or high-valent metal di-, tri-, or even tetroxides [7].

It should be clearly pointed out, however, that these considerations so far only concern mere thermodynamic effects without addressing any kinetic aspects. A particularly instructive example in this respect is the usage of N_2O as a terminal oxidant in the gas phase. From a mere thermochemical point of view, N_2O has a rather low O-atom affinity and can hence transfer its oxygen atom to all metal species with $D([M]-O) > 167\,kJ/mol$. Experimentally, it turns out, however, that many atomic metal ions experience a considerable kinetic hindrance with regard to O-atom transfer from N_2O [9, 10]. Despite the considerable bond strength of $D(Cr^+-O)$ at 360 kJ/mol [6], bare Cr^+, for example, does not undergo any reaction with N_2O at thermal conditions. Hence, experimental studies explicitly addressing the re-oxidation step also form a key aspect in the development of a more comprehensive understanding of oxidation catalysis [11].

2.2 Two-State Reactivity

Despite its seeming simplicity and its obviously limited relevance for applied catalysis, the reaction of diatomic FeO^+ with dihydrogen has received quite some attention [12–21]. This particular interest is due to several experimental observations that give a somewhat confusing picture upon first sight [18]. Thus, the reaction of FeO^+ with H_2 proceeds only once in about 100 collisions, but yet shows the typical negative temperature dependence of exothermic gas-phase ion/molecule reactions. While such a behavior may be rationalized by involving the oxidation of dihydrogen as rate-determining step, the reaction does not show a particularly pronounced kinetic isotope effect. This in turn suggests that H – H bond cleavage is not involved in the rate-determining step. Accordingly, the FeO^+/H_2 system has been extensively studied by both experiment and theory. A mechanistic solution for the seemingly contradicting experimental findings was provided by ab initio calculations [14, 16, 17, 19–21]. These computational studies demonstrated that even though the overall reaction is spin allowed – both Fe^+ and FeO^+ have sextet ground states, and H_2 as well as H_2O are singlets – the crucial insertion intermediate $HFeOH^+$ has a quartet ground state and, even more importantly, the lowest-lying transition structure corresponds to a quartet (Fig. 1).

These state orderings lead to a situation in which the reactants and products belong to one spin surface, while the intermediates have a different spin multiplicity. The experimental and theoretical evidence indicates that for iron, as a 3d element, the spin-change itself is mediated by spin-orbit coupling and is in fact rate-determining for the occurrence of the overall reaction; this scenario can account for all experimental observations.

The detailed studies of this particular, rather simple reaction also formed the basis for the generalized concept of two-state reactivity [22], according to which thermal reactions are not necessarily confined to the spin

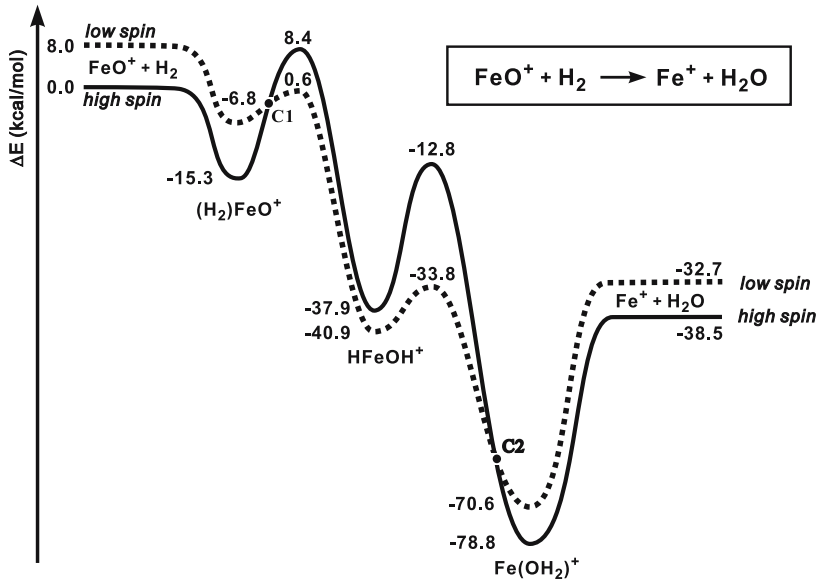

Fig. 1 Simplified potential-energy surface of the FeO^+/H_2 system

surface of the electronic ground-state, but rather spin-crossing effects can dramatically affect many features of numerous organometallic transformations. Thus, a number of other gas-phase oxidations mediated by the FeO^+ cation also involve changes of spin multiplicity as a key step [23, 24]. Further, two-state scenarios play a crucial role in the gas-phase reactions of other metal-oxide ions. In the case of the gas-phase oxidation of simple alkanes by the VO_2^+ cation, for example, small structural variations of the hydrocarbon substrates lead to drastic changes in product distributions, which can be attributed to the decisive role of spin changes for product formation with these substrates [25, 26].

In subsequent research, it turned out that two-state reactivity can also provide a concept for the understanding of oxidation reactions way beyond the scope of gas-phase ion chemistry and can actually resolve a number of existing mechanistic puzzles. In enzymatic oxidations involving cytochrome P450, for example, changes in spin multiplicity appear to act as a kind of mechanistic distributor for product formation [27–29], and in the case of manganese-catalyzed epoxidation reactions, two-state scenarios have been put forward to account for the experimentally observed stereoselectivities [30–32]. Two-state reactivity is not restricted to oxidation reactions, and similar scenarios have been proposed for a number of other experimentally studied reactions of 3d metal compounds [33–37]. Moreover, two-state scenarios have recently also been involved in the chemistry of main group elements [38]. The concept of two-state reactivity developed from the four-atomic system FeO^+/H_2

in the idealized gas phase has hence turned out as a rather useful, wide-ranging paradigm in chemistry [39–43]. As far as O-atom transfer reactions by $[M]O^+$ cations are concerned, the gas-phase studies allow some rather general conclusions. Thus, most monoxides of middle and late transition metals bear high-spin ground states and the passage via low-energy pathways for bond activation requires the occurrence of a spin flip and thus involves two-state reactivity. While spin inversion is facile for 4d and particularly 5d elements, the change of spin multiplicity may be rate-determining in the case of 3d metals.

3
Mononuclear Metal-Oxide Ions

3.1
Oxidation of Methane

Gas-phase studies revealed the existence of two distinctly different mechanistic routes for the oxygenation of methane to methanol by a metal-oxo species (Scheme 3). The first variant proceeds via an addition of a C – H bond of methane across the [M]O unit to yield an insertion species of the type $CH_3 – [M] – OH$ as a reaction intermediate, from which methanol can be liberated via reductive elimination. Alternatively, the metal oxide can act as a mere hydrogen atom abstractor without any interaction between the metal and carbon centers, which requires that the newly formed O – H is stronger than the C – H bond of methane. Experimentally, these two routes can be distinguished by means of the associated kinetic isotope effects (KIEs) for C – H- versus C – D bond activation. Thus, the FeO^+ cation, which reacts via the insertion route, bears a KIE of about 4.6 in the reaction with CH_2D_2 [44]. For the high-valent iron oxide cation $OFeOH^+$ an even larger KIE is found [45]. Somewhat lower, but still rather significant KIEs have been observed for MgO^+ (*KIE* = 2.1) [46] as well as MoO_3^+ (*KIE* = 2.0) [47]. In contrast, the $V_4O_{10}^+/CH_2D_2$ system, which can be regarded as a prototype of a simple hydrogen-atom abstraction mechanism, shows a *KIE* of only 1.35 [48], which is similar to the *KIE* of about 1.3 for the H(D)-atom abstraction from methane by free OH radicals [49].

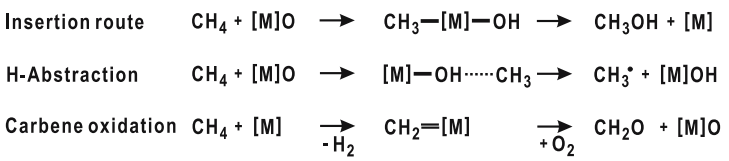

Scheme 3

Another conceptual route for the oxygenation of methane begins with the exclusive activation of methane by a transition-metal ion followed by oxidation of the primary product with a suitable oxygen donor. Due to relativistic effects operating in the formation of metal–carbon multiple bonds [50], several bare cations of 5d elements, for example, are able to dehydrogenate methane under formation of the corresponding metal–carbene cations MCH_2^+ (M = Ta, W, Os, Ir, Pt) [2]. These MCH_2^+ species can subsequently undergo oxygenation reactions. Thus, the $PtCH_2^+$ cation reacts with molecular oxygen to afford oxygenation products such as the couple $PtO^+ + CH_2O$, of which the former is able to convert methane into methanol [51, 52]. Also noteworthy in this context is the (stoichiometric) coupling of methane and carbon dioxide to ketene, in which $TaCH_2^+$ is formed as the key intermediate from bare Ta^+ and methane [53, 54].

3.2 The Selectivity Problem

The particularly high reactivity of gaseous metal-oxide cations is, of course, also associated with some drawbacks. Thus, several metal-oxo species predicted to be rather reactive are on the other hand quite difficult to generate in yields and purities sufficient for ion-reactivity studies. Thermochemical as well as theoretical data suggest, for example, that the diatomic copper-oxide cation CuO^+ should be highly reactive with regard to both H atom abstraction as well as oxygen atom transfer [55]. Nevertheless, diatomic CuO^+ by so far has not yet been made in yields that permit further reactivity studies. Moreover, there has evolved a general problem in chemical reactivity, because highly reactive species that are capable of activating rather robust substrates, such as methane, often bear disappointing selectivities when it comes to even slightly more complex substrates. Thus, bare FeO^+ is capable of activating methane, but already with propane as a substrate, the discrimination between primary and secondary C – H bonds is rather poor [56, 57], and with transition-metal dioxide cations the site-selectivities often even decrease further [58, 59]. The reaction of the PtO_2^+ cation with methane may serve as a particularly impressive example in that this pair of reactants affords no less than eight different product channels with a substrate as simple as methane (Scheme 4) [59].

Another related problem is associated with over-oxidation of the substrate, in the extreme case resulting in complete combustion. In the case of methane oxidation by FeO^+, for example, the activation of methane occurs with about 10% of the gas-kinetic collision rate, whereas those of the putative oxygenation products CH_3OH, CH_2O, and HCOOH occur on every collision [60]. With regard to applied catalysis this would imply that the oxidation products are oxidized faster by about one order of magnitude compared to methane as the initial substrate. In the particular context of heterogeneous oxidation

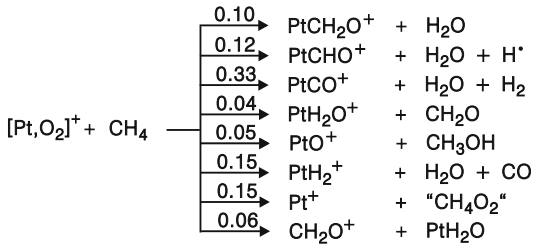

Scheme 4

catalysis it is also to be expected that the polar, oxygenated products bear much larger residence times on the catalyst than the non-polar methane, thereby even further increasing the propensity of over-oxidation.

One way to address the selectivity problems outlined above is the deliberate usage of ligand effects. In the case of the copper-oxide cation, for example, the introduction of an additional phenanthroline (phen) ligand permits the generation of the ligated (phen)CuO^+ cation in yields sufficient for reactivity studies, and this ligated cation is in fact able to activate small hydrocarbons such as propane [61]. We note in passing that for (phen)CuO^+ also, the hydroxylation of propane involves a two-state scenario. Likewise, additional ligands have been used successfully for the modification of the reactivity of other metal-oxide cations [62–64]. Inversion of the sequence of oxidation and interaction with the substrate can also increase oxygenation yields [65]. In many cases, however, either the oxidation activity of the metal-oxo species is quenched by the ligand or the ligand itself undergoes oxidation upon attachment to the metal core. Nevertheless, reactivity studies of ligated metal-oxo species in the gas phase form a promising area for future research.

4 Gas-Phase Catalysis

Experiments conducted with mass-selected ions do not bear any direct relevance for applied catalysis, simply because the number densities of the ionic species are rather low (typically about 10^6 particles per cm^3). Nevertheless, the advantages associated with the handling and the detection of ionic species render gas-phase studies as an ideal tool for the investigation of the elementary steps in oxidation reactions. In the same vein, this holds true for the investigation of the separate mechanistic steps, and in appropriate mass spectrometers that are able to store ions for extended timescales this can also be extended to real catalytic cycles [66]. The time-honored prototype of such a catalysis was reported by Kappes and Staley who demonstrated that bare Fe^+ ions initiate a catalytic conversion of CO into CO_2 in the presence of N_2O [67]. In the following decades, a number of other catalytic cycles involv-

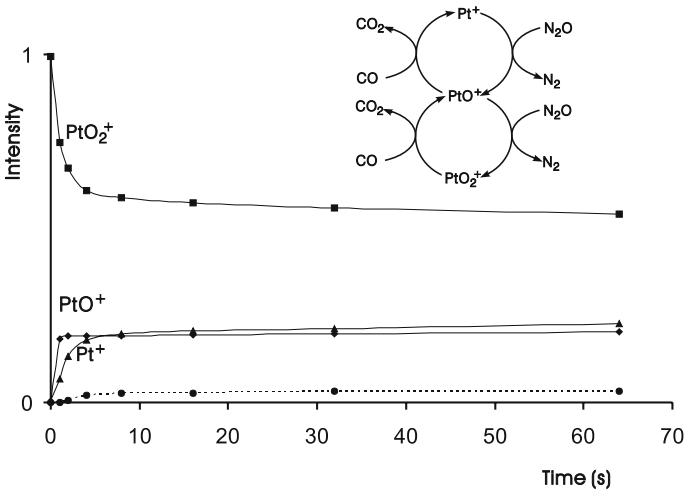

Fig. 2 Time-dependent intensity profiles of Pt^+ (▲), PtO^+ (♦), PtO_2^+ (■), and the sum of all side products (●) when reacting mass-selected $[Pt, O_2]^+$ with a mixture of N_2O and CO. The *inset* shows the two different catalytic cycles involved

ing gaseous FeO^+ were reported [44, 63, 68, 69]. Figure 2 shows an example of such a gas-phase catalysis, in which gaseous Pt^+ initiates two catalytic cycles for the oxidation of CO to CO_2 with N_2O as an oxidant. In this example, the turnover number is only limited by reactions with impurities present in the supplied gases or in the background vacuum of the mass spectrometer.

Beyer and coworkers later extended these reactions to platinum clusters Pt_n^+ and have demonstrated that similar reaction sequences for the oxidation of carbon monoxide can occur with larger clusters [70]. In addition, they were able to demonstrate poisoning effects as a function of surface coverage and cluster size. A related sequence for Pt_n^- anions was proposed by Shi and Ervin who employed molecular oxygen rather than N_2O as the oxidant [71]. Further, the group of Bohme has screened the mononuclear cations of almost the entire transition metal block for this particular kind of oxidation catalysis [72, 73]. Another catalytic system has been proposed by Waters et al. in which a dimolybdate anion cluster brings about the oxidation of methanol to formaldehyde; with nitromethane, however, a rather unusual terminal oxidant was employed [74].

5 Metal-Oxide Clusters

It goes without saying that mononuclear metal-oxo species can only be considered as first-order models for the processes occurring in partial oxidations

on heterogeneous catalysts. In fact, it has be questioned whether the reactions of a diatomic species, such as FeO^+, can at all mimic the reactions occurring in real oxidation catalysis. Compared to the reactions of mononuclear species, the knowledge about the gas-phase reactivities of transition-metal oxide cluster ions is still quite limited. Nevertheless, considerable achievements have been obtained in recent years, mostly dealing with vanadium, nickel, platinum, silver, and gold.

Castleman and coworkers have initiated systematic studies of $V_mO_n^+$ ions with a broad variety of neutral substrates [75], not only including hydrocarbons [76–78], as well as methanol [79], but also other reagents such as haloalkanes [80–82]. Moreover, these experimental studies were recently augmented by inclusion of ab initio investigations of the key intermediates, thereby providing a rather profound insight into the gas-phase chemistry of transition-metal oxide clusters [83]. It is to be noted, however, that the instrumental setup used in the earlier studies of Castleman and coworkers had a somewhat limited mass resolution and some results needed to be revised later [78]. Nevertheless, these studies have provided a wealth of knowledge so far unachieved in the gas-phase chemistry of transition-metal oxide-clusters.

$$V_mO_n^+ + C_oH_p \rightarrow V_mO_nH_2^+ + C_oH_{p-2} \quad (2)$$

A reaction of particular relevance with respect to applied catalysis is the oxidative dehydrogenation (ODH) of hydrocarbon by $V_mO_n^+$ ions according to reaction 2, which involves a two-electron reduction of the cluster. By means of a systematic study of the reactions of various $V_mO_n^+$ ions as well as the related oxo-vanadium hydroxides $V_mO_nH^+$ ions with a set of C_4-hydrocarbons, it was demonstrated recently that the ODH activity of the cluster ions shows a clear correlation with the formal valence of vanadium in the cluster ions with a maximum reactivity for formal vanadium (V) (Fig. 3) [84]. In such a kind of reactivity screening, it is essential to include more than a single reagent as a probe for the reactivity of the different ions in order to reduce interferences by kinetic barriers of one particular combination of neutral and ionic reactants [85]. Accordingly, the sums of the relative rate constants for the ODH reactions of the four different butenes are considered and normalized to the most reactive ion studied, which turns out to be the formally pure vanadium (V) compound $V_3O_7^+$. In addition to isomeric butenes, *n*-butane was also studied, but has not been included in the screening, because of all ions investigated only $V_4O_{10}^+$ reacts with the saturated alkane.

These results further prompted ab initio investigations of the reactions of $V_3O_7^+$ and $V_4O_{10}^+$ with hydrocarbons. Thus, in a model study of the reactions of $V_3O_7^+$ with propane and 1-butene it was found that the initial C – H bond activation of the substrate acts as the rate-determining step. In the case of the saturated hydrocarbon C_3H_8, the associated barrier is slightly

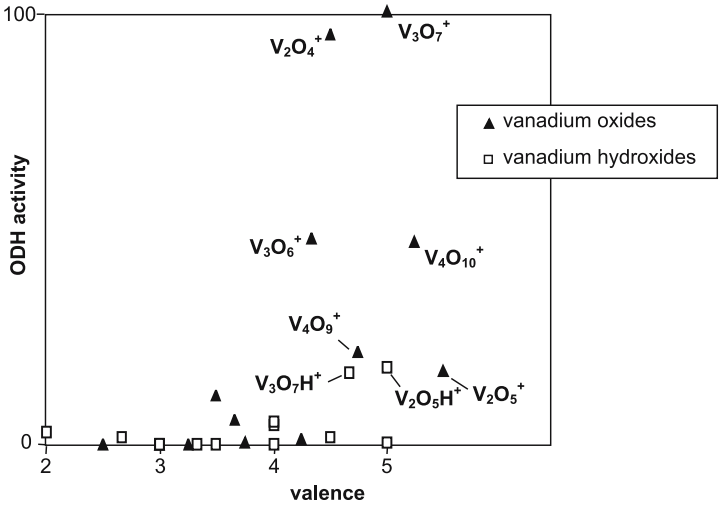

Fig. 3 ODH activities for 1-butene, *cis*-butene, *trans*-butene, and *iso*-butene versus the formal valence of vanadium in the $V_mO_nH_o^+$ clusters

too high for the occurrence of bond activation at room temperature. However, the weaker allylic C – H bond in 1-butene, in conjunction with the larger energy gain upon complexation of the unsaturated hydrocarbon by the metal-oxide cations, promotes a rapid oxidation of the neutral substrate according to reaction 2 [86]. In marked contrast, the formally hypervalent cation radical $V_4O_{10}^+$ is even capable of activating methane under thermal conditions (reaction 3) [48]:

$$V_4O_{10}^+ + CH_4 \rightarrow V_4O_{10}H^+ + CH_3^{\cdot} \quad (3)$$

A detailed theoretical analysis further revealed that this reaction can be considered to proceed as a barrier-free H atom abstraction without any significant additional interaction between the methyl radical formed and the remaining cluster ion. Consistent with this mechanistic interpretation, the kinetic isotope effect associated with C – H(D) bond activation of CH_2D_2 is rather low (*KIE* = 1.35).

The oxidation of CO to CO_2 by metal-oxide clusters has received quite some attention, in part due to its relevance for the catalytic converters in automobiles, in part also because carbon monoxide is often used as a probe molecule in surface science and the reasonable simplicity of the system may still permit adequate theoretical treatments. In addition to the various systems involving $Pt_mO_n^+$ cations as well as $Pt_mO_n^-$ anions (see above), considerable efforts have been devoted to cluster anions of silver and gold, as reviewed recently [87]. A particular highlight is a conceptual catalytic cycle for the Au_2^--mediated oxidation of CO with molecular oxygen, for which

the reaction intermediates were carefully characterized by experiment and theory [88]. Also in the context of exhaust-gas treatment, Castleman and coworkers have investigated the behavior of $Ni_mO_n^+$ cations towards nitric oxides [89]. As far as oxidations of organic substrates are concerned, more recent results have been obtained for the dinuclear clusters $Mg_2O_2^+$ [46], $Fe_2O_2^+$ [90], and $Ni_2O_2^+$ [91] and a series of $M_2O_n^-$ anions (n = 3, 4) [92]. In general, the metal-oxide cluster ions turn out to be considerably less reactive than their mononuclear congeners. Thus, MgO^+, FeO^+ and NiO^+ are all capable of activating methane, whereas none of the corresponding dinuclear $M_2O_2^+$ clusters can fulfill this task. Nevertheless, these clusters are still able to dehydrogenate other small hydrocarbons such as butane (reaction 4 with M = Mg, Fe, and Ni):

$$M_2O_2^+ + C_4H_{10} \rightarrow M_2O_2H_2^+ + C_4H_8 \quad (4)$$

Quite obviously, however, further work – both experimental and computational – is needed to understand the behavior of metal-oxide clusters in more detail and thereby to identify reactive clusters, with options to also tune their reactivity by changing the cluster size. In this context, a final aspect should be mentioned briefly, which is related to the generation of metal-oxide cluster ions in the gas phase. The most common approach involves the use of a Smalley-type source in which a laser beam evaporates a metal followed by subsequent aggregation in an (oxidant-doped) supersonic expansion of a suitable gas (usually helium). It has been demonstrated, however, that these conditions can lead to the formation of dioxygen complexes rather than the desired high-valent metal-oxide clusters [93–95]. Direct laser desorption of solid metal oxides can be used as an alternative approach [92], but ion yields are only moderate and the instrumentation is considerably contaminated by the ablated material. However, this technique is unique in some respects and the prospects for the gas-phase chemistry of actinides [96] are particularly noteworthy. Other approaches involve the oxidation of pure metal cluster ions in the gas phase [97], but this approach is often associated with degradation of the clusters to smaller, if not even mononuclear entities [98, 99]. We have recently introduced a completely different approach based on electrospray ionization of appropriate inorganic precursors and so far have produced several $M_mO_n^+$ clusters for the metals magnesium, vanadium, and iron [46, 84, 100, 101]. The successful generation of binary metal-oxide clusters requires, however, that the bonds to the outer inorganic and organic ligands are weaker than those of the metal-oxide core, and thus related strategies have failed in the generation of $Ti_mO_n^+$ and $Zn_mO_n^+$ from seemingly suitable molecular precursors [102, 103].

Acknowledgements Generous financial support by the Academy of Sciences of the Czech Republic, the Deutsche Forschungsgemeinschaft (Sfb 546), and the Fonds der Chemischen Industrie is gratefully acknowledged.

References

1. Weiss W, Schlögl R (2000) Top Catal 13:75
2. Schwarz H, Schröder D (2000) Pure Appl Chem 72:2319
3. Lunsford JH (2000) Catal Today 63:165
4. Labinger JA (2004) J Mol Catal 220:27
5. Berkowitz J, Ellison GB, Gutman D (1994) J Phys Chem 98:2744
6. Freiser BS (ed) (1996) Organometallic ion chemistry. Kluwer, Dordrecht
7. Schröder D, Shaik S, Schwarz H (2000) Struct Bond 97:91
8. Linstrom PJ, Mallard WG (eds) (2005) NIST chemistry webbook NIST standard reference database number 69, version June 2005
9. Kappes MM, Staley RH (1981) J Phys Chem 85:942
10. Lavrov VV, Blagojevic V, Koyanagi GK, Orlova G, Bohme DK (2004) J Phys Chem A 108:5610
11. Blagojevic V, Koyanagi GK, Caraiman D, Blagojevic V, Bohme DK (2002) J Phys Chem A 106:4581
12. Schröder D, Fiedler A, Ryan MF, Schwarz H (1994) J Phys Chem 98:68
13. Clemmer DE, Chen Y-M, Khan FA, Armentrout PB (1994) J Phys Chem 98:6522
14. Fiedler A, Schröder D, Shaik S, Schwarz H (1994) J Am Chem Soc 116:10734
15. Baranov V, Javahery G, Hopkinson AC, Bohme DK (1995) J Am Chem Soc 117:12801
16. Shaik S, Danovich D, Fiedler A, Schröder D, Schwarz H (1995) Helv Chim Acta 78:1393
17. Danovich D, Shaik S (1997) J Am Chem Soc 119:1773
18. Schröder D, Schwarz H, Clemmer DE, Chen Y-M, Armentrout PB, Baranov VI, Böhme DK (1997) Int J Mass Spectrom Ion Processes 161:177
19. Filatov M, Shaik S (1998) J Phys Chem A 102:3835
20. Irigoras A, Fowler JE, Ugalde JM (1999) J Am Chem Soc 121:8549
21. Matxain JM, Mercero JM, Irigoras A, Ugalde JM (2004) Mol Phys 102:2635
22. Schröder D, Shaik S, Schwarz H (2000) Acc Chem Res 33:139
23. Harris N, Shaik S, Schröder D, Schwarz H (1999) Helv Chim Acta 82:1784
24. Shiota Y, Yoshizawa K (2003) J Chem Phys 118:5872
25. Harvey JN, Diefenbach M, Schröder D, Schwarz H (1999) Int J Mass Spectrom 182/183:85
26. Engeser M, Schlangen M, Schröder D, Schwarz H, Yumura T, Yoshizawa K (2003) Organometallics 22:3933
27. Shaik S, Filatov M, Schröder D, Schwarz H (1998) Chem Eur J 4:193
28. Shaik S, de Visser SP, Ogliaro F, Schwarz H, Schröder D (2002) Curr Opin Chem Biol 6:556
29. Schoeneboom JC, Cohen S, Lin H, Shaik S, Thiel W (2004) J Am Chem Soc 126:4017
30. Adam W, Roschmann K, Saha-Möller CR (2000) Eur J Org Chem 3519
31. Brandt P, Norrby PO, Daly AM, Gilheany DG (2002) Chem Eur J 8:4299, and references cited therein
32. Cavallo L, Jacobsen H (2003) J Phys Chem A 107:5466
33. Fiedler A, Schröder D, Zummack W, Schwarz H (1997) Inorg Chim Acta 259:227
34. Kretzschmar I, Schröder D, Schwarz H, Rue C, Armentrout PB (1998) J Phys Chem A 102:10060
35. Rue C, Armentrout PB, Kretzschmar I, Schröder D, Harvey JN, Schwarz H (1999) J Chem Phys 110:7858
36. Bärsch S, Kretzschmar I, Schröder D, Schwarz H, Armentrout PB (1999) J Phys Chem A 103:5925

37. Hess JS, Leelasubcharoen S, Rheingold AL, Doren DJ, Theopold KH (2002) J Am Chem Soc 124:2454
38. Perez P, Andres J, Safont VS, Contreras R, Tapia O (2005) J Phys Chem A 109:4178
39. Plattner DA (1999) Angew Chem Int Ed 38:82
40. Harvey JN, Poli R, Smith KM (2003) Coord Chem Rev 238/239:347
41. Poli R, Harvey JN (2003) Chem Soc Rev 32:1
42. Schwarz H (2004) Int J Mass Spectrom 237:75
43. Shaik S, Cohen S, de Visser SP, Sharma PK, Kumar D, Kozuch S, Ogliaro F, Danovich D (2004) Eur J Inorg Chem 207
44. Schröder D, Schwarz H (1990) Angew Chem Int Ed Engl 29:1433
45. Schröder D, Schwarz H (1991) Angew Chem Int Ed Engl 30:991
46. Schröder D, Roithová J (2006) Angew Chem Int Ed (in press), published online 21 July 2006
47. Kretzschmar I, Fiedler A, Harvey JN, Schröder D, Schwarz H (1997) J Phys Chem A 101:6252
48. Feyel S, Döbler J, Schröder D, Sauer J, Schwarz H (2006) Angew Chem Int Ed 45(28):4681
49. Saueressig G, Crowley JN, Bergamaschi P, Bruhl C, Brenninkmeijer CAM, Fischer H (2001) J Geophys Res Atmos 106:23127
50. Schwarz H (2003) Angew Chem Int Ed Engl 42:4442
51. Wesendrup R, Schröder D, Schwarz H (1994) Angew Chem Int Ed Engl 33:1174
52. Pavlov M, Blomberg MRA, Siegbahn PEM, Wesendrup R, Heinemann C, Schwarz H (1997) J Phys Chem 101:1567
53. Wesendrup R, Schwarz H (1995) Angew Chem Int Ed Engl 34:2033
54. Sändig N, Koch W (1998) Organometallics 17:2344
55. Irigoas A, Elizade O, Silanes I, Fowler JE, Ugalde JM (2000) J Am Chem Soc 122: 114
56. Trage C, Schröder D, Schwarz H (2003) Organometallics 22:693, addendum (2003) 22:1348
57. Yumura T, Yoshizawa K (2001) Organometallics 20:1397
58. Fiedler A, Kretzschmar I, Schröder D, Schwarz H (1996) J Am Chem Soc 118:9941
59. Brönstrup M, Schröder D, Kretzschmar I, Schwarz H, Harvey JN (2001) J Am Chem Soc 123:142
60. Yumura T, Amenomori T, Kagawa Y, Yoshizawa K (2002) J Phys Chem A 106:621
61. Schröder D, Holthausen MC, Schwarz H (2004) J Phys Chem B 108:14407
62. Stöckigt D, Schwarz H (1994) Chem Ber, p 2499
63. Stöckigt D, Schwarz H (1995) Liebigs Ann, p 429
64. Brönstrup M, Schröder D, Schwarz H (1999) Can J Chem 77:774
65. Ryan MF, Stöckigt D, Schwarz H (1994) J Am Chem Soc 116:9565
66. Böhme DK, Schwarz H (2005) Angew Chem Int Ed 44:2336
67. Kappes MM, Staley RH (1981) J Am Chem Soc 103:1286
68. Buckner SW, Gord JR, Freiser BS (1988) J Am Chem Soc 110:6606
69. Schröder D, Schwarz H (1990) Angew Chem Int Ed Engl 29:1431
70. Balaj OP, Balteanu I, Rossteuscher TTJ, Beyer MK, Bondybey VE (2004) Angew Chem Int Ed 43:6519
71. Shi Y, Ervin KM (1998) J Chem Phys 108:1757
72. Blagojevic V, Jarvis MJY, Flaim E, Koyanagi GK, Lavrov VV, Bohme DK (2003) Angew Chem Int Ed 42:4923
73. Blagojevic V, Orlova G, Bohme DK (2005) J Am Chem Soc 127:3545
74. Water T, O'Hair RA, Wedd AG (2003) J Am Chem Soc 125:3384

75. Zemski KA, Justes DR, Castleman AW Jr (2002) J Phys Chem B 106:6136
76. Bell RC, Zemski KA, Kerns KP, Denkg HT, Castleman AW Jr (1998) J Phys Chem A 102:1733
77. Zemski KA, Justes DR, Castleman AW Jr (2001) J Phys Chem A 105:10237
78. Bell RC, Castleman AW Jr (2002) J Phys Chem A 106:9893
79. Justes DR, Moore NA, Castleman AW Jr (2004) J Phys Chem B 108:3855
80. Bell RC, Zemski KA, Castleman AW Jr (1998) J Phys Chem A 102:8293
81. Bell RC, Zemski KA, Castleman AW Jr (1999) J Phys Chem A 103:1585
82. Bell RC, Zemski KA, Castleman AW Jr (1999) J Phys Chem A 103:2992
83. Justes DR, Mitric R, Moore NA, Bonacic-Koutecky V, Castleman AW Jr (2003) J Am Chem Soc 125:6289
84. Feyel S, Schröder D, Schwarz H (2006) J Phys Chem A 110:2647
85. Cornehl HH, Heinemann C, Schröder D, Schwarz H (1995) Organometallics 14:992
86. Feyel S, Schröder D, Rozanska X, Sauer J, Schwarz H (2006) Angew Chem Int Ed 45(28):4677
87. Bernhardt TM (2005) Int J Mass Spectrom 243:1
88. Socaciu LD, Hagen J, Bernhardt TM, Wöste L, Heiz U, Häkkinen H, Landman U (2003) J Am Chem Soc 125:10437
89. Vann WD, Castleman AW Jr (1999) J Phys Chem A 103:847, and references cited therein
90. Jackson P, Harvey JN, Schröder D, Schwarz H (2001) Int J Mass Spectrom 204:233
91. Koszinowski K, Schlangen M, Schröder D, Schwarz H (2005) Eur J Inorg Chem 2464
92. Oliveira MC, Marcalo J, Vieira MC, Ferreira MAA (1999) Int J Mass Spectrom 185/186/187:825
93. Brümmer M, Kaposta C, Santambrogio G, Asmis KR (2003) J Chem Phys 119:12700
94. Asmis KR, Meijer G, Brümmer M, Kaposta C, Santambrogio G, Wöste L, Sauer J (2004) J Chem Phys 120:6461
95. Koyanagi GK, Bohme DK, Kretzschmar I, Schröder D, Schwarz H (2001) J Phys Chem A 105:4259
96. Gibson JK, Marcalo J (2006) Coord Chem Rev 250:776
97. Gehret O, Irion MP (1996) Chem Eur J 2:598
98. Engeser M, Weiske T, Schröder D, Schwarz H (2003) J Phys Chem A 107:2855
99. Koszinowski K, Schröder D, Schwarz H (2003) J Phys Chem A 107:4999
100. Schröder D, Engeser M, Brönstrup M, Daniel C, Spandl J, Hartl H (2003) Int J Mass Spectrom 228:743
101. Schröder D, Roithová J, Schwarz (2006) Int J Mass Spectrom (in press) published online 5 July 2006 (doi:10.1016/j.imjs.2006.05.024)
102. Khitrov GA, Strouse GF, Gaumet J-J (2004) J Am Soc Mass Spectrom 15:260
103. Schröder D, Schwarz H, Polarz S, Driess M (2005) Phys Chem Chem Phys 7:1049

Top Organomet Chem (2007) 22: 17–37
DOI 10.1007/3418_038

Published online: 8 July 2006

Dioxygen Activation by Organometallics of Early Transition Metals

Klaus H. Theopold

Department of Chemistry and Biochemistry, Center for Catalytic Science and Technology, University of Delaware, Newark, DE 19716, USA
theopold@udel.edu

Abstract Organometallic compounds of the early transition metals (i.e., groups 3–6) react readily with oxygen (O_2). The different reaction pathways governing these reactions are distinguished and relevant examples from the recent organometallic literature are described. Catalytic aerobic oxidations are rare for these metals. However, the investigations of individual reaction steps contribute to the fundamental knowledge of organometallic chemistry, and they are valuable for the design of catalytic oxidations.

Keywords Organometallics · Dioxygen · Early transition metals · Oxygen atom transfer

1 Introduction

The utilization of dioxygen (O_2) in all manner of catalytic oxidation reactions is a highly attractive option for the preparation of oxygenated molecules. O_2 is a readily available, nontoxic reagent, and a common byproduct of aerobic oxidations is the innocuous substance water (H_2O). Thus, chemical processes using dioxygen are a goal of "green" or "sustainable" chemistry.

The reactions of O_2 with organic molecules are generally strongly favored in a thermodynamic sense (see Eqs. 1–3 for some prototypical examples).

$$CH_{4(g)} + 1/2O_{2(g)} \rightarrow CH_3OH_{(l)} \qquad \Delta G^o = -115.4\,kJ/mol \qquad (1)$$

$$H_2C = CH_{2(g)} + 1/2O_{2(g)} \rightarrow CH_2CH_2O_{(l)} \qquad \Delta G^o = -79.8\,kJ/mol \qquad (2)$$

$$C_6H_{6(l)} + 1/2O_{2(g)} \rightarrow C_6H_5OH_{(s)} \qquad \Delta G^o = -174.5\,kJ/mol\,. \qquad (3)$$

However, they face substantial kinetic barriers, and none of the reactions shown above proceed with appreciable rate under mild conditions. Hence there arises the need for catalysts to facilitate the reactions. Besides, the desired reaction products—i.e., methanol, ethylene oxide, and phenol—are of course just kinetic products. The thermodynamic products for the three reactions shown, i.e., CO_2 and H_2O, are the same undesirable two in each case. Thus selectivity is called for, and once again catalysis will be the answer. Based on these fundamental considerations, much effort has already been expended on the search for selective catalysts for O_2-driven oxidations [1], and the need for future innovation remains strong.

Commercially practiced oxidation catalysis employing O_2 as terminal oxidant comprises examples of both heterogeneous and homogeneous catalysis; herein we are mostly concerned with the latter. In further narrowing the scope of this volume, we are considering only those reactions that involve "organometallic" species—i.e., molecules containing a direct metal–carbon bond—either as reactants, products, or intermediates. As both O_2 and hydrocarbon substrates can interact with and bind to metal complexes, there exist at least two general approaches to catalyzing oxidations. The more common approach involves the so-called "activation" of O_2 via coordination to a metal center [2] and its subsequent transformation into a reactive species (e.g., a high-valent metal oxo complex, such as the ferryl moiety commonly considered the reactive oxidant of the cytochrome P450 family of enzymes [3]). A second conceivable strategy relies upon "activation" of the hydrocarbon substrate by coordination to a metal, i.e., forming an organometallic species, which is subject to reaction with free O_2. Actually, even the "O_2-activation" approach may involve organometallic compounds, if the ancillary ligands of the catalyst include carbon-based ones.

This chapter is dedicated to a review of the recent organometallic chemistry of early transition metals (i.e., groups 3–6) with O_2. The oxophilic nature of these electropositive metals might suggest that they will resist complete the transfer of oxygen atoms to carbon, up to and including release of oxygenated products. Nevertheless, there are some examples of catalysis as well as many stoichiometric reactions, which shed light upon the mechanistic details of individual reaction steps comprising catalytic cycles of catalytic oxidations.

2 Reactions with O_2

The number of reactions of organometallic molecules with O_2 yielding well-characterized products in good yield is notably small. It is no accident that the typical synthetic organometallic laboratory is equipped with inert atmosphere glove boxes and Schlenk lines, and that rigorous exclusion of air by means of inert gas techniques and scrupulously dried and deoxygenated solvents pervade our daily routine [4]. Indeed, one's colleagues may receive the report of a reaction with O_2 with a thinly veiled contempt for sloppy laboratory technique.

Considering the potential utility of catalytic oxidations, and the need for a better understanding of the fundamental reaction steps involved, this relative paucity of systematic studies is unfortunate. It is an area that needs more work, and the scientific payoff warrants the occasional—if deplorable—transformation of a perfectly good organometallic compound into a black, smoldering tar.

Any reaction of the type to be considered here begins with the interaction of an organometallic compound with O_2. This may lead to the formation of a dioxygen complex, however fleeting its existence. Further reactions may ensue. In the following sections we summarize the available results, organized by type of transformation. We begin with the evidence for coordination of O_2.

2.1 Binding of O_2

The reaction of organometallic compounds with O_2 may produce more or less stable dioxygen complexes. An early and unambiguous example of this kind of transformation was provided in the report by van Asselt et al. of the isolation of a series of stable peroxo alkyl complexes of the type $Cp^*_2Ta(\eta^2\text{-}O_2)R$ (R = Me, Et, Pr, Bn, Ph) [5]. As shown in Scheme 1, O_2 presumably oxidatively adds to the 16-electron fragments $Cp^*{}_2TaR$, which are in rapid equilibrium with the 18-electron olefin hydrides or alkylidene hydrides.

The benzyl derivative $Cp^*_2Ta(\eta^2\text{-}O_2)Bn$ was structurally characterized by X-ray diffraction; the O_2-ligand is side-on coordinated and lies in the equatorial plane of the bent metallocene fragment. The O – O distance of 1.477(8) Å and the O – O stretching frequency ($\nu_{O-O} = 863\ cm^{-1}$) are consistent with a peroxo ligand ($O_2{}^{2-}$) coordinated to tantalum in its highest possible formal oxidation state (+V). Notably, base appears to stabilize these complexes; i.e., in the presence of triethylamine $Cp^*_2Ta(\eta^2\text{-}O_2)Me$ did not decompose even when heated to 80 °C.

Another organometallic dioxygen complex was found to be the first-formed intermediate in the transformation shown in Eq. 4 ($Cp^{TMS} = \eta^5$-

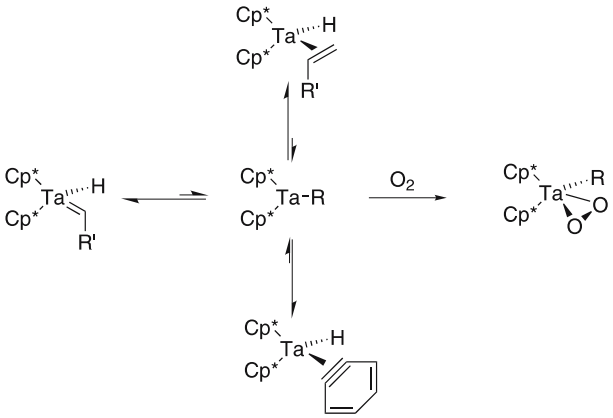

Scheme 1 Formation of a tantalum peroxo complex

$C_5H_4SiMe_3$), which is obviously a multi-step reaction [6].

$$1/x[Cp^{TMS}{}_2NbCl]_x + x/2O_2 \rightarrow Cp^{TMS}{}_2Nb(O)Cl\,. \tag{4}$$

The oxo complex was the final product of prolonged exposure of $[Cp^{TMS}{}_2Nb Cl]_x$ to air. However, rapid reaction with pure O_2 yielded the peroxo complex $Cp^{TMS}{}_2Nb(\eta^2\text{-}O_2)Cl$ as the major product. Its identity was confirmed by independent synthesis following literature precedent. Thus, the analogous $Cp_2Nb(\eta^2\text{-}O_2)Cl$ had been prepared earlier by reaction of Cp_2NbCl_2 with hydrogen peroxide [7]. The proposed series of events leading to the formation of $Cp^{TMS}{}_2Nb(O)Cl$ is shown in Scheme 2; note that the direct reaction of $Cp^{TMS}_2Nb(\eta^2\text{-}O_2)Cl$ with $[Cp^{TMS}{}_2NbCl]_x$ immediately gave $Cp^{TMS}{}_2Nb(O)Cl$, and that the bridging oxo complex $[Cp^{TMS}{}_2NbCl]_2(\mu - O)$ has also been isolated. This series or reaction steps must be considered a probable scenario for any reaction producing oxo complexes from O_2, even when the intermediates shown here are not directly observable.

An organometallic dioxygen adduct of an even more fleeting kind was observed in the reaction of the divalent chromium phenyl complex $Tp^{tBu,Me}Cr$-

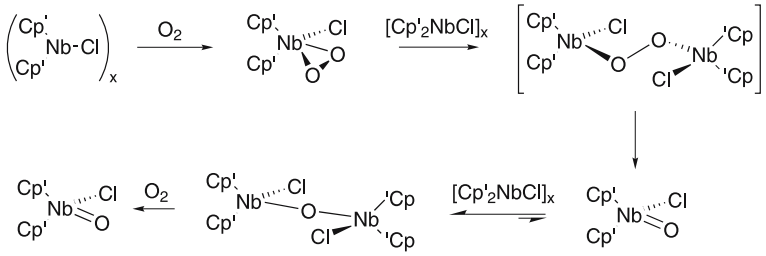

Scheme 2 Formation of a niobium peroxo intermediate and subsequent reactions

Ph ($Tp^{tBu,Me}$ = hydrotris(3-*tert*-butyl-5-methylpyrazolyl)borate) with O_2 [8]. While the ultimate product of the reaction is the product of an O_2 insertion into the Cr – C bond (Sect. 3.1), the first identifiable step is the binding of O_2 to chromium. At – 45 °C, a color change of the solution from the brilliant blue of $Tp^{tBu,Me}$Cr-Ph to a dark red indicated the formation of a new compound, which is stable at this low temperature. Monitoring the reaction by in-situ IR spectroscopy revealed the appearance of a new band at 1027 cm^{-1}, which shifted to 969 cm^{-1} when $^{18}O_2$ was used. These vibrational data are consistent with the formation of a chromium(III) superoxide complex, namely $Tp^{tBu,Me}Cr(O_2)Ph$ (Scheme 3, top).

While most superoxo complexes—in contrast to peroxo compounds—have been assigned a "bent, end-on" coordination mode [9], the superoxide ligand of $Tp^{tBu,Me}Cr(O_2)Ph$ was suggested to exhibit the more unusual "side-on" (η^2) coordination [10]. The reactivity of the complex did not allow for the determination of its molecular structure; however, close analogs could be isolated, crystallized and structurally characterized by X-ray diffraction. For example, the reaction of $[Tp^{tBu,Me}Cr(pz'H)]$BARF (pz′H = 3-*tert*-butyl-5-methylpyrazole, BARF = tetrakis(3,5-bis(trifluoromethyl)phenyl)borate) with O_2 produced the stable dioxygen complex $[Tp^{tBu,Me}Cr(pz'H)(\eta^2\text{-}O_2)]$BARF (Scheme 3, bottom), which featured a side-on bound superoxide ligand (d_{O-O} = 1.327(5) Å, ν_{O-O} = 1072 cm^{-1}) [11]. Other structurally characterized

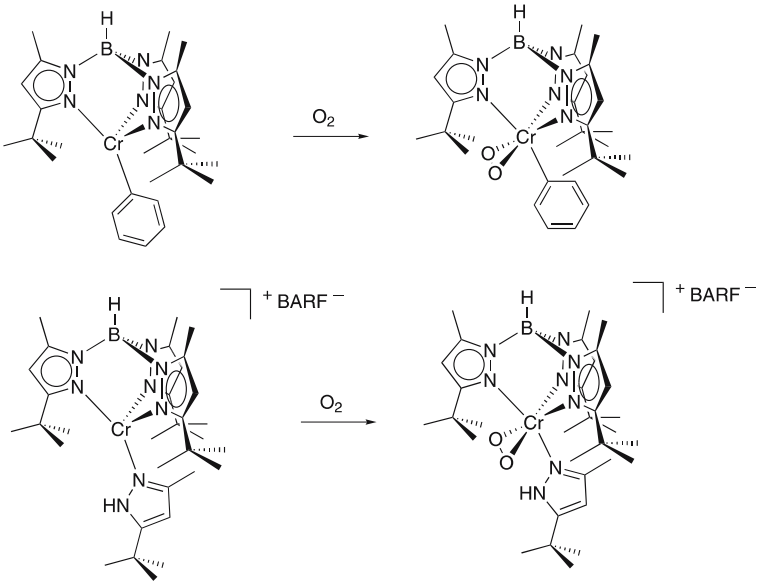

Scheme 3 Formation of a chromium phenyl superoxo intermediate and a stable analog thereof

representatives of this class of molecules include $Tp^{tBu,Me}Cr(\eta^2\text{-}O_2)Cl$ and $Tp^{tBu,Me}Cr(pz')(\eta^2\text{-}O_2)$ [12].

The Tp ligands (i.e., tris(pyrazolyl)borates or scorpionates [13]) are close analogs to the Cp ligands (i.e., η^5-cyclopentadienyl), and in connection with the chemistry of the $Tp^{tBu,Me}Cr$ complexes mentioned above, a recent example of O_2-binding from vanadium chemistry is of interest, even though it is formally not organometallic chemistry. Reaction of the V(IV) complex $Tp^{iPr2}V(O)(OH)(OH_2)$ with oxygen yields two products in a 1 : 1 ratio as shown in Eq. 5 [14].

$$Tp^{iPr2}V(O)(OH)(OH_2) + L + O_2 \rightarrow Tp^{iPr2}V(O)_2(L) + Tp^{iPr2}V(O)(O_2)(L)$$
$$(L = 3,5\text{-diisopropylpyrazole})\,. \qquad (5)$$

The crystal structure of the dioxygen complex $Tp^{iPr2}V(O)(O_2)(L)$ has been determined, and revealed a side-on bonded O_2 ligand. Based on the O – O distance of 1.379(6) Å and ν_{O-O} of 960 cm^{-1} it was formulated as a V(V) peroxo complex, even though these values are on the borderline between the peroxo and superoxo designations. The mechanism of this reaction is curious. Reaction with $^{18}O_2$ showed incorporation of ^{18}O solely in the O_2 ligand and not in the oxo groups. It appears that the O_2 binding step must be preceded by a disproportionation (2 V(IV) → V(III) + V(V)) followed by reaction of V(III) with O_2.

The examples summarized above demonstrate that organometallic derivatives of early transition metals can and will form dioxygen complexes, even though the stability of these adducts varies widely. The availability of some d-electrons is required; i.e., d^0-complexes do not show this mode of reactivity, presumably because binding of O_2 requires some degree of electron transfer (oxidation of the metal).

2.2 Formation of Oxo Complexes

The exposure of organometallic compounds to O_2 frequently results in the formation of metal oxo complexes. The oxygen atom may be bound as a terminal ligand or bridging several metals. The oxide ion (O^{2-}) is a good π-donor and interacts strongly with early metals in high oxidation states, due to the availability of empty d-orbitals of appropriate symmetry [15]. As shown in Sect. 2.1, the formation of oxo complexes may be mechanistically complex (Scheme 2), but the large thermodynamic driving force for the formation of the final product [16] often renders intermediates so short-lived as to evade detection. Nevertheless, the intervention of dioxygen complexes must be considered probable unless the organometallic reagent has a d^0-configuration.

There are many examples of organometallic compounds containing oxygen atoms as ligands; an appreciable number of these resulted from reactions with O_2. Early work has been reviewed by Bottomley and Sutin [17]. Thus we concentrate on more recent reports, and those of particular interest.

Legzdins et al. have reported the formation of oxo alkyls of tungsten and molybdenum in moderate yields (45–60%) according to Eq. 6 [18, 19].

$$Cp'M(NO)R_2 + O_2 \rightarrow Cp'M(O)_2R \quad (6)$$

(Cp' = Cp or Cp^*, M = Mo or W, R = Me, Np, Bn, CH_2SiMe_3, CH_2CMe_2Ph) .

An interesting, albeit unexplained, observation was the beneficial effect of adventitious water upon the reaction yield (10–15% increase in yield). When the oxygenation of $Cp^*W(NO)(CH_2SiMe_3)_2$ was carried out with $^{18}O_2$, the products were a mixture of $Cp^*W(^{16}O)_2(CH_2SiMe_3)$ (12%), $Cp^*W(^{16}O)(^{18}O)(CH_2SiMe_3)$ (35%), and $Cp^*W(^{18}O)_2(CH_2SiMe_3)$ (53%). Thus the majority of the oxo ligands were derived from O_2. The formation of the ^{16}O isotopologs is consistent with the suggested reaction mechanism, shown in Scheme 4.

Insertion of coordinated NO into one of the metal alkyls would yield a nitrosoalkane, which could dissociate and in turn react with the starting material via O-atom transfer. The independent observation that PhNO reacted with $Cp^*W(NO)(CH_2SiMe_3)_2$ to form $Cp^*W(O)_2(CH_2SiMe_3)$ in low yield supports the role of the nitrosoalkane as an alternative oxidant.

An unusual Mo(IV) dioxo complex was formed in the reaction of $(Cp^{TMS})_2Ti(CCSiMe_3)_2$ with $Mo(CO)_3(NCMe)_3$, followed by air oxidation. $\{(Cp^{TMS})_2Ti(CCSiMe_3)_2\}Mo(CO)_4$ is a likely intermediate; its reaction with O_2 yields the dioxo species $\{(Cp^{TMS})_2Ti(CCSiMe_3)_2\}Mo(O)_2$ [20].

Paramagnetic chromium alkyls in the +II and +III oxidation states have been reacted with O_2. For example, treatment of $Cp^*Cr(py)Me_2$ [21] or

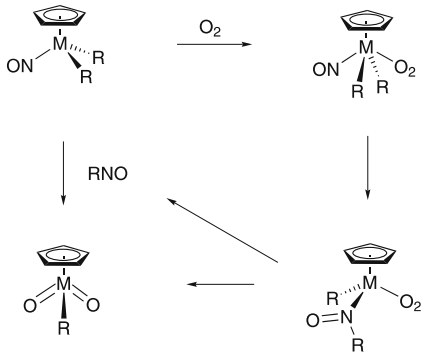

Scheme 4 Formation of high-valent oxo alkyls

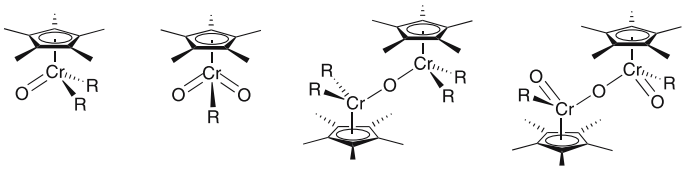

Scheme 5 Various chromium oxo alkyls

$[Cp^*Cr(\mu\text{-}Me)]_2$ [22] yielded a set of oxo alkyls ranging in oxidation state from +IV to +VI. Scheme 5 summarizes the structural types, most of which have been confirmed by X-ray crystallography.

In view of the high formal oxidation state of some of these molecules, their pronounced stability was quite surprising. Notably, these reactions do not produce alkoxide derivatives, i.e., an insertion of oxygen in the Cr – C bond was not observed. The mechanism of formation of the compounds shown in Scheme 4 probably involves the kinds of steps shown in Scheme 2. The direct reaction of $[Cp^*Cr(\mu\text{-}Me)]_2$ to yield $Cp^*Cr(O)_2Me$ may represent an unusual example of the 4-electron oxidative addition of O_2 to a single metal center. The formation of the same Cr(VI) alkyl from $Cp^*Cr(py)Me_2$ presumably follows the same pathway, but results in homolytic cleavage of a Cr – Me bond, so as to not exceed the highest possible oxidation state of chromium. Corroborating evidence comes from the transformations shown in Eqs. 7 and 8; the reaction of a metal oxo group with H_2O_2 frequently results in the formation of a metal peroxo moiety (here a Cr(V) peroxo alkyl). In this case, the peroxo dialkyl intermediate is not observed; however, it is reminiscent of the tantalum complexes $Cp^*{}_2Ta(\eta^2\text{-}O_2)R$ (Scheme 1). The weak Cr – C bond of the first row transition metal presumably confers little protection against further oxidation to Cr(VI) .

$$2Cp^*CrR_2 + O_2 \rightarrow 2Cp^*Cr(O)R_2 \tag{7}$$

$$Cp^*Cr(O)R_2 + H_2O_2 \rightarrow [Cp^*Cr(\eta^2 - O_2)R_2] \rightarrow Cp^*Cr(O)_2R \tag{8}$$

$(R = CH_2SiMe_3)$.

The alkyl complexes mentioned above are very electron rich, and thus their susceptibility to reaction with O_2 is not a great surprise, though the formation of stable organometallic oxidation products may be. Somewhat more unusual is the reaction of metal(III) halides with O_2. Relatively recent results in this area begin with the report by Morse et al. of the oxidative addition of O_2 to $[Cp^*CrBr(\mu - Br)]_2$, see Eq. 9 [23].

$$[Cp'CrBr(\mu - Br)]_2 + O_2 \rightarrow 2Cp'Cr(O)Br_2 \tag{9}$$

$(Cp' = Cp^*$ or Cp) .

The reaction proceeds within minutes in CH_2Cl_2, although coordinating solvents (e.g., THF, CH_3CN) inhibit the reaction rate. The authors also noted that

"concentrated solutions of $[Cp^*CrBr(\mu-Br)]_2$ (> 100 mM) are not noticeably O_2 sensitive". These observations are probably best explained by an obligatory dissociation of the dinuclear complex into coordinatively unsaturated Cp^*CrBr_2 fragments, which can bind O_2.

A very similar set of reactions producing the analogous vanadium compound $Cp^*V(O)Cl_2$ was published independently and contemporaneously by the groups of Bottomley [24] and Doherty [25], see Eq. 10.

$$2[Cp^*VCl_2]_3 + 3O_2 \rightarrow 6Cp^*V(O)Cl_2 \,. \tag{10}$$

Finally, we have reported the analogous syntheses of $Cp^*Cr(O)Cl_2$ and $CpCr(O)Cl_2$ via reaction of the corresponding cyclopentadienyl chromium(III) chlorides with O_2 (Eq. 11) [26]. While these reactions are slow (days at room temperature) they produce the oxo complexes in high yield.

$$[Cp'CrCl(\mu-Cl)]_2 + O_2 \rightarrow 2Cp'Cr(O)Cl_2 \tag{11}$$
$$(Cp' = Cp^*, Cp, \text{or } Cp^{TMS}) \,.$$

The facile activation of dioxygen by these simple organometallic complexes generates high-valent (V(V), Cr(V)) metal oxo complexes, which may undergo oxygen atom transfer reaction with organic substrates, and thus serve as catalysts for aerobic oxidations (Sect. 3.3).

2.3 Radical Chain Reactions

When the organometallic reactant has a d^0-configuration, the formation of a dioxygen adduct of significant stability or lifetime does not appear possible. Dioxygen complexes invariably feature some degree of charge transfer to O_2 (falling either into the superoxo or peroxo rubric), and a d^0-metal center cannot easily give up another electron. However, this does not preclude a reaction between O_2 and an electron-rich alkyl from taking place. Removal of an electron from a metal–carbon bonding MO weakens the metal alkyl bond and induces homolytic cleavage. Thus reactions of early metal alkyls in high oxidation states often involve radical processes.

Early examples of this kind of reactivity include reports about the oxygenation of alkylzirconium(IV) complexes of the type $Cp_2Zr(R)Cl$, yielding the corresponding alkoxides $Cp_2Zr(OR)Cl$, which can be hydrolyzed to the alcohols [27], and similar autoxidation reactions of Cp_2ZrR_2 [28]. A more recent case is the formation of a tantalum(V) alkoxide by the reaction shown in Eq. 12 [29].

$$(2,6\text{-}^i Pr_2ArO)_2TaMe_3 + xs\, O_2 \rightarrow [(2,6\text{-}^i Pr_2ArO)_2Ta(OMe)_2(\mu-OMe)]_2 \,. \tag{12}$$

A detailed mechanistic study of this type of reaction was carried out by Lubben and Wolczanski, who investigated the reactions of a series of alkoxy alkyls of group 4 (M = Ti, Zr, Hf) with O_2 [30]. Thus, exposure to O_2 of the methyl complexes, shown in Eqs. 13 and 14, rapidly generated methoxide derivatives.

$$(^t\mathrm{Bu_3CO})_2\mathrm{MMe_2} + \mathrm{O_2} \rightarrow (^t\mathrm{Bu_3CO})_2\mathrm{M(OMe)_2} \quad (13)$$

M = Ti, Zr, Hf

$$(^t\mathrm{Bu_3CO})\mathrm{TiMe_3} + x/2\mathrm{O_2} \rightarrow (^t\mathrm{Bu_3CO})\mathrm{TiMe_{3-}}_x(\mathrm{OMe})_x \quad (14)$$

$x = 1–3$.

The formation of methylperoxy intermediates—i.e., the product of a formal insertion of O_2 into the metal–methyl bond—was substantiated by the observation of epoxidation of allylic alkoxides (Scheme 6), in analogy to the proposed mechanism for the Sharpless epoxidation utilizing *tert*-butylhydroperoxide (TBHP). A similar oxygen atom transfer from a coordinated alkylperoxide to olefin was also postulated for the epoxidation of olefins with TBHP catalyzed by $Cp^*Mo(O)_2Cl$ [31]. The use of organomolybdenum oxides in olefin epoxidation catalysis (albeit not with O_2) has recently been reviewed [32].

A crossover experiment demonstrated scrambling of the methyl groups between metal atoms during the oxygenation, and various other observations indicated the occurrence of a radical chain process. The conclusion regarding the mechanism of this O_2 insertion was that it parallels the autoxidation of main group alkyls (e.g., BR_3, AlR_3, ZnR_2) and proceeds by an S_H2 homolytic substitution process [33]. As shown in Scheme 7, interaction with O_2 results in homolysis of a metal–carbon bond and provides the initiation step. The methyl radical is trapped by O_2 in a diffusion controlled reaction, and the resulting methylperoxy radical attacks another metal alkyl under displacement of its methyl group (the propagation step of the chain reaction). The methylperoxy ligand delivers an oxygen atom to another alkyl (or an alkene), and scrambling of alkoxide ligands between metal atoms ensures complete oxidation of all alkyl ligands.

An informative recent case study from magnesium chemistry highlights the parallels of the group 4 chemistry described above to the behavior of

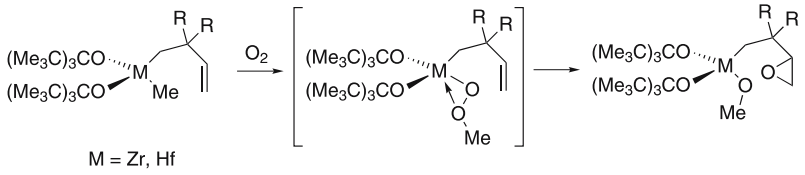

Scheme 6 Intramolecular oxygen transfer from methylperoxo ligand to an olefin

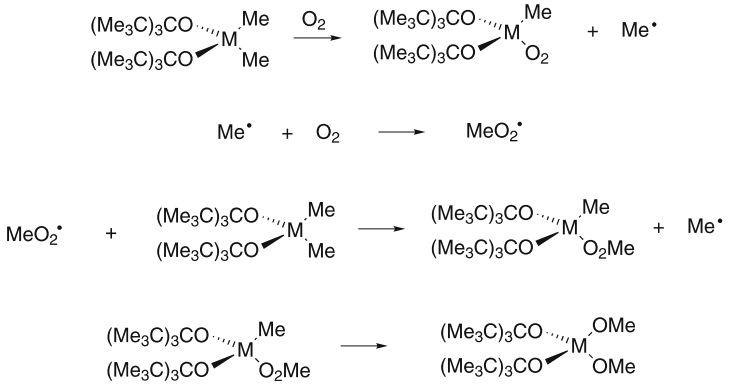

Scheme 7 Radical chain mechanism for the autoxidation of Zr(IV) alkyls

representative elements. The reaction of a β-diketiminate magnesium benzyl compound with O_2 led, for he first time, to the isolation and structural characterization of a alkylperoxy compound, which crystallized as a dimer with $\mu - \eta^2 : \eta^1$ benzylperoxo groups. The proposed mechanism for the overall transformation involves dioxygen insertion into the Mg – C bond followed by oxygen atom transfer to a further magnesium alkyl to ultimately form benzyloxy derivatives, see Scheme 8 [34]. On the basis of several lines of evidence, the mechanism of this O_2 insertion was assigned to be a radical chain process much like the one outlined in Scheme 7. In particular, the relative stability of the benzyl radical was held responsible for the rapid initiation step and thus the unprecedented isolation of the benzylperoxy intermediate.

Despite the radical character of these autoxidations, they may exhibit some selectivity. This can, for example, be seen in a recent report by Kim et al., which notes the selective transformation of a titanium(IV) diamido dimethyl complex into a mixed alkoxide alkyl (Eq. 15) and the complete lack of reactivity of the corresponding dibenzyl complex with O_2 [35]. Both of these observations are probably the result of steric protection. When the metal complex becomes too hindered to allow close interaction with O_2, the oxidation can no longer be initiated.

$$(CH_2)_n Si(NBu^t)_2 TiMe_2 + O_2 \rightarrow [(CH_2)_n Si(NBu^t)_2 TiMe(\mu - OMe)]_2 . \quad (15)$$

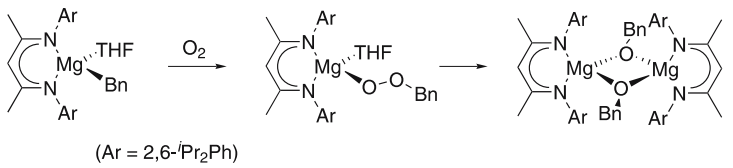

Scheme 8 Autoxidation of a magnesium alkyl

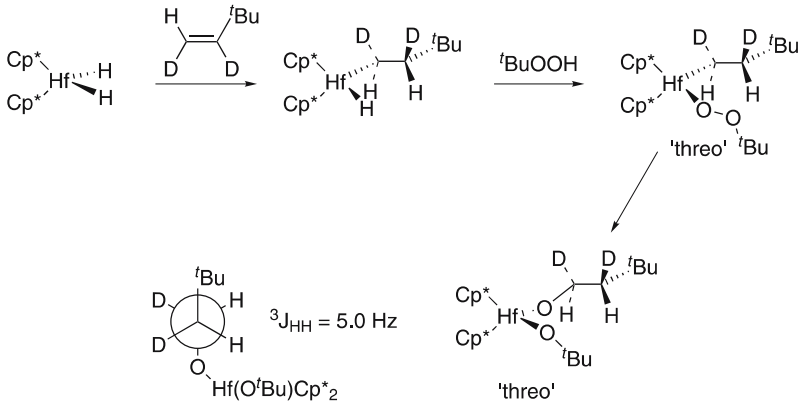

Scheme 9 Retention of configuration in oxygen transfer to an alkyl

Regarding the delivery of an oxygen atom from an alkylperoxy ligand to a neighboring alkyl group, there arises the question of stereochemistry. In the early work on zirconium alkyls, a mixture of 50% racemization and 50% retention of stereochemistry of the α-carbon was observed [36]; this was interpreted as the result of complete racemization in the formation of the alkylperoxide (by a radical chain mechanisms), coupled with retention of configuration in the O-atom transfer step. The latter step has been probed directly by the indirect synthesis of a hafnium alkyl alkylperoxide, and the monitoring of the stereochemical result of the oxygen transfer [37]. Scheme 9 shows the synthesis and stereochemical outcome of the compounds. These experiments confirm the suggestion that the insertion of the oxygen atom into the alkyl proceeds with retention of configuration at the migrating carbon center.

There would appear to be two distinct modes of reactivity of early transition metal alkyls with O_2. When the metal is not in its highest oxidation state, an O_2 complex of variable stability may form, and its subsequent reactivity may or may not involve the metal–carbon bond. The formation of remarkable stable oxo alkyls is an example of this pathway. In contrast, d^0-alkyls react with O_2 by a radical chain mechanism that invariable leads to formation of alkoxide complexes; labile alkylperoxo ligands are clearly implicated as intermediates in these reactions.

3 Reactions of Oxygenated Complexes

As outlined above, the initial reaction of early transition metal organometallics with O_2 may produce a variety of complexes containing oxygen atoms—in the form of superoxo (O_2^-), peroxo (O_2^{2-}), oxo (O^{2-}), or alkylperoxo (RO_2^-)

ligands. These functional groups may give rise to further transformations, such as insertion reactions or oxygen atom transfer. This section is dedicated to a review of these follow-up reactions.

3.1 Dioxygen Insertion

Leaving aside the autoxidations of d^0-alkyls, which only formally yield O_2 insertion products, there are a very few examples of reactions where migratory insertion of a coordinated O_2 into a metal alkyl bond seems indicated. Thus, heating of $Cp^*_2Ta(\eta^2\text{-}O_2)Me$ (Sect. 2.1) in solution in the absence of any base results in its transformation into $Cp^*_2Ta(O)OMe$ [1]. Lewis acids were noted to catalyze the reaction. While there is no direct evidence for the formation of an alkylperoxo intermediate, the final product could easily be rationalized as resulting from an α-alkoxide elimination (Scheme 10).

The parallel to the mechanism of the reaction of $Cp^*_2Hf(OOCMe_3)(R)$ to $Cp^*_2Hf(OCMe_3)(OR)$ was noted, with CMe_3^+ serving as the electrophile, implying the formation of the peroxyalkyl, aided by coordination of an electrophile at the exo-oxygen atom during the migration. It is worth noting that in none of the cases described in this section was the peroxyalkyl stable enough to be isolated or even spectroscopically observed. Apparently, such compounds of the early transition metals are stable only in the d^0-configuration—see e.g., $Cp^*_2Hf(OOCMe_3)(R)$ above, which was prepared not by a reaction with O_2, but rather according to Eq. 16 [38].

$$Cp^*_2Hf(R)(H) + HOOCMe_3 \rightarrow Cp^*_2Hf(R)(OOCMe_3)\,. \qquad (16)$$

Another probable candidate for an O_2 insertion is the reaction of $Cp^*_2W=O$ with O_2. The product of this reaction was the structurally characterized $Cp^*W(O)_2(OC_5Me_5)$ [39, 40]. In this case, neither an O_2-complex nor the peroxyalkyl intermediate was detected, leading the authors to equivocate on the exact mode of product formation (Scheme 11). However, the d^2-configuration of the starting material makes the initial formation of an O_2 adduct reasonably likely, even though this might require an $\eta^5 \rightarrow \eta^1$ shift of one Cp^*

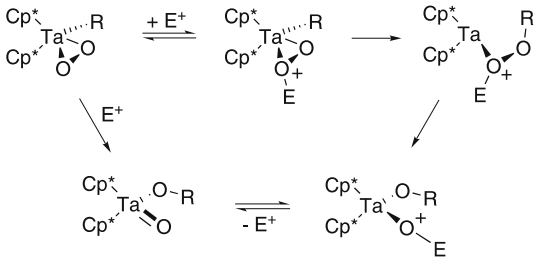

Scheme 10 Electrophile assisted O_2 insertion into tantalum alkyl

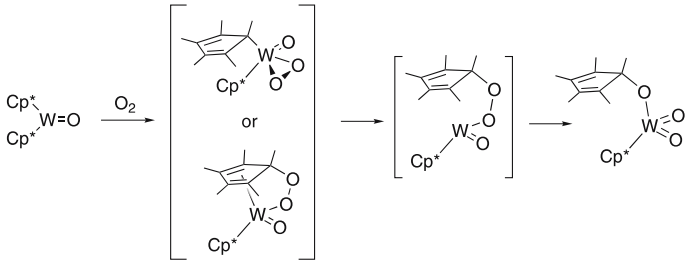

Scheme 11 O_2 insertion into a tungsten cyclopentadienyl

ligand so as to not exceed an 18-electron configuration. This adduct could then undergo an insertion of O_2 into the metal–carbon bond, followed by an α-alkoxide elimination to produce the final product.

The related alkyl complexes $Cp^*W(O)(O_2)R$ (R = Me, CH_2SiMe_3), which have been prepared according to Eq. 17 [10], provide precedent for the existence of the postulated dioxygen complex. However, neither of these two alkyls undergo the subsequent O_2 insertion, leaving in some ambiguity the mechanism of the transformation shown in Scheme 10.

$$Cp^*W(O)_2R + H_2O_2 \rightarrow Cp^*W(O)(\eta^2\text{–}O_2)R\,. \tag{17}$$

Finally, a well-characterized O_2-insertion transforms $Tp^{tBu,Me}Cr(O_2)Ph$ into the paramagnetic oxo alkoxide $Tp^{tBu,Me}Cr(O)OPh$, see Scheme 12 [4]. This reaction proceeds below room temperature, and the starting material has only been characterized by in-situ IR spectroscopy. However, analogous O_2 complexes were isolated and characterized by X-ray crystallography, so there can be little doubt about its assignment as a side-on bonded Cr(III) superoxo complex.

In order to rule out a radical chain process akin to those described in Sect. 2.3, a crossover experiment was carried out. The result, shown in Eq. 18, establishes the intramolecular nature of the transformation. While this does not strictly rule out homolytic events along the reaction pathway (Cr – Ph or O – O bond cleavage), any resulting radicals must be very short-lived and

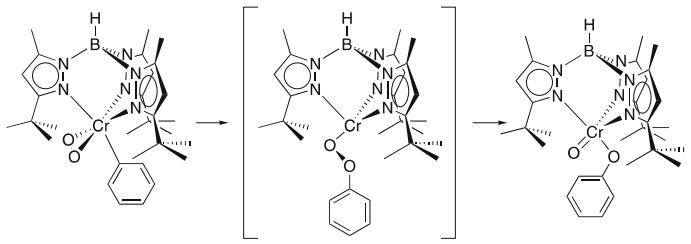

Scheme 12 Intramolecular O_2 insertion into chromium phenyl bond yield oxo alkoxide

cannot escape the solvent cage in which they are generated.

$$Tp^{tBu,Me}Cr(O_2)C_6D_5 + Tp^{tBu}Cr(O_2)C_6H_5 \rightarrow Tp^{tBu,Me}Cr(O)OC_6D_5 + Tp^{tBu}Cr(O)OC_6H_5 \,. \quad (18)$$

Another possible mechanism for this transformation would be oxidative addition of the O_2 to chromium, yielding $Tp^{tBu,Me}Cr(O)_2Ph$, followed by an insertion of an oxo ligand. However, as we shall show in the next section, such insertions are exceedingly rare. Accordingly, $Cp^*Cr(O)_2Me$ (Scheme 5)—a close analog of the hypothetical $Tp^{tBu,Me}Cr(O)_2Ph$—shows no tendency to insert an oxygen ligand into the methyl group.

The above examples indicate the feasibility of the insertion of coordinated O_2 into early transition metal alkyls. The resulting alkylperoxides apparently suffer rapid α-elimination to oxo-alkoxides. In all likelihood, this reflects the strong stabilization of the higher oxidation states of these oxophilic metals by oxygen π-donors. To actually isolate the insertion product requires a late transition metal or a d^0-configuration (the α-elimination is formally a 2-electron oxidation). To wit, the insertion of coordinated O_2 into a rhodium alkyl gives rise to an isolable methylperoxo intermediate [41]. Peroxyalkyls of early transition metal in their highest oxidation states have been isolated as well. Their chemistry is dominated by oxygen atom transfer and or homolytic cleavage of the O – O bond [42].

3.2 Oxygen Insertion

The insertion of a metal bound oxo group into a metal carbon σ-bond (Eq. 19), e.g., of an alkyl or aryl, has great appeal as an elementary step in the oxygenation of organic molecules.

$$L_nM(=O)R \rightarrow L_nM-OR \,. \quad (19)$$

However, the number of well-characterized examples of this transformation is inversely proportional to its desirability. Specifically, there is currently only one system that demonstrably follows this reaction pathway. The metal involved is rhenium and thus not really within the purview of this chapter. However, given the importance of this reaction, a quick summary is provided here.

Following earlier reports of a photochemically driven phenyl-to-oxo migration [43, 44], Brown and Mayer published a study of a related system that exhibits a thermal insertion of an oxo group into a rhenium phenyl bond [45]. The reaction is shown in Eq. 19; it exhibits clean first order kinetics, with activation parameters of $\Delta H^{\ddagger} = 14.8(7)$ kcal/mol and $\Delta S^{\ddagger} = -20.5(25)$ eu (half

life of 4 minutes at 25 °C!).

$$[TpRe(O)_2Ph]OTf + L \rightarrow [TpRe(O)(OPh)L]OTf \quad (L = Py, Me_2SO) . \tag{20}$$

The key to this unique chemistry appears to be the high electrophilicity of the oxo ligands in the cationic Re(VII) precursor. While there are many examples of oxo alkyls of the early transition metals (Sect. 2.2), none of them show any indication of O-insertion chemistry. For example, $Cp^*Cr(O)_2Me$ might be expected to feature fairly electrophilic oxo ligands, and yet it does not produce any methoxide derivatives. In summary, the insertion of oxo ligands into metal alkyls must be considered a highly unusual transformation associated with a large kinetic barrier. It becomes viable only under very special circumstances. The discovery of further examples of this fundamental transformation would be a significant step forward in organometallic oxidation chemistry.

3.3 Oxygen Atom Transfer

Intermolecular oxygen atom transfer from a metal complex to an organic substrate is an archetypical reaction step in oxidation catalysis. As the transformation of O_2 into metal oxo groups by oxidative addition is a well-precedented process (Sect. 2.2), its combination with transfer of the oxygen atom to an oxidizable substrate ("S") constitutes a catalytic cycle for aerobic oxidations (Eq. 21). Examples of such cycles exist in organometallic chemistry, by virtue of oxo complexes with carbon-based ancillary ligands.

$$2L_nM + O_2 + 2S \rightarrow 2L_nM{=}O + 2S \rightarrow 2L_nM + 2SO . \tag{21}$$

Transfer of metal bound oxo ligands will be facilitated by high electrophilicity of the complex, and by weak metal–oxo bonds. For these reasons, electron-withdrawing ligands and first-row transition metals in high oxidation states would seem to be the obvious place to look for oxygen atom transfer chemistry. It is no accident that hexavalent chromium has a long history of use as a stoichiometric and catalytic oxidant [46]; hence electron deficient organometallic chromium oxo complexes—related to chromyl chloride [47]—should be a good place to look for oxygen atom transfer, especially when they can be formed by reaction of a low valent precursor with O_2.

$Cp^*Cr(O)Br_2$ was an early example, but its potential as an oxidant was not explored extensively [14]. The complex was reported to catalyze the aerobic oxidation of PPh_3, but it does not react with Et_2S. According to a footnote, less electron rich $CpCr(O)Br_2$ did "oxygenate Et_2S", but no further detail was given.

We have investigated the analogous chlorides and found them to be more reactive; there are issues that render them inefficient as catalysts, but the basic concept of Eq. 21 is realized. Cyclopentadienyl chromium(III) chlorides react with O_2 to form the corresponding Cr(V) oxo derivatives $Cp'Cr(O)Cl_2$ ($Cp' = Cp^*$, Cp, Cp^{TMS}). $Cp^*Cr(O)Cl_2$ transfers oxygen to a variety of substrates. Thus, it oxidizes PPh_3 and $AsPh_3$, but not MeSPh, or MeS(O)Ph. The oxidation of PPh_3 to $OPPh_3$ is catalytic, whereas the reaction with $AsPh_3$ is stoichiometric, generating the arsine oxide complex $Cp^*Cr(OAsPh_3)Cl_2$. The latter is apparently so stable ($OAsPh_3$ does not dissociate) that it cannot be reoxidized by O_2. Product inhibition is one of the significant problems of this system, as many of the oxidation products form stable pseudooctahedral chromium(III) complexes of the oxidized substrates. Other molecules that react with $Cp^*Cr(O)Cl_2$ are 1,4-cyclohexadiene ($\rightarrow$ benzene), 9,10-dihydroanthracene ($\rightarrow$ anthracene) and 1,2-diphenylhydrazine ($\rightarrow$ azobenzene). The dehydrogenation of 1,4-cyclohexadiene is catalytic and produces H_2O as byproduct. After several turnovers, the resting state of the catalyst becomes the water adduct $Cp^*Cr(OH_2)Cl_2$; this has been isolated and structurally characterized [48]. $Cp^*Cr(O)Cl_2$ does not react with ordinary olefins.

One of the interesting features of these oxygen atom transfer reactions is that they comprise an example of "two state reactivity" [49–52], i.e., the reactants and products have different spin states. $Cp'Cr(O)Cl_2$ contains a d^1-ion and has a doublet ground state ($S = 3/2$), whereas the products feature Cr(III) (d^3, $S = 3/2$) in a quartet ground state. Somewhere along the reaction coordinate the reaction must cross over from the doublet potential energy surface (PES) to the quartet PES. There has been much interest in the effects of spin state on chemical reactivity [51, 53–55], and this has motivated us to perform calculations on this system. Figure 1 shows the two intersecting reaction paths on the doublet and quartet PES, respectively, for the epoxidation of ethylene by $Cp'Cr(O)Cl_2$. It can be seen that the reaction on the doublet PES proceeds through an intermediate, in which one oxygen—carbon bond has been formed. However, instead of continuing on this surface, the reaction reaches a "minimum energy crossing point" (MECP) close to the intermediate, which obviates the traversing of the second (higher) barrier on the doublet surface and leads smoothly to the quartet product.

In the course of the above-mentioned calculations, it became clear that the activation energy for the epoxidation reaction was predicted to be significantly lower for the unsubstituted complex $CpCr(O)Cl_2$. Indeed, $CpCr(O)Cl_2$ and its more soluble analogue $Cp^{TMS}Cr(O)Cl_2$ reacted with various olefins to yield products of oxygen atom transfer (Scheme 13) [56]. Among the olefins investigated, only norbornene and β-methylstyrene produced the corresponding epoxides, along with other oxygenates, whereas styrene and α-methylstyrene gave oxygenated products that can—in part—be rationalized as products of subsequent ring opening of the epoxide (Scheme 12). In support of this hypothesis, we have shown that the reaction of norbornene

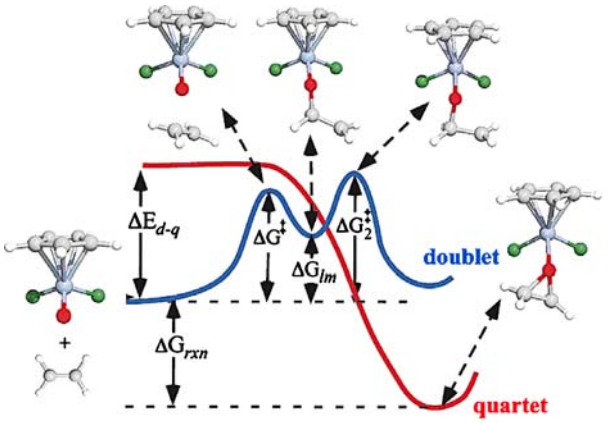

	ΔG_{rxn}	$\Delta G^{‡}$	$\Delta G^{‡}_{2}$	ΔG_{im}	ΔE_{d-q}
$CpCr(O)Cl_2$	-16.3	+20.0	+24.6	+11.2	+34.0
$Cp^*Cr(O)Cl_2$	-10.7	+22.3	-----	+13.6	+36.2

Fig. 1 Doublet and quartet potential energy surfaces for the epoxidation of ethylene with $Cp'Cr(O)Cl_2$

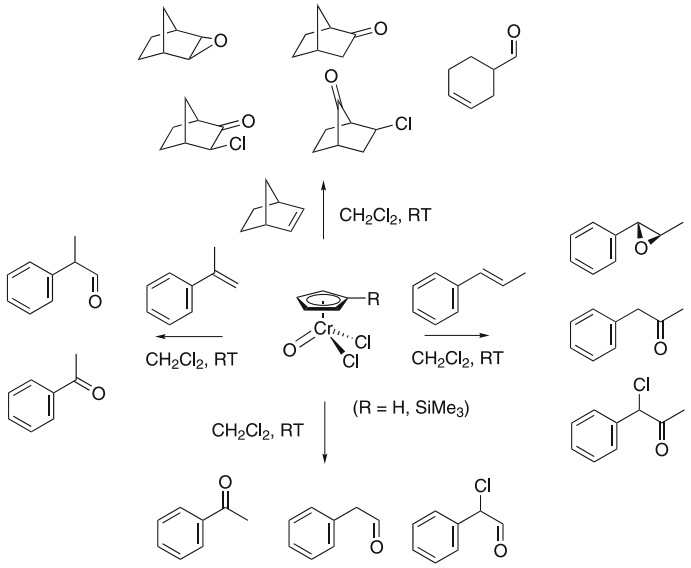

Scheme 13 Oxygen atom transfer from chromium to olefins yields variety of products

oxide with $[Cp'Cr(\mu\text{-}Cl)(Cl)]_2$ produces all the same byproducts that are formed in the reaction of $Cp'Cr(O)Cl_2$ with norbornene.

There are some surprises, such as the occurrence of chlorinated products. The chlorine derives form the metal complex and not from the chlo-

rinated solvent, as the same products formed when the reactions were run in nitromethane. Their formation is consistent with a radical intermediate (Fig. 1) [57, 58], which can abstract a chlorine atom from the metal in an intramolecular fashion. Another curious observation is the formation of benzaldehyde in the oxidation of styrene; one wonders how the cleavage of the C = C double bond occurs.

These reactions are not catalytic, and the oxygenation of the Cr(III) precursors is very slow, presumably reflecting the lesser oxygen affinity of the less electron rich complexes. Nevertheless, they are proof of the concept that an organometallic complex can mediate the oxidation of organic substrates by O_2. The product distributions also point out some of the problems that must be addressed to make this chemistry synthetically useful. They include—inter alia—the ring opening of the primary epoxide products, the incorporation of coligands (here chloride), and the slow reaction rates. Furthermore, there is obviously a tradeoff between the rate of the reaction of the reduced form of the catalyst with O_2 and the reactivity of the oxidized form with organic substrates. However, appropriate ligand design may solve all of these problems. It is reasonable to suggest that a catalytic aerobic epoxidation of substituted olefins is possible.

4 Conclusions

Organometallic derivatives of the early transition metal react with O_2 in a variety of ways. While the formation of stable O_2 adducts is possible for these metals, the number of characterized examples of such complexes is small. The high oxophilicity of the electropositive metals, and the availability of empty d-orbital for L $\rightarrow$ M π-donation favor the formation of oxo complexes via cleavage of the O – O bond, most often in bimolecular reactions. However, under the right circumstances, high-valent metal oxo complexes can transfer oxygen atoms to organic substrates, thus offering a possible pathway for catalytic aerobic oxidations.

Early metal alkyls in the highest formal oxidation states (i.e., with d^0-configurations) react with O_2 by a radical chain mechanism. The alkylperoxo intermediates thus formed are highly reactive; they can transfer oxygen to other alkyl groups (forming alkoxides), or to oxidizable organic functional groups (e.g., olefins). In the absence of O-acceptors they suffer facile O – O bond homolysis.

Early transition metals have a high affinity for oxygen. This is especially true for electron-rich organometallic compounds. Accordingly, the final products of reactions with O_2 will often feature metal oxygen bonds. In this neighborhood of the periodic table, complete transfer of oxygen to an organic

substrate is the exception rather than the rule. Knowing this is a valuable lesson to heed when looking for catalytic oxidations.

Acknowledgements I thank the graduate students, post-docs, and collaborators who have carried out some of the work described above; their names can be found in the references. Our research in organometallic chemistry has been funded by NSF (CHE-0132017), and our work on O_2-activation is supported by DOE (DE-FG02-92ER14273).

References

1. Punniyamurthy T, Velusamy S, Iqbal J (2005) Chem Rev 105:2329
2. Martell AE, Sawyer DT (1988) Oxygen Complexes and Oxygen Activation by Transition Metals. Plenum Press, New York, p 1–341
3. Ortiz de Montellano PR (2004) Cytochrome P450: structure mechanism, and biochemistry. Kluwer Academic/Plenum, New York
4. Shriver DF, Drezdzon MA (1986) The Manipulation of Air-Sensitive Compounds. Wiley, New York
5. Van Asselt A, Trimmer MS, Henling LM, Bercaw JE (1988) J Am Chem Soc 110:8254
6. Thiyagarajan B, Kerr ME, Bruno JW (1995) Inorg Chem 34:3444
7. Salapala J, Roue J, Guerchais JE (1980) J Mol Catal 7:141
8. Hess A, Hörz MR, Liable-Sands LM, Lindner DC, Rheingold AL, Theopold KH (1999) Angew Chem Int Ed 38:166
9. Dickmann MH, Pope MT (1994) Chem Rev 94:569
10. Cramer CJ, Tolman WB, Theopold KH, Rheingold AL (2003) Proc Natl Acad Sci USA 100:3635
11. Qin K, Incarvito CD, Rheingold AL, Theopold KH (2002) Angew Chem Int Ed 41:2333
12. Qin K (2003) Dioxygen Chemistry of Hydrotris(pyrazolyl)borate Chromium(II) Complexes. PhD Thesis, University of Delaware
13. Trofimenko S (1999) Scorpionates. Imperial College Press, London
14. Kosugi M, Hikichi S, Akita M, Moro-oka Y (1999) J Chem Soc, Dalton Trans 1369
15. Nugent WA, Mayer JM (1988) Metal-Ligand Multiple Bonds. Wiley, New York
16. Luo L, Lanza G, Fragala IL, Stern CL, Marks TJ (1998) J Am Chem Soc 120:3111
17. Bottomley F, Sutin L (1988) Adv Organomet Chem 28:339
18. Legzdins P, Phillips EC, Sanchez L (1989) Organometallics 8:940
19. Legzdins P, Phillips EC, Rettig SJ, Sanchez L, Trotter J, Yee VC (1988) Organometallics 7:1877
20. Mansilla N, Rheinwald G, Lang H (2000) J Organomet Chem 602:72
21. Noh SK, Heintz RA, Haggerty BS, Rheingold AL, Theopold KH (1992) J Am Chem Soc 114:1892
22. Heintz RA, Ostrander RL, Rheingold AL, Theopold KH (1994) J Am Chem Soc 116:11387
23. Morse DB, Rauchfuss TB, Wilson SR (1988) J Am Chem Soc 110:8234
24. Abernethy CD, Bottomley F, Decken A, Thompson RC (1997) Organometallics 16:1865
25. Aistars A, Newton C, Ruebenstahl T, Doherty NM (1997) Organometallics 16:1994
26. Hess JS, Leelasubcharoen S, Rheingold AL, Doren DJ, Theopold KH (2002) J Am Chem Soc 124:2454
27. Blackburn TP, Labinger JA, Schwartz J (1975) Tetrahedron Lett 16:3041
28. Brindley PB, Scotton MJ (1981) J Chem Soc Perkin Trans 2:419

29. Wang R, Folting K, Huffman JC, Chamberlain LR, Rothwell IP (1986) Inorg Chim Act 120:81
30. Lubben TV, Wolczanski PT (1987) J Am Chem Soc 109:424
31. Trost MK, Bergman RG (1991) Organometallics 10:1172
32. Kuhn FE, Santos AM, Herrmann WA (2005) Dalton Trans 2483
33. Davies AG, Roberts BP (1973) In: Kochi JK (ed) Free Radicals (Reactive Intermediates in Organic Chemistry), vol I. Wiley, New York, p 547
34. Bailey PL, Coxall RA, Dick CM, Fabre S, Henderson LC, Herber C, Liddle ST, Lorono-Gonzalez D, Parkin A, Parsons S (2003) Chem Eur J 9:4820
35. Kim SJ, Choi DW, Lee YJ, Chae BH, Ko JJ, Kang SO (2004) Organometallics 23:559
36. Labinger JA, Hart DW, Seibert WE, Schwartz J (1975) J Am Chem Soc 97:3851
37. Coughlin EB, Bercaw JE (1992) Organometallics 11:465
38. Van Asselt A, Santarsiero BD, Bercaw JE (1986) J Am Chem Soc 108:8291
39. Parkin G, Bercaw JE (1989) J Am Chem Soc 111:391
40. Parkin G, Bercaw JE (1988) Polyhedron 7:2053
41. Ahijado M, Braun T, Noveski D, Kocher N, Neumann B, Stalke D, Stammler HG (2005) Angew Chem Int Ed 44:6947
42. DiPasquale AG, Kaminsky W, Mayer JM (2002) J Am Chem Soc 124:14534
43. Brown SN, Mayer JM (1994) J Am Chem Soc 116:2219
44. Brown SN, Mayer JM (1995) Organometallics 14:2951
45. Brown SN, Mayer JM (1996) J Am Chem Soc 118:12119
46. Muzart J (1992) Chem Rev 92:113
47. Limberg C (2000) Chem Eur J 6:2083
48. Leelasubcharoen S (2001) Pentamethylcyclopentadienyl Chromium Complexes in Ethylene Polymerization and Oxidation Reactions. PhD Thesis, University of Delaware
49. Schroder D, Shaik S, Schwarz H (2000) Acc Chem Res 33:139
50. Plattner DA (1999) Angew Chem Int Ed 38:82
51. Harvey JN, Poli R, Smith KM (2003) Coord Chem Rev 238:347
52. Li C, Wu W, Kumar D, Shaik S (2006) J Am Chem Soc 128:394
53. Poli R (2004) J Organomet Chem 689:4291
54. Poli R, Harvey JN (2003) Chem Soc Rev 32:1
55. Landis CR, Morales CM, Stahl SS (2004) J Am Chem Soc 126:16302
56. Salisbury BA (2004) Synthesis and Reactivity of Chromium(III) Pyrrolatodiimine Complexes, Chromium(III) Constrained Geometry Complexes and Chromium(V) Oxo Complexes. PhD Thesis, University of Delaware
57. Samsel EG, Srinivasan K, Kochi JK (1985) J Am Chem Soc 107:7606
58. Limberg C (2003) Angew Chem Int Ed 42:5932

Top Organomet Chem (2007) 22: 39–77
DOI 10.1007/3418_029

Published online: 10 June 2006

Organorhenium and Organomolybdenum Oxides as Heterogenised Catalysts

Christelle Freund[1] · Wolfgang Herrmann[1] · Fritz E. Kühn[1,2] (✉)

[1]Lehrstuhl für Anorganische Chemie der Technischen Universität München, Lichtenbergstrasse 4, 85747 Garching, Germany
fritz.kuehn@ch.tum.de

[2]Departamento de Química, Instituto Tecnológico e Nuclear (ITN), Estrada National 10, 2686-953 Sacavém, Portugal

Abstract A variety of organomolybdenum and organorhenium complexes, most prominently methyltrioxorhenium(VII) (MTO), are applicable as efficient and selective oxidising agents in the presence of organic hydroperoxides (molybdenum complexes) or hydrogen peroxide (rhenium complexes). Besides strictly homogeneous oxidation catalysis, there is increasing interest in immobilizing homogeneous catalysts, both on carrier materials and in ionic liquids. Several methods that differ mainly in the anchoring mode and the nature of the supporting material have been described, and the resulting materials were applied to oxidation catalysis. Chiral oxidation catalysis with the compounds mentioned in the title is still in its infancy, but initial results point towards a promising future. The supported catalysts combine properties of homogeneous catalysts (reactivity,

control and selectivity) and heterogeneous catalysts (enhanced stability and reusability). Homogeneous catalysts have a clearly defined composition, and mechanistic examinations are usually less problematic than with bulk (heterogeneous) catalysts, where the active sites are less clearly defined. It is also more straightforward to modify homogeneous catalysts by fine-tuning their ligand environments.

Keywords Organomolybdenum complexes · Organorhenium complexes · Oxidation catalysis · Heterogenisation

Abbreviations

acac	acetylacetonate
bpy	2,2′-bipyridyl
Cp	cyclopentadiene
dppa	bis(diphenylphosphino)amine
Et	ethyl
EXAFS	extended X-ray absorption fine structure
IR	infrared
MCM	mobile crystalline material
Me	methyl
MTO	methyltrioxorhenium
NMR	nuclear magnetic resonance
PBI	polybenzimidazole
PEO	polyethylene oxide
Ph	phenyl
PPO	polypropylene oxide
PS	polystyrene
PSHPAMP	polystyrene–divinylbenzene resin carrying an *N*-(2-hydroxypropyl)-2-aminomethylpyridine ligand
PVP	poly(4-vinylpyridine)
PVPN	poly(4-vinylpyridine-*N*-oxide)
RT	room temperature
RTIL	room temperature ionic liquid
TBHP	*tert*-butyl hydroperoxide
UHP	urea hydroperoxide

1 Introduction

The heterogenisation of homogeneous transition metal catalysts has received considerable attention in recent years, since such heterogenised homogeneous catalysts (surface organometallic catalysts) may combine the most advantageous properties of both homogeneous and heterogeneous systems: easier product/catalyst separation and high activity and selectivity. Many attempts have been made to enhance the activities of heterogenised complexes, which are usually lower than those of homogeneous systems due to low loadings and problems concerning the accessibility of catalytic sites. The latter

point may, however, be an advantage, as the selectivity observed is often better when using supported catalysts rather than homogeneous catalysts. Since (sometimes severe) leaching occurs in some cases, some of the activity in fact results from a homogeneous catalyst. It is therefore important to check the true nature of the process. In particular, recyclability is important for industrial applications but is often not easy to obtain. This contribution deals with the particular case of the heterogenisation of organorhenium(VII) and organomolybdenum(VI) complexes, which are very important catalysts for many reactions in the homogeneous phase.

2
Heterogenisation of Molybdenum(VI) Complexes

Molybdenum(VI) complexes are versatile catalysts for the oxidation of organic substrates [1–8]. Since the late 1960s they have been used in the industrial epoxidation of propylene with *tert*-butyl hydroperoxide (TBHP) (HALCON [9, 10] and ARCO [11]). Heterogenisation of molybdenum catalysts on inorganic supporting materials, especially mesoporous sieves [12–14], is a very active research field. Different techniques of immobilisation have been developed, ranging from direct grafting [15–17] to tethering via a functionalised spacer ligand introduced either on the complex [16, 18–21] or on the support [15, 16, 19, 22–27]. Other supports are being developed, like hybrid materials [28, 29], polymers [30–34] or ionic liquids [35, 36].

2.1
Inorganic Supports

Among the various supporting materials studied, the mesoporous silicates designated by Mobil scientists as MCM-41 and MCM-48 [12] have very high surface areas (ca. 1000 m^2g^{-1}), high pore volumes (ca. 1 cm^3g^{-1}), very narrow pore size distributions, a large number of surface silanol groups, high chemical and thermal stabilities, and are promising candidates for use as catalysts and catalyst supports. MCM-41 and MCM-48 are members of the M41S family of ordered mesoporous siliceous materials formed by surfactant templating methods [12, 13]. They have properties intermediate between those of amorphous refractory oxides and microporous crystalline molecular sieves. The structure of MCM-41 can be described as a hexagonal arrangement of cylindrical pores embedded in a matrix of amorphous silica. The inner surface is covered with nucleophilic silanol groups. MCM-48 possesses a three-dimensional pore structure, with a silica interface that can be modelled by a minimal surface of the gyroid type [14]. MCM-48, therefore, has some advantages over MCM-41 as a catalyst support material.

2.1.1
Immobilisation Techniques

The two main immobilisation techniques on a mesoporous material are direct grafting and indirect grafting (tethering), as shown in Scheme 1. In the former case, the complex interacts directly with the matrix. In the latter case, the complex is tethered to the supporting material via a spacer ligand, which is either introduced first on the support (as shown on the upper part of Scheme 1) or integrated into the complex before being anchored onto the support (lower part of Scheme 1).

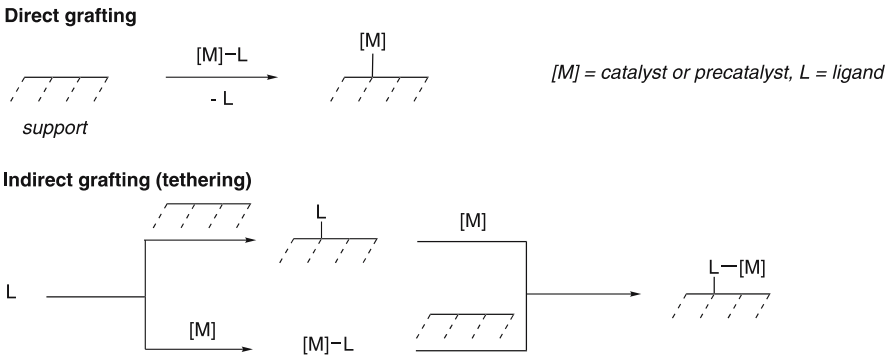

Scheme 1 Schematic drawing of direct and indirect grafting

Modified mesoporous materials are usually characterised by various methods, such as elemental analysis (EA). This often involves studying the loading of the metal and performing powder X-ray diffraction (XRD), N_2 adsorption, magic angle spinning (MAS) NMR spectroscopy (^{13}C, ^{29}Si), IR spectroscopy and in some cases EXAFS spectroscopy.

The catalytic behaviour of the resulting immobilised complex is (for the cases we discuss in this work, anyway) usually evaluated in terms of activity, selectivity and recyclability by olefin epoxidation. The extent of leaching is also addressed.

2.1.2
Direct Grafting

Exchanging a ligand from the complex with a silanol group from a zeolite leads to direct bonding between the metal and support. Dioxomolybdenum complexes $MoO_2X_2(THF)_2$ (X = Cl, Br) can thus be directly grafted through the reaction of the halogen ligand with a hydroxyl group from the mesoporous sieves MCM-41 and MCM-48 (with concomitant HX elimination) by solvent impregnation [15] (Scheme 2).

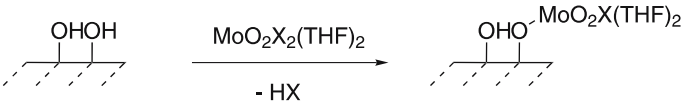

Scheme 2 Direct grafting of dioxomolybdenum complexes $MoO_2X_2(THF)_2$ onto MCM-41 and MCM-48

Loadings of 0.5–1.0 wt % molybdenum can be achieved and they allow an efficient catalysis of cyclooctene epoxidation with TBHP. For example, after 2 h, 31% conversion with 100% selectivity to the epoxide is observed with MCM-41-$MoO_2Cl(THF)_2$ (entry 1, Table 1). The same reaction with MCM-41-$MoO_2Br(THF)_2$ is slower and less selective (only 17% conversion with 56% selectivity after 2 h, entry 2, Table 1). This difference in activity between dichlorodioxomolybdenum complexes and their bromine analogues has already been noted for the homogeneous catalytic epoxidation of cyclooctene with complexes of the type $MoO_2X_2L_n$ (L = mono- and bidentate nitrogen and oxygen ligands, X = Cl, Br) [37].

Recently, it has been shown that compounds like $Cp'Mo(CO)_3Cl$ (Cp′ = Cp or ring-substituted derivatives) can be used as olefin epoxidation catalyst precursors. They are oxidised in situ to molybdenum(VI) catalysts with the general formulae $Cp'MoO_2Cl$ and $Cp'MoO(O_2)Cl$. An advantage of these catalysts over the direct application of the more sensitive molybdenum(VI) species $Cp'MoO_2Cl$ is that the more stable carbonyl complex can be stored easily for long periods of time. Furthermore, these complexes significantly surpass most other molybdenum (VI) dioxo complexes in their catalytic activity. Therefore, immobilisation of such a precatalyst was of great in-

Table 1 Cyclooctene epoxidation with TBHP/MCM-supported $MoO_2X_2(THF)_2$

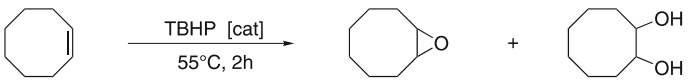

Entry	Support	Precursor	Conversion %	Epoxide selectivity %	TOF h^{-1}	Refs.
1	MCM-41	$MoO_2Cl_2(THF)_2$	31	100	130	[15]
2	MCM-41	$MoO_2Br_2(THF)_2$	17	56	60	[15]
3	MCM-48	$MoO_2Cl_2(THF)_2$	[a]	99	80	[15]
4	MCM-48	$MoO_2Br_2(THF)_2$	[a]	52	50	[15]

Reaction conditions: TBHP (5.5 M in decane), Mo loading = 0.5–1.0 wt %, Mo/TBHP/cyclooctene = 1/1200/800 or 1/600/400. TOFs calculated after 2 h of reaction.

[a] Similar results to the corresponding MCM-41 supported catalysts were obtained

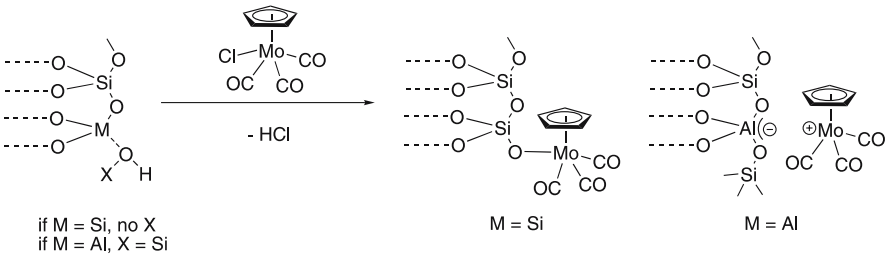

Scheme 3 Direct grafting of $CpMo(CO)_3Cl$ onto zeolites containing alumina (zeolite-β, zeolite-Y, AM-41, AM-48) and zeolites not containing alumina (SM-41, SM-48)

terest. The complex $CpMo(CO)_3Cl$ can be grafted directly onto protonated zeolite-Y [16], zeolite-β [16], MCM-41 [17], MCM-48 [17] or SBA-15 [38] through the reaction of the chloro ligand with the hydroxyl groups of the mesoporous sieves without significant loss of order in the carrier materials (Scheme 3).

Higher molybdenum loadings are observed when greater amounts of aluminium are present in the material (see Table 2, zeolite-Y versus zeolite-β, AM-41(48) versus SM-41(48)). The presence of aluminium enhances the ionic character of the H–OSi bond, which in turn favours a higher molybdenum loading. The grafted samples are active and highly selective epoxidation catalysts. TOFs are comparable ($370\,h^{-1}$ for zeolite-Y-[Mo] and $300\,h^{-1}$ for zeolite-β-[Mo], entries 2 and 3, respectively, Table 2) with the respective homogeneous catalyst $CpMo(CO)_3Cl$ [39] (entry 1, Table 2). In general it can be said that the higher the amount of aluminium, the better the catalytic activity. This again can be ascribed to the greater amount of aluminium in the framework, enhancing the Lewis acidity of the molybdenum in this system and the activation of TBHP by the aluminium sites.

Control experiments show that, in all cases, activity is not due significantly to catalyst leaching. During the course of the reaction the velocity slows with all of the grafted samples. This reduction in rate can be assigned to the interaction of the catalyst with the by-product *tert*-butanol. The zeolite-Y and zeolite-β supported catalysts show TOFs that are lower (ca. $300–400\,h^{-1}$) than the respective homogeneous catalyst $CpMo(CO)_3Cl$ ($1300\,h^{-1}$), whereas immobilisation reactions on MCM supports lead to very high TOFs. The catalysts can be reused several times, albeit with a decrease in conversion and selectivity (entries 2, 3 and 8 in Table 2). According to the authors, the decreased activity may be due, at least partially, to an increased amount of chemisorbed organic molecules on the surfaces of the materials.

Table 2 Catalytic cyclooctene epoxidation with TBHP/zeolite-supported $MoCp(CO)_3Cl$

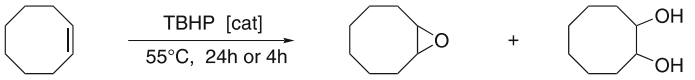

Entry	Support	Loading wt%	Conversion % Run 1	Run 2	Run 3	Epoxide Selectivity % Run 1	Run 2	Run 3	TOF h^{-1}	Refs.
1	–	–	100			100			1300	[39]
2	zeolite-Y [a]	2.8	100	99	95	100	92	78	370	[16]
3	zeolite-β [b]	1.3	98	95	85	79	84	68	300	[16]
4	SM-41 [c]	0.8	70			100			> 4000	[17]
5	AM-41 [d]	1.3	100			100			> 4000	[17]
6	SM-48 [c]	0.9	70			100			> 4000	[17]
7	AM-48 [d]	1.6	100			100			> 4000	[17]
8	SBA-15	1.5	100	81	81	100	88	86	1500	[38]

[a] zeolite-Y: Si/Al = 2.5
[b] zeolite-β: Si/Al = 12.5
[c] SM-41(48) = MCM-41(48) (0% Al_2O_3)
[d] AM-41(48) = MCM-41(48) containing 0.025% Al_2O_3. Reaction conditions: TBHP (5.5 M in decane), reaction time is 24 h, apart for entry 1 (4 h). Mo/TBHP/cyclooctene = 1/200/100 (entry 1), 1/300/150 (entries 2, 4-8), 1/700/350 (entries 3, 8), TOFs calculated after 5 min of reaction

2.1.3 Indirect Grafting: Tethering

Another useful strategy for the confinement of metal centres in molecular sieves is the covalent attachment of coordination complexes via a spacer ligand (tethering). The use of surface-fixed *N*-donor ligands (Lewis base ligands) coordinating dioxomolybdenum MoO_2 moieties has been described mainly by Thiel et al. [22, 23, 28, 29] and Gonçalves et al. [15, 24, 40].

2.1.3.1 Spacer Ligands Introduced Onto the Complex

Chiral $MoO_2(acac)(L^*)$ complexes, where L* is a chiral bidentate *O,O*-ligand derived from (L)-*trans*-4-hydroxyproline bearing a $Si(OEt)_3$ moiety, have been successfully heterogenised on zeolite-Y and tested for the epoxidation of allylic alcohols (geraniol and nerol) with TBHP (Scheme 4) [18].

Whatever the configuration and the nature of the process, all of the catalysts examined show high activities and selectivities of up to 90%, but low enantioselectivity (in the best case 64% ee; data reported in Table 3). Heterogenised catalysts (entries 2 and 4, Table 3) are slightly better in terms of both

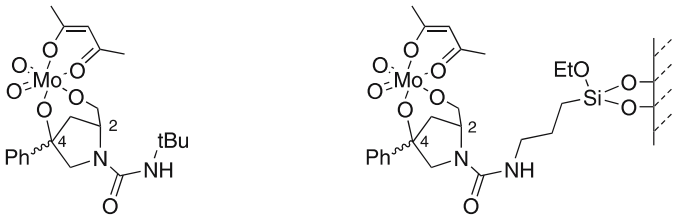

Scheme 4 Chiral $MoO_2(acac)(L^*)$ complexes tethered via a bidentate *O*,*O*-ligand on zeolite-Y

activity and selectivity than the corresponding homogeneous precursors (entries 1 and 3, Table 3). Despite a slight decrease in conversion, more than 95% of the metal is still retained after five runs, therefore allowing recycling and reuse of the catalyst materials.

A series of cyclopentadienylmolybdenum complexes containing a siloxane functional group, either directly attached to the metal center or to the cyclopentadienyl moiety, have recently been described and tested under homogeneous conditions [41]. These complexes have been successfully grafted onto MCM-41 and MCM-48 [19, 42] (Scheme 5).

The grafted samples are active and highly selective catalysts for cyclooctene epoxidation with TBHP (entries 4–9, Table 4), but are less efficient and selective than the corresponding homogeneous precursors (entries 1–3, Table 4). TOFs are the highest for the materials with longer hydrocarbon bridges between the molybdenum atoms and the surface Si – O groups of the support (entries 4–7 for longer hydrocarbon bridges versus entries 8–9 for shorter hydrocarbon bridges, Table 4). Indeed, the influence of the electron

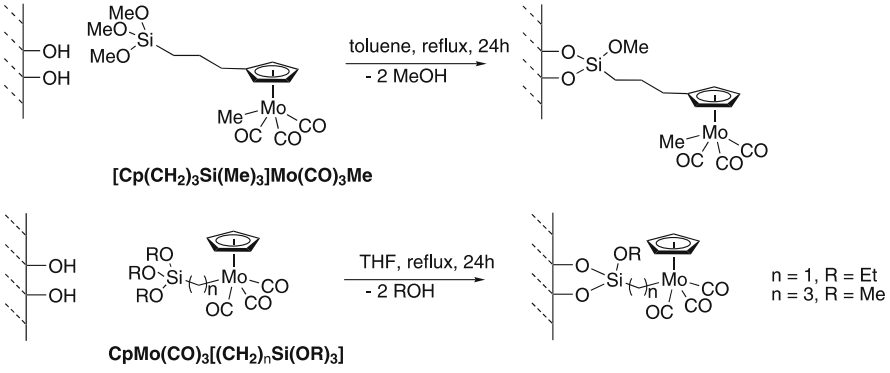

Scheme 5 Heterogenisation of complexes $Cp'Mo(CO)_3R$ bearing a siloxane group on MCM-41 and MCM-48

Table 3 Allylic alcohol epoxidation with TBHP/dioxomolybdenum $MoO_2(acac)(L^*)$ catalysts, where the catalysts were homogeneous or zeolite-Y-supported

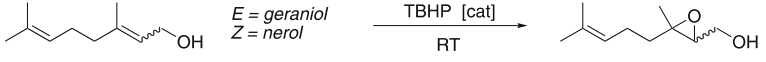

Entry		Time h	Geraniol Conversion %	Selectivity %	ee %	Time h	Nerol Conversion %	Selectivity %	ee %	Refs.
1	(2S,4R)	4	40	92	12	5	60	94	5	[18]
2	(2S,4R)-zeolite	4/18	40/82	99	–	5	78	98	–	[18]
3	(2S,4S)	4	80	91	28	4	94	92	10	[18]
4	(2S,4S)-zeolite	4/18	75/90	96	47	3	98	99	64	[18]

Reaction conditions: TBHP (in CH_2Cl_2), Mo/TBHP/cyclooctene = 1/300/200

Table 4 Cyclooctene epoxidation with TBHP/MCM–spacer ligand–tethered Cp′Mo(CO)$_3$R complexes

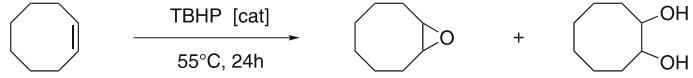

Entry	Support	Precursor	Loading wt %	Conversion % (run)	Epoxide selectivity % (run)	TOF h^{-1}	Refs.
1	–	$[Cp(CH_2)_3Si(OMe)_3]Mo(CO)_3Me$	–	100	100	410	[41]
2	–	$CpMo(CO)_3[(CH_2)_3Si(OMe)_3]$	–	100	100	400	[41]
3	–	$CpMo(CO)_3[CH_2Si(OEt)_3]$	–	100	100	360	[41]
4	MCM-41	$[Cp(CH_2)_3Si(OMe)_3]Mo(CO)_3Me$	2.3	95 (1) 46 (3)	79 (1) 98 (3)	100	[19]
5	MCM-48	$[Cp(CH_2)_3Si(OMe)_3]Mo(CO)_3Me$	3.4	100 (1) 73 (3)	100 (1) 90 (3)	80	[19]
6	MCM-41	$CpMo(CO)_3[(CH_2)_3Si(OMe)_3]$	1.7	95 (1) 57 (3)	87 (1) 91 (3)	80	[19]
7	MCM-48	$CpMo(CO)_3[(CH_2)_3Si(OMe)_3]$	1.8	100 (1) 80 (3)	100 (1) 70 (3)	100	[19]
8	MCM-41	$CpMo(CO)_3[CH_2Si(OEt)_3]$	0.3	33 (1) 27 (3)	73 (1) 89 (3)	50	[19]
9	MCM-48	$CpMo(CO)_3[CH_2Si(OEt)_3]$	0.4	46 (1) 29 (3)	78 (1) 95 (2)	60	[19]
10	MCM-41	$CpMo(CO)_3((CH_2)_3Si(OMe)_3)$	0.1	58 (1) 55 (2) 54 (3)	92 (1) 89 (2) 90 (3)		[42]

Notations: see Scheme 5. Reaction conditions: TBHP (5.5 M in decane), Mo/TBHP/cyclooctene = 1/200/100 (entries 1–3), 1/300/150 (entries 4–9), 1/700/350 (entry 10). TOFs calculated after 5 min of reaction

donor ability of the support's surface on the Lewis acidity of the catalytic centre is reduced due to the longer hydrocarbon bridges. Moreover, the steric bulk is lower for the methoxy groups (entries 6–7, Table 4) than for the ethoxy groups (entries 8–9, Table 4).

Leaching of the molybdenum complexes is not significant, but an important decrease in activity (ca. 50%) is observed after three runs. Despite this, the selectivity remains high and sometimes even improves. These significant decreases are only avoided when very low loadings are applied (entry 10, Table 4).

Scheme 6 offers two other examples of cyclopentadienylmolybdenum $Cp'Mo(CO)_3Cl$ tethered to MCM by a functional group of the cyclopentadienyl moiety.

In example (a) in Scheme 6, $[CpCONH(CH_2)_3Si(OEt)_3]Mo(CO)_3Cl$ is grafted onto MCM-41 through the siloxane-containing arm of the cyclopentadienyl ligand. An oxidative carbonylation with excess TBHP leads in situ to the supported dioxomolydenum complex $[CpCONH(CH_2)_3Si(OEt)_3]MoO_2Cl$ [20]. The synthesis is accompanied by some metal leaching (Mo loading decreases from 13 to 9 wt %). Both the grafted carbonyl precursor and the dioxo complexes were tested for cyclooctene epoxidation catalysis (data reported in Table 5, entries 3 and 4, respectively). The results are very similar and are in agreement with the fast in situ conversion of the tricarbonyl complex to the dioxo analogue under the catalytic conditions of the reaction. Although the selectivity to the epoxide is very high, the activities are moderate (63% conversion at best). This low activity is very likely due to the presence of the pendant siloxane arm and its functional groups, particularly the R – N(H) – C(O) – moiety, since the precursor complex (entry 2, Table 5) is much less active than the unsubstituted complex $CpMo(CO)_3Cl$

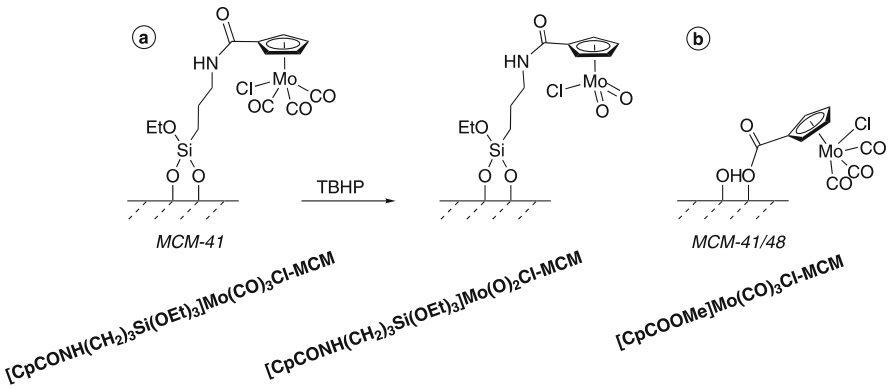

Scheme 6 **a** $[CpCONH(CH_2)_3Si(OEt)_3]Mo(CO)_3Cl$ immobilised on MCM-41 by a siloxane functionality. Further oxidation into the dioxo analogue is accomplished by TBHP. **b** $[CpCOOMe]Mo(CO)_3Cl$ immobilised on MCM-41/48 by an ether oxide moiety

Table 5 Cyclooctene epoxidation with TBHP/MCM-supported $[CpCONH(CH_2)_3Si(OEt)_3]Mo(CO)_3Cl$, $[CpCONH(CH_2)_3Si(OEt)_3]Mo(O)_2Cl$ and $[CpCOOMe]Mo(CO)_3Cl$ complexes

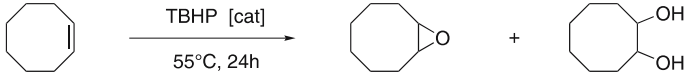

Entry	Support	Precursor	Loading wt %	Conversion %	Epoxide selectivity % (run)	TOF h^{-1}	Refs.
1	–	$CpMo(CO)_3Cl$	–	100	100	140	[20]
2	–	$[CpCONH(CH_2)_3Si(OEt)_3]Mo(CO)_3Cl$	–	82	100	15	[20]
3	MCM-41	$[CpCONH(CH_2)_3Si(OEt)_3]Mo(CO)_3Cl$	13.0	63 (1) 57 (2) 51 (3)	100	10	[20]
4	MCM-41	$[CpCONH(CH_2)_3Si(OEt)_3]MoO_2Cl$*	9.0	52 (1) 46 (2) 39 (3)	100	10	[20]
5	–	$[CpCOOMe]Mo(CO)_3Cl$	–	100	100	40	[20]
6	MCM-41	$[CpCOOMe]Mo(CO)_3Cl$	0.3	58 (1) 53 (2) 51 (3)	97 (1) 96 (2) 89 (3)	[b]	[21]
7	MCM-48	$[CpCOOMe]Mo(CO)_3Cl$	0.3	64 (1) 60 (2) 56 (3)	100 (1) 100 (2) 100 (3)	[b]	[21]

[a] Synthesised by in situ oxidation of the grafted complex $[CpCONH(CH_2)_3Si(OEt)_3]Mo(CO)_3Cl$. Reaction conditions: TBHP (5.5 M in decane), Mo/TBHP/cyclooctene = 1/80/50 (entries 1–5), 1/800/400 (entries 6 and 7). TOFs calculated after 18 min of reaction (entries 1–5)

[b] No TOF calculated (entries 6, 7)

(entry 1, Table 5) under homogeneous conditions. Upon recycling, the activity decreases slightly run after run. In example (b) in Scheme 6, the grafting of the complex [CpCOOMe]$Mo(CO)_3Cl$ onto MCM-41 and MCM-48 occurs through the reaction between an available silanol group in the mesoporous materials and the ester group, COOMe, of the complex [21]. Both MCM-41- and MCM-48-supported systems catalyse the epoxidation of cyclooctene with high yield and selectivity, and show very good recyclability (entries 6 and 7, Table 5). The slightly better results obtained with MCM-48 versus MCM-41 may be connected to the three-dimensional pore openings in the case of the former compared to the one-dimensional pore openings of the latter.

2.1.3.2 Spacer Ligands Introduced Onto the Support

The syntheses of the materials $CpMo(CO)_3(CH_2)_nSi(OR)-MCM$ ($n = 1$, R = Et; $n = 3$, R = Me; MCM = MCM-41, MCM-48) were explained above via the functionalisation of the complex (vide supra). Another strategy that has also been implemented functionalises the mesoporous framework instead of the complex [19] (Scheme 7). Here, the loading appears to be independent of the length of the siloxane bridge (1.0 and 0.9 wt % for $n = 1$, R = Me and $n = 3$, R = Et, respectively, in the complexes $CpMo(CO)_3(CH_2)_nSi(OR)-MCM-41$).

The results for cyclooctene epoxidation with TBHP show that the method of heterogenisation plays a decisive role in the activity (Table 6). Indeed, the materials obtained from the complex grafted onto a functionalised matrix (odd entries, Table 6) are less active (seen by comparing TOF values) than those synthesised via the tethering of functionalised complexes on a mesoporous material (even entries, Table 6).

The $CpMo(CO)_3$ moiety has also been grafted onto mesoporous materials, MCM-41 [25], MCM-48 [25], and SBA-15 [38], previously modified by the use of *p*-(iodomethyl)phenyltrimethoxysilane (Scheme 8).

The MCM samples show about 90–95% cyclooctene epoxidation with TBHP, with nearly 100% selectivity after a reaction time of 24 h (entries 2 and 3, Table 7). Conversion is lower with the SBA-15 catalysts (entry 4, Table 7). The TOFs are about one order of magnitude lower than the respective homo-

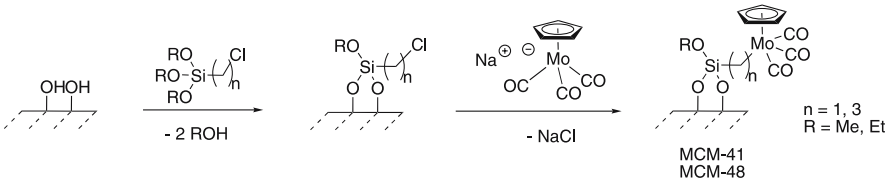

Scheme 7 Functionalisation of the mesoporous material prior to the grafting of the complex via an alkyl-siloxane spacer ligand

Table 6 Cyclooctene epoxidation with TBHP/MCM–spacer ligand–tethered $Cp'Mo(CO)_3R$ complexes

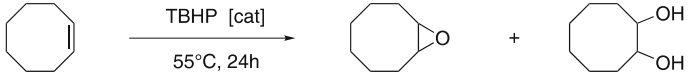

Entry	Support	Precursor	Loading wt %	Conversion %	Epoxide selectivity % (run)	TOF h^{-1}	Refs.
1	MCM-41	$CpMo(CO)_3((CH_2)_3Si(OMe)_3)$ matrix functionalised	1.0	68 (1) 31 (3)	100 (1) 44 (2)	30	[19]
2	MCM-41	$CpMo(CO)_3((CH_2)_3Si(OMe)_3)$ complex functionalised	1.7	95 (1) 57 (3)	87 (1) 91 (3)	80	[19]
3	MCM-41	$CpMo(CO)_3(CH_2Si(OEt)_3)$ matrix functionalised	0.9	35 (1) 28 (3)	82 (1) 64 (3)	30	[19]
4	MCM-41	$CpMo(CO)_3(CH_2Si(OEt)_3)$ ligand functionalised	0.3	33 (1) 27 (3)	73 (1) 89 (3)	50	[19]
5	MCM-48	$CpMo(CO)_3((CH_2)_3Si(OMe)_3)$ matrix functionalised	1.2	66 (1) 33 (3)	99 (1) 80 (3)	50	[19]
6	MCM-48	$CpMo(CO)_3((CH_2)_3Si(OMe)_3)$ ligand functionalised	1.8	100 (1) 80 (3)	100 (1) 70 (3)	100	[19]
7	MCM-48	$CpMo(CO)_3(CH_2Si(OEt)_3)$ matrix functionalised	1.3	63 (1) 47 (3)	92 (1) 64 (2)	30	[19]
8	MCM-48	$CpMo(CO)_3(CH_2Si(OEt)_3)$ ligand functionalised	0.4	46 (1) 29 (3)	78 (1) 95 (2)	60	[19]

Reaction conditions: TBHP (5.5 M in decane), Mo/TBHP/cyclooctene = 1/300/150. TOFs calculated after 5 min of reaction

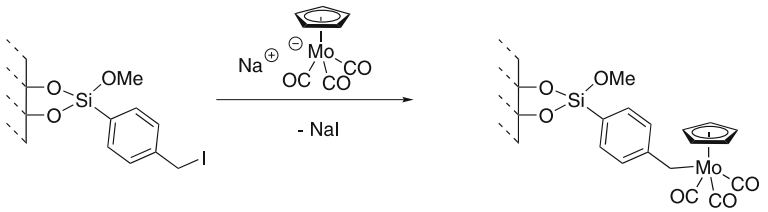

Scheme 8 $[Mo(CO)_3]Na$ tethering on a *p*-(iodomethyl)phenyltrimethoxysilane-functionalised MCM

Table 7 Cyclooctene epoxidation with TBHP/zeolite-spacer ligand-tethered $Cp'Mo(CO)_3R$ complexes

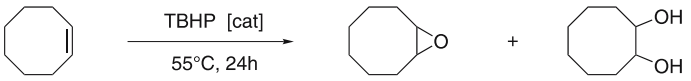

Entry	Support functionalised	Precursor	Loading wt %	Conversion %	Epoxide selectivity % (run)	TOF h^{-1}	Refs.
1	–	$CpMo(CO)_3Cl$	–			1700	[38]
2	MCM-41	$CpMo(CO)_3Na$	6.4	91[a] (1)	100[a] (1)	110[a]	[25]
				87[a] (2)	80[a] (2)	180[b]	
				85[a] (3)	76[a] (3)	200[c]	
				89[b]	100[b]	480[d]	
				77[c]	100[c]		
				68[d]	100[d]		
3	MCM-48	$CpMo(CO)_3Na$	8.3	95[a] (1)	100[a] (1)	130[a]	[25]
				92[a] (2)	71[a] (2)	230[b]	
				91[a] (3)	72[a] (3)	360[c]	
				92[b]	100[b]	520[d]	
				85[c]	100[c]		
				77[d]	100[d]		
4	SBA-15	$CpMo(CO)_3Na$	4.9	57 (1)	100 (1)	1500	[38]
				56 (2)	84 (2)		
				49 (3)	95 (3)		

Reaction conditions: TBHP (5.5 M in decane), Mo/TBHP/cyclooctene = 1/700/350 (entry 4)
[a] 1/120/60
[b] 1/240/120
[c] 1/360/180
[d] 1/1000/500
TOFs calculated after 5 min of reaction

geneous catalyst $CpMo(CO)_3Cl$ for the MCM-supported complexes. The conversion decreases only slightly with recycling, whereas the selectivity, after decreasing from 100% to ca. 75%, seems to stabilize. The influence of the ratio catalyst/TBHP/cyclooctene was also studied. This shows that the TOF is higher with lower amounts of catalyst. In this way, higher TOFs than those observed for $CpMo(CO)_3Cl$ directly grafted onto MCM can be reached.

Dioxomolybdenum catalysts have also been heterogenised on zeolites functionalised by *N*-donor or *N*,*N*-donor ligands. Complexes of the type MoO_2Cl_2LL' have thus been introduced to MCM previously functionalised by a nitrile ligand $NC(CH_2)_nSi(OEt)_3$ [15, 26], or a bipyridine ligand [24] (Scheme 9). Introduction of oxodiperoxo $MoO(O_2)_2(DMF)_2$ onto MCM-41 functionalised with the *N*,*N*-ligand 3-triethoxysilylpropyl[3-(2-pyridyl)-1-pyrazolyl]acetamide has also been done [22, 23]. The reaction between the iodo moiety of a modified MCM and the amino functional group of a chiral hydrosalendioxomolybdenum complex has been successfully applied for grafting [27] (Scheme 9).

After functionalisation, the matrix is usually further silylated using Me_3SiCl in order to remove the residual Si – OH groups on the surface of the mesoporous material, which are assumed to be unfavourable for catalytic reactions. Indeed, the adsorption characteristics of MCM-41 for polar molecules greatly depend upon the concentration of surface silanol groups [43]. Modification of MCM by silylation with Me_3SiCl makes the surface more hydrophobic. Moreover, stability with respect to moisture and mechanical compression is also improved [44].

When $MoO_2Cl_2(THF)_2$ is introduced into functionalised MCM (MCM-41 or MCM-48), cyclooctene epoxidation results are better than those observed

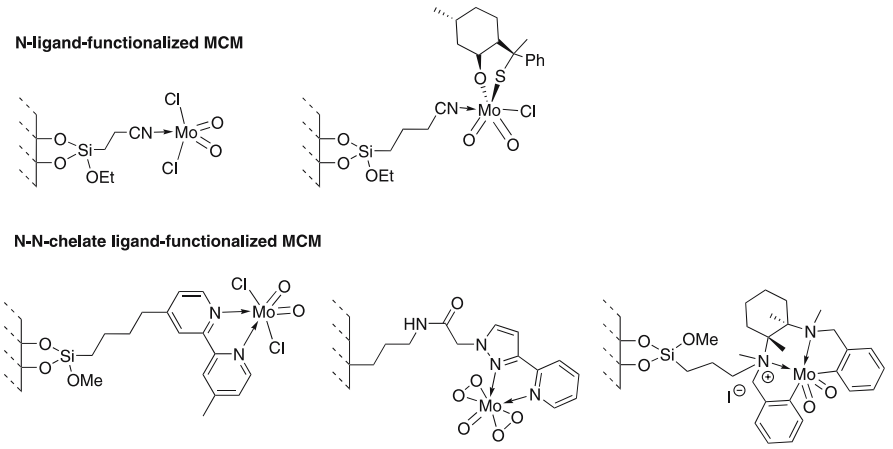

Scheme 9 Heterogenisation of dioxo and oxodiperoxo molybdenum complexes on MCM functionalised with *N*-ligands or *N*,*N*-ligands

Table 8 Catalytic cyclooctene epoxidation with TBHP/MCM-spacer ligand-supported dioxo- and oxodiperoxomolybdenum complexes

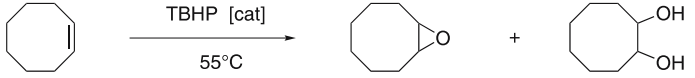

Entry	Support functionalised	Precursor	Loading wt %	Conversion % (run)	Epoxide selectivity % (run)	TOF h^{-1}	Refs.
1	MCM-41-L_1	$MoO_2Cl_2(THF)$	0.5–1	–	100	120	[15]
2	MCM-41	L_1'-MoO_2Cl_2	3.5	–	93	40	[15]
3	MCM-41-Si(OMe)-L_2	$MoO_2Cl_2(THF)$	8.3	74 (1) 45 (2)	100 (1) 95 (2)	–	[24]
4	homogeneous	L_2-$MoO_2Cl_2(THF)$	–	97	100	–	[24]

Reaction conditions: TBHP (5.5 M in decane), reaction time = 24 h (entries 3, 4), Mo/TBHP/cyclooctene = 175 mg cat/11 mmol TBHP/7.3 mmol cyclooctene (entries 1–4). TOFs calculated after 2 h of reaction. L_1 = $Si(OEt)(CH_2)_2CN$, L_1' = $(EtO)_3Si(CH_2)_2CN$, L_2 = 4,4′-dimethyl-2,2′-bipyridine

with materials obtained from grafting functionalised transition metal complexes onto MCM [15]. This is true for both the activity (TOFs after 2 h are $120\,h^{-1}$ and $40\,h^{-1}$ for grafted and nongrafted MCM, respectively) as well as for the selectivity (100% versus 93%, entries 1 and 2, Table 8). Bipyridine-functionalised MCM-41 offers high encapsulating ability for $MoO_2Cl_2(THF)_2$, leading to a final material with a metal loading as high as 8.3 wt % [24]. When tested for cyclooctene epoxidation, this heterogeneous catalyst shows high activity and selectivity, comparable to the homogeneous precursor (entries 3 and 4 for the heterogeneous and homogeneous catalysts, respectively, Table 8), but the results from heterogeneous catalyst recycling experiments are disappointing. By contrast, the covalent grafting of oxodiperoxo molybdenum $MoO(O_2)_2(DMF)_2$ onto MCM bearing a pyrazolylpyridine ligand [22, 23] provides remarkable stability against leaching and very good recycling ability (the catalytic properties are almost fully recovered after a second run).

Some attempts to introduce chirality into heterogeneous molybdenum(VI) complexes have also been reported. The complex $MoO_2Cl(THF)(L^*)$ (L^* = 8-phenylthioneomenthol) tethered via a $NC(CH_2)_3Si(OEt)_3$ spacer ligand on MCM-41 have been proven to be inappropriate for the preparation of enantioselective catalysts for cyclooctene epoxidation because of the lability of the chiral ligand [26]. Optically active dioxomolybdenum(VI) complexes bearing substituted hydrosalen ligands have been successfully grafted onto MCM. The resulting heterogenised compounds provide only moderate optical induction (enantiomeric excesses of 31% at best) in the asymmetric epoxidation of *trans*-β-methylstyrene and *cis*-β-methylstyrene.

2.2 Other Supports

2.2.1 Hybrid Supporting Material

One of the drawbacks of grafting procedures is the low loading of organic functionalities, which is limited by the distribution of reactive Si – OH groups and by diffusion through the mesoporous channels. Hybrid organic–inorganic materials allow higher catalyst loading. Thus, $MoO(O_2)_2$ was heterogenised on a hybrid support synthesised by sol-gel copolymerisation of the *N*,*N*-chelate ligand (3-triethoxysilylpropyl)[3-(2-pyridyl)-1-pyrazol]acetamide and tetraethoxysilane [28, 29] (Scheme 10). The material offers loadings as high as 23.0 wt % of the chelate ligand. This is more than twice the content of the samples obtained by normal grafting procedures, leading to a final loading of up to 6.7 wt % of metal. Hydrolysis and cocondensation processes can be catalysed either by the ligand itself, since it bears basic moieties, or with the help of a base like $EtNH_2$ or an acid like $HCl \cdot EtNH_2$. Depending on the method of cocondensation, the chelating sites can be made

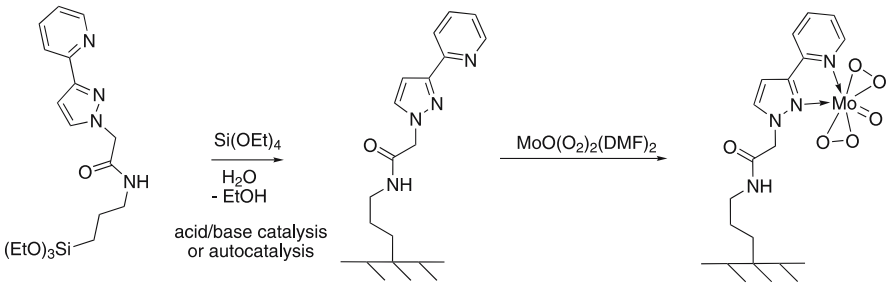

Scheme 10 $Mo(O)O_2(DMF)_2$ grafting on a hybrid sol-gel material

either more or less accessible for molybdenum complex binding. As a result, in some cases leaching becomes significant (materials obtained by external base or acid catalysis). No leaching occurs with materials synthesised by autocatalysis.

Materials synthesised by autocatalysis provide high activity (100% conversion in 3 h) and selectivity (100%) for cyclooctene epoxidation with TBHP, as well as excellent recycling ability (the catalytic properties are almost fully recovered after three runs).

2.2.2 Polymer-Supported Complexes

Highly active and selective polymer-supported molybdenum(VI) catalysts for olefin epoxidation using TBHP as oxidant have been being developed since the 1990s [30–34, 45–47]. The earliest examples employed polystyrene- and polymethacrylate-based resins to which nitrogen base ligands like aminomethylpyridine were attached [30, 31]. Later, compounds involving highly thermo-oxidatively stable resins were developed, such as polybenzimidazole (PBI) [32, 33, 45, 46] and polyimides [34] (Scheme 11). In the case of

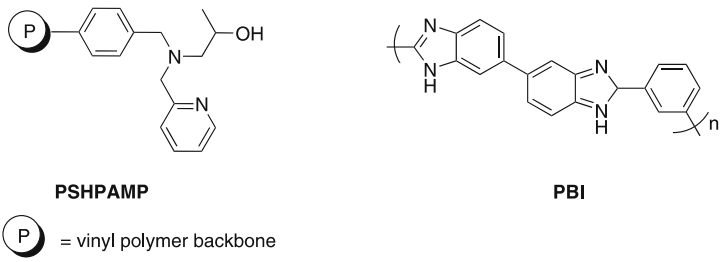

Scheme 11 Examples of polystyrene- and polybenzimidazole-based resins: PSHPAMP(polystyrene–divinylbenzene resin carrying an *N*-(2-hydroxypropyl)-2-aminomethylpyridine ligand), and PBI (polybenzimidazole)

the PBI resin, no additional Lewis base ligand was needed, since the benzimidazole residues of the backbone act as coordination sites for the metal centres which were introduced as $MoO_2(acac)_2$. The materials show loadings of ca. 2 mmol of Mo/g.

Without activation prior to use for olefin epoxidation, polystyrene- and polymethacrylate-based catalysts show long induction periods. By contrast, PBI · Mo does not require any pretreatment and acts as a highly active, selective and stable catalyst. For catalytic cyclohexene epoxidation with TBHP, PBI · Mo provides higher conversion (100%) than the homogeneous precursor $MoO_2(acac)_2$ (96%) and the PSHAMP · Mo system (23%) [33]. PBI · Mo can also be recycled with almost no leaching (leaching < 5% for the first run, then < 0.2% for all further runs) [46].

2.2.3 Ionic Liquids

In the last decade, room-temperature ionic liquids (RTILs) have been attracting considerable attention as alternatives to conventional molecular solvents. This is due to their unique physical properties, such as nonvolatility, nonflammability, thermal stability and high polarity. Additionally, they enable solubilisation of inorganic complexes whilst being immiscible with most hydrocarbons. Therefore, they provide a nonaqueous alternative for two-phase catalysis in which the catalyst is "immobilised" in the ionic liquid and then separated from the products (i.e., recycled). RTILs have been used in several types of reactions but are just emerging with regard to epoxidation catalysis. A manganese(II) salen complex which catalyses asymmetric epoxidation in an ionic liquid was reported a few years ago [48]. Since then, RTILs have been successfully applied to olefin epoxidation with manganese(III) porphyrin [49, 50]. A series of imidazolium-based RTILs have

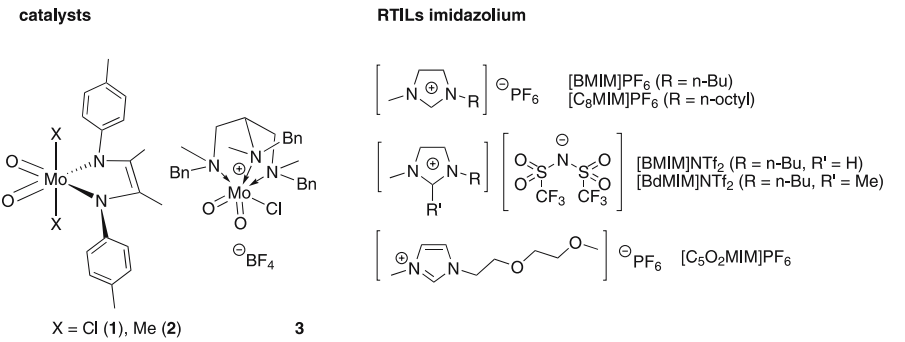

Scheme 12 Dioxomolybdenum complexes **1–3** tested in several imidazolium-based RTILs for olefin epoxidation

Table 9 Cyclooctene epoxidation with TBHP/complexes $MoX_2O_2L_2$ (X = Cl, Me; L = Lewis base) **1–3** and $CpMo(CO)_3Me$, $CpMo(CO)_3Cl$, $Me_5CpMo(CO)_3Me$ in different RTILs

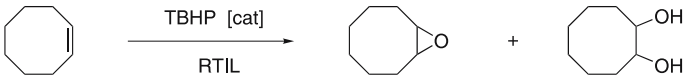

Entry	Catalyst	Solvent	Conversion %	Epoxide selectivity %	TOF h^{-1}	Refs.
1	**1**	–	100	100	(55)	[35]
2	**1**	DCE	94	100	11 (32)	[35]
3	**1**	$[BMIM]PF_6$	73	100	7 (77)	[35]
4	**2**	–	100	100	(73)	[35]
5	**2**	DCE	100	100	12 (53)	[35]
6	**2**	$[BMIM]PF_6$	90	100	8 (24)	[35]
7	**2**	$[BMIM]PF_6$	73	100	6	[35]
8	**2**	$[BMIM]PF_6$ [a]	34	100	2	[35]
9	**2**	$[C_8MIM]PF_6$	94	100	8 (25)	[35]
10	**2**	$[BMIM]NTf_2$	96	100	10 (34)	[35]
11	**2**	$[BdMIM]NTf_2$	53	100	4 (7)	[35]
12	**2**	$[C_5O_2MIM]PF_6$	14	100	1 (2)	[35]
13	**2**	$[(d\text{-}h)_2dmg]PF_6$	92	100	9 (27)	[35]
14	**3**	–	64	75	8 (48)	[35]
15	**3**	DCE	71	97	6 (19)	[35]
16	**3**	$[BMIM]PF_6$	71	85	9 (40)	[35]
17	**3**	$[BMIM]NTf_2$	93	85	11 (47)	[35]
18	$CpMo(CO)_3Me$	–	100 [b]		820	[36]
19	$CpMo(CO)_3Me$	$[BMIM]PF_6$	0 [b]		316	[36]
20	$CpMo(CO)_3Me$	$[BMIM]NTf_2$	100 [b]		33	[36]
21	$CpMo(CO)_3Me$	$[BMIM]BF_4$	38 [b]		14	[36]
22	$CpMo(CO)_3Cl$	–	100 [b]		960	[36]
23	$CpMo(CO)_3Cl$	$[BMIM]PF_6$	0 [b]		528	[36]
24	$CpMo(CO)_3Cl$	$[BMIM]NTf_2$	100 [b]		46	[36]
25	$CpMo(CO)_3Cl$	$[BMIM]BF_4$	31 [b]		15	[36]
26	$Me_5CpMo(CO)_3Me$	–	100 [b]		270	[36]
27	$Me_5CpMo(CO)_3Me$	$[BMIM]PF_6$	0 [b]		144	[36]
30	$Me_5CpMo(CO)_3Me$	$[BMIM]NTf_2$	83 [b]		24	[36]
29	$Me_5CpMo(CO)_3Me$	$[BMIM]BF_4$	27 [b]		10	[36]

[a] Reaction conditions: T = 55 °C (entries 1–7, 9–29); 35 °C (entry 8), Mo/TBHP/cyclooctene = 1/150/100 (1–6, 9–17) 1/100/100 (entries 7–8), 1/200/100 (entries 18–29). TOFs calculated after 8 h of reaction for entries 1–17 (values in *brackets* are calculated after 1 h of reaction), after 5 min of reaction for entries 18–29. Conversion and selectivity calculated after 30 h of reaction (entries 1–17), after 24 h of reaction (18–29)

[b] Epoxide yield

been tested as solvents for catalytic cyclooctene epoxidation with TBHP as an oxidising agent and dioxomolybdenum complexes $MoX_2O_2L_2$ (X = Cl, Me; L = Lewis base) [35] (Scheme 12), and cyclopentadienyltricarbonyl complexes $CpMo(CO)_3R$ as catalysts [36].

TBHP and the molybdenum catalysts are soluble in imidazolium-based RTILs. The system becomes biphasic when the olefinic substrate is added. In all cases, the TOFs of the catalytic reactions are considerably lower with the ionic solvent than when performed without the ionic solvent (data reported in Table 9). This slower catalytic reaction may be due to dilution effects and phase transfer problems, especially with the olefin, which is quite insoluble in the RTIL. The conversion appears to be strongly temperature-dependent, as decreasing the temperature from 55 °C to 35 °C reduces the conversion by ca. 50% (entries 7 and 8, Table 9). With the dioxomolybdenum complexes **1** and **2**, the epoxidation reaction proceeds with 100% selectivity (Table 9), whereas some diol is formed with the catalyst **3**.

As recycling is conducted via an extraction operation with an organic solvent, recovering the catalyst is linked to the affinity of the catalyst to the RTIL on one side and its affinity to the extracting organic solvent on the other side. For example, in $[BMIM]PF_6$ and $[C_8MIM]PF_6$ the cyclooctene conversion decreases to ca. 94% after the "recycling" of catalyst **2**, whereas in $[BMIM]NTf_2$ and $[BdMIM]NTf_2$, the loss is less dramatic (ca. 40%). Complete recycling of the catalyst $CpMo(CO)_3Me$ is achieved if a mixture of $[BMIM]NTf_2$ and $[BMIM]PF_6$ in a volume ratio of 4 : 1 is used as the RTIL. Increasing the amount of $[BMIM]PF_6$ applied, however, pushes the reaction towards diol formation, which is the only reaction product in systems containing pure $[BMIM]PF_6$ as the RTIL (in spite of a very high TOF).

3 Heterogenisation of MTO

Methyltrioxorhenium(VII) (MTO) was first described more than 25 years ago and has been closely examined after becoming easily available synthetically. It shows remarkable catalytic activity for oxyfunctionalisations such as epoxidation, heteroatom oxidation and C – H and Si – H oxidations. The oxidation occurs by activating cheap and environmentally friendly hydrogen peroxide (H_2O_2). The drawbacks of the MTO/H_2O_2 oxidation system lie in the appreciable formation of side products, in particular diols, and the facile decomposition of MTO to perrhenates. For example, in epoxidations the epoxide ring is opened quite readily to the diol, which undergoes a pinacol-type rearrangement and cleavage. In silane oxidations, the undesirable disiloxane is frequently formed as the major product through acid-catalysed condensation. Pyridine and pyrazole as Lewis bases overcome these drawbacks by coordination to the metal centre, thereby reducing the Lewis acidity of the catalyst and

promoting stability against decomposition to perrhenates. Significant efforts have been dedicated to the immobilisation of MTO on various supports [51] such as niobia, [52–57] zeolites [58–64], urea [65–69], polymers [70–76] and ionic liquids [77, 78]. The immobilised catalysts were evaluated for their activity in various reactions, like olefin epoxidation, silane oxidation, metathesis and Baeyer–Villiger reactions.

3.1 Inorganic Supports

3.1.1 Unfunctionalised Inorganic Oxides

MTO supported on acidic metal oxides was quickly discovered to form metathesis catalysts that are active without the need for additives, even for functionalised olefins [70]. Standard supports are zeolites and niobia (Nb_2O_5), and the activity was reported to be related to the surface acidity [79].

3.1.1.1 Niobia

Niobia-supported MTO has been prepared either by the deposition of sublimed MTO onto the support, or by the impregnation of the support by a solution of MTO, and has been well characterised [54]. A large variety of oxidation reactions were efficiently performed with niobia-supported MTO, such as olefin metathesis catalysis [53, 54], reactions of ethyl diazoacetate, heteroatom oxidation (amine and phosphine oxidations) and olefin epoxidation with hydrogen peroxide [55] (Scheme 13).

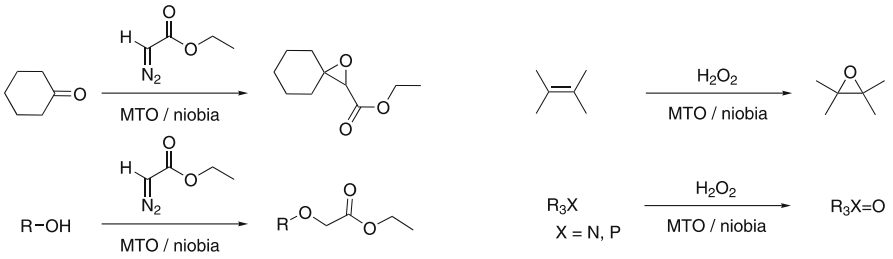

Scheme 13 Examples of oxidation reactions catalysed by niobia-supported MTO

Olefin epoxidation by hydrogen peroxide catalysed by MTO on niobia in the presence of urea was successfully applied with better results than under homogeneous conditions, thereby transforming simple olefin substrates to unsaturated fatty acids and esters [56, 57].

3.1.1.2 Zeolites

A series of zeolite-Y hosts containing different proton concentrations has been used for MTO encapsulation [80], and the resulting materials were studied for 1-hexene metathesis. The MTO molecule was activated by intra-zeolite protons, and simultaneously blocks their isomerisation activity. The ability to tune intra-zeolite acidity and the doping levels of the intact MTO precatalyst permits control over selectivity in the metathesis reaction.

The MTO-catalysed oxidation of silanes to silanols (data reported in Table 10) and epoxidation of olefins (data reported in Table 11) by aqueous H_2O_2 proceeds in high yields and excellent product chemoselectivities (no siloxane and no diol are observed as byproducts) in the presence of zeolite-Y [64], which are better than those obtained under homogeneous conditions (data in Table 11). For example, only 26% of $PhMe_2SiH$ is converted with as low as 20% selectivity towards silanol in 24 h when reacted with 85% H_2O_2 and catalysed by MTO (entry 5, Table 10). However, in the presence of zeolite-Y, 99% conversion is reached with 99% selectivity (entry 6, Table 10). The confinement of the oxidative species inside the 12 Å supercages

Table 10 Silane oxidation with aqueous H_2O_2/zeolite-Y-supported MTO

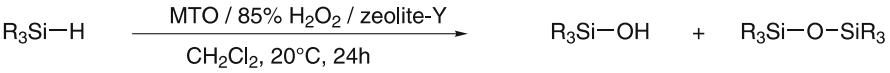

Entry	Silane	Oxidant	Nature	Conversion %	Selectivity silanol/ disiloxane %	Refs.
1	$EtMe_2SiH$	85% H_2O_2	homo	55	5/95	[66]
2	$EtMe_2SiH$	NaY/85% H_2O_2	hetero	72	99/1	[64]
3	$tBuMe_2SiH$	85% H_2O_2	homo	70	99/1	[66]
4	$tBuMe_2SiH$	NaY/85% H_2O_2	hetero	99	99/1	[64]
6	$PhMe_2SiH$	85% H_2O_2	homo	26	20/80	[66]
7	$PhMe_2SiH$	NaY/85% H_2O_2	hetero	99	99/1	[64]
8	Et_3SiH	85% H_2O_2	homo	54	54/46	[66]
9	Et_3SiH	NaY/85% H_2O_2	hetero	86	99/1	[64]

Reaction conditions for entries 2, 4, 6, 8: 330 μmol of substrate, 2 mol % of MTO, 2 eq of H_2O_2 (ratio MTO/oxidant/substrate = 2/200/100) in the presence of 35 mg of NaY zeolite; for entries 1, 3, 5, 7: MTO (1–20% solution in CH_2Cl_2), 1–10 eq oxidant

of the zeolite prevents bimolecular condensation of silanol to siloxane by steric means.

In the case of olefin epoxidation, the formation of the diol is prevented since MTO and the epoxide are topologically separated (MTO is absorbed in the zeolite whereas the epoxide remains in solution). As a consequence, selectivities are very high (95%, Table 11) except with 1-methylcyclohexene (entry 2, Table 11).

Table 11 Olefin epoxidation with aqueous H_2O_2/zeolite-Y supported MTO

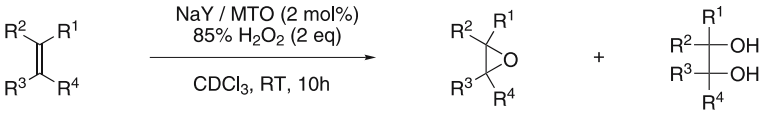

Entry	Substrate	Conversion %	Selectivity epoxide/diol %	Refs.
1		47	95/5	[64]
2		42	75/25	[64]
3		33	95/5	[64]
4		65	95/5	[64]
5		89	95/5 exo/endo ratio: 82/18	[64]
6	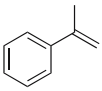	43	95/5	[64]
7	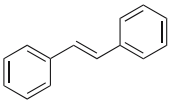	95	95/5	[64]
8	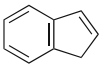	52	95/5	[64]

3.1.2
Functionalised Silica Matrices

MTO has been heterogenised inside the porous systems of hybrid silica matrices [59, 60]. Thus, it has been supported on silica functionalised by polyethers [59]. These polyethers are covalently attached to a silicate particle using sol-gel procedures and act as the solvent for the catalyst (Scheme 14).

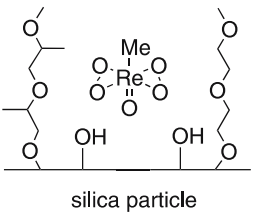

Scheme 14 Encapsulation of MTO in silica functionalised by polyethylene oxide (PEO) and polypropylene oxide (PPO)

In the absence of an organic solvent, this assembly catalyses cyclohexene epoxidation with 30% aqueous H_2O_2 with high selectivity, especially when

Table 12 Influence of the nature of the tethered polyether on cyclohexene epoxidation with H_2O_2/MTO

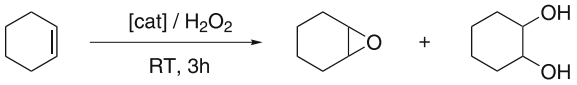

Entry	Tethered polyether	Conversion %	Epoxide selectivity %	Refs.
1	–	1	–	[59]
2	5% PEO	10	12	[59]
3	10% PEO	70	0	[59]
4	20% PEO	79	9	[59]
5	10% PEO, 5% PPO	82	57	[59]
6	10% PEO, 10% PPO	100	86	[59]
7	10% PEO, 20% PPO	33	85	[59]
8	4% PPO	92	56	[59]
9	10% PPO	20	64	[59]
10	20% PPO	1	–	[59]

Reaction conditions: 1 mmol cyclohexene, 2 mmol H_2O_2 (30%), 0.02 mmol MTO (ratio MTO/oxidant/substrate = 1/100/50) and polyether tethered silica (100 mg)

the ring-opening products (diols) often observed in homogeneous media are considered (data reported in Table 12). A balanced amount of polyethylene oxide PEO (hydrophilic) and polypropylene oxide PPO (hydrophobic) gives the best results (entry 6, Table 12) including an improved selectivity over homogeneous conditions (entry 1, Table 12).

The oxidation of various other alkenes using the optimal heterogeneous system (10% PEO–10% PPO) was compared to a typical homogeneous reaction using MeOH as solvent (data reported in Table 13). Compared to the homogeneous standard, the polyether tethered–silica-encapsulated catalysts show somewhat lower activity but much better selectivity.

Table 13 Comparative olefin epoxidation with H_2O_2/MTO under heterogeneous conditions (10% PEO–10% PPO silica support) and homogeneous conditions

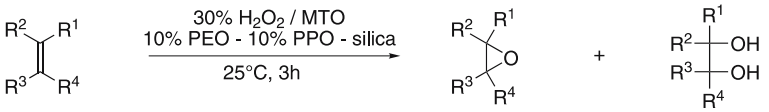

Entry	Substrate	Conversion %		Epoxide selectivity %		Refs.
		Homogeneous	Heterogeneous	Homogeneous	Heterogeneous	
1		100	100	0	86	[59]
2		100	94	28	71	[59]
3	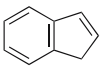	100	89	0	94	[59]
4	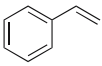	100	84	0	34	[59]
5	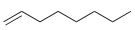	100	63	63	100	[59]
6	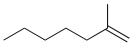	100	80	0	79	[59]
7	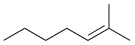	100	73	0	93	[59]

Reaction conditions (heterogeneous): 1 mmol substrate, 3 mmol H_2O_2 (30%), 0.02 mmol MTO on 10% PEO – 10% PPO – SiO_2 (100 mg); (homogeneous): 1 mmol substrate, 2 mmol H_2O_2 (30%), 0.02 mmol MTO, MeOH (1 mL)

MTO has also been confined in mesoporous material functionalised with *N*-donors like pyridine or *N*,*N*-donor ligands such as bipyridine. Hybrid silica matrices bearing pyridine moieties were prepared via sol–gel methods using 1,4-bis(triethoxysilyl)benzene as a cocondensation agent and 4-((3-triethoxysilyl)propylamino)pyridine hydrochloride as a hydrolysable ligand [60] (Scheme 15, *N*-donor). Combined with MTO and H_2O_2, the resulting agents proved to be highly selective and recyclable as olefin heterogeneous epoxidation catalysts. MTO has also been immobilised on the mesoporous silica material MCM-41 functionalised by pendant bipyridyl groups (bpy) (4-[(-O)$_3$Si(CH$_2$)$_4$]-4′-CH$_3$-2,2′-bipyridine) to form a hybrid MCM-41-bpy/MTO material [61] (Scheme 15, *N*,*N*-donor). When the metal loading is very high (10.24 wt %, giving an Re:N molar ratio of 1 : 1.1), analyses show that in fact some rhenium atoms remain uncoordinated in the MCM channels. This material has not yet been tested for catalysis.

Another route to immobilising an organorhenium (VII) oxide derived from MTO on the surface of an iodosilane-modified MCM-41 was applied (Scheme 16).

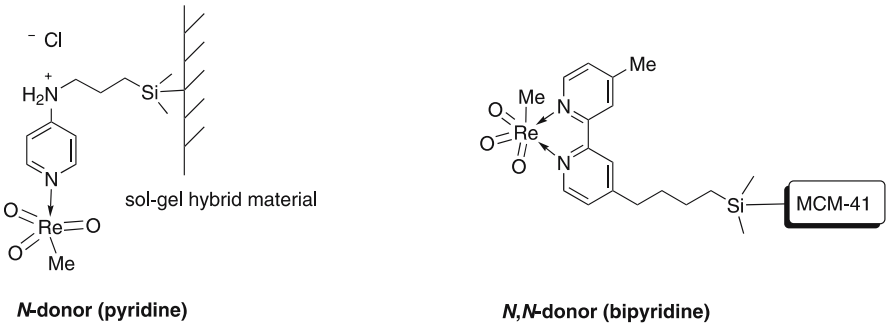

Scheme 15 MTO confined in silica matrices functionalised with *N*-donors and *N*,*N*-donors

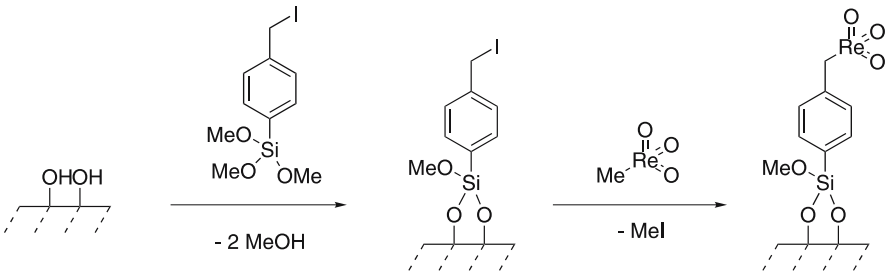

Scheme 16 Immobilisation of trioxorhenium(VII) derived from MTO on an iodosilane-modified MCM

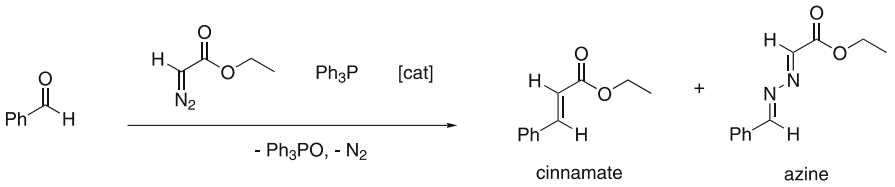

Scheme 17 Benzaldehyde olefination with ethyl diazoacetate/triphenylphosphine/MCM-supported trioxorhenium(VII) catalyst

The resulting material contains 1.25 wt % Re. As it is not stable in the presence of H_2O_2, it could not be used for olefin epoxidation. Instead, it was tested for aldehyde olefination reactions [62] (Scheme 17). The catalytic activity is lower than that observed for the homogeneous process but is retained even after three catalytic runs.

3.2
Organic Supports

3.2.1
MTO/UHP (Urea Hydroperoxide) System

One of the most important drawbacks of olefin epoxidation with MTO/H_2O_2 lies in the epoxide ring-opening reactions which lead to the corresponding diol. These undesirable reactions can be partially prevented when operating under anhydrous conditions in *tert*-butanol. The system MTO/UHP (UHP = urea hydrogen peroxide) was also proven to be an excellent alternative. The urea, and therefore the inclusion complex formed by MTO with urea, is insoluble in most organic solvents. As a result, the system MTO/UHP/organic phase is heterogenous. The MTO/UHP combination was found to be very efficient for olefin epoxidation [65] and silane oxidation [66], providing higher yields and selectivities than those obtained in the homogeneous processes. This can be attributed to an increased stability of MTO when inclusion complexes with urea are formed. Since the reaction is supposed to take place inside the helical urea channels, the condensation of the silanol produced is prevented for steric reasons. Thus, an improved chemoselectivity for silanol versus disiloxane, similar to the case of the zeolite-supported MTO already described, results (vide supra). The results for the MTO-catalysed Si – H insertion of the silanes with UHP or 85% H_2O_2 are given in Table 14.

The conversion and selectivity towards silanols are very high when a heterogeneous MTO/UHP system is used (entries 2 and 5; Table 14: conversion > 85%, selectivity > 94% for $EtMe_2SiH$ and $PhMe_2SiH$ as substrates) and significantly better than the homogeneous MTO/85% H_2O_2 combination (conversion < 55%, selectivity < 20%, entries 1 and 4, Table 14). The presence of urea is not only beneficial to the efficiency and the chemoselectivity, but also

to the stereoselectivity. Thus (+)-(α-Np)PhMeSiH is converted with retention of its configuration to (+)-(α-Np)PhMeSiOH with a high enantiomeric excess (91%) using the MTO/UHP system (entry 8, Table 14), whereas almost no enantioselectivity is observed with MTO/85% H_2O_2 (entry 7, Table 14). Even steroidal dienes, uracil, and purine have been successfully oxidised by the MTO/UHP system [67–69] (Scheme 18).

Table 14 Silane oxidation with the MTO/UHP system

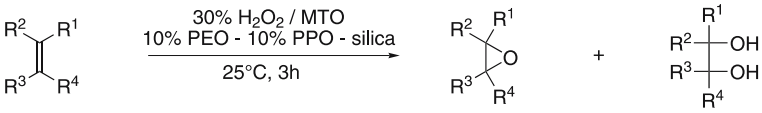

Entry	Silane	Support/Oxidant	Time h	Conversion %	Selectivity Silanol/ Disiloxane % (ee %)	Refs.
1	$EtMe_2SiH$	85% H_2O_2	18	55	5/95	[66]
2	$EtMe_2SiH$	UHP	18	95	94/6	[66]
3	$EtMe_2SiH$	NaY/85% H_2O_2	24	72	99/1	[64]
4	$PhMe_2SiH$	85% H_2O_2	13	26	20/80	[66]
5	$PhMe_2SiH$	UHP	13	87	98/2	[66]
6	$PhMe_2SiH$	NaY/85% H_2O_2	13	99	99/1	[64]
7	(+)-(α-Np)PhMeSiH	85% H_2O_2	14	2	90 (1)/10	[66]
8	(+)-(α-Np)PhMeSiH	UHP	14	12	96 (91)/4	[66]

Reaction conditions: entries 1, 2, 4, 5, 7, 8: MTO 1–20 mol % in solution, oxidant 1–10 eq, urea 1–10 eq (135 wt % silica, entry 7), entries 3, 6: 330 μmol of substrate, 2 mol % MTO, 2 eq H_2O_2 in the presence of 35 mg of zeolite-Y

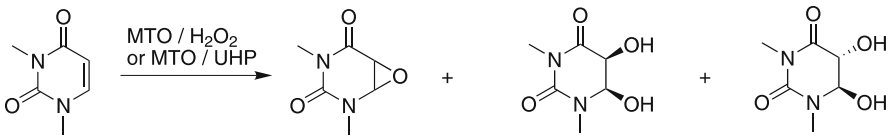

oxidant			
MTO / H_2O_2	45 %	22 %	0 %
MTO / UHP	82 %	7 %	

Scheme 18 Oxidation of an uracil derivative by the MTO/H_2O_2 system or the MTO/UHP combination

3.2.2
Organic Polymers

Herrmann and coworkers prepared heterogeneous MTO compounds of the general formula polymer/MTO in which MTO was assumed to be bound to the support by coordination with one nitrogen atom [70, 71]. Nonreticulated poly(4-vinylpyridine), poly(2-vinylpyridine), poly(vinylpyrrolidone), polyacrylamide), and nylon 6 were used as organic supports. When applied to the epoxidation of olefins (cyclohexene, methyl oleate, allyl alcohols) with dried H_2O_2 in *tert*-butanol, these systems led to low yields (20–27%) of epoxide. Ten years later, Saladino and coworkers used this concept to prepare two families of organic polymer-supported MTO [72]. PVP/MTO and PVPN/MTO systems are based on **p**oly(4-**v**inyl**p**yridine) and **p**oly(4-**v**inyl**p**yridine-***N***-oxide), respectively, whereas PS/MTO are obtained from **p**oly**s**tyrene. Cross-linkage is accomplished by divinylbenzene (Scheme 19).

Depending on the loading factor (0.5 or 1.0 mmol MTO/g support) and more importantly on the reticulation grade, these catalytic systems proved to be very efficient and selective for olefin epoxidation with H_2O_2 (Table 15). For example, cyclohexene is oxidised by H_2O_2 with 78% conversion (and 91% selectivity) within 1 h using the PVP–2%/MTO catalyst (entry 1, Table 15). When dividing the loading factor by two (0.5 instead of 1.0%), the reaction time required to reach the same conversion (80%) is also divided by two (0.5 h). Moreover, the selectivity is increased (98%, entry 4, Table 15). Using 0.5% as the loading factor and increasing the cross-linkage from 2% to 25% leads to 98% conversion with 98% selectivity in 0.5 h (entry 5, Table 15).

The exceptional recyclability of the PVP/MTO system (the catalytic activity is maintained for at least five recycling experiments, see entries 1–3,

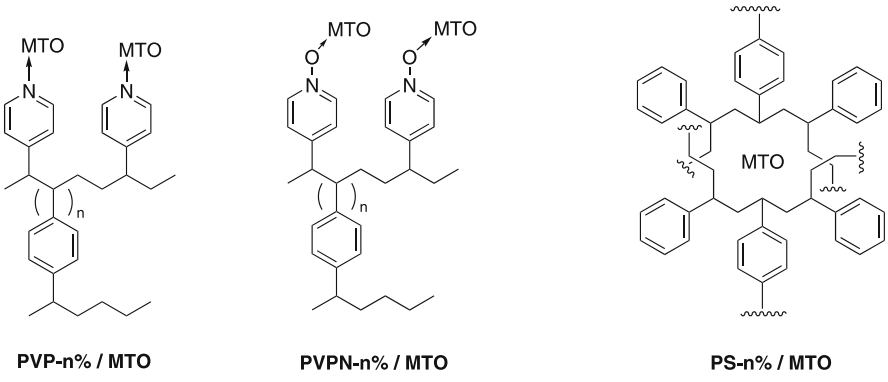

Scheme 19 The poly(4-vinylpyridine)-based supports PVP-*n*% and PVPN-*n*%/MTO, and the polystyrene-based supports PS-*n*%/MTO, where *n* is the cross-linkage percentage with divinylbenzene

Table 15 Olefin epoxidation with H_2O_2/polymer-supported MTO

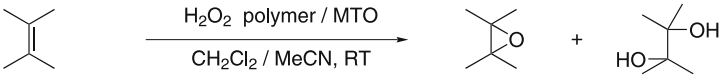

Entry	Olefin	Polymer	Loading %	Time h	Conversion % (Run)	Epoxide Selectivity %(Run)	Refs.
1	cyclohexene	PVP-2%	1.0	1.0	78 (1) 80 (2) 74 (3) 72 (4) 75 (5)	91 (1) 86 (2) 83 (3) 90 (4) 92 (5)	[72]
2	cyclohexene	PVP-25%	1.0	1.5	94 (1) 91 (2) 89 (3) 93 (4) 95 (5)	95 (1) 95 (2) 92 (3) 94 (4) 93 (5)	[72]
3	cyclohexene	PVPN-2%	1.0	0.5	98 (1) 96 (2) 94 (3) 98 (4) 98 (5)	82 (1) 80 (2) 81 (3) 81 (4) 84 (5)	[72]
4	cyclohexene	PVP-2%	0.5	0.5	80	98	[72]
5	cyclohexene	PVP-25%	0.5	0.5	98	98	[72]
6	cyclohexene	PS-2%	1.0	1.5	98 (1) 97 (2) 95 (3) 88 (4) 77 (5)	55 (1) 53 (2) 54 (3) 55 (4) 53 (5)	[72]
7	cyclohexene	PVP-2%	1.0	0.5	98	98	[72]
8	cyclooctene	PVP-25%	1.0	0.5	98	98	[72]
9	cyclooctene	PVPN-2%	1.0	0.5	96	98	[72]
10	cyclooctene	PS-2%	1.0	0.5	94	98	[72]
11	cyclooctene	PVP-2%	1.0	2.0	98	70	[72]
12	styrene	PVP-25%	1.0	6.5	98	98	[72]
13	styrene	PVPN-2%	1.0	18.0	85	88	[72]
14	styrene	PS-2%	1.0	2.0	60	80	[72]
15	styrene	PVP-2%	1.0	12.0	95	75	[72]
16	α –methylstyrene	PVP-25%	1.0	3.5	98	98	[72]
17	α –methylstyrene	PVPN-2%	1.0	7.0	98	54	[72]
18	α –methylstyrene	PS-2%	1.0	1.0	98	78	[72]
19	*trans*-stilbene	PVP-2%	1.0	6.0	98	46	[72]
20	*trans*-stilbene	PVP-25%	1.0	6.0	98	98	[72]
21	*trans*-stilbene	PVPN-2%	1.0	1.0	98	98	[72]
22	*trans*-stilbene	PS-2%	1.0	1.0	93	98	[72]

Reaction conditions: H_2O_2 (30% aqueous solution). Ratio catalyst/H_2O_2/olefin = 1/240/200 (loading factor 0.5%) or 1/120/100 (loading factor 1%)

Table 15) highlights the stability of this system compared to the PS/MTO system (entry 6, Table 15), which shows a decrease in activity during recycling. This difference in behaviour may be due to the weaker interaction between MTO and the PS polymer, which is only accomplished by the physical envelopment of the benzene ring. The PVP/MTO combination was successfully used for other compounds of biological interest, such as terpenes. Even highly sensitive terpenic epoxides, like α-pinene oxide, can be obtained in excellent yields using polymer-supported MTO catalysts [73] (Scheme 20, Table 16).

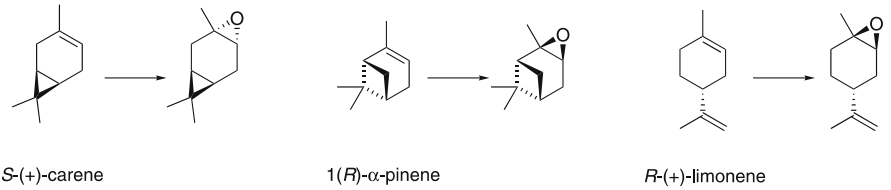

Scheme 20 Epoxidation of terpenes with H_2O_2/polymer-supported MTO at room temperature in CH_2Cl_2/MeCN

Table 16 Epoxidation of terpenes with H_2O_2/polymer-supported MTO at room temperature in CH_2Cl_2/MeCN

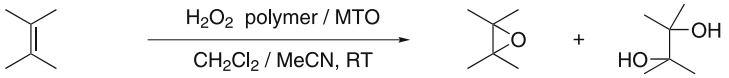

Entry	Substrate	Catalyst	Time h	Conversion %	Epoxide Selectivity %	Refs.
1	*S*-(+)-carene	MTO/pyridine	1.0	98	75	[73]
2	*S*-(+)-carene	PVP-2%/MTO	3.5	68	85	[73]
3	*S*-(+)-carene	PVP-25%/MTO	2.5	98	96	[73]
4	*S*-(+)-carene	PVPN-2%/MTO	2.5	75	84	[73]
5	*S*-(+)-carene	PS-2%/MTO	3.0	98	91	[73]
6	α –pinene	MTO/pyridine	1.0	–	90	[73]
7	α –pinene	PVP-2%/MTO	2.0	76	95	[73]
8	α –pinene	PVP-25%/MTO	0.5	81	88	[73]
9	α –pinene	PVPN-2%/MTO	1.0	70	98	[73]
10	α –pinene	PS-2%/MTO	1.5	98	98	[73]
11	*R*-(+)-limonene	MTO/pyridine	1.0	96	79	[73]
12	*R*-(+)-limonene	PVP-2%/MTO	1.5	75	83	[73]
13	*R*-(+)-limonene	PVP-25%/MTO	1.5	79	89	[73]

Reaction conditions: H_2O_2 (35% aqueous solution), catalyst loading factor 1.0

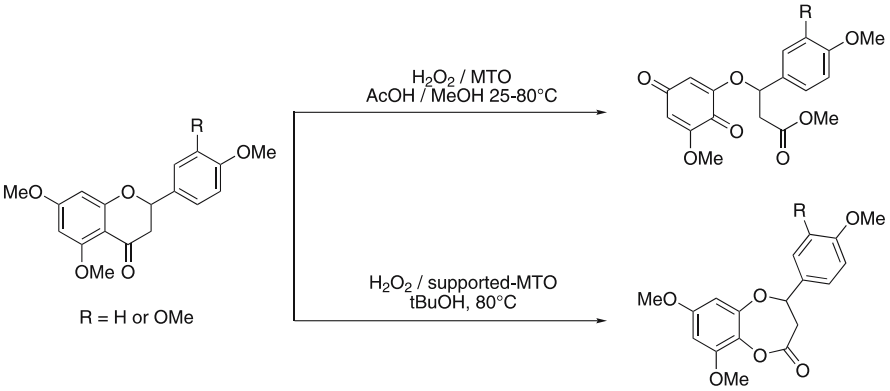

Scheme 21 Baeyer–Villiger reaction catalysed by the PVP/MTO/H_2O_2 system

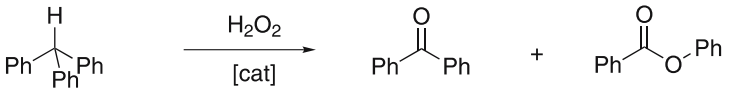

Scheme 22 Example of C – H insertion reactions catalysed by the PVP/MTO/H_2O_2 system

Compared to homogeneous conditions with MTO in the presence of pyridine, selectivities improve using polymer-supported MTO (for example, compare the selectivity of entry 1 with those of entries 2–5 in Table 16). Conversions are generally good-to-excellent.

The heterogeneous PVP/MTO/H_2O_2 system was additionally proven efficient and selective for the conversion of naringenin and hesperetin into lactones by a Baeyer–Villiger reaction [74] (Scheme 21). In less than 8 h, 75–100% conversion was reached with 35–80% selectivity.

C – H insertion reactions with H_2O_2 catalysed by PVP/MTO were also achieved, starting from hydrocarbons and producing ketones and alcohols [75] (Scheme 22).

3.3 Ionic Liquids

The catalytic potential of the MTO/UHP oxidation system has also been tested in the room-temperature ionic liquid [EMIM][BF_4], in which it is soluble [77]. In contrast, the olefin is poorly soluble in such solvents. Therefore, the whole system is biphasic. Excellent conversions and selectivities for the epoxides of a wide number of olefinic substrates were reached under these anhydrous conditions. The exception was 1-decene (data collected in Table 17), for which poor conversion (entry 9, Table 17) may result in phase transfer problems, since it is the least soluble substrate in the ionic liquid.

Table 17 Epoxidation of various substrates with MTO/UHP in $[EMIM]BF_4$

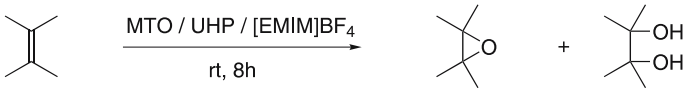

Entry	Substrate	Conversion %	Selectivity %	Refs.
1		95	99	[77]
2		95	95	[77]
3		95	95	[77]
4	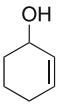	99	95	[77]
5	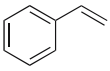	95	95	[77]
6	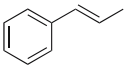	95	95	[77]
7		95	95	[77]
8		99	85	[77]
9	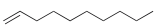	46	99	[77]

Reaction conditions: ratio MTO/UHP/olefin = 1/100/50

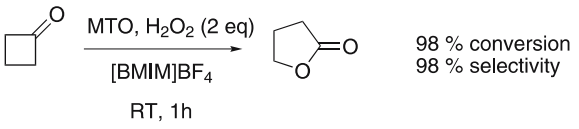

Scheme 23 Example of Baeyer–Villiger oxidation achieved by MTO (2%)/H_2O_2 (50% aqueous) system in RTIL $[BMIM][BF_4]$

Table 18 Recyclability of the PS-2%/MTO/H_2O_2/RTIL [BMIM]PF_6 system used for oxidation reactions

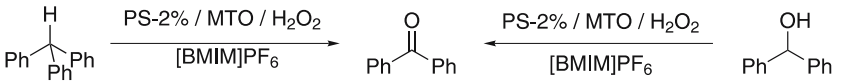

triphenylmethane benzophenone benzhydrol

Entry	Reagent	Product	Conversion % (run)	Selectivity % (run)	Refs.
1	triphenylmethane	benzophenone	49 (1) 47 (2) 45 (3)	88 (1) 88 (2) 86 (3)	[76]
2	benzhydrol (diphenylmethanol)	benzophenone	94 (1) 85 (2) 83 (3)	78 (1) 78 (2) 77 (3)	[76]

Reaction conditions: temperature = 25–60 °C, 100 mg supported catalyst, loading factor = 1, H_2O_2 (4–6 eq)

Remaining reactants and products are both easily removed from the reaction mixture via extraction with an organic solvent such as diethyl ether which is immiscible with the ionic liquid. Unfortunately, MTO cannot be retained in ionic liquids during the liquid/liquid extraction of the reaction mixture for recycling due to its high solubility in a wide range of molecular solvents. However, when MTO is additionally supported by an organic polymer, recycling becomes possible. For example, the system PS-2%/MTO/H_2O_2 in RTIL [BMIM]PF_6, which is an efficient and selective catalytic system for various oxidation reactions, can be fully recovered [76] (Table 18).

The Baeyer–Villiger oxidation of cyclic ketones was also achieved by the MTO/H_2O_2 system in the ionic liquid [BMIM][BF_4] [78] (Scheme 23). Kinetic investigations have additionally been performed in order to follow the formation of the catalytically active peroxorhenium intermediates in the RTILs [81, 82].

4 Conclusion

Considerable improvements have been made in the field of organorhenium and organomolybdenum oxide catalyst heterogenisation over the last decade. These include, in particular, the application of zeolites and mesoporous materials as supporting systems. Such heterogeneous systems have proven to be, in most cases, efficient and selective catalysts in various reactions, especially olefin epoxidation and (to a lesser extent) silane oxidation, other oxidation

reactions, metathesis, and the Baeyer–Villiger reaction. Supports other than mesoporous materials and zeolites have also been developed. The MTO/UHP system constitutes another very attractive combination. Polymer-supported catalysts and the use of RTILs have also been successfully applied. Under optimised conditions, such systems are indeed highly active, selective and recyclable. Very promising results have been attained in the heterogenisation of organorhenium and organomolybdenum complexes so far. Future developments are expected to achieve better recyclability, and the possibility of obtaining highly enantioselective heterogeneous epoxidation catalysts tolerating a wide variety of substrates exists.

Acknowledgements The authors are greatly indebted to the Fonds der Chemischen Industrie and to the Bayerische Forschungsstiftung (postdoctoral grant for C.F.) for financial support. M.A. Fredricks is acknowledged for helping to edit this work.

References

1. Kumar SB, Chaudhury M (1991) J Chem Soc Dalton Trans p 2169
2. Palanca P, Picher T, Sanz V, Gomez-Romero P, Llopis E, Domenech A, Cervilla A (1990) J Chem Soc Chem Commun p 531
3. Wilshire JP, Leon L, Bosserman P, Sawyer DT (1979) J Am Chem Soc 101:3379
4. Berg JM, Holm RH (1985) J Am Chem Soc 107:925
5. Caradonna JP, Harlan EW, Holm RH (1986) J Am Chem Soc 108:7856
6. Fehrer FJ, Rahimian K, Budzichowski TA, Ziller JW (1995) Organometallics 14:3920
7. Clarke R, Gahagan M, Mackie RK, Foster DF, Cole-Hamilton DJ, Nicol M, Montford AW (1995) J Chem Soc Dalton Trans p 1221
8. Backhouse JR, Lowe HM, Sinn E, Suzuki S, Woodward S (1995) J Chem Soc Dalton Trans p 3329
9. Kollar J (Halcon International Inc.) (1967) US Patent 3 350 422
10. Kollar J (Halcon International Inc.) (1967) US Patent 3 351 635
11. Sheng MN, Zajaczek GJ (ARCO) (1968) UK Patent: GB 1 136 923
12. Kresge CT, Leonowicz ME, Roth WJ, Vartuli JC, Beck S (1992) Nature 359:710
13. Beck S, Vartuli JC, Roth WJ, Leonowicz ME, Kresge CT, Schmitt KD, Chu CT-W, Olson DH, Sheppard EW, McCullen SB, Higgins JB, Schlenker JL (1992) J Am Chem Soc 114:10834
14. Alfredsson V, Anderson M (1996) Chem Mater 8:1141
15. Ferreira P, Gonçalves IS, Kühn FE, Lopez AD, Martins MA, Pillinger M, Pina A, Rocha J, Romão CC, Santos AM, Santos TM, Valente AA (2000) Eur J Inorg Chem p 2263
16. Sakthivel A, Zhao J, Kühn FE (2005) Catal Lett 102:115
17. Sakthivel A, Zhao J, Hanzlik M, Kühn FE (2004) Dalton Trans p 3338
18. Corma A, Fuerte A, Iglesias M, Sanchez F (1996) J Mol Catal A–Chem 107:225
19. Sakthivel A, Zhao J, Hanzlik M, Chiang AST, Herrmann WA, Kühn FE (2005) Adv Synth Catal 347:473
20. Abrantes M, Gago S, Valente AA, Pillinger M, Gonçalves IS, Santos TM, Rocha J, Romão CC (2004) Eur J Inorg Chem 4914
21. Sakthivel A, Abrantes M, Chiang AST, Kühn FE (2006) J Organomet Chem 691:1007

22. Jia M, Thiel WR (2002) Chem Commun p 2392
23. Jia M, Seifert A, Thiel WR (2003) Chem Mater 15:2174
24. Nunes CD, Valente AA, Pillinger M, Fernandes AC, Romão CC, Rocha J, Gonçalves IS (2002) J Mater Chem 12:1735
25. Sakthivel A, Zhao J, Raudaschl-Sieber G, Kühn FE (2005) J Organomet Chem 690:5105
26. Gonçalves IS, Santos AM, Romão CC, Lopez AD, Rodriguez-Borges JE, Pillinger M, Ferreira P, Rocha J, Kühn FE (2001) J Organomet Chem 626:1
27. Sakthivel A, Zhao J, Raudaschl-Sieber G, Hanzlik M, Chiang AST, Kühn FE (2005) Appl Cat A 281:267
28. Jia M, Seifert A, Berger M, Giegengack H, Schulze S, Thiel WR (2004) Chem Mater 16:877
29. Jia M, Seifert A, Thiel WR (2004) J Catal 221:319
30. Sherrington DC, Simpson S (1991) J Catal 131:115
31. Sherrington DC, Simpson S (1993) React Polym 19:13
32. Miller MM, Sherrington DC (1994) J Chem Soc Perkin Trans 2:2091
33. Miller MM, Sherrington DC (1995) J Catal 152:368
34. Ahn JH, Sherrington DC (1996) J Chem Soc Chem Commun p 643
35. Valente AA, Petrovski Z, Branco LC, Afonso CAM, Pillinger M, Lopez AD, Romão CC, Nunes CD, Gonçalves IS (2004) J Mol Catal A–Chem 218:5
36. Kühn FE, Zhao J, Abrantes M, Sun W, Afonso CAM, Branco LC, Gonçalves IS, Pillinger M, Romão CC (2005) Tetrahedron Lett 46:47
37. Kühn FE, Lopes AD, Santos AM, Herdtweck E, Haider JJ, Romão CC, Santos AG (2000) J Mol Catal A–Chem 151:147
38. Sakthivel A, Zhao J, Kühn FE (2005) Micropor Mesopor Mater 86:341
39. Abrantes M, Santos AM, Mink J, Kühn FE, Romão CC (2003) Organometallics 22:2112
40. Gago S, Pillinger M, Valente AA, Santos TM, Rocha J, Gonçalves IS (2004) Inorg Chem 43:5422
41. Zhao J, Sakthivel A, Santos AM, Kühn FE (2005) Inorg Chim Acta 358:4201
42. Sakthivel A, Zhao J, Kühn FE (2005) Bull Catal Soc India 4:79
43. Zhao XS, Lu GQ (1998) J Phys Chem B 102:1556
44. Tatsumi T, Koyano A, Tanaka Y, Nakata S (1998) Stud Surf Sci Catal 117:143
45. Miller MM, Sherrington DC (1994) J Chem Soc Chem Commun 55
46. Miller MM, Sherrington DC (1995) J Catal 152:377
47. Leinonen S, Sherrington DC, Sneddon A, McLoughlin D, Corker J, Canevali C, Morazzoni F, Reedjik J, Spratt SPD (1999) J Catal 183:251
48. Song CE, Roh EH (2000) Chem Commun p 837
49. Li Z, Xia C-G (2003) Tetrahedron Lett 44:2069
50. Li Z, Xia C-G, Ji M (2003) Appl Cat A–Gen 252:17
51. Kühn FE, Santos AM, Herrmann WA (2005) Dalton Trans p 2483
52. Buffon R, Leconte M, Basset J-M, Touroude R, Herrmann WA (1992) J Mol Catal A–Chem 72:139
53. Buffon R, Choplin A, Leconte M, Basset J-M, Touroude R, Herrmann WA (1992) J Mol Catal A–Chem 72:L7
54. Buffon R, Auroux A, Lefebvre F, Leconte M, Choplin A, Basset J-M, Herrmann WA (1992) J Mol Catal A–Chem 76:287
55. Zhu Z, Espenson JH (1997) J Mol Catal A–Chem 121:139
56. Bouh AO, Espenson JH (2003) J Mol Catal A–Chem 200:43
57. Li M, Espenson JH (2004) J Mol Catal A–Chem 208:123
58. Herrmann WA, Kuchler JG, Felixberger JK, Herdtweck E, Wagner W (1988) Anal Chem 27:394

59. Neumann R, Wang T-J (1997) J Chem Soc Chem Commun p 1915
60. Dallmann K, Buffon R (2000) Catal Commun 1:9
61. Nunes CD, Pillinger M, Valente AA, Gonçalves IS, Rocha J, Ferreira P, Kühn FE (2002) Eur J Inorg Chem p 1100
62. Sakthivel A, Raudaschl-Sieber G, Kühn FE (2006) Dalton Trans p 468
63. Wang T-J, Li D-C, Bai J-H, Huang M-Y, Jiang Y-Y (1998) J Macromol Sci Pure 35:531
64. Adam W, Saha-Möller CR, Weichold O (2000) J Org Chem 65:2897
65. Adam W, Mitchell CM (1996) Angew Chem Int Ed 35:533
66. Adam W, Mitchell CM, Saha-Möller CR, Weichold O (1999) J Am Chem Soc 121:2097
67. Saladino R, Carlucci P, Danti MC, Crestini C, Mincione E (2000) Tetrahedron 56:10031
68. Sica D, Musumeci D, Zollo F, de Marino S (2001) Eur J Org Chem 19:3731
69. Sica D, Musumeci D, Zollo F, de Marino S (2001) J Chem Soc Perkin Trans 1:1889
70. Herrmann WA, Wagner W, Flessner UN, Volkhardt U, Komber H (1991) Angew Chem Int Ed 30:1636
71. Herrmann WA, Fritz-Meyer-Weg DM, Wagner W, Kuchler JG, Weichselbaumer G, Fischer RW (Hoechst AG) (1992) US Patent 155 247
72. Saladino R, Neri V, Pellicia AR, Caminiti R, Sadun C (2002) J Org Chem 67:1323
73. Saladino R, Neri V, Pelliccia AR, Mincione E (2003) Tetrahedron 59:7403
74. Bernini R, Mincione E, Cortese M, Saladino R, Gualandi G, Belfiore MC (2003) Tetrahedron Lett 44:4823
75. Bianchini G, Crucianelli M, De Angelis F, Neri V, Saladino R (2004) Tetrahedron Lett 45:2351
76. Bianchini G, Crucianelli M, De Angelis F, Neri V, Saladino R (2005) Tetrahedron Lett 46:2427
77. Owens GS, Abu-Omar MM (2000) Chem Commun p 1165
78. Bernini R, Coratti A, Fabrizi G, Goggiamani A (2003) Tetrahedron Lett 44:8991
79. Rost AMJ, Schneider H, Zoller JP, Herrmann WA, Kühn FE (2005) J Organomet Chem 690:4712
80. Bein T, Huber C, Moller K, Wu CG, Xu L (1997) Chem Mater 9:2252
81. Owens GS, Abu-Omar MM (2002) J Mol Catal A–Chem 187:215
82. Owens GS, Durazo A, Abu-Omar MM (2002) Chem Eur J 8:3053

Top Organomet Chem (2007) 22: 79–95
DOI 10.1007/3418_055

Published online: 29 July 2006

The SOHIO Process as an Inspiration for Molecular Organometallic Chemistry

Christian Limberg

Institut für Chemie, Humboldt-Universität zu Berlin, Brook-Taylor-Straße 2, 12489 Berlin, Germany
christian.limberg@chemie.hu-berlin.de

Abstract In the SOHIO process, propene is oxidized with O_2 or ammonoxidised with O_2 and NH_3 to give acrolein and acrylonitrile, respectively. For both conversions bismuthmolydates are serving as catalysts, and organometallic surface intermediates containing allylmolybdenum units are suggested as intermediates. This review summarises attempts of the past 10 years to model these and other surface species with molecular compounds. Furthermore, recent achievements with respect to the modelling of potentially active Mo – O – Bi sites on bismuthmolybdate catalysts are presented: the first molecular compounds containing such moieties could be isolated due to a partial shielding of the metal centre by organic ligands.

Keywords Organometallics · Molybdenum · Bismuth · SOHIO · Model complexes · Metal oxo complexes

1 Introduction

Acrolein is needed industrially on a great scale, and to obtain it selectively from propene and O_2 various different heterogeneous catalysts have been investigated. In 1957–1962 Standard Oil of Ohio (SOHIO) developed the MoO_3/Bi_2O_3-catalyst system [1, 2], that did not lead to a high propene conversion but yielded a fairly good selectivity. Furthermore, acrylonitrile can be obtained instead of acrolein if NH_3 is added to the system (ammonoxidation of propene, Eq. 1).

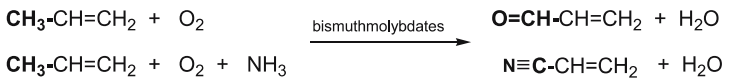

Equation 1

In the ensuing decades, catalyst performance has been significantly improved and the predominant commercial processes now use multicomponent catalysts that are still based on bismuth molybdates but which also contain metal oxide additives. Today, all of the US capacity and approximately 90% of the world capacity for acrylonitrile (ca. 5 mio t) is covered by the SOHIO process [3]. While the ammonoxidation of propene is highly selective, at present the maximum acrolein yield at high propene conversion (90–95%) using commercial catalysts is approximately 80% in average (acrylic acid forms as a byproduct with yields of 5–15%) [3]. Hence, despite the long history of the process an improvement of the selectivity is still desirable, as the capacities of acrolein production are rather high, too. However, neither the exact functioning of the mixed metal oxide catalysts employed nor the reasons for their uniqueness are clear today making their rational replacement by catalysts capable of reaching higher selectivities difficult. A summary of some mechanistic proposals made in the 1980s based on the results obtained in experiments with isotopically labelled substrates and spectroscopic investigations involving the actual heterogeneous catalysts themselves [4–8] is shown in Scheme 1. It is assumed that propene is coordinated/chemisorbed initially at the catalysts surface (**A**), followed by a rate-determining step in which an H atom is abstracted—presumably at a bismuth site (Bi = O, Bi – O – Bi, Bi – O – Mo; only Bi = O shown in Scheme 1, → **B**). This step that was proposed to be identical in both processes, oxidation and ammonoxidation of propene, leads to an allyl radical, that is π-bonded symmetrically at a molybdenum centre (**B**) before it is trapped in a fast subsequent step (**C**). Early work [4–8] assigned *terminal* oxo ligands (or imido ligands in the ammonoxidation, respectively) the role of the trapping site and this theory is still discussed today [4–11]. The results of more recent work [11–14], however, casted doubt on this contend: they put forward the alternative idea, that in heterogeneous oxidation catalysis with MoO_3/Bi_2O_3 (α-[Bi_2MoO_6]) *bridging* oxo ligands (or terminal ligands being in close contact to a second metal) might be the ultimate oxygenation sites, i.e., in the propene oxidation the allyl radical would then be trapped by a μ-oxo-type function at the metal. In any case, a subsequent second H atom transfer, probably to a Mo = O group (**D**), finally yields acrolein, and oxidation of the reduced catalyst with O_2 under elimination of water then leads back to the starting situation **A**. In the ammonoxidation a similar mechanism was proposed starting with the trapping of the allyl radical by a nitrogen-containing ligand (imido or amido) formed in-situ at the surface.

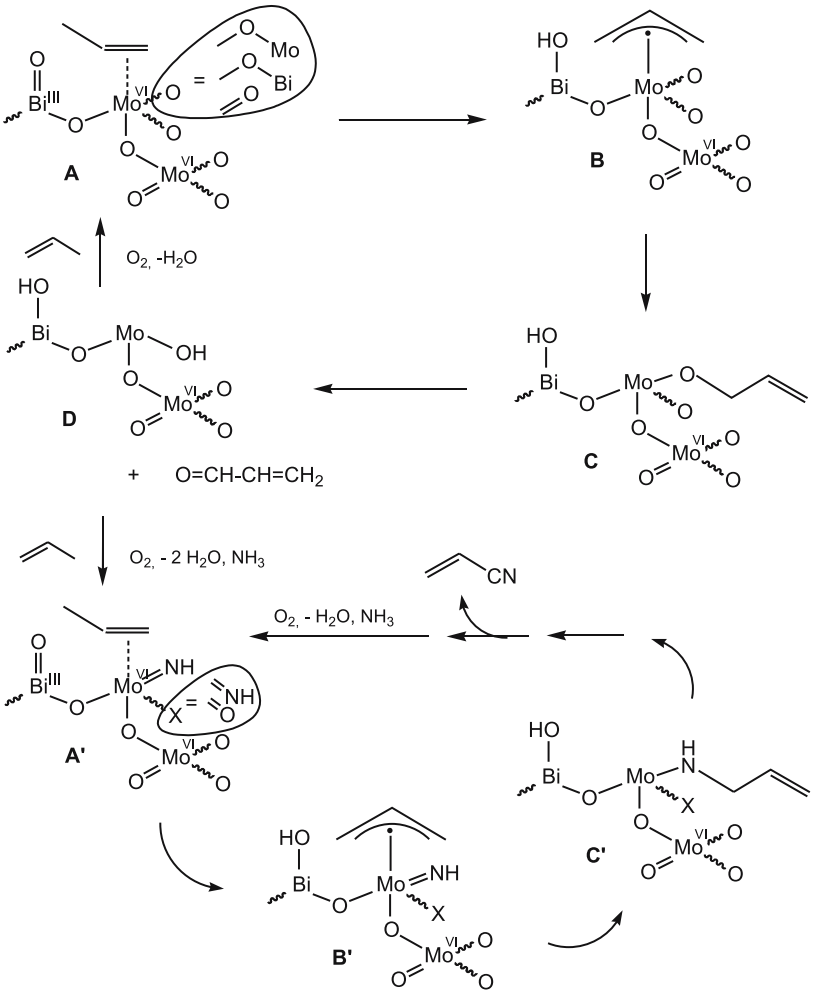

Scheme 1 Mechanistic proposals for the oxidation and ammonoxidation of propene on bismuthmolybdates

As the occurring short-lived intermediates (such as **A**–**D** and **A′**–**C′**, Scheme 1) occur on bismuthmolybdate surfaces, they are difficult to investigate or to identify directly, and at the end of the 1980s obviously a limit for the information available via investigations with the authentic catalysts was nearly reached [11]. However, the results of surface studies can represent an inspiration also for molecular chemists, and in the mid-1980s, the first molecular model compounds began to appear in the literature that had been prepared to support or dispute mechanistic postulates. Some accounts dealing with such model complexes have appeared already [11, 15–17]: the

most recent one [11] focuses on the role of bismuth in the SOHIO process and additionally covers models for the species **C/C′** as well as the state of the art for Mo/Bi models until the year 2003. With respect to Mo/Bi compounds, this review concentrates on the most recent literature, which afforded the first Mo – O – Bi complexes making use of the principles of organometallic chemistry. Furthermore, it summarises the activities of the last years concerning the organometallic intermediates **B/B′**.

2
Models for Surface Intermediates and Sites

2.1
Models for Intermediates B

Species **A** is proposed to consist of a high oxidation state Mo centre, embedded in a "hard" oxo environment, binding a π-accepting, soft organic ligand in addition. The latter combination naturally casted some doubt on this suggestion but nowadays such a species **A** does not appear as exotic as in the former times, bearing in mind that the last years spawned several precedent cases, where coordination of an olefin to a d^0-metal centre has been testified [18–23]. Moreover, the binding of olefins to $O = Mo^{IV}$-units [24] and interactions of olefins with $O = Mo^{V}$-moieties [25] have been demonstrated, too. Considering the reactivity proposed for **A** (**A**→ **B**) it has to be reemphasised that the H abstraction not necessarily has to proceed at Bi = O sites as shown in Scheme 1; Bi – O – Bi and Bi – O – Mo functions are discussed in this context, too, [11] as they could undergo M – O bond homolyses to give

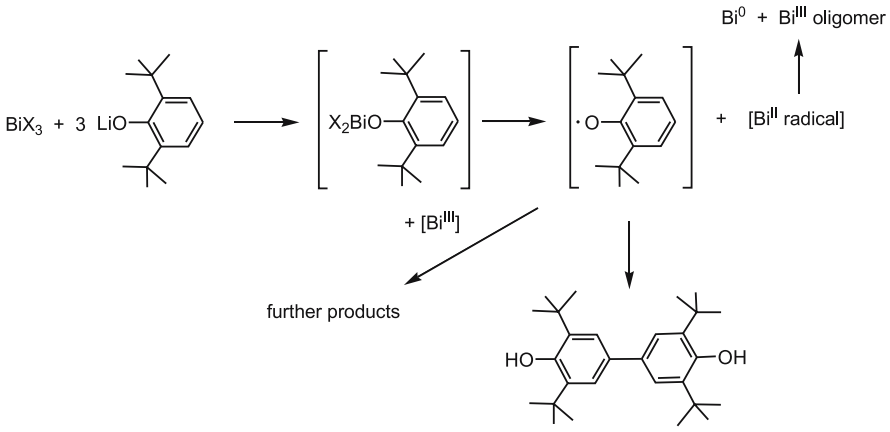

Scheme 2 Bond homolysis in bismuth aryloxides leading to Bi^{II} radicals

H abstracting M – O radicals, while the respective second metal is getting reduced (→ e.g., Bi^{II}). With this background, some recent model studies are noteworthy [26] showing that bismuth alkoxides, $Bi(OR)_3$, with bulky ligands (R = 2,6-di-*tert*-butylphenyl) decompose via homolytic Bi – O bond cleavage (Scheme 2) yielding unstable Bi^{II} radicals, as they are proposed to form by way of H atom abstraction from propene in the SOHIO process. Furthermore, investigating $Bi(OR)_3$ complexes an illustration of C – H activation using Bi^{III} could be given (Hanna TA, personal communication).

However, models for surface intermediates **B**, which according to Scheme 1 decompose to give allyloxymolybdenum complexes, are not yet known. This does not seem surprising as **B** was often termed "radical-like π-allylmolybdenum complex" [4–8], which could mean two things (and thus a formal assignment of oxidation states in Scheme 1 has been avoided): On the one hand it could be formulated as a chemisorbed radical weakly bound to a Mo^{VI}-centre. Alternatively, it is discussed, that the electron that is transferred together with a proton onto a Bi = O (or Bi – O – Mo) group, "flows back" to the Mo centre, thereby lowering its oxidation state to +V. This Mo centre is proposed to subsequently form a π-complex with the allyl radical, although stabilisation via back bonding is hardly possible for the electron deficient metal centre. However, considering that today the organometallic chemistry of metals also in their highest oxidation states as well as organometaloxo chemistry is well established [27–32] the occurrence of an intermediate with a π-allyl ligand bound to a Mo^{VI} centre under catalytic conditions today seems not as unrealistic as to the times of its first mentioning. Compounds designed to model these intermediates structurally or functionally should contain a π-allylmolybdenum group covalently bound to an oxo ligand as a minimum requirement, and one precedent case for a complex, fulfilling this requirement is worth mentioning [33]: Compound **1** (Structure 1) contains—in form of a $Mo_4(\mu\text{-}OH)_3(\mu\text{-}O)$-moiety—an oxomolybdenum core with allyl ligands bound at the surface. **1** shows an interesting fluxional behaviour in solution [33]: The allyl$(CO)_2$ ligand set rotates with respect to the oxygen donor set, and this might give an impression, how mobile allylmolybdenum

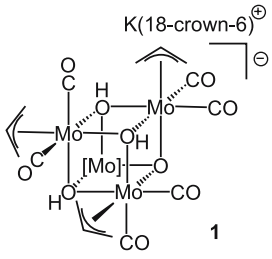

[Mo] = $(\pi\text{-}C_3H_5)(CO)_2Mo$

Structure 1

units could be also on the surfaces of molybdenum oxide solids. While **1** can thus be viewed as a structural model for **B**, its Mo atoms are all in the oxidation states +II and thus lower than those discussed for the corresponding centres in **B**. In fact, this will be the reason why **1** is stable, while **B** rapidly decomposes via an allyl shift.

In order to synthesize model complexes that are somewhat more authentic, it could certainly be attempted to simply raise the oxidation state, however, as outlined above, this would naturally cause problems with respect to the isolability, since the allyl-Mo unit would then certainly become very unstable and easily eliminate an allyl radical. To obtain tractable systems, thus a further measure of stabilization has to be applied to the system. One such measure could be the chelating effect, that is, it should be possible to fix the allyl ligand at a high valent Mo atom via a tether. The first experiments in this direction were performed [34] starting from high-valent molybdenum oxo complexes, and hence for the anchoring a hard oxo donor function (carrying a charge) was chosen. The latter was linked via an aryl ring as the tether to a propenyl residue, and the resulting aryloxide **PO**$^-$ was anticipated to represent a potential chelating aryloxo/olefin ligand. According to Eq. 2 employment of **POH** indeed led to a corresponding oxo molybdenum(VI)aryloxide **2** where, however, the olefin functions remained dangling, and it proved impossible to introduce them into the coordination sphere of the molybdenum centres [34]. Therefore an alternative route was followed, which did result in a high-valent allyl molybdenum complex as envisioned (albeit without oxo ligands) and thus in a proof of concept. Mo(II) complexes were employed as starting materials, which were supposed to be oxidized in a later step—after introduction of the tethered allyl ligand. In accordance with the lower oxidation state, a phosphane donor function was chosen instead of the O$^-$ function used before, and the resulting potential phosphane/olefin chelating ligand **PP** was first of all coordinated to a CpMoCl(CO) complex metal fragment (Eq. 3) [35]. As a cis/trans mixture of **PP** had been employed a corresponding cis/trans olefin complex mixture **3** was obtained. Both isomers could be separated from each other by crystallization. The trans complex represented the main prod-

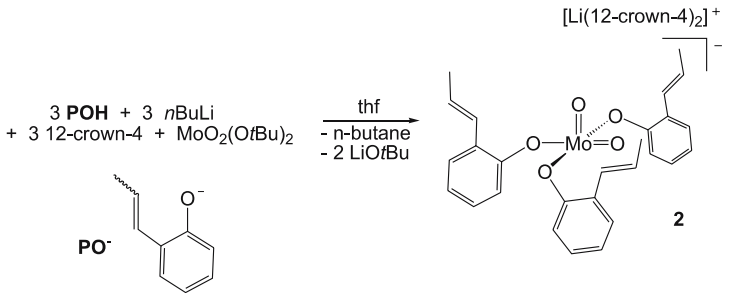

Equation 2

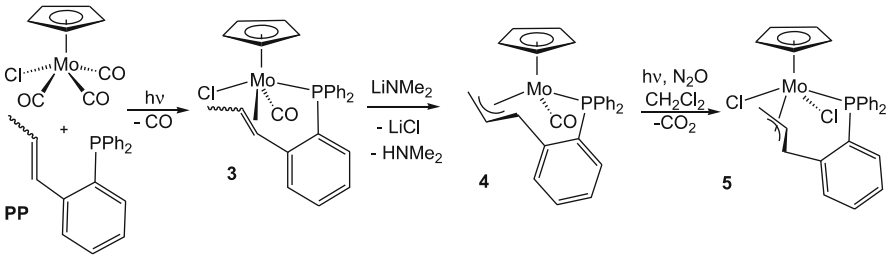

Equation 3

uct and its crystal structure already indicates that the methyl group of the propenyl unit and the chloride ligand are located in close proximity to each other. They are therefore ideally preorientated for an HCl elimination which in fact can be realized, if lithium dimethylamide is employed as the base—the olefin ligand is then converted into an allyl ligand so that **4** is formed [35]. **4** still contains a residual CO ligands that represent a point of attack for an increase of the Mo oxidation state through an oxidative elimination. Hence, **4** was photolysed in the presence of N_2O as a mild oxidant in CH_2Cl_2 solution. This indeed led to a complex with the oxidation state +IV but instead of the expected oxo ligand two chloride ligands were bound to the Mo centre. The latter have their origin in the solvent, and as dichloromethane is not known as an oxidizing solvent but rather as a source for HCl it is reasonable to assume that the original plan of introducing an oxo ligand had worked out. Then, however, the oxo ligand has been replaced by two chloride ligands in the course of a reaction with HCl under elimination of water [35]. So far a few allyl molybdenum(IV) compounds are known (see discussion in [35]) which, however, all exclusively wear organic ligands. The latter make the molybdenum centres—despite their comparatively high oxidation states—reasonably soft, so that an additional allyl ligand is bound strongly. **5** contains two "hard" chloride ligands in addition to the allyl ligand; nonetheless it is stable due to the posphane tether. Attempts to isolate comparable complexes lacking a tether—like [AllylMoBr_2(Cp)CO]—failed [36]. Hence, the tethering concept was successful, and currently attempts are made to use it for the preparation of isolable allyl(oxo)molybdenum(IV/V/VI) complexes.

There is of course another strategy that can be applied for the preparation of functional model compounds: instead of increasing the oxidation state at the allyl binding Mo centre allylmolybdenum(II) units could be connected to *Mo^{VI}centres via oxo ligands* to achieve a weakening of the allylmolybdenum bonds, which in this form are easily cleaved homolytically, for instance by warming. A situation comparable to the one of **B** could this way be generated in situ and it seemed interesting to investigate how the individual components (allyl radical and molybdenumoxo unit) behave. Hence, **6** was synthesised [37, 38] as a representative compound (Eq. 4) containing a moi-

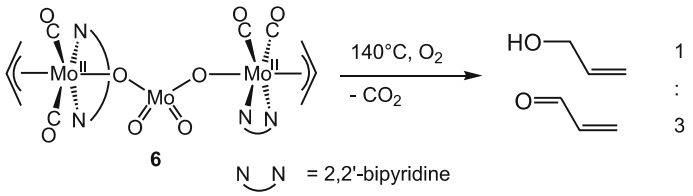

Equation 4

eties as mentioned above (oxo bridges between allylmolybdenum units and a Mo^{VI} centre). The Mo^{VI} centre in **6** enhances the model character in comparison to **1**, already, and indeed on warming **6** generates allyl radicals, which, however, are not trapped by the oxo ligands. They rather abstract hydrogen atoms to yield propene. No immediate conclusions should be drawn from such a finding to the mechanism of the propene oxidation during the SOHIO process, since—although the constitution of the model is already quite acceptable—there remains a topological problem: while the allyl and oxo groups are located in close proximity on the catalysts surface, they receive a maximum of separation within **6**, so that competing reaction paths gain in importance. Nevertheless, **6** can also serve to generate neighboring allyl and oxo groups in-situ if O_2 is admitted to the system, as this leads to the oxidation of the CO ligands to CO_2 and thus to a replacement of CO by O^{2-} [39]. This increases the oxidation state of the molybdenum atom and leads to a concomitant production of allyl radicals, so that allylmolybdenum carbonyl complexes in a dioxygen atmosphere can act—in principle—as sources for both, allyl radicals and high-valent molybdenum oxo species. Thermolysis of **6** in the presence of O_2 yielded as the volatile products not only allylalcohol but also acrolein [16, 17]. Accordingly, not only the generation and trapping of allyl radicals has been achieved but also a reaction in analogy to the subsequent step (**B** $\rightarrow$ **C**) in Scheme 1, the second H atom abstraction to give acrolein. Hence, a molybdenum compound like **6** is capable of mimicking the steps **B** $\rightarrow$ **D** of the mechanism in Scheme 1.

2.2 Models for Intermediates B′

An intermediate proposed to occur during the ammonoxidation of propene and that would correspond to the intermediate **B** suggested for the oxidation of propene is **B′** as shown in Scheme 1. Compounds designed to model these intermediates structurally or functionally should contain a π-allylmolybdenum group covalently bound to an imido ligand as a minimum requirement, ideally an oxo ligand should be bound in addition.

M.L.H. Green et al. were able to prepare a [$CpMo^{IV}(=NR)(\pi$-allyl)] complex (**7** in Structure 2) [40]. J. Sundermeyer et al. reported the synthesis of

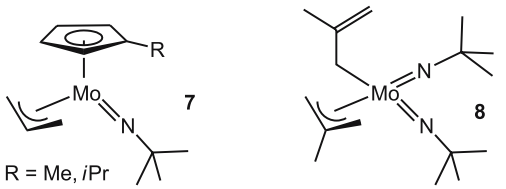

Structure 2

the compound $[(t\text{-BuN}=)_2Mo^{VI}(metallyl)_2]$, which could not be characterised structurally, but spectroscopic investigations hinted to a π-coordination of one of the allyl ligands (**8** in Structure 2) [41]. Since the bismuthmolybdate surface during the SOHIO process might contain both oxo and imido ligands at Mo^{VI} sites beside each other [4–10, 15] complexes containing O=Mo=NR units that are capable of binding olefin or allyl ligands are of special interest. However, as the oxo ligand therein makes the metal centre "harder" in comparison to a situation where the first imido ligand is joined by a Cp ligand (**7**) or a second imido ligand (**8**, vide supra), it should be more difficult to coordinate the "soft" organic functions. Bearing in mind that it has proved possible to isolate an allylmolybdenum(IV) complex with "hard" co-ligands via tethering of the allyl ligand to a coordinating donor function [35], the question arose whether allyl and/or olefin ligands could be stabilised in the coordination sphere of oxo/imido molybdenum complex metal fragments, when these are tethered to the imido ligand. Hence, the syntheses of a mixed oxo/imido molybdenum(VI) complex with a pendant olefin arm was pursued, as such a compound would contain all ingredients to model the situation where propene binds to the above-mentioned $O = Mo^{VI} = NH$ units before the first H atom abstraction occurs during the SOHIO process. A complex containing

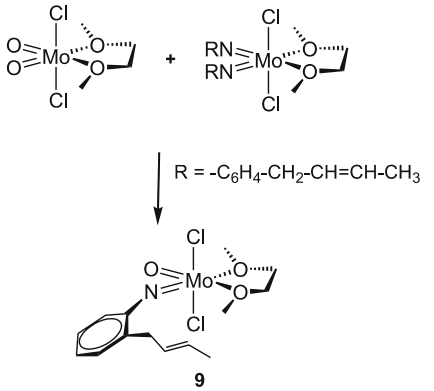

Equation 5

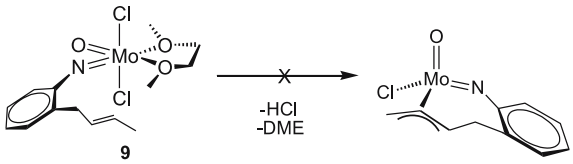

Equation 6

the $O = Mo^{VI} = N - C_6H_4 - CH_2 - CH = CH - CH_3$ moiety would thus contain all "ingredients" to model such a situation. Indeed, it proved possible to synthesise such a compound $[Cl_2Mo(= O)(= N - C_6H_4 - CH_2 - CH = CH - CH_3)(dme)]$, **9**, either by treatment of Na_2MoO_4 with $H_2N - C_6H_4 - CH_2 - CH = CH - CH_3$ and trimethylchlorosilane, or via synthesis of the corresponding diimido compound that can then be reacted with the dioxo complex $[(dme)Cl_2Mo(= O)_2]$ according to Eq. 5 [42].

In principle, **9** is ideally suited for an abstraction of an anionic ligand to coordinate the pendant olefinic function or even additional proton abstraction (→ altogether HCl elimination) to convert it into an allyl ligand (Eq. 6). However, so far, attempts to realise any kind of interaction were unsuccessful; possibly the ligand chosen is not suited to bind to a Mo^{VI} centre in a chelating allyl/imido or olefin/imido mode.

3
Models for Mo – O – Bi Sites on Bismuthmolybdate Surfaces

Naturally, homometallic molybdenum compounds cannot model the first step in the catalytic cycle—the primary H atom abstraction, which undoubtedly proceeds with bismuth participation (Bi = O, Bi – O – Bi, Bi – O – Mo) [11]. Bi might be involved in another step, too: it is not clear yet whether the allyl radical generated is trapped by a Mo = O, a Mo – O – Mo or else by a Mo – O – Bi moiety [11]. In so far it seemed of course very interesting to gain access to *molecular* Mo – O – Bi compounds in order to see how those behave and whether any conclusions can be drawn for the corresponding surface sites.

Bearing in mind that the synthesis of the first Mo/Bi alkoxides could be achieved by shielding part of the coordination sphere at the Mo centres by organic ligands [43–50], a similar approach was pursued in order to prepare the first Mo – O – Bi complexes.

3.1
Complexes with an Oxo Bridge Between Mo^{VI} and Bi^{V}

Motivating in this context was an older publication [51] by W.G. Klemperer et al.: they reported in 1980 that the reaction between $[Ph_3BiBr_2]$ and two

equivalents of $[Bu_4N]_2[MoO_4]$ leads to a salt whose anion is composed of Ph_3Bi and molybdate units. A formula $[NBu_4]_2[Ph_3Bi(MoO_4)_2] \cdot 3H_2O$ was deduced from the results of elemental analysis, IR- and NMR spectroscopy, and ^{17}O-NMR data hinted to the existence of Bi – O – Mo moieties, however, no structural evidence was given [51].

Hence, it seemed plausible to follow the strategy that had led to the successful isolation of the first Mo/Bi alkoxides already: the introduction of organic ligands, i.e., the replacement of the "naked" hard molybdate as starting material by an organomolybdate, namely $[Cp^*MoO_3]^-$. Treatment of $[Ph_3BiBr_2]$ with $[NBu_4][Cp^*MoO_3]$ provided in a clean reaction the desired metathesis product $[Ph_3Bi\{\mu\text{-}O - MoO_2Cp^*\}_2]$, **10**, which was isolated in pure crystalline form (Eq. 7) [52, 53], so that for the first time a Mo – O – Bi unit could be structurally characterised in a molecular compound.

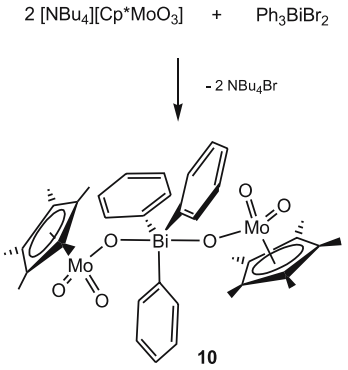

10

Equation 7

The X-ray crystal structure analysis showed, that the Bi atom is located at the centre of a slightly distorted trigonal bipyramid, in which the oxygen atoms occur at the apical sites. The Mo – O – Bi moieties are bent (Mo – O – Bi 139.5(3) and 152.8(3)°). Compounds like **10** seem to be unstable, when a solution containing them is heated above approximately 60 °C and decompose with the formation of the corresponding hydroxyarenes, $[(Cp^*MoO_2)_2O]$ and Bi^{III} molybdate anions like **17** (Eq. 10; Roggen and Limberg, personal communication).

The successful isolation of **10**, that apparently—rather paradoxically—was enabled by the embedding of the hard $Mo^{VI} - O - Bi^{V}$ unit in a shell of soft organic ligands represented a major step forward with regard to the development of model compounds, however, bearing in mind the original goal, the mimicking of catalytically relevant bismuthmolybdate surface species in molecular compounds **10** still exhibits a flaw: the bismuth centre is in the oxidation state +V which is only considered to be relevant during the SOHIO process by a minority [9, 10]. Hence, the next target was obvious:

3.2 Complexes with an Oxo Bridge Between Mo^{VI} and Bi^{III}

Prior to the organometallic Mo – O – Bi^{V} chemistry described in Sect. 3.1 and the successive work that finally led to the first covalent Mo – O – Bi^{III} compounds discussed in the second part of this chapter, some complexes had been reported containing $MoOBi^{III}$ units that can be considered rather a hybrid between Mo – O – Bi and Mo = O···Bi moieties.

In $[NBu_4]_3[Bi\{Mo_5O_{13}(OMe)_4(NO)\}_2]$, **11** [54] a Bi^{III} cation is surrounded by eight O atoms in form of two monovacant Lindqvist-type-nitrosyl polyoxomethoxomolybdates ($[Mo_5O_{13}(OMe)_4(NO)]^{3-}$). **11** is prepared by the reaction between equimolar amounts of $[NBu_4]_2[\{Na(MeOH)\}Mo_5O_{13}(OMe)_4(NO)]\cdot 3$ MeOH and $BiCl_3$ and its crystal structure is shown in Fig. 1.

More recently, some other compounds containing polyoxometallates coordinated to Bi^{III} were reported by U. Kortz et al., who investigated the interactions of amino acids with polyoxomolybdates in the presence of *inter alia* Bi^{3+}-ions [55, 56]. A series of ionic compounds with anions of the general formula $[XMo_6O_{21}(\text{amino acid})_3]^{3-}$ (X = As^{III}, Sb^{III}, Bi^{III}) were prepared. In case of the bismuth derivatives the amino acids $HOOC(CH_2)_nNH_2$ (n = 1, 2, 3) and L– $HOOCCH[(CH_2)_4NH_2]NH_2$ were reacted with Na_2MoO_4, Bi_2O_3 and KCl in an aqueous medium (Eq. 8).

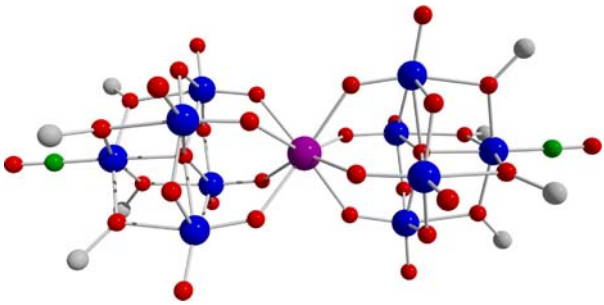

Fig. 1 Molecular structure of the anion $[Bi\{Mo_5O_{13}(OMe)_4(NO)\}_2]^{3-}$ in **11**

$$6\ Na_2MoO_4 + {}^1/_2\ Bi_2O_3 + 6\ \textit{amino acid} + 6\ KCl \xrightarrow[pH = 3.5]{} K_3[BiMo_6O_{21}(\textit{amino acid})_3]$$

amino acid =	$HOOCCH_2NH_2$	**12**
	$HOOC(CH_2)_2NH_2$	**13**
	$HOOC(CH_2)_3NH_2$	**14**
	L-$HOOCCH[(CH_2)_4NH_2]NH_2$	**15**

Equation 8

Samples of $K_3[BiMo_6O_{21}\{O_2C(CH_2)_nNH_3\}_3]$, ($n = 1$ **12**, 2 **13**, 3 **14**) were obtained in good yields, while for the isolation of a $[BiMo_6O_{21}(L\text{–}O_2CCH[(CH_2)_4NH_2]NH_3\}_3]^{3-}$ salt additional treatment of **15** with CsCl was necessary, thus allowing for the isolation of a corresponding Cs-salt. As single crystal X-ray analyses could not be performed for the Bi compounds, their molecular geometry was deduced from IR-spectroscopic data as well as from the X-ray crystal structures determined for the related compounds with As^{III} and Sb^{III}. On this basis the polyanions $[BiMo_6O_{21}(\text{amino acid})_3]^{3-}$ were suggested to contain bismuth atoms surrounded by a ring of six MoO_6 octahedra which alternately share edges and corners. Each of the three amino acid molecules is bound as zwitterion to two edge-sharing Mo centres via its carboxylate group on the same side of the ring. The central heteroatom, located slightly above the plane of the six molybdenum atoms, is coordinated by three μ_3-oxo groups which leads to a trigonal-pyramidal coordination geometry [55, 56].

In this context is might also be worth mentioning that the importance of the bismuthoxo component in the SOHIO catalysts also provided the impetus for more general studies concerning the synthesis of molecular bismuthoxo compounds (clusters), their structures and their behaviour in dependence of the cluster size [57–61].

This was the state of the art until the year 2005 that led to the first structural characterisation of a $Mo-O-Bi^V$ complex as described in Sect. 3.1. Bearing in mind the experiences made in Bi^V chemistry, the route to corresponding Bi^{III} compounds seemed to be straight forward: the reaction of Ph_2BiBr with $[NBu_4][Cp^*MoO_3]$. However, Bi^{III} compounds such as Ph_2BiBr are Lewis acidic and readily accept an additional anionic ligand to form a hypervalent compound. Hence, the $[NBu_4]Br$ generated in the metathesis reaction was trapped by unconsumed starting material leading to a non-uniform course of the reaction, and besides $[NBu_4][Ph_2BiBr_2]$ no other pure compound could be isolated from the mixture [52, 53]. It was therefore decided to employ $[(o\text{-tolyl})_2Bi(hmpa)_2]SO_3CF_3$ (o-tolyl = 2-$(CH_3)C_6H_4$) instead of Ph_2BiBr as the starting material, as it seemed to offer several advantages with respect to the above-mentioned problems: The o-tolyl residues are sterically somewhat more demanding than phenyl residues are, the hmpa ligands can occupy vacant coordination sites where necessary, and moreover in contrast to halide ions triflate anions are very weak ligands. The reaction between $[(o\text{-tolyl})_2Bi(OTf)(hmpa)_2]$ and one equivalent of $[NBu_4][Cp^*MoO_3]$ indeed afforded the first $Mo-O-Bi^{III}$ complex $[\{(o\text{-tolyl})_2Bi\}\text{-}\mu\text{-}O-MoO_2Cp^*]_n$, **16**, [52, 53] in a clean conversion. $[NBu_4]$ SO_3CF_3 was eliminated and hmpa ligands can be found in **16** neither, so that initially the fictive molecule $(o\text{-tolyl})_2Bi\text{-}\mu\text{-}O-MoO_2Cp^*$ (bold in Eq. 9) will have formed. However, the latter contains Lewis basic $Mo=O$ groups on the one end and a Lewis acidic Bi^{III} centre being prone to undergo secondary bonding on the other end, and such a situation naturally leads to a coordination polymer as depicted

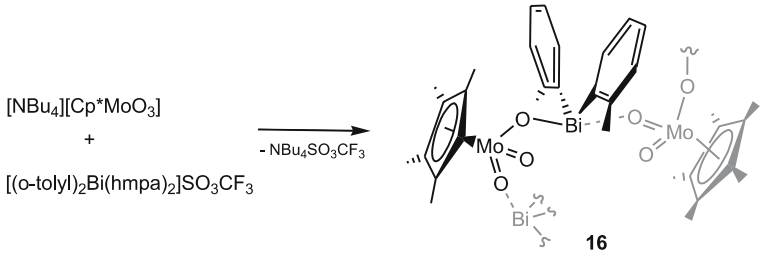

Equation 9

in Eq. 9. The O – Bi···O is nearly linear (170.46(9)°) indicating a strong secondary Mo = O···Bi bond. This is further reflected in the great similarity of the primary Bi – O and secondary Bi···O bond (2.310(2) and 2.385(2) Å, respectively).

As many coordination polymers **16** is only sparingly soluble in most organic solvents so that attempts were made to break it up in order to get more soluble compounds. Hyphenation points would be the bonds where the Lewis acidic Bi centres are coordinatively saturated by Mo = O units of "neighbouring molecules"—very efficiently considering that hmpa ligands could be found theoretically at these position, too. Hence, contemplating external donors Mo=O donor functions suggest themselves, and the obvious reagent was yet again $[NBu_4][Cp^*MoO_3]$.

If a suspension of **16** in CH_2Cl_2 is reacted with one equivalent of $[NBu_4][Cp^*MoO_3]$ a bright yellow solution is formed. Evaporation of the solvent yields the ionic compound $[NBu_4][(o\text{-tolyl})_2Bi(\mu\text{-O} - MoO_2Cp^*)_2]$, **17** [62] as anticipated (Eq. 10).

In the anion of **17** two $Cp^*MoO_3^-$ moieties are bound via an oxygen atom to a $(o\text{-tolyl})_2Bi^+$-fragment forming a 10 electron four-coordinate bismuth centre. As anticipated coordination of the second Cp^*MoO_3 unit saturates the Lewis acidity of the Bi^{III} centre thereby avoiding the formation of a polymeric structure as in **16**. Even though **17** is a monomeric complex the

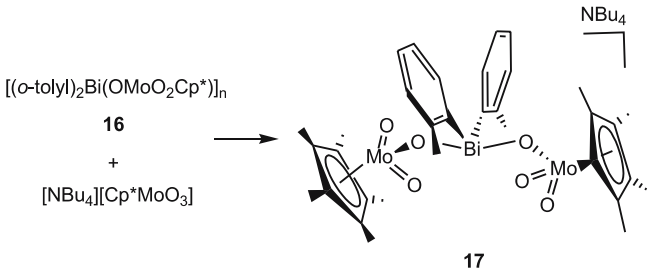

Equation 10

overall coordination geometry of **17** is very similar to the one observed in polymeric **16.**

At that stage, the access to molecular Mo – O – Bi^{III} and Mo – O – Bi^{V} compounds finally seemed to have been achieved, and curiosity concerning the constitution of the original Klemperer compound $[NBu_4]_2[Ph_3Bi(MoO_4)_2]\cdot 3H_2O$ [51] resurrected. The synthesis starting from triphenylbismuthdibromide and molybdate was therefore revisited under strictly anhydrous conditions to avoid formation of a water solvate. Indeed, anhydrous $[NBu_4]_2[Ph_3Bi(OMoO_3)_2]$, **18**, was obtained (Eq. 11), also in form of single crystals so that its crystal structure could be determined [62].

The crystals of **18** contain discrete molecular dianions which exhibit a crystallographical C_2-axis. Surprisingly, in contrast to **10** the Mo – O – Bi moieties are nearly linear (Mo – O – Bi 173.6(2)°), while remaining structural features are similar to those of **10** [62]. For an explanation, DFT calculations were carried out on the B3LYP/Lanl2dz level of theory. Analysis of the charge distribution revealed that both the bridging O atoms and the Bi centre carry unusually high charges (O: – 1.142 and Bi: 2.497, respectively), a feature that hints to ionic MoO/Bi interactions, and indeed an NBO analysis failed to detect a hybrid orbital between Bi and O. The interaction is thus of an electrostatic nature, and this is the explanation for the linear Mo – O – Bi arrangement. This finding naturally called for corresponding investigations concerning the compounds **10**, **16** and **17**. Exemplarily, **17** was chosen, whose crystal structure results were used as starting geometry for calculations using DFT-methods. An NBO analysis revealed a charge distribution between the O and Bi atoms that supports a covalent bonding within the Mo – O – Bi units [62].

Hence, the last 3 years have finally brought access to organometallic complexes with covalent Mo – O – Bi moieties—a previously unknown and long-

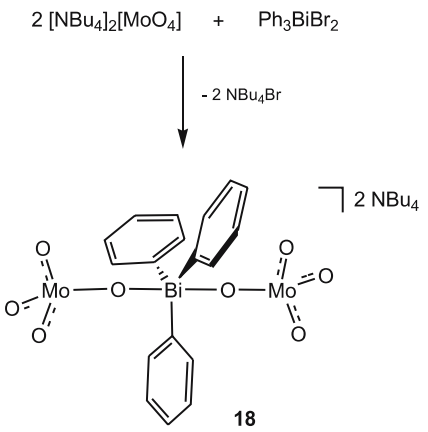

18

Equation 11

sought class of compounds—so that finally their chemical properties can be explored on the molecular level, i.e., their behaviour in the presence of hydrocarbons like olefines, substrates with weak C – H bonds as well as organic radicals, to fathom their potential as functional models for Mo – O – Bi units on bismuthmolybdate surfaces.

4 Conclusions

In conclusion, the mechanism proposed to be active during the SOHIO process represents a copious stimulus for the synthesis of novel complexes that may display interesting reactivities. These compounds are worthwhile objects of study in their own right, but they might as well be regarded as models that can help to confirm or dispute mechanistic suggestions and potential intermediates. This review has focused on intermediates **B/B′** as well as on Bi – O – Mo active sites; others gave an overview concerning intermediates **C/C′** and the step **A**→**B** [11]. The combined research performed so far on this topic has laid the basis for even more elaborate models—that may even prove to be active as (homogeneous) catalysts themselves—and for reactivity studies in the future.

References

1. Idol JD (1959) US Patent No. 2,904,580
2. Callahan JL, Foreman RW, Veatch F (1962) US Patent No. 3,044,966
3. Arntz D, Höpp M, Jacobi S, Sauer J, Ohara T, Sato T, Shimizu N, Prescher G, Schwind H, Weiberg O (2002) In: Ullmann's Encyclopedia of Industrial Chemistry. Wiley, Weinheim
4. Keulks GW, Krenzke LD, Notermann TM (1978) Adv Catal 27:183
5. Grasselli RK, Burrington JD (1981) Adv Catal 30:133
6. Grasselli RK, Burrington JD (1984) Ind Eng Chem Prod Res Dev 23:394
7. Anderson AB, Ewing DW, Kim Y, Grasselli RK, Burrington JD, Brazdil JF (1985) J Catal 96:222
8. Grasselli RK (1997) In: Ertl G, Knozinger H, Weitkamp J (eds) Handbook of Heterogeneous Catalysis. VCH Verlagsgesellschaft mbH, Weinheim, p 2302
9. Jang YH, Goddard WA III (2002) J Phys Chem B 106:5997
10. Jang YH, Goddard WA III (2001) Top Catal 15:273
11. Hanna TA (2004) Coord Chem Rev 248:429
12. Ono T, Ogata N, Mijaryo Y (1996) J Catal 161:78
13. Ono T, Numata H, Ogata N (1996) J Mol Catal 105:31
14. Nugent WA, Mayer JM (eds) (1988) Metal-Ligand Multiple Bonds. Wiley, New York
15. Belagem J, Osborn JA, Kress J (1994) J Mol Catal 86:267
16. Limberg C (2003) Angew Chem 115:6112
17. Limberg C (2003) Angew Chem Int Ed 42:5932
18. Kress J, Osborn JA (1992) Angew Chem 104:1660

19. Kress J, Osborn JA (1992) Angew Chem Int Ed 31:1585
20. Casey CP, Hallenbeck SL, Pollock DW, Landis CR (1995) J Am Chem Soc 117:9770
21. Witte PT, Meetsma A, Hessen B (1997) J Am Chem Soc 119:10561
22. Nalewajski RF, Michalak A (1996) J Phys Chem 100:20076
23. Wu Z, Jordan RF, Peterson JL (1995) J Am Chem Soc 117:5867
24. Mayer JM, Hall KA (1992) J Am Chem Soc 114:10402
25. Limberg C, Boese R, Schiemenz B (1997) J Chem Soc, Dalton Trans, p 1633
26. Hanna TA, Rieger AL, Rieger PH, Wang X (2002) Inorg Chem 41:359
27. Compare contributions of Kühn F, Herrmann WA and Theopold K in this volume
28. Adam W, Putterlik J, Schuhmann RM, Sundermeyer J (1996) Organometallics 15:4586
29. Pfennig V, Seppelt K (1996) Science 271:626
30. Radius U, Sundermeyer J (1992) Chem Ber 125:2183
31. Sundermeyer J, Putterlik J, Pritzkow H (1993) Chem Ber 1993 126:289
32. Schrock RR (2002) Chem Rev 102:145
33. Borgmann C, Limberg C, Cunskis S, Kircher P (2001) Eur J Inorg Chem 349
34. Wippert-Rodrigues C, Limberg C, Pritzkow H (2004) Eur J Inorg Chem 3644
35. Wippert Rodrigues C, Antelmann B, Limberg C, Pritzkow H (2001) Organometallics 20:1825
36. Faller JW, Ma Y (1986) Organometallics 5:1949
37. Borgmann C, Limberg C, Zsolnai L (1998) Chem Commun, p 2729
38. Wippert-Rodrigues C, Limberg C, Pritzkow H (2004) Chem Commun, p 2734
39. Almond MJ (1994) Chem Soc Rev, p 309
40. Green MLH, Konidaris PC, Mountford P (1994) J Chem Soc, Dalton Trans, p 2975
41. Radius U, Sundermeyer J, Peters K, Schnering HG v (2002) Z Anorg Allg Chem 628:1226
42. Siewert I, Limberg C, Ziemer B (2006) Z Anorg Allg Chem 632:1078
43. Hunger M, Limberg C, Kircher P (1999) Angew Chem 111:1171
44. Hunger M, Limberg C, Kircher P (1999) Angew Chem Int Ed 38:1105
45. Hunger M, Limberg C, Kircher P (2000) Organometallics 19:1044
46. Hunger M, Limberg C, Kaifer E, Rutsch P (2002) J Organomet Chem 641:9
47. Limberg C, Hunger M, Habicht W, Kaifer E (2002) Inorg Chem 41:3359
48. Roggan S, Schnakenburg G, Limberg C, Sandhöfner S, Pritzkow H, Ziemer B (2005) Chem Eur J 11:225
49. Roggan S, Limberg C, Ziemer B, Brandt M (2004) Angew Chem 116:2906
50. Roggan S, Limberg C, Ziemer B, Brandt M (2004) Angew Chem Int Ed 43:2846
51. Klemperer WG, Liu RS (1980) Inorg Chem 19:3863
52. Roggan S, Limberg C, Ziemer B (2005) Angew Chem 117:2
53. Roggan S, Limberg C, Ziemer B (2005) Angew Chem Int Ed 44:5259
54. Villanneau R, Proust A, Robert F, Gouzerh P (1999) J Chem Soc, Dalton Trans, p 421
55. Kortz U, Savelieff MG, Abou Ghali FY, Khalil LM, Maalouf SA, Sinno DI (2002) Angew Chem 114:4246
56. Kortz U, Savelieff MG, Abou Ghali FY, Khalil LM, Maalouf SA, Sinno DI (2002) Angew Chem Int Ed 41:4070
57. Mansfeld D, Mehring M, Schürmann M (2005) Angew Chem 117:250
58. Mansfeld D, Mehring M, Schürmann M (2005) Angew Chem Int Ed 44:245
59. Mehring M, Mansfeld D, Paalasmaa S (2006) Eur J Inorg Chem 735
60. Mehring M, Mansfeld D, Paalasmaa S (2006) Chem Eur J 12:1767
61. Mehring M, Palasmaa S, Schurmann M (2005) Eur J Inorg Chem 4891
62. Roggan S, Limberg C, Brandt M, Ziemer B (2005) J Organomet Chem 690:5282

Top Organomet Chem (2007) 22: 97–124
DOI 10.1007/3418_045

Published online: 16 September 2006

Catalysis and Organometallic Chemistry of Rhodium and Iridium in the Oxidation of Organic Substrates

Cristina Tejel (✉) · Miguel A. Ciriano

Departamento de Química Inorgánica, Instituto de Ciencia de Materiales de Aragón, CSIC-Universidad de Zaragoza, Pedro Cerbuna 12, 50009 Zaragoza, Spain
ctejel@unizar.es

Abstract The purpose of this chapter is to present a survey of the organometallic chemistry and catalysis of rhodium and iridium related to the oxidation of organic substrates that has been developed over the last 5 years, placing special emphasis on reactions or processes involving environmentally friendly oxidants. Iridium-based catalysts appear to be promising candidates for the oxidation of alcohols to aldehydes/ketones as products or as intermediates for heterocyclic compounds or domino reactions. Rhodium complexes seem to be more appropriate for the oxygenation of alkenes. In addition to catalytic allylic and benzylic oxidation of alkenes, recent advances in vinylic oxygenations have been focused on stoichiometric reactions. This review offers an overview of these reactions

as well as some comments on key questions related to achieving the desired C – O bond formation.

Keywords Rhodium · Iridium · Catalysis · Oppenauer-type oxidations · Allylic oxygenations · Oxetanes · Dioxolanes · N-based ligands · Dioxygen · Hydrogen peroxide

1 Introduction

Oxidation of organic compounds is a basic tool in chemistry, covering a broad spectrum of stoichiometric and catalytic reactions ranging from the production of bulk chemicals to chiral compounds in which enantioselectivity is of particular importance. However, oxidation reactions yielding valuable products from organic raw materials are one of the most problematic transformations, although they constitute industrial core technologies. In particular, converting the basic materials of the industry, olefins and hydrocarbons, into oxygenated species such as alcohols, diols, epoxides, and carbonyl compounds is of general importance [1]. Moreover, the current main challenge and the goal in oxidation is to carry out these reactions with no waste and using environmentally friendly oxidants such as oxygen [2] or hydrogen peroxide [3, 4], which require new, selective, and efficient catalytic processes.

The most widely developed catalytic methods in oxidation involve complexes of the early and middle transition metals, generally in high-oxidation state and some late transition metals such as palladium and copper [5], but this is a wide field and under continuous development [6]. Rhodium and iridium compounds are less known as oxygenation catalysts than other metals, although their ability to form dioxygen complexes and their use as hydrogen transfer catalysts has been known of for a long time [7, 8]. However, after promising initial reports in the 1980s and early 1990s, they were then overlooked until quite recently when new results began to appear.

In this chapter we describe recent developments in the catalytic dehydrogenation of alcohols and related reactions as well as the organometallic chemistry of rhodium and iridium based on the oxygenation of coordinated alkenes.

2
Catalytic Oxidations Based on Rhodium and Iridium

2.1
Historical Background

2.1.1
Oxygenation of C = C Bonds

Most of the catalytic studies on the oxygenation of alkenes were carried out in the 1970s and 1980s in which typical rhodium complexes [9, 10] such as $[RhCl(PPh_3)_3]$ [11], or even $Rh^{III}Cl_3$ [12–14] with or without co-catalysts (Cu^{II} [14, 15] or Bi^{III} [16]), and some iridium compounds such as $[\{Ir^{III}(\mu\text{-}Cl)HCl(cod)\}_2]$ [17] were used as catalyst precursors.

Rhodium complexes were generally found to be more effective than iridium, but on the whole they show moderate activity in alkene oxygenation reactions. Significantly, epoxides, a typical product of the oxidation of olefins catalyzed by the middle transition metals, have rarely been evoked as products [18–22]. Although allylic alcohols [23] or ethers [24] have sometimes been described as products, the above cited rhodium and iridium complexes are characterized by an excellent selectivity in the oxygenation of terminal alkenes to methyl ketones.

With the exception of the binary system $RhCl_3/Cu(ClO_4)_2$ [9, 24], which incorporates the two atoms of dioxygen to the substrate (dioxygenase activity) (Eq. 1) all the rest show monooxygenase activity, incorporating only one oxygen atom to the substrate.

$$2\ R\text{-}CH{=}CH_2 + O_2 \xrightarrow[EtOH,\ 20 - 80^{\circ}\ C]{RhCl_3 + Cu(ClO_4)_2} 2\ R\text{-}CO\text{-}CH_3$$

Equation 1

The second oxygen atom is trapped either by PPh_3 to $OPPh_3$ [11] (Eq. 2a), or with H_2 to H_2O [25] (Eq. 2b), or more commonly by alcohols [26] that behave as two hydrogen donors to give H_2O and the corresponding aldehyde/ketone (Eq. 2c).

From a mechanistic point of view, the behavior of these catalysts represents a complicated puzzle [27], still poorly understood today, in which the original proposed catalytic cycles reveal several critical points in the light of present

$$R\text{-}CH{=}CH_2 + PPh_3 + O_2 \xrightarrow{[RhCl(PPh_3)_3]} R\text{-}CO\text{-}CH_3 + OPPh_3$$

Equation 2a

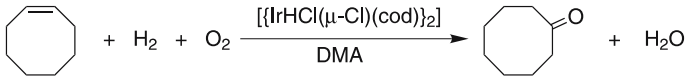

Equation 2b

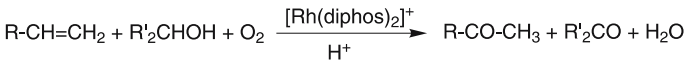

Equation 2c

knowledge on rhodium and iridium chemistry, covered by an excellent review by de Bruin [28]. Moreover, similar substrates give different products depending on the conditions, so that more than one single mechanism, that is still unclear, could be operative. For example, 1,5-cyclooctadiene (cod) can be oxygenated either to 1,4-cyclohexadione (Eq. 3a) [29] or to 4-cyclohexenone (Eq. 3b) [16].

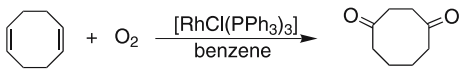

Equation 3a

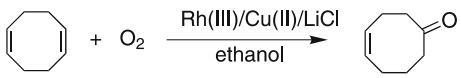

Equation 3b

On the whole, all proposed mechanisms contain three relevant steps: (1) coordination of the olefin and oxygen, (2) C – O bond formation, (3) elimination of the ketone with regeneration of the catalytically active species. In recent years, rather than searching for new catalytic systems based on rhodium and iridium compounds, attention has been focused on understanding the organometallic chemistry involved in the oxygenation of C = C bonds, as described in Sect. 3.

2.1.2 Allylic Oxygenation

Although the catalytic reactions described above involve mononuclear Rh^{I} and Rh^{III} complexes, dinuclear Rh^{II} compounds have also been studied as catalyst precursors in oxygenation reactions. The system $[Rh_2(\mu\text{-}OAc)_4]$/*t*-BuOOH is effective in the oxidation of cyclic alkenes such as cyclopentene, cyclohexene and cycloheptene, mainly to α,β-unsaturated ketones and allylic acetates, but with poor yields (Eq. 4) [30, 31].

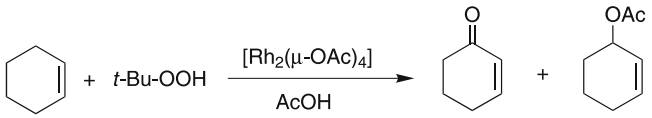

Equation 4

The mechanism operating in these reactions seems to follow a radical path that could be related to the classic Haber-Weiss radical-chain sequence [32] based on the couple $[Rh_2^{II}(\mu\text{-}OAc)_4]/[Rh_2^{II,III}(\mu\text{-}OAc)_4]$.

2.2
Allylic and Benzylic Oxygenation of Alkenes

The low effectiveness of the $[Rh_2^{II}(\mu\text{-}OAc)_4]$ system [31] in the oxygenation of alkenes has been attributed to its high oxidation potential to form the mixed-valence complex $[Rh_2^{II,III}(\mu\text{-}OAc)_4]$ on the basis of a relationship between the ability of the complexes to transfer one electron and the effectiveness of the catalysts in allylic oxidation, suggested by Kochi [33].

The related dirhodium(II) α-caprolactamate (cap) complex $[Rh_2(\mu\text{-cap})_4]$ undergoes a one-electron oxidation process at quite a lower potential (11 mV) than the acetate complex (1170 mV). In agreement with the Kochi hypothesis, the α-caprolactamate complex has recently been found to be an exceptional catalyst for the allylic oxidation of alkenes under mild conditions. A wide range of cyclohexenes, cycloheptenes, and 2-cycloheptenone (Eq. 5) are rapidly converted to enones and enediones in 1 h with only 0.1 mol % of $[Rh_2(\mu\text{-cap})_4]$ and yields ranging from 60 to 90%, in the presence of potassium carbonate [34].

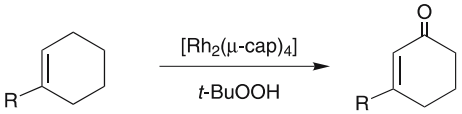

Equation 5

The proposed mechanism (Scheme 1) involves the mixed-valence compounds $[Rh_2^{II,III}(\mu\text{-cap})_4(OH)]$ and $[Rh_2^{II,III}(\mu\text{-cap})_4(OO\textit{t}\text{-Bu})]$ formed from the homolytic cleavage of *t*-BuOOH. The *t*-BuOO$^{\cdot}$ radicals in the medium promote a selective hydrogen abstraction from the alkene to give the allylic alkenyl radical. This species traps the peroxide in $[Rh_2^{II,III}(\mu\text{-cap})_4(OO\textit{t}\text{-Bu})]$ to produce the alkenyl hydroperoxide, which rapidly decomposes to the isolated products, thus regenerating the catalyst.

This system also catalyzes the benzylic oxidation of 1,2,3,4-tetrahydronaphthalene [35] (Eq. 6) and hydrocarbons containing benzyl groups with

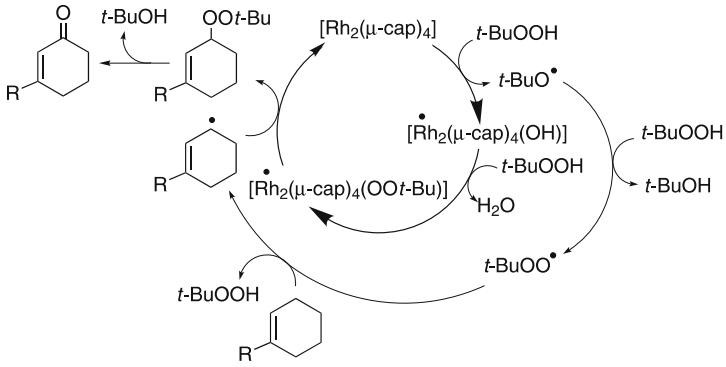

Scheme 1

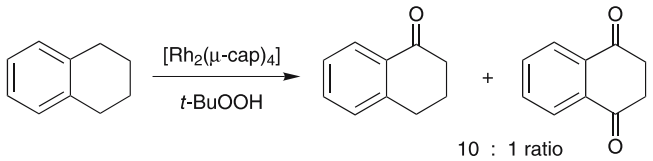

Equation 6

yields of up to 99% in 16 h in the presence of sodium hydrogencarbonate as base.

Moreover, this catalyst is also effective in the oxidation of a spirocyclic acetal of 5-methoxy-1,2,3,4-tetrahydronaphthalenone to palmarumycin CP_2 [35], a biosynthetic precursor to the preussomerin class of natural products exhibiting a wide range of biological activity.

2.3 Oxidation of Ethers

The cationic complex $[Rh(nbd)(PMe_2Ph)_3](BF_4)$ catalyzes the oxygenation of several ethers (Eq. 7) by O_2/CO_2 mixtures with moderate turnovers (1,000 in 8 days at 60 °C for γ-butyrolactone) [36], accompanied by the reduction of CO_2 to formic acid. In the absence of CO_2, 2-hydroperoxidetetrahydrofuran is the major product.

More recently, Vaska's compound $[IrCl(CO)(PPh_3)_2]$, was found to be a better catalyst than the cationic rhodium complex in the oxidation of THF

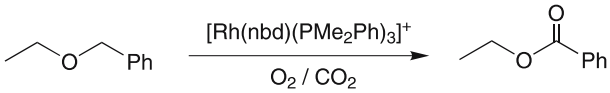

Equation 7

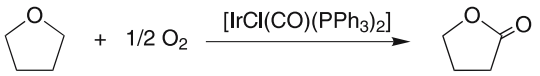

Equation 8

to γ-butyrolactone (Eq. 8) under ambient conditions with a TON (turnover number) of 150 in 48 h, along with 4-hydroxybutyraldehyde [37].

2.4 Oxidation of Alcohols

Recent advances in alcohol oxidations by rhodium and iridium complexes have mainly focused on Oppenauer-type oxidations or reactions in which this type of oxidation is an intermediate step. An independent result is the oxidation of allylic (Eq. 9) and benzylic alcohols with *t*-BuOOH to the corresponding α,β-unsaturated ketones [38] with $[Rh_2(\mu\text{-}OAc)_4]$. The reactions were carried out at room temperature in dichloromethane and yields of up to 92% (by GC) in 24–48 h have been described.

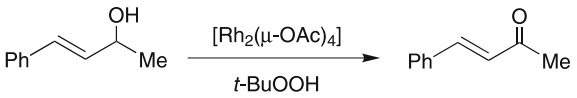

Equation 9

2.4.1 Simple Oppenauer-type Oxidations

For a long time, rhodium and iridium complexes have been known to be highly effective homogeneous catalysts for hydrogen-transfer reactions. Initially, they were used to promote hydrogen transfer from isopropanol to organic substrates in hydrogenation reactions giving acetone [39, 40]. The hydrogen transfer reaction has been also used for the hydrogenation of ketones to alcohols (Eq. 10) [41, 42].

Since these are chemical equilibrium reactions, by modifying the reaction conditions, i.e., using acetone as solvent instead of isopropanol, the reaction can be reversed, and therefore used for the oxidation (dehydrogenation) of alcohols (Oppenauer-type oxidation) [43]. Moreover, since acetone is the hy-

Equation 10

drogen acceptor the reactions are carried out in an environmentally benign fashion.

The mechanism operating in rhodium-catalyzed and iridium-catalyzed hydrogen transfer reactions involves metal hydrides as key intermediates. Complexes such as $[\{M(\mu\text{-}Cl)(L_2)\}_2]$, $[M(cod)L_2](BF_4)$ (M = Rh, Ir; L_2 = dppp, bipy), and $[RhCl(PPh_3)_3]$ are most likely to follow the well-established mechanism [44] via a metal alkoxide intermediate and β-elimination to generate the active hydride species, as shown in Scheme 2.

The system $[\{Ir(\mu\text{-}Cl)Cp^*Cl\}_2]/K_2CO_3$ [45, 46] was recently reported to be a catalyst for the oxidation of primary (Eq. 11) and secondary alcohols to the corresponding carbonyl compounds in acetone.

The catalytic cycle starts with the formation of the metal alkoxide complex with the removal of the hydrogen chloride generated in this step by the base. The base (K_2CO_3 in this case) is indeed necessary to enhance catalytic activity in this system. For example, benzyl alcohol is oxidized to benzaldehyde with a 13% conversion in the absence of K_2CO_3, while the conversion rises to 71% after K_2CO_3 addition. The aldehyde is then produced via β-hydride elimination from the alkoxide to give an iridium hydride complex, which inserts acetone into the Ir – H bond to give the isopropoxide complex. Protonation of isopropoxide by the alcohol releases isopropanol and regenerates the alkoxide complex [46].

The variety of complexes containing the "IrCp*" moiety allows the fine-tuning of the catalyst's properties to enhance selectivities by a careful choice of the remaining ligands. The incorporation of doubly deprotonated aminoalcohols into the "IrCp*" moiety gives neutral complexes, such as $[IrCp^*(OCH_2CPh_2NH)]$ with the N,O based bifunctional ligand (Scheme 3) [47]. This catalyst is also active for the oxidation of alcohols and for the oxidative lactonization of 1,4 or 1,5-diols [48], using acetone

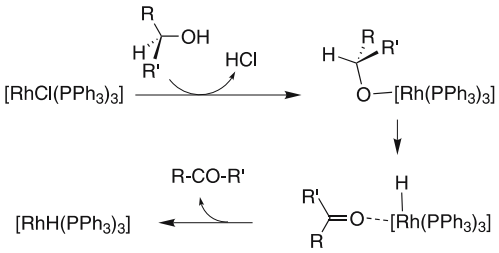

Scheme 2

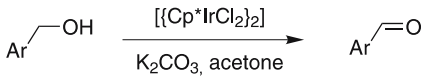

Equation 11

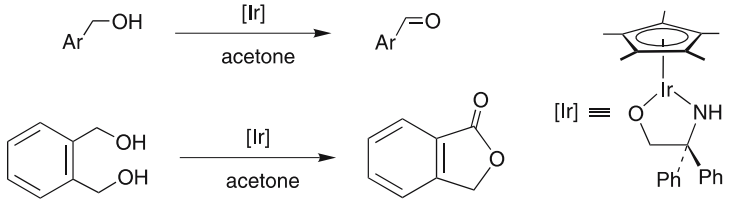

Scheme 3

as the hydrogen acceptor (Scheme 3). Similar complexes containing chiral aminoalcoholates as ligands have shown a good activity for the asymmetric lactonization of several meso-diols [49] to afford the corresponding lactones in a yield of up to 81 ee and 99%.

More recently, it was found that the incorporation of N-heterocyclic carbene ligands to the "Cp*Ir" moiety (Eq. 12) considerably enhances catalyst activity for alcohol oxidation reactions [50, 51]. By way of example, the oxidation of secondary alcohols occurs with high turnovers, up to 3,200 for the oxidation of 1-phenylethanol and 6,640 for that of cyclopentanol (95% yield, 40 °C, 4 h) using the complex with the carbene derived from the tetramethylimidazole (Eq. 12).

This enhancement could be attributed to an increase in the nucleophilicity of the iridium-hydride intermediate, due to the good electron donor ability of this type of ligand, which leads to the acceleration of the hydride transfer to acetone as the hydrogen acceptor.

An interesting case of heterobimetallic catalysis occurs with the complex $[(\eta^5\text{-}C_5Ph_4O)Rh(\mu\text{-}Cl)_3Ru(PPh_3)_2(Me_2CO)]$, which is an efficient catalyst for the oxidation of both primary and secondary alcohols under mild conditions. The cooperation of two metals in this homogeneous bimetallic-catalysis is noteworthy since the homometallic complexes $[\{Rh(\mu\text{-}Cl)(\eta^5\text{-}C_5Ph_4O)\}_2]$ and $[(PPh_3)_2ClRu(\mu\text{-}Cl)_3Ru(PPh_3)_2(Me_2CO)]$ were ineffective for the Oppenauer oxidation [52].

Water-soluble catalysts for Oppenauer-type oxidation of alcohols can be achieved by adding functionalized salts of classical ligands such as dipotassium 2,2′-biquinoline-4,4′-dicarboxylate (BQC) to acetone-water mixtures. In this way, the catalyst system $[\{Ir(\mu\text{-}Cl)(cod)\}_2]$/BQC is highly efficient for the selective oxidation of a wide range of alcohols such as benzylic,

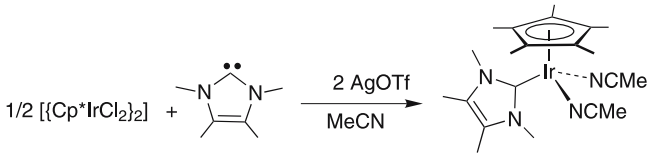

Equation 12

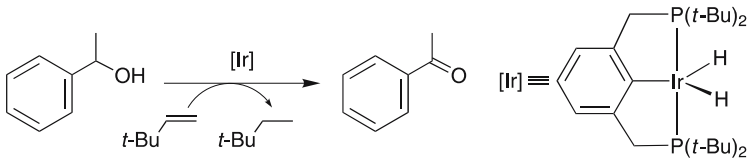

Equation 13

1-heteroaromatic, allylic, and aliphatic secondary alcohols to the corresponding ketones using catalyst/substrate ratios ranging from 0.4 to 2.5% and yields up to 87% in 4 h [53, 54].

A related dehydrogenation of primary and secondary alcohols to the corresponding aldehydes/ketones has been achieved using the dihydride iridium compound $[IrH_2(C_6H_3\text{-}2,6\{CH_2P\text{-}t\text{-}Bu_2\}_2)]$ as the precursor's catalyst and *t*-butylethylene as hydrogen acceptor (Eq. 13). The reactions are carried out at 200 °C with a 99% yield in 18 h (alcohol/Rh = 10/1) [55].

A plausible mechanism involves the reaction of the dihydride precursor with *t*-butylethylene to the 14-e complex $[Ir(C_6H_3\text{-}2,6\{CH_2P\text{-}t\text{-}Bu_2\}_2)]$, which undergoes the oxidative-addition reaction of the alcohol to afford a hydride alkoxide complex. Further β-hydride elimination gives the aldehyde/ketone and regenerates the dihydride active species [55]. In the particular case of 2,5-hexanediol as the substrate, the product is the cyclic ketone 3-methyl-2-cyclopenten-1-one. The formation of this ketone involves the oxidation of both OH groups to 2,5-hexanedione followed by an internal aldol reaction and further oxidation as in the final step of a Robinson annulation reaction [56].

2.4.2
Oxidation and Cyclisation: Synthesis of Indoles and Quinolines

Starting from *ortho*-aminoalcohols as substrates, the products are indoles (Eq. 14) resulting from the condensation of the aldehyde and the amino group. This reaction is catalyzed by the system $[\{Ir(\mu\text{-}Cl)Cp^*Cl\}_2]/K_2CO_3$ in toluene. This catalyst was also efficient for the synthesis of 1,2,3,4-tetrahydroquinolines and 2,3,4,5-tetrahydro-1-benzazepine [57] starting from the corresponding aminoalcohols. Since the reactions are carried out in toluene, a protonation of the iridium hydride by the alcohol with removal of hydrogen has been suggested to regenerate the iridium alkoxide species [57].

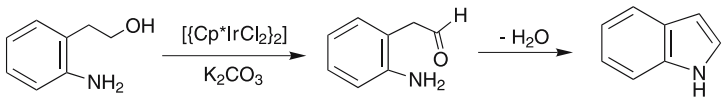

Equation 14

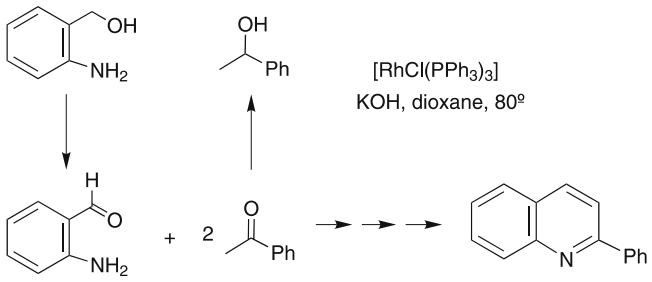

Scheme 4

Quinolines can be prepared from the oxidative coupling and cyclation of the 2-aminobenzyl alcohol and ketones (Scheme 4) catalyzed by the system $[RhCl(PPh_3)_3]$/KOH [58]. The reactions were carried out in dioxane at 80 °C with 85% yield in 24 h (alcohol/Rh = 100/1). However, better yields are obtained with the related ruthenium system $[RuCl_2(=CHPh)(PCy_3)_2]$ [59].

In this case, the 2-aminobenzyl alcohol is oxidized to 2-aminobenzaldehyde, which undergoes an aldol condensation with the ketone to give an α,β-unsaturated ketone. This is followed by cyclodehydratisation to form quinoline. An excess of ketone is necessary to act as a sacrificial hydrogen acceptor.

2.4.3 Domino Reactions

A recent methodology for the synthesis of organic compounds uses the oxidation of alcohols to aldehydes [60] as the first step in a three-step domino reaction sequence to attach the carbon chain of the alcohol to alkanes, amines or ketones. The second step is the well-known condensation of the carbonyl compound with a Wittig reagent, aza-Wittig or amines, and methylketones to give alkenes, imines, and α,β-unsaturated ketones, respectively. Finally, these unsaturated compounds are reduced by hydrogen transfer reactions using the same catalyst introduced for the oxidation of the alcohol. Coupling these three reactions in a one-pot reaction directly affords the products.

Scheme 5 shows a formal explanation of this conceptual idea for alkanes developed by Williams [60]: the alcohol is first oxidized into the aldehyde affording a hydride complex. The aldehyde is then condensed with the Wittig reagent to form the unsaturated compound, which becomes hydrogenated by the hydride complex, thus regenerating the catalyst.

The catalyst for this type of reaction was $[\{Ir(\mu\text{-Cl})(cod)\}_2]$/dppp/$Cs_2CO_3$. For the reaction shown in Eq. 15, a 100% conversion with selectivities of 80% in alkane, 5% in aldehyde and 12% in alkene were obtained for R = COOBn.

An extension of this methodology [61] to amines instead of alkanes, using the same catalyst precursor, is obtained by replacing the Wittig reagent,

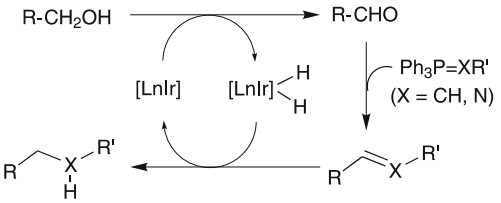

Scheme 5

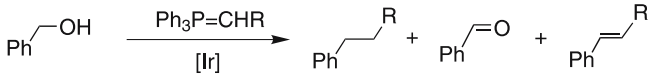

Equation 15

$PPh_3P = CHR$, with the aza-analogue $PPh_3P = NR$ (Scheme 5). The condensation of the aldehyde, generated "in situ", with $PPh_3P = NR$ gives the imine, which was hydrogenated to the amine.

A related process, from this conceptual point of view (Eq. 16), the use of the aldehyde generated "in situ" for further reactions, has allowed the α-alkylation of ketones with primary alcohols [62]. Several ketones have been condensed with 1-butanol or benzyl alcohol affording the corresponding α-alkylated ketones in good yields (up to 96%) in the presence of $[\{Ir(\mu\text{-}Cl)(cod)\}_2]$ and KOH.

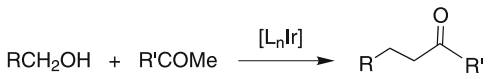

Equation 16

This method is a very convenient route to obtain aliphatic ketones because the carbonyl function can be placed in the desired position by selecting the ketones and alcohols employed.

The N-alkylation of amines with alcohols [63] can also be carried out with Ir^{III} catalysts through a similar domino sequence reaction. In this case, the aldehyde/ketone resulting from oxidation is condensed with an amine to the corresponding imine, which is hydrogenated to the alkylated amine [63]. By way of example, the reaction of benzyl alcohol with aniline in toluene afforded benzylaniline in a 88% isolated yield by using catalytic amounts of $[\{Ir(\mu\text{-}Cl)Cp^*Cl\}_2]/K_2CO_3$.

3
Organometallic Chemistry of Rhodium and Iridium Directed towards Olefin Oxygenation

Most of the recent studies on the stoichiometric oxygenation of C = C bonds coordinated to rhodium and iridium focus on the search for suitable precursors able to promote the desired C – O bond formation reaction between the carbon of the olefin and the oxygen from the oxygen source, typically dioxygen or hydrogen peroxide. Prototype complexes with the "M^{I}(olefin)" framework along with di-, tri- and tetradentate N-based ligands are commonly used for two reasons: (1) the well-known changes in the hapticity of these ligands that allow coordination vacancies to be generated if necessary, and (2) their resistance to oxidation, which is clearly greater than that of posphane ligands. Up to now, ligands with hard donor atoms of the main groups (N, O) seem to create the more appropriate metal environments for the oxidation of olefins. Nevertheless, this is a feature that requires further study, and close observation of the properties of organometallic compounds by practitioner chemists to recognize chemical oxidations.

3.1
Reactions with Dioxygen

The olefin oxygenations carried out with dioxygen seem to be metal-centered processes, which thus require the coordination of both substrates to the metal. Consequently, complexes containing the framework "M^{III}(peroxo)(olefin)" represent key intermediates able to promote the desired C – O bond formation, which is supposed to give 3-metalla^{III}-1,2-dioxolane compounds (Scheme 6) from a 1,3-dipolar cycloinsertion. This situation is quite different from that observed in similar reactions involving middle transition metals for which the direct interaction of the olefin and the oxygen coordinated to the metal, which is the concerted oxygen transfer mechanism proposed by Sharpless, seems to be a more reasonable pathway [64] without the need for prior olefin coordination. In principle, there are two ways to produce the "M^{III}(peroxo)(olefin)" species, shown in Scheme 6, both based on the easy switch between the M^{I} and M^{III} oxidation states for

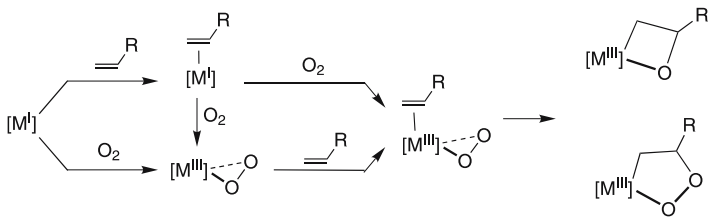

Scheme 6

rhodium and iridium. The first possibility seems to be the most plausible since it combines the ability of these metals in low oxidation state to coordinate olefins with a feasible further oxidation to the desired species, although the simple replacement of the olefin by dioxygen could also be a possible competitive reaction. The second possibility involves the coordination of the olefin to a "M^{III}(peroxo)" complex, but given the low affinity of these metals in the M^{III} oxidation state for olefins, and the inertness of these compounds, this possibility seems to be less likely, although it could be an equilibrium operative for catalytic processes.

3.1.1
Solid-gas Reactions to 3-metalla^{III}-1,2-dioxolane Complexes

Compounds of the 3-metalla^{III}-1,2-dioxolane type were unknown in rhodium and iridium chemistry until 2001 [65] when Gal reported the preparation of some examples through solid-gas reactions, quite an uncommon type of chemistry. They were initially obtained from the cationic complex [Rh(κ^4-tpa)(C_2H_4)]$^+$ (tpa = *N*,*N*,*N*,-tris(2-pyridylmethyl)amine), and then extended to the iridium counterparts and the rhodium [66] compounds [Rh(κ^4-dpda-Me_2)(C_2H_4)]$^+$ (Fig. 1) (the aromatic circles for the pyridine rings have been omitted for clarity).

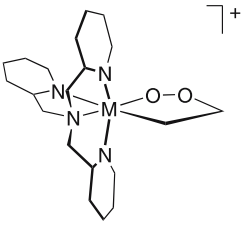

[M(κ^4-tpa)(κ^2-$O_2C_2H_4$)]$^+$

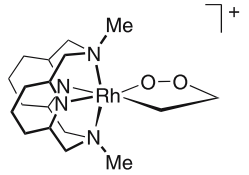

[Rh(κ^4-dpda-Me_2)(κ^2-$O_2C_2H_4$)]$^+$

Fig. 1

These solid-gas reactions represent, at the moment, the single path to 3-metalla^{III}-1,2-dioxolane complexes of rhodium and iridium. Complexes of this type have been widely proposed in catalytic cycles. However, it is unlikely that they take part in oxygenations with rhodium because of their high reactivity (see below) and the special conditions for their preparation.

3.1.2
Reactions in Solution to Peroxo Complexes

Reactions of the above-mentioned ethylene derivatives with dioxygen *in solution* afford mixtures of uncharacterized compounds [67] with minor ex-

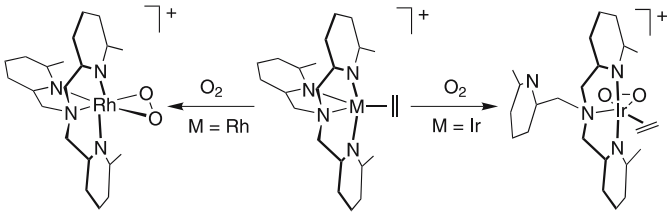

Scheme 7

ceptions. For example, the "Rh^{III}peroxo" complex $[Rh(\kappa^4\text{-}Me_3tpa)(O_2)](PF_6)$ (Me_3tpa = *N*,*N*,*N*-tris[(6-methyl-2-pyridyl)methyl]amine) was obtained in quantitative yield after the clean replacement of ethylene in $[Rh(\kappa^4\text{-}Me_3tpa)(C_2H_4)]$ by dioxygen (Scheme 7) [68]. The iridium counterpart coordinates O_2 without ethylene replacement, to give an "Ir^{III}(peroxo)(ethylene)" compound, $[Ir(\kappa^3\text{-}Me_3tpa)(O_2)(C_2H_4)](PF_6)$ (Scheme 7) in a rather low yield. The incoming of the new ligand is associated with a change in the coordination mode of the ligand from κ^4 to κ^3 [68]. In these reactions, the regioselectivity of the reactions is driven by the nature of the metal.

The iridium complex models one of the proposed intermediates in the catalytic conversion of alkenes to ketones, but the expected C – O bond formation reaction is not observed. A related example in rhodium chemistry, $[RhH(O_2)\{CH_2 = C(CH_2CH_2Pt\text{-}Bu_2)_2\}]$ (Fig. 2) [69], is the only complex in which a peroxide ligand coexists with an olefin moiety, which forms part of the pincer ligand. The lack of C – O bond formation in both complexes could be indicative of a stereochemical requirement or a "further activation" of oxygen for the mentioned coupling, which is not accessible in these complexes. In fact, both show a similar arrangement of the peroxide and the C = C bond in the solid state, both being coplanar and forming a bow tie with the metal, in which the C = C and O – O edges are almost parallel.

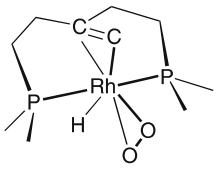

Fig. 2

Thus, although the coordination of the olefin and the dioxygen at the same metal center seems to be a required condition for achieving oxygen transfer, it does not seem to be the only one.

3.1.3
Reactions in Solution to 2-metalla^{III}oxetanes

Rhodium and iridium complexes incorporating diolefins such as 1,5-cyclooctadiene (cod) are more reluctant to react with molecular oxygen than the ethylene analogues. To date, only two cod compounds, [Ir(κ^3-P_3O_9)(cod)](TBA)$_2$ and [Rh(κ^2-PhN$_3$Ph)(cod)] react straightforwardly with dioxygen under mild conditions. The result of the reactions is a mononuclear 2-irida^{III}oxetane-type complex in the case of iridium (Eq. 17) [70], while for rhodium the related 2-rhoda^{III}oxetane complex (Scheme 8) is dinuclear [71]. In both reactions all the oxygen consumed is incorporated in the substrate, thus yielding a 100% atom-economy processes.

The structure of the rhodium compound and the kinetic study of the reaction provide strong evidence of a binuclear activation of dioxygen with complete effective transfer of both oxygen atoms to C = C bonds.

According to the second order of the reaction, the rate-determining step is the formation of a "Rh^{III}(peroxo)(cod)" complex from [Rh(κ^2-PhN$_3$Ph)(cod)] and dioxygen. This peroxo compound undergoes the attack of an intact molecule of [Rh(κ^2-PhN$_3$Ph)(cod)] to complete the dinuclear oxygen cleavage with the formation of two C – O bonds.

Probably, the key to the insertion of each oxygen atom in a C = C bond lies in the characteristics of the proposed intermediate "Rh$_2$(μ-oxo)$_2$" com-

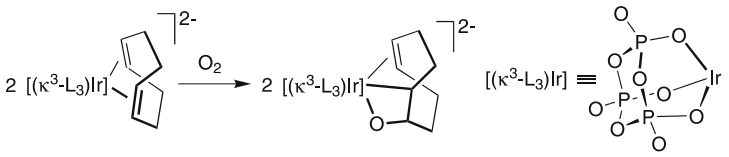

Equation 17

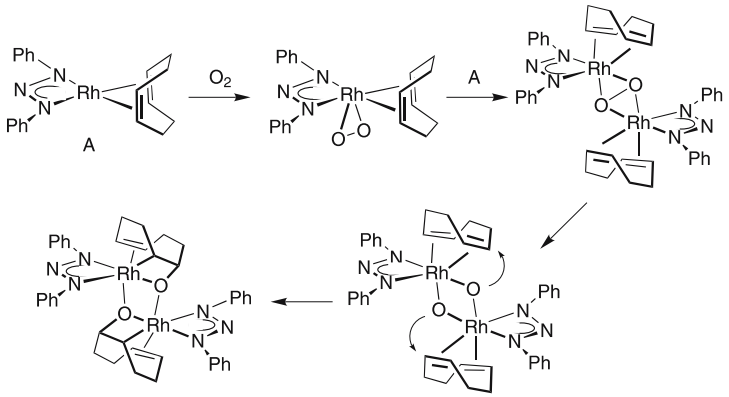

Scheme 8

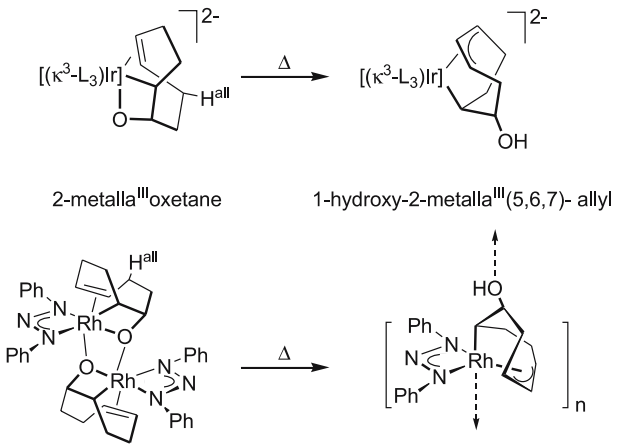

Scheme 9

plex. Thus, the coordination of the second metal to the peroxo ligand cleaves the O – O bond and each oxide ligand is transferred to the closest C = C bond. The most relevant aspect of these two 100% atom economy reactions is a strong indication of the existence of an effective dinuclear pathway to activate dioxygen that produces C – O bonds without waste, which is available for the late transition metals in a relatively low oxidation state.

These two 2-metalla^{III}oxetanes are the isolated kinetic products of the reactions, which transform into 1-hydroxy-2-metalla^{III}(5,6,7)-allyl derivatives through the migration of a proton from the methylene group, specified in Scheme 9, to the oxygen. The regioselectivity of this isomerisation indicates a preference for the activation of the C – H bond at this site through a common yet unknown way. The distinct hapticity of the ancillary ligand in both cases determines the iridium complex to be mononuclear, while the corresponding rhodium system is polymeric in the solid state.

3.1.4
Acid-catalyzed Reactions to 1-hydroxy-2-rhoda^{III}(5,6,7)-allyl Derivatives

The typical reluctance of the cod derivatives to react with dioxygen has been overcome, in some cases, by different approaches. Using catalytic amounts of acid [72], the otherwise inert complex [Rh(κ^3-bpa)(cod)](PF_6) reacts with oxygen to give the 1-hydroxy-2-rhoda^{III}(5,6,7)-allyl derivative [Rh(κ^3-bpa)($C_8H_{11}OH$)](PF_6) (Scheme 10) with a consumption of one mole of O_2 per mol of [Rh(κ^3-bpa)(cod)](PF_6), i.e., it is a 50% atom-economy process.

Probably, the acid protonates one of the pyridine rings to give the 16 electron-valence complex [Rh(κ^2-bpaH)(cod)](PF_6)$_2$. This complex can then react with molecular oxygen to give an "Rh^{III}(peroxo)(cod)" intermediate, which is immediately protonated by the pyridinium group to regenerate

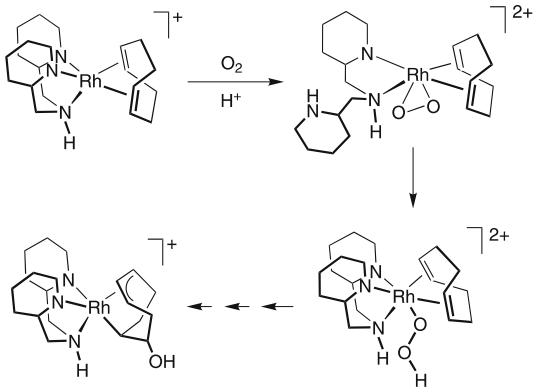

Scheme 10

the κ^3-bpa ligand with formation of the "Rh^{III}(hydroperoxo)(cod)" complex. Then, one oxygen atom is transferred to the C = C bond, while the fate of the other oxygen atom is unknown [72].

3.1.5
Radical-chain Processes Involving Ketone Derivatives

Radical-chain processes that are usually operative in the auto-oxidation of free cod [73] can produce olefin oxygenation in some instances. This is the case of the reaction of [Ir(η^5-Cp′)(cod)] (Cp′ = 3,5-$(Me_3Si)_2$Cp) [74] with dioxygen in tetrachloroethane (TCE) under reflux, where a free-radical chlorine-photosensitized oxidation gave two isomeric ketones (Eq. 18).

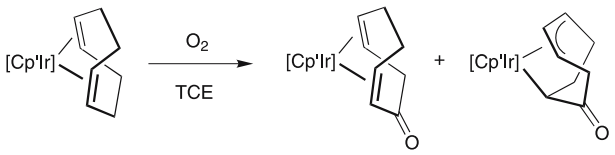

Equation 18

The setereochemistry of the products isolated in this reaction is related to that of the hydroperoxides produced in autoxidation of free cod.

3.1.6
Electron-transfer Reactions Promoting O_2 Activation

An elegant illustration of this feature was provided by the reactivity of the redox-pair [Rh^I(κ^3-dpa)(cod)](PF_6)/[Rh^{II}(κ^3-dpa)(cod)]$(PF_6)_2$ towards dioxygen [75]. The reluctance of the Rh^I complex to react with dioxygen

is overcome by a one-electron oxidation process affording the paramagnetic Rh^{II} complex. This compound, upon treatment with dioxygen, gives a rhodium superoxide complex (Fig. 3) in a reversible fashion. However, the superoxide complex does not transfer oxygen to the coordinated diolefin (cf. the binuclear oxygen activation and formation of C – O bonds discussed above), but rather it decomposes through a C – H bond activation reaction.

Another perhaps more relevant example consists of the redox pair $[Ir^{I}(\kappa^4\text{-}Me_3tpa)(C_2H_4)](PF_6)/[Ir^{II}(\kappa^4\text{-}Me_3tpa)(C_2H_4)](PF_6)_2$ [76]. In this case, while the reaction of the Ir^{I} compound with oxygen affords the olefin-peroxide complex $[Ir(\kappa^3\text{-}Me_2dpa\text{-}Me)(O_2)(C_2H_4)](PF_6)$, as mentioned above, the product of the reaction of the paramagnetic Ir(II) complex with dioxygen in acetonitrile is the diamagnetic formylmethyl complex, $[Ir(\kappa^4\text{-}Me_3tpa)(\kappa^1\text{-}CH_2CHO)(MeCN)](PF_6)_2$ (Scheme 11) [77, 78]. The radical character of the complex $[Ir^{II}(\kappa^4\text{-}Me_3tpa)(C_2H_4)](PF_6)_2$ centered on the non-innocent ethylene ligand could be responsible for facile C – O bond formation, through the collapse of the C-centered radical in $[Ir(\kappa^4\text{-}Me_3tpa)(C_2H_4)](PF_6)_2$ [78] with dioxygen, which is a biradical by itself.

This observation opens up a new possibility in the formation of C – O bonds for the already complicated oxygenation reactions of organic substrates, i.e., the non-innocent behavior of the olefin in open-shell transition metal olefin complexes can allow a direct radical coupling of dioxygen with the coordinated olefin.

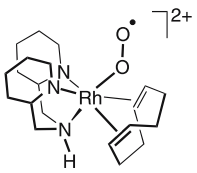

Fig. 3

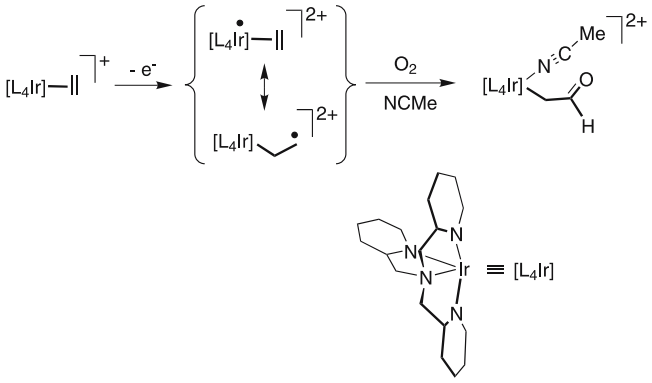

Scheme 11

3.2
Reactions with Hydrogen Peroxide

Hydrogen peroxide is the second environmentally friendly reagent of choice to be used as primary oxidant, since after the transfer of one of the oxygen atoms water is the only by-product. While oxygen is very selective in producing the oxygenation of the olefins coordinated to rhodium and iridium, hydrogen peroxide is more efficient for this purpose. For example, 2-rhoda^{III}oxetanes derived from ethylene (Fig. 4), inaccessible from the reactions of the appropriate precursors with dioxygen, are easily obtained if aqueous hydrogen peroxide is used instead [67, 79, 80].

The greater effectiveness of hydrogen peroxide is also shown in the reactions of the pentacoordinated complexes $[M(\kappa^3\text{-}L_n)(cod)]^+$ supported by N-donor ligands (L_n = dpa-R′ [72, 79], Cn* [79], Py_3S_3 [81]) (Fig. 5). While these complexes are unreactive with molecular oxygen, they react with H_2O_2 to systematically give the 1-hydroxy-2-metalla^{III}(5,6,7)-allyl derivatives (Scheme 12) as the thermodynamic products.

These 1-hydroxy-2-metalla^{III}(5,6,7)-allyl complexes result directly from the reactions of the less sterically crowded complexes [Ir(Cn)(cod)](OTf) (Cn = 1,4,7-triazacyclononane) [82] and $[Rh(\kappa^3\text{-}Py_3S_3)(cod)](BPh_4)$ [81]. Slowing down the reactions by increasing the steric crowding around the metal, the kinetic isomers 2-irida^{III}oxetane and 6,7-oxarhoda^{III}tetracyclodecane can be isolated from the reactions of [Ir(Cn*)(cod)](OTf) [82] and $[Rh(\kappa^3\text{-}L_n)(cod)](PF_6)$ (L_n = Cn*, dpa-R′) [72, 79] with H_2O_2, respectively. The

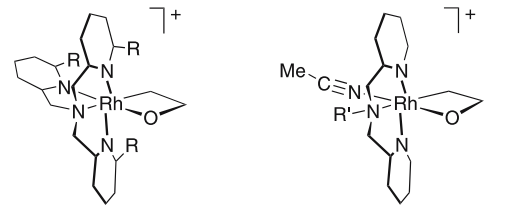

Fig. 4

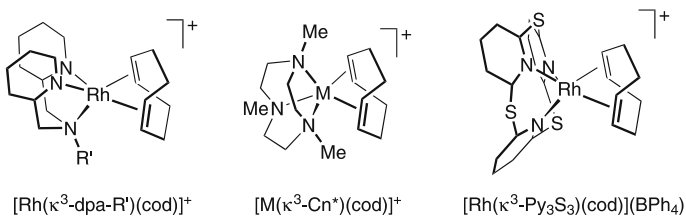

Fig. 5

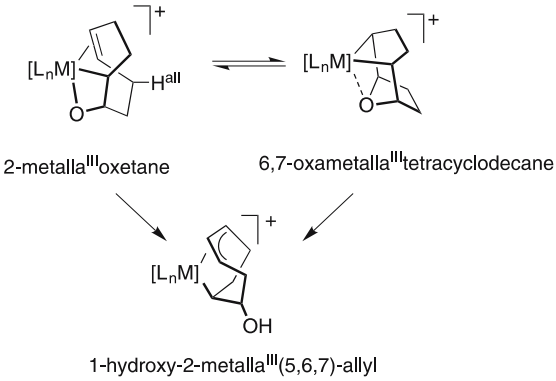

Scheme 12

unique organic fragment in the 6,7-oxarhoda^{III}tetracyclodecanes bonded to rhodium can formally be considered as a tetrahydrofuran derivative. This organic moiety may result from an internal attack of the oxygen atom to the closer olefinic carbon in a preceding 2-rhoda^{III}oxetane compound. Both types of oxametallacycles are transformed into the thermodynamic products, the 1-hydroxy-2-metalla^{III}(5,6,7)-allyl derivatives, on heating or through acid-catalyzed reactions. The conversion of the 2-irida^{III}oxetane is again regioselective (Sect. 3.1.3)

The conversion of the 6,7-oxarhoda^{III}tetracyclodecanes into the 1-hydroxy-2-metalla^{III}(5,6,7)-allyl products is more complicated since it involves the rupture of Rh – C and C – O bonds in the rhodium complexes. In some instances, an equilibrium between both types of complexes, 6,7-oxarhoda^{III}-tetracyclodecanes and 2-rhoda^{III}oxetanes, has been proposed to account for these results [72].

The only exception to this general trend, to date, is the reaction of the pyridophane iridium compound [Ir(κ^3-dpda-Me_2)(cod)](PF_6) with hydrogen peroxide that requires the addition of one molar-equivalent of a strong acid to proceed. The acid not only protonates one arm of the ligand as an intermediate step, but it is consumed to produce the oxidation of the C = C bond to ketone. The product is the complex [Ir(κ^4-dpda-Me_2)(κ^2-$C_8H_{11}O$)](PF_6)$_2$ [83], containing a cyclooct-5-en-2-yl-1-one ligand, in a net four-electron oxidation (Eq. 19).

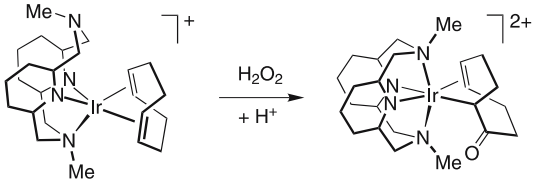

Equation 19

3.3
Reactions of Dioxolane and Oxetane Complexes

The few 3-metalla^{III}-1,2-dioxolane complexes of rhodium and iridium isolated so far have been highly reactive species. Simply by exposure to daylight they rearrange to the very unusual formylmethyl hydroxy complexes [M(κ^4-tpa)M(OH)(η^1-CH_2CHO)](X) and [Rh(κ^4-dpda-Me_2)(OH)(η^1-CH_2CHO)](PF_6) in the solid state (Scheme 13) [84]. An alternative route to these formylmethyl hydroxy complexes is the oxidation of a 2-rhoda^{III}oxetane with hydrogen peroxide [67] (Scheme 13).

These formylmethyl hydroxy compounds could be intermediates [66] in the formation of acetaldehyde, for example, by the direct protonation of the CH_2 group by an external acid. Unfortunately, these formylmethyl hydroxy compounds do not eliminate acetaldehyde but, to the contrary, strong acids protonate the hydroxy group to give the aqua complex while the formylmethyl ligand remains unaltered.

However, the elimination of acetaldehyde from 2-rhoda^{III}oxetanes (Scheme 14) is observed if a coordination vacancy on the metal, necessary for a β-hydrogen elimination, is created. This is achieved by dissociation of an acetonitrile ligand [67] or by protonation [80] of the oxetane moiety.

The β-hydride shift followed by a reductive elimination produces acetaldehyde, while the resulting Rh^I fragment is trapped by cod or ethylene to give

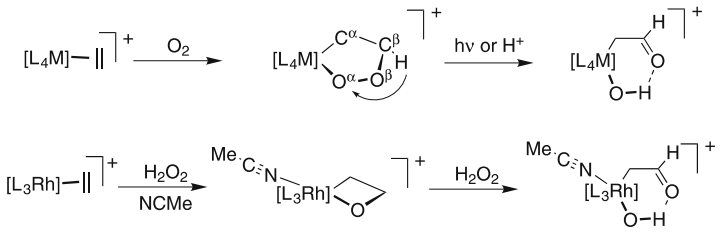

Scheme 13

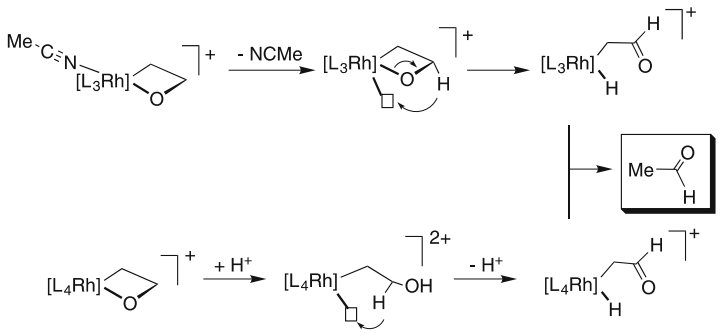

Scheme 14

the Rh^{I} compounds $[Rh(\kappa^3\text{-dpa-Bn})(L)](BPh_4)$ (L = cod, ethylene), respectively.

This β-hydrogen elimination in 2-rhoda^{III}oxetanes is apparently favored over reductive elimination to an epoxide. Moreover, the reverse step, i.e., the oxidative-addition of epoxides to Rh^{I} and Ir^{I} results in 2-rhoda^{III}oxetanes [85] and/or hydrido formylmethyl complexes [86]. Therefore, assuming that 2-metalla^{III}oxetanes are intermediates in the oxygenation of alkenes by group VIII transition metals, the reported reactivity would account for selectivity to ketones in the catalytic reactions based on these metals.

3.4
A Close Look at Alkene Oxygenation Reactions

The recent advances described above confirm the feasibility of oxygenating olefins by oxygen and hydrogen peroxide in rhodium and iridium chemistry. This is not a common reaction of the olefinic complexes of these metals, nor are the products—mainly 2-metalla^{III}oxetane and 3-metalla^{III}-1,2-dioxolane complexes—that were isolated under solid-gas reactions, common products. On the whole, it represents an outstanding advance in the knowledge of the oxidation of olefins mediated by rhodium and iridium; transforming this stoichiometric into catalytic chemistry is a desired goal for the future. Nevertheless, several questions related to the activation and transfer of oxygen to the olefin remain unanswered, and the rationalizations given below should be taken as speculative proposals. For instance, what are the characteristics of the Rh and Ir olefin complexes that produce their effective interaction with dioxygen or hydrogen peroxide? Are there active oxygenated intermediate species? If the answer to the latter question is yes, then what makes them active and how does this occur? Also, in this context, how is the oxygen transferred to the alkene? Is there more than one reaction path?

It can generally be assumed that oxygen adds to d^8 Rh^{I} and Ir^{I} complexes in an oxidative way to form peroxocomplexes. While this reaction is usually reversible for rhodium, iridium peroxo complexes are more stable to dissociation [87]. By combining this reversibility, which is typical of rhodium, with electron-rich metal centers, which can be created by strong electron-donating ancillary ligands, one can expect square-planar 16-*e* metal complexes to be the most appropriate candidates for olefin oxygenation. $[Rh(\kappa^2\text{-}PhN_3Ph)(cod)]$ and $[Ir(\kappa^3\text{-}P_3O_9)(cod)](TBA)_2$, which are neutral and anionic coordinatively unsaturated complexes, fall into this category. In the iridium complex one Ir – O bond is very long (2.70 Å) while the other two are quite shorter (2.18 Å) [74], so that the existence of the coordinatively unsaturated $[Ir(\kappa^2\text{-}P_3O_9)(cod)](TBA)_2$ species in solution seems to be more than probable. Dissociation of one ligand or protonation of one arm of the ligand in pentacoordinated 18-e rhodium complexes with polydentate ligands

described by de Bruin and Gal is another way of achieving a coordination vacancy. However, the addition of dioxygen to the metal cannot be predicted a priori, and olefin replacement is a possible side reaction.

Once the oxidative-addition reaction of dioxygen to metal d^8-ions has occurred, the essentially electrophilic dioxygen becomes a nucleophilic peroxide ligand. Since the oxidation of substrates is associated with electron transfer from the substrate to the oxidant, i.e. in this case the dioxygen adduct, effective oxygenations require a "further activation" to transform the nucleophilic peroxide into an electrophilic species prior to the oxygen transfer.

It may be reasonable to argue that this "further activation" is achieved in several ways. The acid-catalysis required for Gal and de Bruin complex [Rh(κ^3-bpa)(cod)](PF_6) to react with dioxygen can be used to protonate the peroxo compound (Scheme 10) to a hydroperoxo species. This is a way to achieve "further activation" of dioxygen, since it decreases the nucleophilic character of the peroxo ligand and makes interaction with the coordinated olefin easier. Recent works by Moro-oka [88, 89] and Braun [90] (Scheme 15) have shown that peroxorhodium complexes can be protonated to hydroperoxo compounds. However, the addition of a second mole of acid leads to hydrogen peroxide elimination rather than to the highly electrophilic oxo species (M = O) that could result from the heterolytic cleavage of the O – O bond with removal of water.

Oxo species (M = O) are almost unknown in Rh and Ir chemistry with the exception of the unique terminal iridium oxo complex, [Ir = O(mes)$_3$] (mes = 2,4,6-trimethylphenyl) [91]. This compound surprisingly displays little reactivity towards organic substrates, despite its high formal oxidation state. It only oxidizes the most reactive oxygen acceptors such as phosphanes or arsanes [92].

A second way to activate the peroxide ligand for oxygen transfer to C = C bonds could be via homolytic O – O cleavage of the peroxide by coordination to a second metal center. From this point of view, the peroxide ligand is converted into the "[M(μ-O)]$_2$" moiety in which the oxide bridges are now electrophilic and then each oxygen atom from the "M$_2$(μ-oxo)$_2$" core is transferred to a close C = C bond in a *cis* position (Scheme 8). As this conclusion is based on only two reported examples, it should be taken as a working hypothesis.

A third possible way to carry out the addition of oxygen to C = C bonds involves paramagnetic metal complexes in which the unpaired electron resides

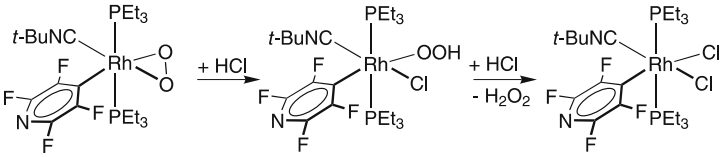

Scheme 15

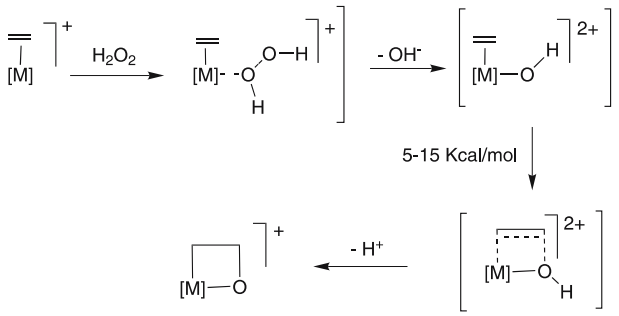

Scheme 16

partly on the olefin ligand. In this case no coordination of dioxygen to the metal is required, but it can attack the olefin directly, with addition occurring as a result of the collapse of free-radicals.

Moving on to the reactions with hydrogen peroxide, a hydroperoxide complex could be also formed by a direct interaction of hydrogen peroxide with metal complexes [93]. The hypothesis of a common intermediate, the hydroperoxo species, could reasonably be assumed in some reactions of rhodium cyclooctadiene complexes carried out with both H_2O_2 and O_2/H^+, since they gave identical products [72]. However, a DFT study [94] indicates that the heterolytic cleavage of the O – O bond by rhodium is most probably the first step in the oxygenation of ethylene with hydrogen peroxide (Scheme 16). The product, a 2-rhoda^{III}oxetane complex would result from an intramolecular nucleophilic attack of the hydroxide group on the coordinated olefin followed by the loss of the proton.

The low values found for the barriers associated with the heterolytic cleavage and cyclisation steps are the main reasons for considering this proposal to be valid.

Finally, it should be pointed out that unknown paramagnetic species are also obtained in some of these reactions, thus complicating the mechanistic panorama of the oxygenation of organic substrates.

4 Conclusions

The last 5 years have witnessed important advances and breakthroughs in the rhodium and iridium chemistry involved in olefin oxygenation and alcohol oxidation (dehydrogenation). After promising results in the 1980s with rhodium-based catalysts for alkene oxygenation there followed a long period of "hibernation". However, rhodium has recently re-emerged as a promising candidate for allylic oxidation of alkenes and to promote C – O bond formation reactions. The outstanding stoichiometric chemistry of alkene oxy-

genation developed recently evidences the need to search for new systems that are able to activate dioxygen with efficient transfer to alkenes. A deeper understanding of the as yet poorly known operating mechanisms and further reactivity studies directed toward discovering the appropriate reductive-elimination steps also needs to be acquired before achieving the desired goal of transforming this stoichiometric into catalytic chemistry.

Moreover, the already known ability of iridium compounds to catalyze hydrogen transfer reactions has been excellently applied in Oppenauer-type and domino-type reactions for valuable organic chemicals; and further developments, including asymmetric variants to kinetic resolution of alcohols and fine chemicals, can be expected.

Since these are still early days in our understanding of these aspects of rhodium and iridium, whether or not they are "rough diamonds" for these reactions is a question to be answered in the future.

Acknowledgements We are grateful to the Spanish Ministry of Education and Science (MEC/FEDER) and the Government of Aragón (DGA) for generous financial support (projects CTQ2005-06807/BQU) and (PIP019/2005), respectively.

References

1. Beller M (2004) Adv Synth Catal 346:107
2. Punniyamurthy T, Velusamy S, Iqbal J (2005) Chem Rev 105:2329
3. Jones CW (1999) Applications of Hydrogen Peroxide and Derivatives. R Soc Chem, Cambridge
4. Moiseev II (1997) J Mol Catal A 127:1
5. Bäckvall JE (ed) (2004) Modern Oxidation Methods. Wiley, Weinheim
6. Simándi LI (ed) (2003) Advances in Catalytic Activation of Dioxygen by Metal Complexes. Kluwer, Dordrecht
7. Hill HAO, Tew DG (1987) Dioxygen, Peroxide and Superoxide. In: Wilkinson G, Gillard RD, McCleverty JA (eds) Comprehensive Coordination Chemistry, vol 2, chap 15.2. Pergamon Press, Oxford, p 315
8. Peris E, Crabtree RH (2004) Coord Chem Rev 248:2239
9. Mimoun H (1987) Metal Complexes in Oxidation. In: Wilkinson G, Gillard RD, McCleverty JA (eds) Comprehensive Coordination Chemistry, vol 6, chap 61.3. Pergamon Press, Oxford, p 317
10. Drago RS (1992) Coord Chem Rev 117:185
11. Read G (1988) J Mol Catal 44:15
12. Faraj M, Brégeault JM, Martin J, Martin C (1985) J Organomet Chem 276:C23
13. Martin C, Faraj M, Martin J, Bregeault JM, Mercier J, Fillaux J, Dizabo P (1986) J Mol Catal 37:201
14. Drago RS, Zuzich A, Nyberg ED (1985) J Am Chem Soc 107:2898
15. Mimoun H (1981) Pure Appl Chem 53:2389
16. Faraj M, Martin J, Martin J, Brégeault JM (1985) J Mol Catal 31:57
17. Atlay MT, Preece M, Strukul G, James BR (1982) J Chem Soc Chem Commun 406
18. Lyons JE, Turner JO (1972) J Org Chem 37:2881

19. Morvillo A, Bressan M (1986) J Mol Catal 37:63
20. Fusi A, Ugo R, Fox F, Pasini A, Cenini S (1971) J Organomet Chem 26:417
21. Lyons JE, Turner JO (1972) Tetrahedron Lett 2903
22. Müller P, Idmoumaz H (1988) J Organomet Chem 345:187
23. Read G, Shaw J (1984) J Chem Soc Chem Commun 1313
24. Mimoun H, Machirant MMP, de Roch IS (1978) J Am Chem Soc 100:5437
25. James BR, Morriis RH, Kvintovics P (1986) Can J Chem 64:897
26. Bressan M, Morandini F, Morvillo A (1985) J Organomet Chem 280:139
27. Fowler P, Read G, Shaw J, Šik V (1991) J Chem Soc Dalton Trans 1087
28. de Bruin B, Budzelaar PHM, Gal AW (2004) Angew Chem Int Ed 43:4142
29. Carlton L, Read G, Urgelles M (1983) J Chem Soc Chem Commun 586
30. Bien S, Segal Y (1977) J Org Chem 42:1685
31. Uemura S, Patil SR (1982) Chem Lett 1743
32. Weiner H, Trovarelli A, Finke RG (2003) J Mol Catal 191:217
33. Srinivassan K, Perrier S, Kochi JK (1986) J Mol Catal 36:297
34. Catino AJ, Forslund RE, Doyle MP (2004) J Am Chem Soc 126:13622
35. Catino AJ, Nichols JM, Choi H, Gottipamula S, Doyle MP (2005) Org Lett 7:5167
36. Fazlur-Rahman AK, Tsai JJ, Nicholas KM (1992) J Chem Soc Chem Commun 1334
37. Shi M (1998) J Chem Res (S) 592
38. Moody CJ, Palmer FN (2002) Tetrahedron Lett 43:139
39. Herman WA, Cornils B (1997) Angew Chem Int Ed Engl 36:1049
40. Crabtree RH, Felkin H, Morris GE (1977) J Organomet Chem 141:205
41. Hillier AC, Lee HM, Stevens ED, Nolan SP (2001) Organometallics 20:4246
42. Albrecht M, Miecznikowski JR, Samuel A, Faller JW, Crabtree RH (2002) Organometallics 21:3596
43. Bäckvall JE (2002) J Organomet Chem 652:105
44. Pàmies O, Bäckvall JE (2001) Chem Eur J 7:5052
45. Fujita K, Yamaguchi R (2005) Synlett 560
46. Fujita K, Furukawa S, Yamaguchi R (2002) J Organomet Chem 649:289
47. Suzuki T, Morita K, Tsuchida M, Hiroi K (2003) J Org Chem 68:1601
48. Suzuki T, Morita K, Tsuchida M, Hiroi K (2002) Org Lett 4:2361
49. Suzuki T, Morita K, Matsuo Y, Hiroi K (2003) Tetrahedron Lett 44:2003
50. Hanasaka F, Fujita K, Yamaguchi R (2004) Organometallics 23:1490
51. Hanasaka F, Fujita K, Yamaguchi R (2005) Organometallics 24:3422
52. Gauthier S, Scopelliti R, Severin K (2004) Organometallics 23:3769
53. Ajjou AA (2001) Tetrahedron Lett 42:13
54. Ajjou AA, Pinet J-L (2005) Can J Chem 83:702
55. Morales-Morales D, Redón R, Wang Z, Lee DW, Yung C, Magnuson K, Jensen CM (2001) Can J Chem 79:823
56. Jung EM (1976) Tetrahedron 32:3
57. Fijita K, Yamamoto K, Yamaguchi R (2002) Org Lett 4:269
58. Cho CS, Seok HJ, Shim SC (2005) J Heterocyclic Chem 42:1219
59. Cho CS, Kim BT, Kim T-J, Shim SC (2001) Chem Commun 2576
60. Edwards MG, Williams JMJ (2002) Angew Chem Int Ed 41:4749
61. Cami-Kobeci G, Williams JMJ (2004) Chem Commun 1072
62. Taguchi K, Nakagawa H, Hirabayashi T, Sakaguchi S, Ishii Y (2004) J Am Chem Soc 126:72
63. Fujita K, Li Z, Ozeki N, Yamaguchi R (2003) Tetrahedron Lett 44:2687
64. Deubel DV, Frenking G, Gisdakis P, Herrmann WA, Rösch N, Sundermeyer J (2004) Acc Chem Res 37:645

65. Krom M, Coumans RGE, Smits JMM, Gal AW (2001) Angew Chem Int Ed 40:2106
66. Krom M, Peters TPJ, Coumans RGE, Sciarone TJJ, Hoogboom J, ter Beek SI, Schlebos PPJ, Smits JMM, de Gelder R, Gal AW (2003) Eur J Inorg Chem 1072
67. de Bruin B, Verhagen JAW, Schouten CHJ, Gal AW, Feichtinger D, Plattner DA (2001) Chem Eur J 7:416
68. de Bruin B, Peters TPJ, Wilting JBM, Thewissen S, Smits JMM, Gal AW (2002) Eur J Inorg Chem 2671
69. Vigalok A, Shimon LJW, Milstein D (1996) Chem Commun 1673
70. Day VW, Klemperer WG, Lockedge SP, Main DJ (1990) J Am Chem Soc 112:2031
71. Tejel C, Ciriano MA, Sola E, del Río MP, Ríos-Moreno G, Lahoz FJ, Oro LA (2005) Angew Chem Int Ed 44:3267
72. de Bruin B, Brands JA, Donners JJJM, Donners MPJ, de Gelder R, Smits JMM, Gal AW, Spek AL (1999) Chem Eur J 5:2921
73. Farrissey WJ, Perry SH, Stehling FC, Chamberlain NF (1964) Tetrahedron Lett 48:3635
74. Day VW, Eberspacher TA, Klemperer WG, Zhong B (1994) J Am Chem Soc 116:3119
75. Hetterscheid DGH, de Bruin B, Smits JMM, Gal AW (2003) Organometallics 22:3022
76. Hetterscheid DGH, Bens M, de Bruin B (2005) Dalton Trans 979
77. de Bruin, Peters TPJ, Thewissen S, Blok ANJ, Wilting JBM, de Gelder R, Smits JMM, Gal AW (2002) Angew Chem Int Ed 41:2135
78. Hetterscheid DGH, Kaiser J, Reijerse E, Peters TJP, Thewissen S, Blok ANJ, Smits JMM, de Gelder R, de Bruin B (2005) J Am Chem Soc 127:1895
79. de Bruin B, Boerakker MJ, Donners JJJM, Christiaans BEC, Schlebos PPJ, de Gelder R, Smits JMM, Spek AL, Gal AW (1997) Angew Chem Int Ed 36:2064
80. de Bruin B, Boerakker M J, Verhagen JAW, de Gelder R, Smits JMM, Gal AW (2000) Chem Eur J 6:298
81. Nishioka T, Onishi Y, Nakajo K, Guo-Xin J, Tanaka R, Kinoshita I (2005) Dalton Trans 2130
82. Flood TC, Iimura M, Perotti JM, Rheingold AL, Concolino TE (2000) Chem Commun 1681
83. Sciarone T, Hoogboom J, Schlebos PPJ, Budzelaar PHM, de Gelder R, Smits JMM, Gal AW (2002) Eur J Inorg Chem 457
84. Krom M, Coumans RGE, Smits JMM, Gal AW (2002) Angew Chem Int Ed 41:575
85. Calhorda MJ, Galvão AM, Ünalerogly C, Zlota AA, Frolow F, Milstein D (1993) Organometallics 12:3316
86. Milstein D (1982) J Am Chem Soc 124:5227
87. Haarman HF, Bregman FR, van Leeuwen PWNM, Vrieze K (1997) Organometallics 16:979
88. Takahashi Y, Hashimoto M, Hikichi S, Moro-oka Y, Akita M (2004) Inorg Chim Acta 357:1711
89. Takahashi Y, Hashimoto M, Hikichi S, Akita M, Moro-oka Y (1999) Angew Chem Int Ed 38:3074
90. Ahijado M, Braun T, Noveski D, Kocher N, Neumann B, Stalke D, Stammler H-G (2005) Angew Chem Int Ed 44:6947
91. Hay-Motherwell RS, Wilkinson G, Hussain-Bates B, Hursthouse MB (1992) J Chem Soc Dalton Trans 3477
92. Jacobi BG, Laitar DS, Pu L, Wargocki MF, DiPascuale AG, Fortner KC, Schuck SM, Brown SN (2002) Inorg Chem 41:4815
93. Lemma K, Bakac A (2004) Inorg Chem 43:4505
94. Budzelaar PHM, Blok ANJ (2004) Eur J Inorg Chem 2385

Top Organomet Chem (2007) 22: 125–148
DOI 10.1007/3418_040

Published online: 5 July 2006

The Role of NHC Ligands in Oxidation Catalysis

Thomas Strassner

Technische Universität Dresden, Physikalische Organische Chemie, Bergstrasse 66, 01069 Dresden, Germany
thomas.strassner@chemie.tu-dresden.de

Abstract During the last decade *N*-heterocyclic carbenes (NHC) have become a very important class of ligands for catalytic applications. They have been employed in reactions like C – C/C – N coupling, olefin metathesis, hydrosilylation and hydrogenation. Recently, also in the field of oxidation catalysis significant progress has been achieved. NHC ligands are known to efficiently activate metal centers and they are surprisingly resistant, even in acidic media. In contrast to phosphine ligands, the metal-NHC bond is also stable under oxidizing conditions. This review covers the oxidation of organic substrates by NHC catalysts as well as the fixation and activation of O_2 and CO_2 by NHC complexes. A variety of oxidation reactions have been studied using NHC catalysts, but the oxidation of alcohols and olefins was of particular interest. Most of the work in this area was conducted with palladium catalysts, which even allow the efficient oxidation of alcohols at ambient temperature using molecular oxygen. Bi- and tridentate NHC ligands are described as well as a variety of complexes with different metals other than palladium. Reactive intermediates like peroxo complexes have been characterized experimentally, while DFT calculations have been used to explain the mechanisms of the oxidation chemistry of transition metal NHC complexes.

Keywords Catalysis · DFT calculations · *N*-heterocyclic carbenes · Oxidation · Palladium

Abbreviations

acac	acetylacetonate
BDE	bond dissociation energy
CDA	charge decomposition analysis
CNC	2,6-bis(butylimidazole-2-ylidene)pyridine

Cp	cyclopentadienyl
Cy	cyclohexyl
DFT	density functional theory
EDA	energy decomposition analysis
Hal	halogen
HF	Hartree–Fock
Me	methyl
NHC	*N*-heterocyclic carbene
OAc	acetate
Ph	phenyl
PPh_3	triphenylphosphine
post-HF	post-Hartree–Fock
TM	transition metal

1 Introduction

For a long time metal carbenes have been either classified as Fischer- or Schrock carbenes, depending on the oxidation state of the metal. Since the introduction of *N*-heterocyclic carbene complexes this classification needs to be extended because of the very different electronic character of these ligands. Carbenes—molecules with a neutral dicoordinate carbon atom—play an important role in all fields of chemistry today. The first examples in the field of organic chemistry were published by Doering and Hoffmann in the 1950s [1], while Fischer and Maasböl introduced them to organometallic chemists about ten years later [2, 3]. But it took another 25 years until the first carbenes could be isolated [4–8].

Especially the report of the successful isolation of a stable carbene by Arduengo [6, 7] (Scheme 1) and the publication of the solid-state structure of a stable imidazole-2-ylidene in 1991 led to a renaissance of these nucleophilic carbenes, which certainly also had an influence on the 2005 Nobel price in chemistry!

The realization of the extraordinary properties of these new ligands stimulated research in this area and many imidazole-2-ylidenes have been synthesized in the last 10 years [8]. The 1,3-diadamantyl derivative **1** of the imidazole-2-ylidenes is stable at room temperature and the 1,3-dimesityl-4,5-dichloroimidazole-2-ylidene [9] is reported to be even air-stable. A variety of stable carbenes has been synthesized in between and it could be shown that steric bulk is not a requirement for the stability (the 1,3-dimethylimidazoline-2-ylidene can be distilled without decomposition [10]), although it certainly influences the long-term stability by preventing dimerization.

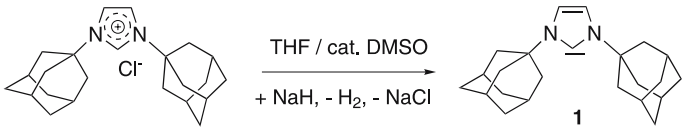

Scheme 1 Synthesis of a stable, "bottle-able" imidazole-2-ylidene

Those *N*-heterocyclic carbenes show a surprising stability which was of interest to organometallic chemists who started to explore the metal complexes of these new ligands. The first examples of this class had been synthesized as early as 1968 by Wanzlick [11] and Öfele [12], only four years after the first Fischer-*type* carbene complex was synthesized [2, 3] and six years before the first report of a Schrock-*type* carbene complex [13]. But at that time their potential as ligands had not been explored. Once the *N*-heterocyclic ligands are attached to a metal they show a completely different reaction pattern compared to the electrophilic Fischer- and nucleophilic Schrock-*type* carbene complexes.

Within the last decade many variations of the basic imidazole-2-ylidene structure (Scheme 2,A) have been synthesized [14–19]. They are not limited to sterically hindered unsaturated cyclic diaminocarbenes like **1**, also 1,2,4-triazolin-5-ylidenes (Scheme 2,B), saturated imidazolidin-2-ylidenes [6, 7, 20] (Scheme 2,C), tetrahydropyrimid-2-ylidenes [21, 22] (Scheme 2,D), acyclic structures [23, 24] (Scheme 2,E), systems with larger ring sizes [25, 26] (Scheme 2,F) or constrained geometry [27, 28] (Scheme 2,G). Reviews on the different possible synthetic routes from various precursors can be found in the literature [29–31].

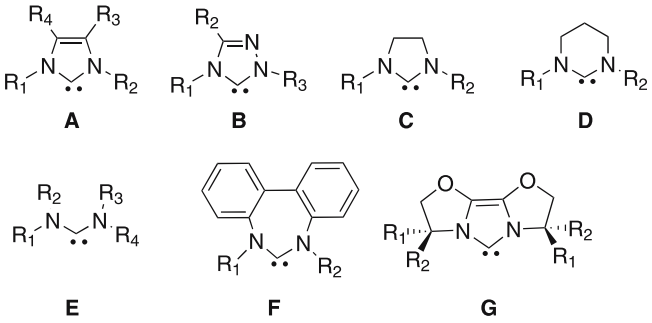

Scheme 2 Different classes of synthesized *N*-heterocyclic carbenes

2
Electronic Structure of *N*-Heterocyclic Carbenes

The electronic structure of the carbene center of an imidazole-2-ylidene can be approximated as a singlet carbene, where the carbene carbon atom is close to a sp^2-hybridization as shown in Scheme 3.

Scheme 3 Electronic structure of an imidazole-2-ylidene

The two substituents and a pair of electrons occupy the three sp^2-hybrid orbitals, while a formally vacant p_π orbital remains at the carbene carbon atom. Because of the similar chemical behavior of these nucleophilic carbenes compared to phosphines, organometallic chemists have in many cases successfully replaced phosphines by stronger donating *N*-heterocyclic carbenes.

It is known today that it is absolutely not necessary to have a cyclic delocalization of π-electrons in those NHC ligands to be able to isolate stable carbenes, as was believed in the beginning, although this provides additional stability [32–34]. Contrary to Fischer-*type* or Schrock-*type* carbene complexes, these ligands generally are formally neutral two-electron donors, which are best described as pure σ-donor ligands without significant metal-ligand π-backbonding [35–38]. It has been proposed that this might be due to a rather high occupancy of the formally empty p_π orbital of the carbene carbon atom by π-delocalization [39].

The electronic structure of these carbenes was investigated by early theoretical studies [36, 40–48] to elucidate the reasons for the surprising stability, which came to different conclusions concerning the importance of the stabilizing effect of the π-delocalization. While early studies predicted that the C – N π-interaction does not play a major role [33], others found that the p_π population at the carbene carbon atom is 30% higher for the unsaturated case, indicating that cyclic delocalization is clearly enhanced in the unsaturated carbene [48].

Frenking [36] could show that the higher stability of the imidazoline-2-ylidenes is caused by enhanced p_π–p_π delocalization leading to a significant electronic charge in the formally "empty" p_π orbital of the carbene carbon atom. The unsaturated imidazoline-2-ylidenes as well as the saturated imidazolidin-2-ylidenes are strongly stabilized by electron donation from the nitrogen lone pairs into the formally "empty" p_π orbital. The cyclic 6π-electron delocalization shows some aromatic character according to energetic and magnetic analysis. The electronically less stable saturated imidazolidin-2-ylidenes need additional steric protection of the carbene carbon atom to become isolable.

3
Synthesis of Metal Complexes

During the last decade *N*-heterocyclic carbene complexes of transition metals have been developed for catalytic applications in many different organic transformations. The most prominent example is probably the olefin metathesis reaction (Nobel price in Chemistry in 2005). *N*-heterocyclic carbenes show a pure donor nature. Comparing them to other monodentate ligands such as phosphines and amines on several metal-carbonyl complexes showed the significantly increased donor capacity relative to phosphines, even to trialkylphosphines, while the π-acceptor capability of the NHCs is on the order of those of nitriles and pyridine [29]. Experimental evidence comes from the fact that it has been shown for several metals, that an exchange of phosphines versus NHCs proceeds rapidly and without the need of an excess quantity of the NHC. This also represents one general pathway for the synthesis of these complexes, the "free carbene pathway" (Scheme 4). After deprotonation of the imidazolium salt by bases like KO^{t}Bu or NaH, the free carbene replaces a weaker bonded ligand in the low valent metal precursor.

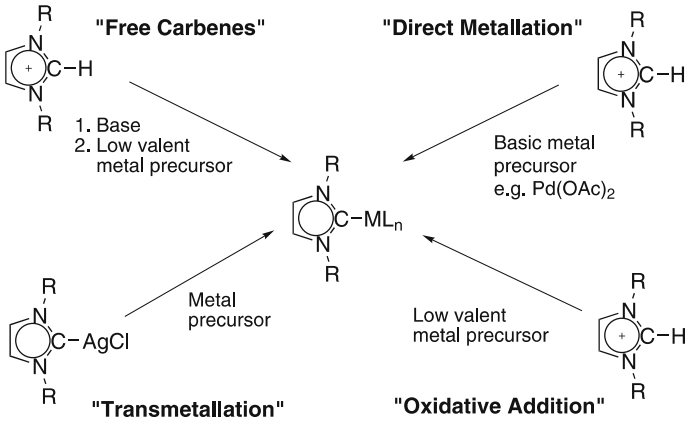

Scheme 4 Pathways for the synthesis of NHC metal complexes

This principle was used in the synthesis of the Grubbs/Herrmann metathesis catalysts [49]. As it was known that the exchange of the triphenylphosphine ligands of **2** by the more electron-donating tricyclohexylphosphines was accompanied by a significantly higher stability and reactivity [50–52], the development of complexes **3** and **4** (Scheme 5) was the logical extension of that concept. Although the metathesis reaction and NHC ligands are intimately connected and could be seen as oxidations, they are not included in this review.

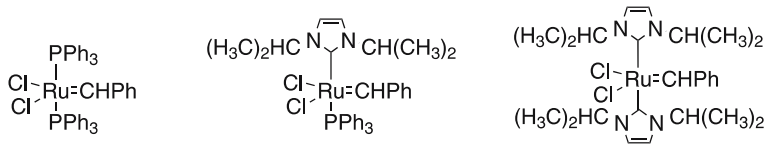

Scheme 5 Ruthenium-NHC complexes, active in the catalytic olefin metathesis

The synthesis of these complexes can easily be accomplished by substitution of one or both PPh_3 groups of **2** by NHC ligands. From the X-ray structure [53] of **4** the differences between the *N*-heterocyclic carbenes and Schrock carbenes becomes obvious just by looking at the significantly different bond lengths: the "Schrock double bond" to the CHPh group is 1.821(3) Å, while the "NHC bond" to the 1,3-diisopropylimidazoline-2-ylidene is 2.107(3) Å, more like a single bond.

The "direct metallation" is not in all cases useful as it depends on the availability of a suitable basic metal precursor, which is able to deprotonate the imidazolium salt. The advantage is that it allows one to deprotonate the imidazolium salts in the presence of groups which are labile towards stronger bases. We found $Pd(OAc)_2$ [54–56] and $Pt(acac)_2$ [57] especially useful in that regard. In cases where no basic metal precursor is available it is often successful to add NaOAc as an external base [58, 59].

Even though the "oxidative addition" pathway of imidazolium salts has been shown to be possible at certain metal complexes under special circumstances, it is far from being generally applicable to the synthesis of NHC complexes [60–67].

Widely applicable is the last pathway shown in Scheme 4, the "transmetallation reaction". Although other reagents have been proposed [68], the use of Ag_2O as introduced by Lin [69, 70] is currently the most important pathway for the synthesis of NHC metal complexes. The imidazolium halide forms a silverhalide-NHC complex which then transfers the carbene ligand to the metal precursor. Scheme 4 shows a general representation of possible pathways for the synthesis of transition metal NHC complexes.

As soon as the carbene complex is formed it shows extraordinary stability, even against strong acids and oxidizing agents like peroxodisulfate [55–57, 59]. Therefore, these complexes can be used in catalytic processes which have not been possible before with the phosphine ligands, e.g. reactions under oxidizing conditions as the tendency to form phosphine oxides is too high.

4
Oxidation Catalysis

NHC transition metal complexes have been used in several different oxidation reactions, which are described in Scheme 6. This review will cover them by reaction type and I do apologize to any author whose work is not cited although I tried hard to include all contributions to the field of oxidation catalysis.

Quite recently transition metal oxo complexes with NHC ligands have been synthesized, e.g. for rhenium [71, 72] and uranium [73], but no oxygen transfer using those complexes has been reported yet.

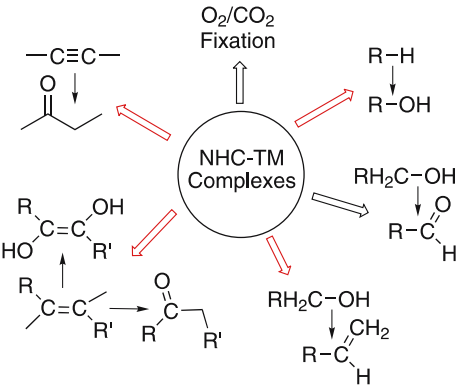

Scheme 6 Oxidation reactions catalyzed by NHC complexes

4.1
$O_2/CO/CO_2$ Fixation

Dioxygen activation at transition metal centers is a fundamentally important process and the catalytic aerobic oxidation by transition metal complexes is a challenging synthetic task. Several groups have succeeded in isolating and characterizing complexes where dioxygen, carbon monoxide or carbon dioxide are bound as ligands in empty coordination sites. One example is the cobalt peroxo complex isolated by Meyer [74]. There has been a longstanding interest in the dioxygen chemistry of cobalt and most of the complexes reported had shown the dioxygen molecule in an end-on binding mode. But cobalt(I) supported by a tripodal NHC ligand **5** binds dioxygen in a side-on, η^2-fashion (Scheme 7).

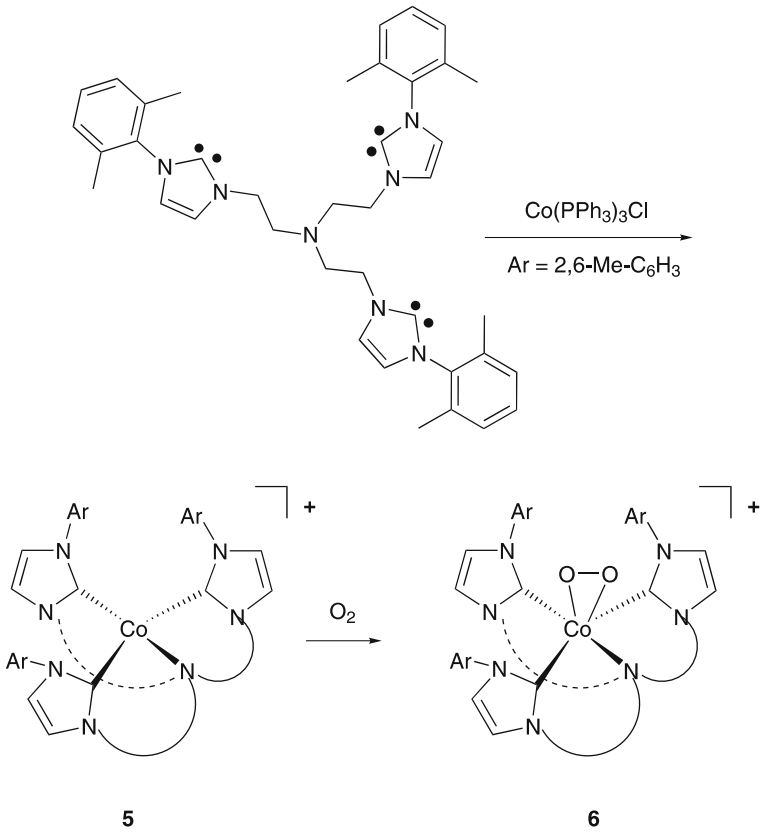

5 **6**

Scheme 7 Synthesis of $[(TIMEN^{xyl})Co(O_2)]BPh_4$ (**6**)

The complex was synthesized by deprotonation of the corresponding imidazolium salt with potassium *tert*-butoxide under formation of the triscarbene ligand tris[2-(3-xylenimidazole-2-ylidene)ethyl]amine ($TIMEN^{xyl}$), followed by the reaction with a cobalt-phosphine complex $Co(PPh_3)_3Cl$. Under inert-gas atmosphere **5** is stable in the solid state, but in THF or CH_3CN solution it slowly oxidizes to yield the cobalt (II) complex $[(TIMEN^{xyz})CoCl]Cl$ (**7**). A solution of **5** reacts cleanly with dioxygen at room temperature to form a 1 : 1 cobalt dioxygen adduct $[(TIMEN^{xyl})Co(O_2)]^+$. On the basis of the O – O stretching frequency observed in the infrared spectra it is classified as a peroxo species. Additionally, the corresponding ^{18}O labelled complex showed an isotopic shift of 50 cm^{-1}, which agrees well with theoretical predictions for a peroxo complex. When the reaction is carried out in THF in the presence of $NaBPh_4$, the resulting complex **6** precipitates from the reaction mixture.

The corresponding CO complex [(TIMEN^{xyz})Co(CO)]Cl (**8**) forms in 85% yield if **5** is reacted with an excess of CO gas. Structures of the complexes have been published [74] and are given in Fig. 1.

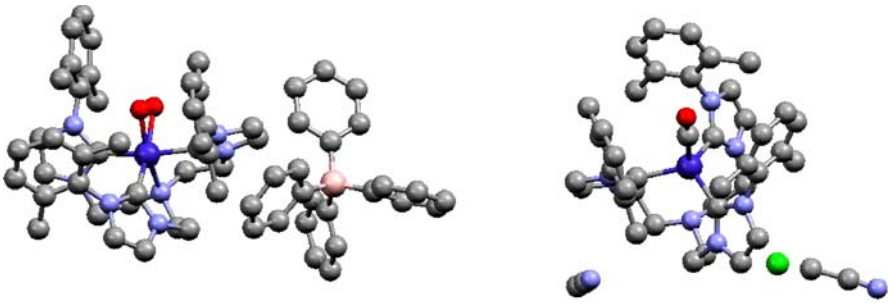

6 **8**

Fig. 1 Solid-state structures of the dioxygen complex **6** and carbon monoxide complex **8** (hydrogen atoms omitted for clarity)

The different ligand properties compared to phosphine ligands can be seen when comparing the NHC complexes with known analogous phosphine chelators. The differences become obvious from the coordination polyhedra and the electronic properties. The TIMEN ligands lead to high spin carbonyl complexes while the phosphine-based systems form diamagnetic complexes.

The dioxygen complex **6** shows almost no electrophilicity as it does not react with alkenes like styrene, cyclohexene or α,β-unsaturated alkenes such as 2-cyclohexene-1-one or 1,4-naphthochinones. Only with electron-deficient alkenes like TCNE or with benzoyl chloride reactivity was observed.

In the case of a π-allylnickel(NHC)chloride complex (**9**) a different reaction with oxygen was observed [75]. The active complex is formed in a one-pot reaction (Scheme 8). Solutions of complex **9** which are exposed to molecular oxygen undergo rapid color changes under precipitation of a purple solid, which has been identified as a μ-hydroxo Ni(II) dimer which is air-stable, but moisture-sensitive. It also was reported to be unstable in solution [75].

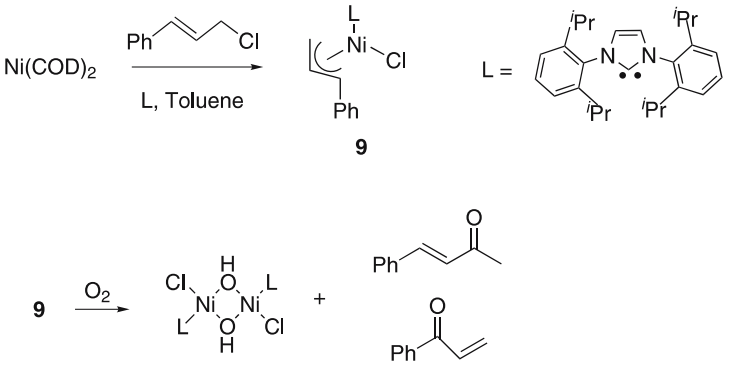

Scheme 8 Synthesis of the π-allylnickel(NHC)chloride complex **9** and its reaction with dioxygen

From the observed products and from studies using labelled material (^{18}O) it can be concluded that the nickel center promotes the splitting of the oxygen–oxygen bond. The proposed mechanism is given in Scheme 8. Reversible binding of dioxygen to the nickel center leads to the activated complex, which then undergoes rate-determining decomposition. Plausible intermediates according to kinetic studies include a Ni(III) peroxide intermediate and a monomeric hydroxonickel compound. Oxygenation of the allyl fragment leads to cinnamaldehyde and phenyl vinyl ketone in a 5 : 3 ratio.

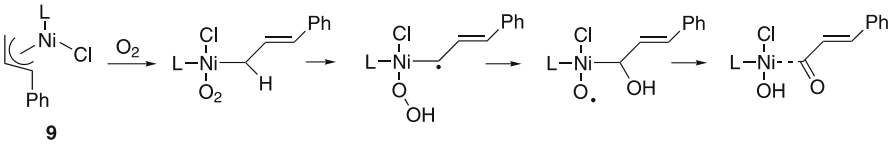

Scheme 9 Proposed mechanism of the observed allylic oxidation

The same group reported the rapid aerobic oxidation of planar bis-μ-hydroxynickel(I) dimers to yield bis-μ-hydroxonickel(II) dimers with concomitant ligand dehydrogenation [76].

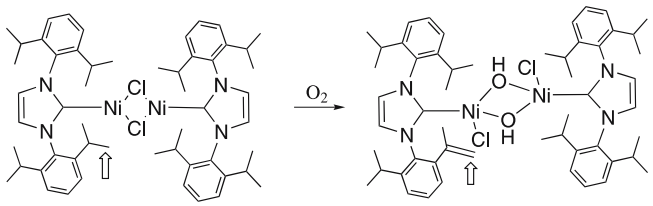

Scheme 10 Oxidation leading to ligand dehydrogenation

In contrast to the biological CO_2 fixation during the dark reaction of photosynthesis where very low concentrations of CO_2 from air can be fixed at room temperature, most reactions with transition-metal complexes or with organic substrates either require high partial pressure of CO_2 or high temperatures. An exception was published quite recently, the rapid fixation of CO_2 and O_2 from air at a palladium(0) complex **10** (Scheme 11) [77].

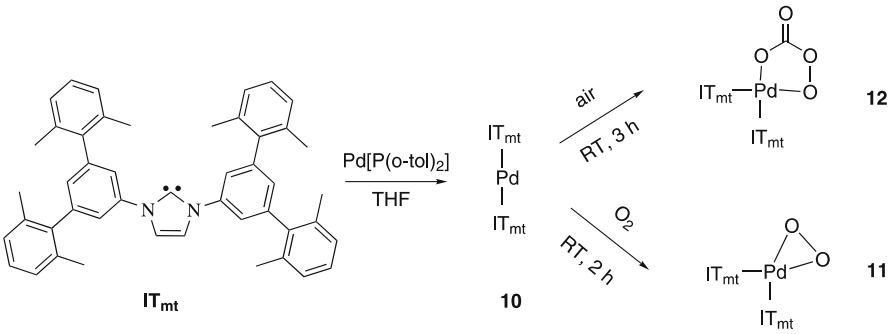

Scheme 11 Fixation of O_2 and CO_2 at a palladium(0) complex **10**

The ligand 1,3-bis(2,2″, 6,6″-tetramethyl-*m*-terphenyl-5′-yl)imidazole-2-ylidene) IT_{mt} was designed to facilitate the formation of low-coordinate species. It has a much higher overall degree of bulkiness than the well-known 1,3-bis(2,4,6-trimethylphenyl)imidazoline-2-ylidene (IMes), but in the vicinity of the carbene center it is less severe because of the absence of substituents in the ortho-position.

Exposure of the crystalline palladium(0) complex **10** to air at room temperature caused a color change from deep red to pale yellow. The formation of the palladium(II)peroxocarbonate complex **12** was confirmed by spectroscopic analysis as well as a solid-state structure. Control reactions revealed that the first intermediate is a palladium(II)peroxo complex **11**.

The analogous dioxygen species $(IMes)_2Pd(O_2)$ was isolated for the $Pd(IMes)_2$ complex, confirming the above analysis [78]. But in this case the peroxo complex does not react with CO_2. Addition of acetic acid to a toluene solution of the peroxo complex produces a hydroperoxopalladium(II) complex species $(IMes)_2Pd(OAc)(OOAc)$. Further protonolysis to yield hydrogen peroxide proceeds quite slowly (Scheme 12). Details are described in another article of this issue by S. Stahl.

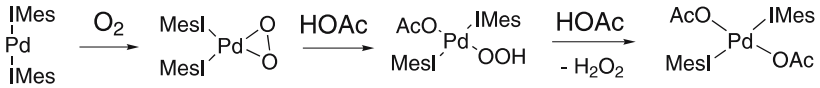

Scheme 12 Palladium dioxo intermediate

A general simplified mechanism for palladium-catalyzed aerobic oxidation reactions and the different intermediates is given in Scheme 13.

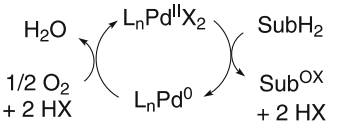

Scheme 13 Palladium-catalyzed aerobic oxidations

4.2 Transformation of Alcohols

But not only palladium(0) complexes can activate CO or O_2, also palladium(II) complexes have been reported to be active in the presence of carbon monoxide or dioxygen as it was shown in the direct synthesis of polycarbonate from CO and phenol or bisphenol A [79, 80]. The authors could confirm the positive influence of the NHC ligand comparing the activity and reactivity of the palladium-carbene complex with the corresponding $PdBr_2$ catalyst. The molecular weights and yields of the polycarbonates improved with increasing steric hindrance of the substituents in the 1,1′-position of the carbene complex.

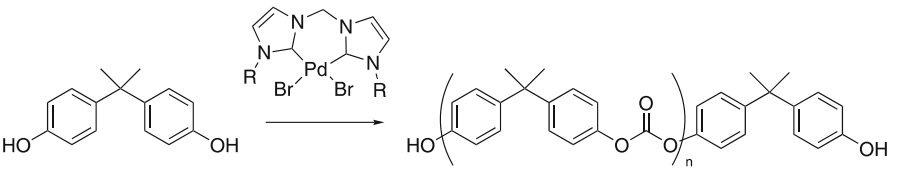

Scheme 14 Palladium(II)biscarbenes as catalysts for the oxidative carbonylation

The oxidation of alcohols to carbonyl compounds is one of the most important transformations in organic synthesis. Although many different methods have been developed, some of the most popular reactions suffer from the necessity to use toxic reagents in stoichiometric amounts or the production of large quantities of waste. Therefore, catalytic reactions using a simple oxidant like oxygen or air are still of interest to the community. Many different metals have been used in the last years, but palladium seems to be the most promising transition metal. While there is a long history for the use of palladium in the oxidation of alcohols [81–84], the benchmarks might be the Uemura system [85–87] (pyridine/$Pd(OAc)_2$) and the Sheldon system [88] (phenantroline/$Pd(OAc)_2$). Although they already succeeded in using low catalyst loadings there was still room for improvement by NHC-palladium complexes. Quite recently reports appeared where carbene ligands

promoted the aerobic oxidation of alcohols even at room temperature [89–91]. A key role is attributed to the acetate counterions in **13**, which according to the authors allow intramolecular hydrogen transfer. The optimized catalytic system is comprised of 0.5 mol % **13**, 2 mol % HOAc, and 3 Å molecular sieve in toluene at 60 °C under a balloon pressure of oxygen. For activated substrates up to 1000 turnovers have been observed. This system converts primary as well as secondary benzylic, allylic and aliphatic substrates to the corresponding carbonyl compounds in high yields.

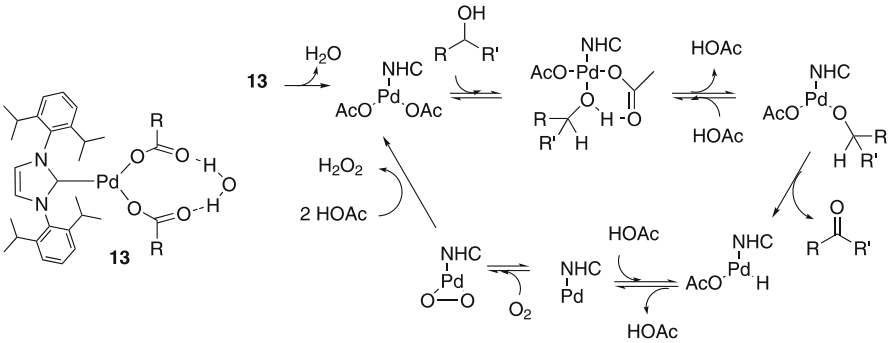

Scheme 15 Alcohol oxidation by a 1,3-bis(2,6-diisopropylphenyl)imidazole-2-ylidene) palladium(II) complex **13**

The proposed mechanism is given in Scheme 15. Initially the dissociation of water, maybe trapped by the molecular sieve, initiates the catalytic cycle. The substrate binds to the palladium followed by intramolecular deprotonation of the alcohol. The alkoxide then reacts by β-hydride elimination and sets the carbonyl product free. Reductive elimination of HOAc from the hydride species followed by reoxidation of the intermediate with dioxygen reforms the catalytically active species. The structure of **13** could be confirmed by a solid-state structure [90]. A similar system was used in the cyclization reaction of suitable phenols to dihydrobenzofuranes [92]. The mechanism of the aerobic alcohol oxidation with palladium catalyst systems was also studied theoretically [93–96].

Even more interesting is the oxidative kinetic resolution of alcohols under aerobic conditions. The system Pd(II)/sparteine/O_2 was reported to convert a racemic alcohol with high selectivity into the ketone and the alcohol [97–99]. This has also been shown to work with palladium carbene complexes (Scheme 16).

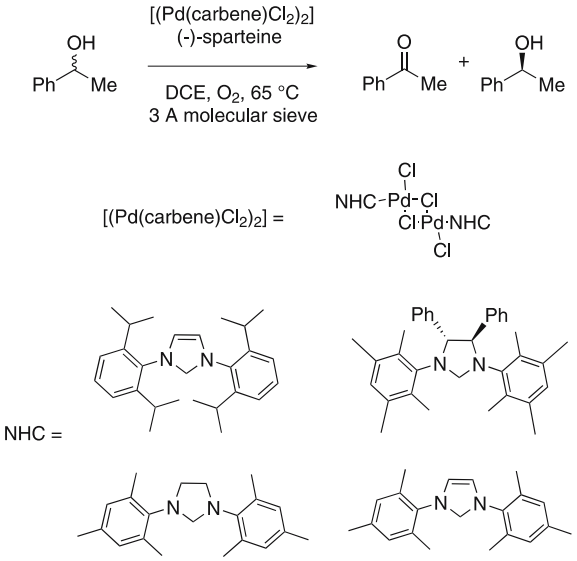

Scheme 16 Aerobic oxidative kinetic resolution of secondary alcohols

Using the catalyst system described above in combination with a rhodium phosphine catalyst Lebel reported the de novo synthesis of alkenes from alcohols [100]. They developed a one-pot process, avoiding the isolation and purification of the potentially instable aldehyde intermediate. They combined the oxidation of alcohols developed by Sigman [89] with their rhodium-catalyzed methylenation of carbonyl derivatives. The cascade process is compatible with primary and secondary aliphatic as well as benzylic alcohols in good yields. They even added another reaction catalyzed by a NHC complex, the metathesis reaction, which has not been addressed in this review as there are many good reviews, which exclusively and in great depth describe all aspects of the reaction.

The three-reaction one-pot procedure allows the conversion of suitable alcohols to cyclic alkenes in relatively good yields, one example is given in Scheme 17.

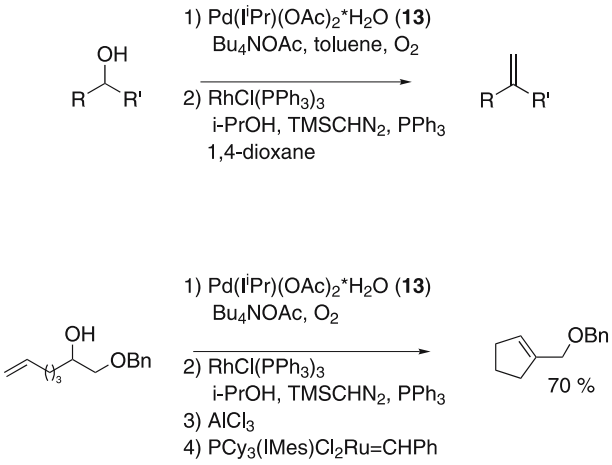

Scheme 17 Multicatalytic oxidation of alcohols

Iridium complexes like $[Cp^*IrCl_2]_2$ have been found to catalyze the Oppenauer-*type* oxidation of alcohols. However, the catalytic activity was not really satisfactory as the turnover numbers were less than 200. But when NHC ligands were introduced, the catalytic activity increased considerably. Treatment of $[Cp^*IrCl_2]_2$ with two equivalents of free carbene resulted in the formation of air-stable complexes of the type $Cp^*Ir(NHC)Cl_2$ in good yields [101]. With AgOTf in acetonitrile they could be converted to the dicationic complexes $[Cp^*Ir(NHC)(CH_3CN)_2]^{2+}$. It turned out that the neutral complexes do not show any activity while for the dicationic complexes (0.10 mol % Ir, 0.10 mol % K_2CO_3, acetone, 40 °C, 4 h) turnover numbers up to 6600 were measured [102]. Control experiments with isoelectronic phosphine ligands revealed the importance of the NHC ligands, as there was no catalytic activity observed for the phosphines. The postulated mechanism together with the most active catalyst **14** is given in Scheme 18 [101].

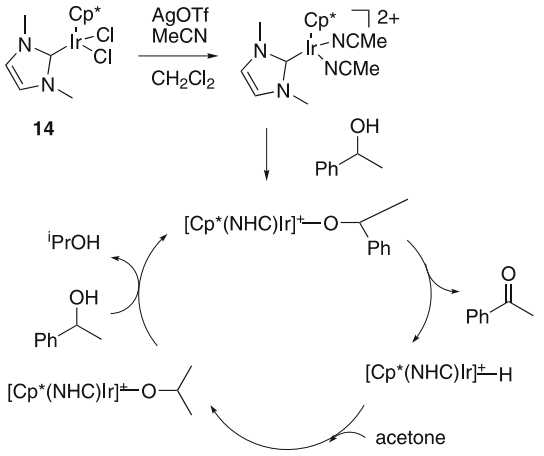

Scheme 18 Oppenauer-*type* oxidation catalyzed by Cp*Ir(NHC) complexes

4.3 Alkyne Oxidation

The hydration of unsaturated carbon-carbon bonds is one of the most environmentally friendly oxidation reactions. It had been reported that highly polar phosphane Au(I) complexes catalyze the addition of nucleophiles to non activated alkynes [103, 104]. Consequently the replacement of the phosphine by a NHC ligand was attempted and tested in the catalytic addition of water to 3-hexyne (Scheme 19). The catalyst (NHC)Au(I)OAc was synthesized from the corresponding chloride complex by addition of AgOAc [105]. Tris-(pentafluorophenyl)borane $B(C_6F_5)_3$ was needed as a co-catalyst to successfully catalyze the water addition. The authors mention that the chloride complex itself had been tested and was not active, indicating the need for a weakly coordinating ligand. The catalysis could be accomplished, but in this case the phosphine ligands provide better conversions.

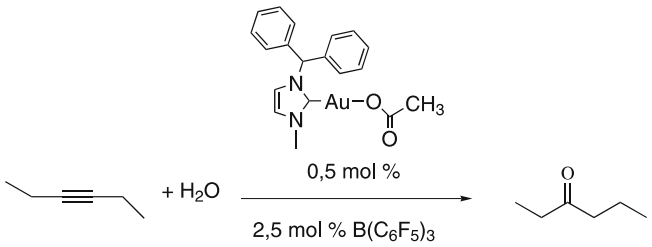

Scheme 19 Catalytically active gold carbene

4.4 Olefin Oxidation

The well-known Wacker oxidation of terminal alkenes to methylketones has been used for many years on a large scale. It requires a catalytic amount of Pd(II) together with stoichiometric $CuCl_2$ under aerobic conditions. But it is limited by palladium decomposition and chlorinated byproducts. Therefore, a lot of research has been devoted to modifying the reaction, but most of the time copper cocatalysts were necessary. Another problem is the often observed cleavage of the double bond and the production of aldehydes.

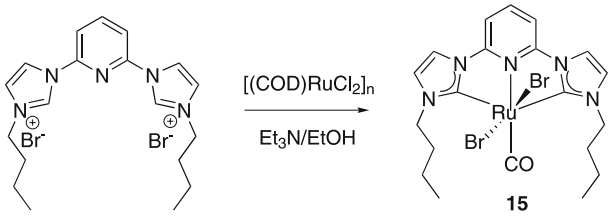

Scheme 20 Synthesis of $Ru(CNC)(CO)Br_2$ **15**

This was observed for a ruthenium(II) pincer complex $Ru(CNC)(CO)Br_2$ **15** (CNC = 2,6-bis(butylimidazole-2-ylidene)pyridine), which can be obtained in moderate yield from the direct reaction of $[(COD)RuCl_2]_n$ and 2,6-bis(1-*n*-butylimidazolium-3-yl)pyridine bromide in refluxing ethanol in the presence of NEt_3 (Scheme 20) [106]. The source of the CO in this reaction is believed to be oxidative addition of CH_3CHO followed by CH_3 migration and reductive CH_4 elimination. A similar mechanism is known from the synthesis of $RuHCl(CO)(PPh_3)_3$ [107]. Reaction of $RuCl_3$ with the ligand under similar conditions leads to the formation of $[Ru(CNC)_2](PF_6)_2$ (CNC = 2,6-bis(butylimidazole-2-ylidene)pyridine) **16**, where two pincer ligands occupy all six positions of a distorted octahedral geometry. This compound proved to be very stable and no catalytic activity was reported, but **15** catalyzes hydrogen transfer as well as the clean oxidation of olefins to aldehydes without unwanted byproducts. The catalytic system consists of 1 mol % catalyst and $NaIO_4$ in $CDCl_3/H_2O$ (9 : 1).

The oxidation to methyl ketones without cleavage of the double bond was reported recently for a palladium NHC complex [108]. When the authors used the previously described catalyst **13** in THF with dioxygen for the oxidation of styrene they found that together with the phenylmethylketone a significant amount of γ-butyrolactone was formed. Analysis of the mechanism led to the conclusion that THF is oxidized to a hydroperoxide species which is the real oxidant. They therefore tried *tert*-butylhydroperoxide (TBHP) and found immediate conversion without any induction period. Optimized conditions include 0.75 mol % of the previously described dimeric complex

[(Pd(NHC)Cl_2)$_2$] (Scheme 16) together with 3 mol % AgOTf and 5.5 eq. TBHP in methanol under aerobic conditions at 35 °C.

The oxidation of alkenes to diols via 1,2-bis(boronate) esters was reported for a silver(I) NHC complex **17** [109]. 1-Methyl-3-(+)-methylmenthoxide imidazolium chloride was used as the precursor together with an excess of Ag_2O (Scheme 21). The resulting complex was significantly more active than when prepared in situ from Ag_2O and the imidazolium salt.

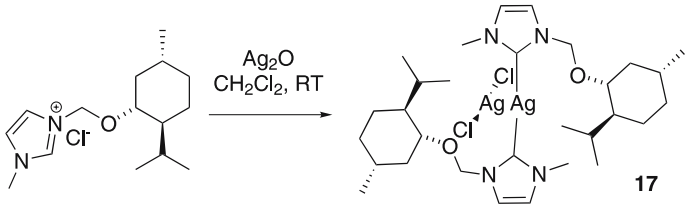

Scheme 21 Catalytically active silver carbene complex **17**

Bis(catecholato)diboron was added to internal and terminal alkenes in the presence of 5 mol % catalyst **17** in THF at room temperature. The resulting diborane complex was oxidized to the corresponding diol by a $NaOH/H_2O_2$ mixture. The conversions are strongly dependent on the electronic situation of the double bond. Vinylcyclohexane proved to be the most active substrate at 90% conversion compared to 76% conversion of styrene. Substituents in the para position of the styrene dramatically reduced the conversion (F: 12%; Cl: 14%; CF_3: 10%). Although the ligand is chiral, no asymmetric induction was observed in the reaction.

4.5 Alkane Oxidation

The CH-activation of alkanes and especially of methane and their catalytic conversion to alcohols is one of the major challenges for chemists. Methane as the major part of natural gas is currently the cheapest source of hydrocarbons and the need for methanol will increase in the near future. Methane conversion to methanol would make a conveniently transportable fuel and also a new carbon source for the chemical industry.

The catalytic homogeneous oxidation at low temperatures is therefore economically interesting, but also very difficult to achieve due to the high stability of CH-bonds. Partial oxidation is particularly hard in alkanes as classical oxidation procedures tend to overoxidize them. In the case of methane this would result in the formation of CH_2O, CO and CO_2. Low valent transition metals, however, are capable of activating the CH bond and rendering that problem less important as the difference in reactivity between the CH bond in methane and methanol is not that big.

Palladium- and platinum compounds have been successfully used for the functionalization of alkanes [110–112]. An efficient and highly selective catalytic system is a platinum complex with a bipyrimidine ligand [$Pt(bpym)Cl_2$], which provides up to 72% yield of methanol. The major drawback of the system is the reaction medium. Oleum leads to a large amount of diluted sulfuric acid when the formed ester is hydrolized.

While the research in the direction of the CH activation had its advances, the central problem is still not solved. There is no selective and efficient catalytic functionalization reaction known for unactivated sp^3 CH bonds. Only a small number of systems have been published that are capable of functionalizing methane catalytically [113–115], many of them dealing with the direct carbonylation to acetic acid [116–119].

We reported the use of *N*-heterocyclic carbene complexes (NHC) for the catalytic activation of methane [55, 56]. We found that solutions of *N*-heterocyclic carbene complexes of palladium(II) in carboxylic acids catalyze the conversion of methane to the corresponding methylesters. The high thermal stability of palladium(II) carbene complexes could be shown for complex **18** (Scheme 22), which we also structurally characterized [120]. An extraordinary feature is the unprecedented resistance of the palladium-NHC-complexes **18–22** under the acidic oxidizing conditions which are necessary for the CH-activation and functionalization.

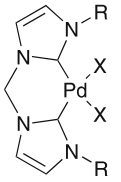

18: R = *t*Bu, X = Br
19: R = *t*Bu, X = I
20: R = Me, X = Br
21: R = Me, X = I

Scheme 22 Palladium biscarbene complexes **18–22**

A suspension of potassiumperoxodisulfate in a mixture of trifluoroacetic acid and trifluoroacetic acid anhydride at a methane pressure of 20–30 atmospheres methane and 80–100 °C in the presence of catalytic amounts of **18** and **20** leads to the formation of the trifluoroacetic acid methylester. Scheme 23 shows the oxidative character of the reaction which formally can be described as $CH_4 \rightarrow [CH_3]^+ + H^+ + 2e^-$.

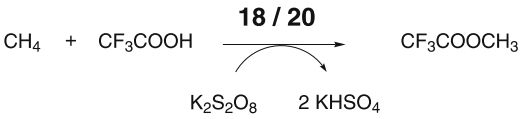

Scheme 23 Conversion of methane into the methylester of the trifluoroaceticacid

The analogous platinum complexes could be synthesized by a new synthetic route and have been structurally characterized [58], but can not be used as catalysts, since they immediately decompose in trifluoroacetic acid under formation of platinum black, whereas compounds **18–22** form clear yellow solutions in the same solvens, which even after 20 hours do not show signs of decomposition according to a NMR analysis. Reprotonation of the carbene ligands to the corresponding bisimidazolium salts can be excluded. The complexes are also stable against the addition of strong oxidants and no precipitation of palladium(II) salts was observed.

Therefore, these palladium-NHC-complexes fulfill the requirements for catalysts which are suitable for the CH-activation: a strong acid can be used as the reaction medium to protect the formed alcohols against overoxidation by forming an ester; the NHC-ligands stabilize the strong *Lewis*-acidic metal centers, which can bind the methyl species formed from methane by activation of a CH-bond and the extraordinary thermal and chemical stability allows reactions at higher temperatures in the presence of strong oxidants.

For the catalytic functionalization of methane 0.21 mmol of compound **18** and 100 equivalents $K_2S_2O_8$ are suspended in a mixture of 60 mL trifluoroacetic acid and 10 mL trifluoroacetic acid anhydride and are transferred into an autoclave. With an initial methane pressure of 20 atmospheres and a temperature of 80 °C the only product is trifluoroacetic acid methylester (510% yield relative to palladium).

The choice of the counterion has a significant influence on the activity of the catalyst, no methylester is produced by complex **19**. Similar results were obtained for compounds **20** (980%) and **21** (0%), where the steric demand of the ligands R (= methyl) is significantly lower. Additional reactions under different conditions show that the yields can be improved. After 14 hours at 90 °C catalyst **20** yielded 3000% relative to palladium (TON 30) [55].

The use of trifluoroacetic acid has the additional advantage that the formed ester can easily be removed from the reaction mixture by distillation due to the difference in boiling point between the acid and the ester. After hydrolysis, the recovered acid together with unreacted methane can be transferred back into the reactor, the catalysis could be run as a cyclic process.

DFT calculations indicated that the mechanism most likely involves three steps: electrophilic substitution, oxidation and reductive elimination. The inactivity of the iodine complexes prompted us to investigate the counterion dependence. For the methyl-substituted complexes (Scheme 23, R = CH_3) we synthesized the acetate (X = $OCOCH_3$) **22** and the chloride complex (X = Cl) **23**. The catalytic conversions are within experimental error identical to the results of the bromide complex **20**. This indicates that the dissociation of a counterion is a necessary condition for the activity of the complex [59].

We recently succeeded in synthesizing platinum-NHC complexes which are stable under the reaction conditions [57]. Introduction of aromatic substituents (Scheme 24, R= NO_2, Cl, Br, OCH_3, COOEt) in the imidazole changed the properties of the complexes quite significantly.

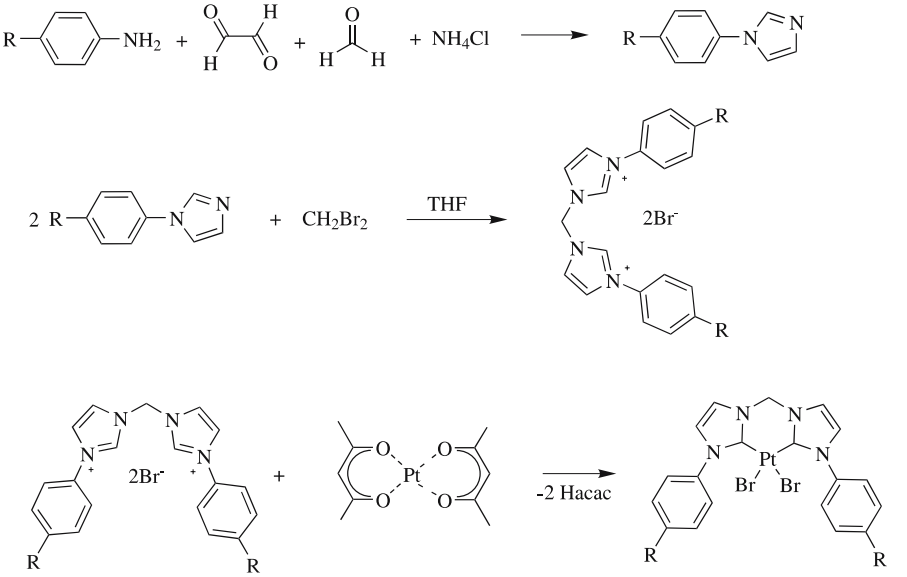

Scheme 24 Synthesis of acid stable platinum-NHC-complexes

Unfortunately, these new complexes do not show higher activities than the palladium complexes **18** and **20**, further optimization of the catalysts and reaction conditions is necessary to improve the reaction to a point where it becomes economically interesting.

References

1. Doering WvE, Hoffmann AK (1954) J Am Chem Soc 76:6162
2. Fischer EO, Maasboel A (1964) Angew Chem 76:645
3. Fischer EO (1974) Angew Chem 86:651
4. Igau A, Grutzmacher H, Baceiredo A, Bertrand G (1988) J Am Chem Soc 110:6463
5. Bourissou D, Bertrand G (1999) Adv Organomet Chem 44:175
6. Arduengo AJ III, Harlow RL, Kline M (1991) J Am Chem Soc 113:2801
7. Arduengo AJ III, Harlow RL, Kline M (1991) J Am Chem Soc 113:361
8. Arduengo AJ III (1999) Accounts Chem Res 32:913
9. Arduengo AJ III, Davidson F, Dias HVR, Goerlich JR, Khasnis D, Marshall WJ, Prakasha TK (1997) J Am Chem Soc 119:12742
10. Fischer J (1996) Dissertation, Technische Universität München, Germany

11. Wanzlick HW, Schoenherr HJ (1968) Angew Chem Int Ed Engl 7:141
12. Oefele K (1968) J Organomet Chem 12:P42
13. Schrock RR (1974) J Am Chem Soc 96:6796
14. Koecher C, Herrmann WA (1997) J Organomet Chem 532:261
15. Herrmann WA, Goossen LJ, Artus GRJ, Koecher C (1997) Organometallics 16:2472
16. Herrmann WA, Goossen LJ, Koecher C, Artus GRJ (1997) Angew Chem Int Ed Engl 35:2805
17. Herrmann WA, Koecher C, Goossen LJ, Artus GRJ (1996) Chem A Eur J 2:1627
18. Herrmann WA, Elison M, Fischer J, Koecher C, Artus GRJ (1996) Chem A Eur J 2:772
19. Herrmann WA, Elison M, Fischer J, Koecher C, Artus GRJ (1995) Angew Chem Int Ed Engl 34:2371
20. Denk MK, Thadani A, Hatano K, Lough AJ (1997) Angew Chem Int Ed Engl 36:2607
21. Alder RW, Blake ME, Bortolotti C, Bufali S, Butts CP, Linehan E, Oliva JM, Orpen AG, Quayle MJ (1999) Chem Commun (Cambridge), p 1049
22. Alder RW, Blake ME, Bortolotti C, Bufali S, Butts CP, Linehan E, Oliva JM, Orpen AG, Quayle MJ (1999) Chem Commun (Cambridge), p 241
23. Alder RW, Blake ME (1997) Chem Commun (Cambridge), p 1513
24. Alder RW, Allen PR, Murray M, Orpen AG (1996) Angew Chem Int Ed Engl 35:1121
25. Scarborough CC, Popp BV, Guzei IA, Stahl SS (2005) J Organomet Chem 690:6143
26. Scarborough CC, Grady MJW, Guzei IA, Gandhi BA, Bunel EE, Stahl SS (2005) Angew Chem Int Ed 44:5269
27. Altenhoff G, Goddard R, Lehmann Christian W, Glorius F (2004) J Am Chem Soc 126:15195
28. Altenhoff G, Goddard R, Lehmann Christian W, Glorius F (2003) Angew Chem Int Ed 42:3690
29. Herrmann WA, Weskamp T, Bohm VPW (2001) Adv Organomet Chem 48:1
30. Weskamp T, Bohm VPW, Herrmann WA (2000) J Organomet Chem 600:12
31. Herrmann WA (2002) Angew Chem Int Ed 41:1290
32. Wanzlick HW (1962) Angew Chem 74:129
33. Arduengo AJ III, Dias HVR, Dixon DA, Harlow RL, Klooster WT, Koetzle TF (1994) J Am Chem Soc 116:6812
34. Arduengo AJ III, Goerlich JR, Marshall WJ (1995) J Am Chem Soc 117:11027
35. Lehmann JF, Urquhart SG, Ennis LE, Hitchcock AP, Hatano K, Gupta S, Denk MK (1999) Organometallics 18:1862
36. Boehme C, Frenking G (1996) J Am Chem Soc 118:2039
37. Boehme C, Frenking G (1998) Organometallics 17:5801
38. Heinemann C, Mueller T, Apeloig Y, Schwarz H (1996) J Am Chem Soc 118:2023
39. McGuinness DS, Yates BF, Cavell KJ (2002) Organometallics 21:5408
40. Gleiter R, Hoffmann R (1968) J Am Chem Soc 90:5457
41. Dixon DA, Arduengo AJ III (1991) J Phys Chem 95:4180
42. Cioslowski J (1993) Int J Quantum Chem, Quantum Chem Symposium 27:309
43. Kutzelnigg W (1984) Angew Chem 96:262
44. Gobbi A, Frenking G (1994) J Am Chem Soc 116:9287
45. Kutzelnigg W (1980) Israel J Chem 19:193
46. Schindler M, Kutzelnigg W (1982) J Chem Phys 76:1919
47. Hansen AE, Bouman TD (1985) J Chem Phys 82:5035
48. Heinemann C, Thiel W (1994) Chem Phys Lett 217:11
49. Schmidt B (2003) Angew Chem Int Ed 42:4996
50. Schwab P, Grubbs RH, Ziller JW (1996) J Am Chem Soc 118:100

51. Schwab P, France MB, Ziller JW, Grubbs RH (1995) Angew Chem Int Ed Engl 34:2039
52. Nguyen ST, Grubbs RH, Ziller JW (1993) J Am Chem Soc 115:9858
53. Weskamp T, Schattenmann WC, Spiegler M, Herrmann WA (1998) Angew Chem Int Ed Engl 37:2490
54. Zeller A, Herdtweck E, Strassner T (2005) Acta Crystallograph C: Cryst Struct Commun C61:m46
55. Muehlhofer M, Strassner T, Herrmann WA (2002) Angew Chem Int Ed 41:1745
56. Maletz G, Schmidt F, Reimer A, Strassner T, Muehlhofer M, Mihalios D, Herrmann W (2003) Ger Offen (Sued-Chemie AG, Germany) De, p 10
57. Ahrens S, Herdtweck E, Goutal S, Strassner T (2006) Eur J Inorg Chem 6:1268
58. Muehlhofer M, Strassner T, Herdtweck E, Herrmann WA (2002) J Organomet Chem 660:121
59. Strassner T, Muehlhofer M, Zeller A, Herdtweck E, Herrmann WA (2004) J Organomet Chem 689:1418
60. Viciano M, Poyatos M, Sanau M, Peris E, Rossin A, Ujaque G, Lledos A (2006) Organometallics 25:1120
61. Duin MA, Clement ND, Cavell KJ, Elsevier CJ (2003) Chem Commun (Cambridge), p 400
62. Clement Nicolas D, Cavell Kingsley J, Jones C, Elsevier Cornelis J (2004) Angew Chem Int Ed 43:1277
63. McGuinness DS, Cavell KJ, Yates BF, Skelton BW, White AH (2001) J Am Chem Soc 123:8317
64. McGuinness DS, Yates BF, Cavell KJ (2001) Chem Commun (Cambridge), p 355
65. Clement ND, Cavell KJ (2004) Angew Chem Int Ed 43:3845
66. Hawkes KJ, McGuinness DS, Cavell KJ, Yates BF (2004) Dalton Trans, p 2505
67. Bacciu D, Cavell Kingsley J, Fallis Ian A, Ooi L-L (2005) Angew Chem Int Ed 44:5282
68. Rubio RJ, Andavan GTS, Bauer EB, Hollis TK, Cho J, Tham FS, Donnadieu B (2005) J Organomet Chem 690:5353
69. Wang HMJ, Lin IJB (1998) Organometallics 17:972
70. Garrison JC, Youngs WJ (2005) Chem Rev (Washington, DC) 105:3978
71. Royo B, Herdtweck E, Romao CC (2004) Eur J Inorg Chem, p 3305
72. Kueckmann TI, Abram U (2004) Inorg Chem 43:7068
73. Evans WJ, Kozimor SA, Ziller JW (2004) Polyhedron 23:2689
74. Hu X, Castro-Rodriguez I, Meyer K (2004) J Am Chem Soc 126:13464
75. Dible BR, Sigman MS (2003) J Am Chem Soc 125:872
76. Dible BR, Sigman MS, Arif AM (2005) Inorg Chem 44:3774
77. Yamashita M, Goto K, Kawashima T (2005) J Am Chem Soc 127:7294
78. Konnick MM, Guzei IA, Stahl SS (2004) J Am Chem Soc 126:10212
79. Okuyama K-I, Sugiyama J-I, Nagahata R, Asai M, Ueda M, Takeuchi K (2003) Macromolecules 36:6953
80. Okuyama K-i, Sugiyama J-i, Nagahata R, Asai M, Ueda M, Takeuchi K (2003) J Mol Catal A: Chem 203:21
81. Muzart J (2005) Tetrahedron 61:9423
82. Muzart J (2005) Tetrahedron 61:5955
83. Muzart J (2005) Tetrahedron 61:4179
84. Muzart J (2003) Tetrahedron 59:5789
85. Nishimura T, Maeda Y, Kakiuchi N, Uemura S (2000) J Chem Soc Perkin Trans 1:4301
86. Nishimura T, Kakiuchi N, Onoue T, Ohe K, Uemura S (2000) J Chem Soc Perkin Trans 1:1915

87. Nishimura T, Onoue T, Ohe K, Uemura S (1999) J Org Chem 64:6750
88. ten Brink G-j, Arends IWCE, Sheldon RA (2000) Science (Washington, DC) 287:1636
89. Jensen DR, Schultz MJ, Mueller JA, Sigman MS (2003) Angew Chem Int Ed 42:3810
90. Mueller JA, Goller CP, Sigman MS (2004) J Am Chem Soc 126:9724
91. Schultz MJ, Hamilton SS, Jensen DR, Sigman MS (2005) J Org Chem 70:3343
92. Muniz K (2004) Adv Synth Catal 346:1425
93. Keith JM, Nielsen RJ, Oxgaard J, Goddard WA III (2005) J Am Chem Soc 127:13172
94. Nielsen RJ, Keith JM, Stoltz BM, Goddard WA III (2004) J Am Chem Soc 126:7967
95. Privalov T, Linde C, Zetterberg K, Moberg C (2005) Organometallics 24:885
96. Keith JA, Oxgaard J, Goddard WA III (2006) J Am Chem Soc 128:3132
97. Jensen DR, Sigman MS (2003) Org Lett 5:63
98. Nicholas KM, Ferreira EM, Stoltz BM, Jensen DR, Pugsley JS, Sigman MS (2001) Chemtracts 14:654
99. Ferreira EM, Stoltz BM (2001) J Am Chem Soc 123:7725
100. Lebel H, Paquet V (2004) J Am Chem Soc 126:11152
101. Hanasaka F, Fujita K-i, Yamaguchi R (2004) Organometallics 23:1490
102. Hanasaka F, Fujita K, Yamaguchi R (2005) Organometallics 24:3422
103. Mizushima E, Sato K, Hayashi T, Tanaka M (2002) Angew Chem Int Ed 41:4563
104. Teles JH, Brode S, Chabanas M (1998) Angew Chem Int Ed Engl 37:1415
105. Schneider SK, Herrmann WA, Herdtweck E (2003) Zeitschr Anorg Allgem Chem 629:2363
106. Poyatos M, Mata JA, Falomir E, Crabtree RH, Peris E (2003) Organometallics 22:1110
107. Robinson SD, Levison JJ (1970) J Chem Soc [Section] A: Inorganic, Physical, Theoretical, p 2947
108. Cornell CN, Sigman MS (2005) J Am Chem Soc 127:2796
109. Ramirez J, Corberan R, Sanau M, Peris E, Fernandez E (2005) Chem Commun (Cambridge), p 3056
110. Jia C, Kitamura T, Fujiwara Y (2001) Acc Chem Res 34:633
111. Periana RA, Taube DJ, Gamble S, Taube H, Satoh T, Fujii H (1998) Science (Washington, DC) 280:560
112. Gol'dshleger NF, Tyabin MB, Shilov AE, Shteinman AA (1969) Zh Fiz Khim 43:2174
113. Wolf D (1998) Angew Chem Int Ed Engl 37:3351
114. Crabtree RH (1995) Chem Rev 95:987
115. Stahl S, Labinger JA, Bercaw JE (1998) Angew Chem Int Ed Engl 37:2181
116. Lin M, Sen A (1994) Nature (London) 368:613
117. Taniguchi Y, Hayashida T, Shibasaki H, Piao D, Kitamura T, Yamaji T, Fujiwara Y (1999) Org Lett 1:557
118. Asadullah M, Taniguchi Y, Kitamura T, Fujiwara Y (2000) Appl Catal A 194–195:443
119. Nakata K, Yamaoka Y, Miyata T, Taniguchi Y, Takaki K, Fujiwara Y (1994) J Organomet Chem 473:329
120. Herdtweck E, Muehlhofer M, Strassner T (2003) Acta Crystallogr E: Structure Reports Online E59:m970

Top Organomet Chem (2007) 22: 149–189
DOI 10.1007/3418_039

Published online: 22 July 2006

Palladium-Catalyzed Oxidation Reactions: Comparison of Benzoquinone and Molecular Oxygen as Stoichiometric Oxidants

Brian V. Popp · Shannon S. Stahl (✉)

Department of Chemistry, University of Wisconsin-Madison, 1101 University Ave., Madison, WI 53706, USA
stahl@chem.wisc.edu

Abstract Palladium-catalyzed oxidation reactions are among the most diverse methods available for the selective oxidation of organic molecules, and benzoquinone is one of the most widely used terminal oxidants for these reactions. Over the past decade, however, numerous reactions have been reported that utilize molecular oxygen as the sole oxidant. This chapter outlines the fundamental reactivity of benzoquinone and molecular oxygen with palladium(0) and their catalyst reoxidation mechanisms. The chemical similarities

between benzoquinone and dioxygen are reinforced by catalytic reactions that undergo successful catalytic turnover with either or both of these oxidants. The results highlight substantial opportunities for the development of new aerobic oxidation reactions.

Keywords Palladium · Oxidation · Dioxygen · Benzoquinone · Catalysis

Abbreviations

Ar-Bian	1,2-Bis[(2,6-diisopropylphenyl)imino]acenaphthene
bc	Bathocuproine (2,9-dimethyl-4,7-diphenyl-1,10-phenanthroline)
Bn	Benzyl
bpy	2,2′-Bipyridine
BQ	Benzoquinone
BOC	*t*-Butoxycarbonyl
bpym	Bipyrimidine
Cbz	Benzyloxycarbonyl
*chex*DAB	*N*,*N*′-Dicyclohexylethylenediimine
COD	1,5-Cyclooctadiene
dafe	4,5-Diazofluorene
dafo	4,5-Diazafluorenone
dba	Dibenzylideneacetone
dh-phen	5,6-Dihydro-1,10-phenanthroline
DIPEA	Diisopropylethylamine
DMA	*N*,*N*-Dimethylacetamide
DME	1,2-Dimethoxyethane
DMF	*N*,*N*-Dimethylformamide
dmphen	2,9-Dimethyl-1,10-phenanthroline
DMSO	Dimethyl sulfoxide
EWG	Electron-withdrawing group
HOAc	Acetic acid
HQ	Hydroquinone
IMes	1,3-Dimesitylimidazolin-2-ylidene
ITmt	1,3-Bis(2,6,2″,6″-tetramethyl-[1,1′;3′,1″]terphenyl-5′-yl)-2,3-dihydro-1*H*-imidazol-2-ylidene
MeO-BIPHEP	(*R*)-(6,6′-Dimethoxybiphenyl-2,2′-diyl)bis(3,5-di-*tert*-butylphenyl-phosphine)
MOM	Methoxymethyl
(*M*,*S*,*S*)-ip-SPRIX	(*M**,3a*S**,3a′*S**)-3,3′,3a,3a′,4,4′,5,5′-octahydro-3,3,3′,3′-tetramethyl-6,6′-spirobi[6*H*-cyclopent[*c*]isoxazole]
NHC	*N*-Heterocyclic carbene
NMM	*N*-Methylmorpholine
NQ	Naphthoquinone
Ns	Benzenesulfonyl
ns	*trans*-β-Nitrostyrene
NSN	Bis(2-pyridylmethyl)sulfide
OAc	Acetate
P2Bn	1,2-Bis[(di-*tert*-butylphosphino)methyl]benzene
PAd-Ph	2,4,6-Trioxa-8-phosphatricyclo[3.3.1.13,7]decane, 1,3,5,7-tetramethyl-8-phenyl
PAd-*o*Tol	2,4,6-Trioxa-8-phosphatricyclo[3.3.1.13,7]decane, 1,3,5,7-tetramethyl-8-(2-methylphenyl)

Pc	Phthalocyanine
PG	Protecting group
salophen	[α,α′-(*o*-phenylenedinitrilo)di-*o*-cresolato]$^{2-}$
phen	1,10-Phenanthroline
Q	Quinone
SNS	2,6-Bis(methylthiomethyl)pyridine
sp	(–)-Sparteine
(*S*,*S*)-ip-boxax	Oxazole, (1*R*)-2,2′-[1,1′-binaphthalene]-2,2′-diylbis[4,5-dihydro-4-(1-methylethyl)-, (4*S*,4′S)]
TBDMS	*t*-Butyldimethylsilyl
TFA	Trifluoroacetate
TFAH	Trifluoroacetic acid
TIPS	Triisopropylsilyl
tmeda	*N*,*N*,*N*′,*N*′-Tetramethyl-1,2-ethylenediamine
TMS	Trimethylsilyl
Ts	Tosyl, *p*-toluenesulfonyl
TPP	*meso*-Tetraphenylporphyrinato
2-pymeim	2-Pyridinylmethylene-4-methoxyaniline

1 Introduction

The Wacker process (Eq. 1) was developed nearly 50 years ago [1–3] and represents one of the most successful examples of homogeneous catalysis in industry [4–9]. This palladium-catalyzed method for the oxidation of ethylene to acetaldehyde in aqueous solution employs a copper cocatalyst to facilitate aerobic oxidation of Pd^0 (Scheme 1). Despite the success of this process, certain features of the reaction have limited the development of related aerobic oxidation reactions. Many organic molecules are only sparingly sol-

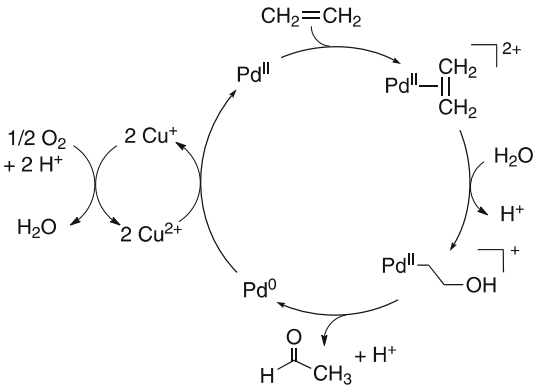

Scheme 1 Catalytic mechanism for the Wacker process

uble in water, the industrial reaction medium, and the copper cocatalysts often are less effective in organic solvents. In the absence of efficient catalyst reoxidation, Pd^0 generally decomposes into inactive metallic palladium. Such factors contribute to the fact that the majority of Pd-catalyzed reactions developed in subsequent decades consist of nonoxidative methods, such as cross-coupling reactions [10].

$$CH_2{=}CH_2 + 1/2\ O_2 \xrightarrow[H_2O]{[Pd]/[Cu]} CH_3CHO \qquad (1)$$

Oxidation reactions remain among the most important reactions in organic chemistry because they intrinsically *increase* functionality within the organic substrate. Palladium(II) is widely recognized as a versatile and selective oxidant, but its high cost limits its utility as a stoichiometric reagent. This limitation has been addressed by the identification of cooxidants and/or cocatalysts that permit the use of palladium in catalytic quantities. The $CuCl_2/O_2$ combination employed in the Wacker process (Scheme 1) is perhaps the best-known cooxidant mixture; however, a number of other reagents have also been used, including benzoquinone, polyoxometallates, stoichiometric Cu^{II} salts, and organic and inorganic peroxides [11]. Benzoquinone (BQ) is perhaps the most widely used stoichiometric oxidants for small-scale Pd-catalyzed oxidation reactions.

Molecular oxygen is perhaps the most attractive terminal oxidant. Over the past decade, numerous Pd-catalyzed oxidation reactions have been identified that undergo direct dioxygen-coupled turnover, namely, in the absence of redox-active cocatalysts or cooxidants. These reactions, which have been the subject of a number of recent reviews [12–18], are thought to proceed via a two-stage "oxidase" mechanism in which the Pd^{II} catalyst oxidizes the organic substrate (Scheme 2, step A) and the reduced catalyst is oxidized by molecular oxygen (Scheme 2, step B) [13]. This class of aerobic oxidation reactions is quite attractive because it permits a wide range of oxidation reactions to be achieved with molecular oxygen as the stoichiometric oxidant. The substrate does not react directly with molecular oxygen (or an activated oxygen intermediate). Therefore, the reactions are not limited to oxygenation of the organic substrate. As the Wacker process reveals, however, oxygen-atom transfer reactions are still possible by using water as the oxygen-atom source.

The catalytic mechanism for BQ-coupled Pd-catalyzed oxidation reactions is formally identical to that of the aerobic oxidation reactions (Scheme 2). Benzoquinone replaces O_2 as the oxidant for Pd^0 and hydroquinone is formed as a by-product. This similarity suggests that it might be possible to convert

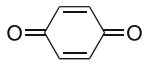

benzoquinone (BQ)

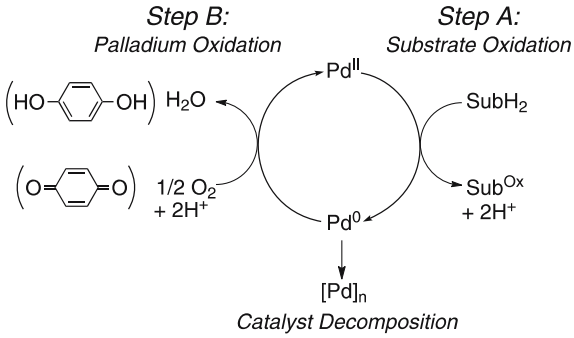

Scheme 2 Simplified catalytic cycle for palladium-catalyzed aerobic oxidation ("oxidase") reactions

BQ-coupled oxidation reactions into direct dioxygen-coupled oxidation reactions. In many studies of Pd-catalyzed oxidation reactions, however, BQ and dioxygen were not compared directly. Historically, the reaction between molecular oxygen and Pd^0 was commonly thought to be disfavored kinetically, for example, by the spin-forbidden nature of the reaction (see Fig. 1; dioxygen is a ground-state electronic triplet, Pd^0 is a closed-shell singlet). For cases in which both BQ and O_2 have been tested, neither oxidant has proven to be universally better in catalytic reactions. These observations suggest the catalytic cycle presented in Scheme 2 is overly simplified. Nevertheless, recent research results reveal that the reactivity of dioxygen and benzoquinone in Pd-catalyzed oxidation reactions may be more closely related than previously appreciated.

In this chapter, we analyze the chemistry of dioxygen and benzoquinone in the context of palladium-catalyzed oxidation reactions. After a brief histor-

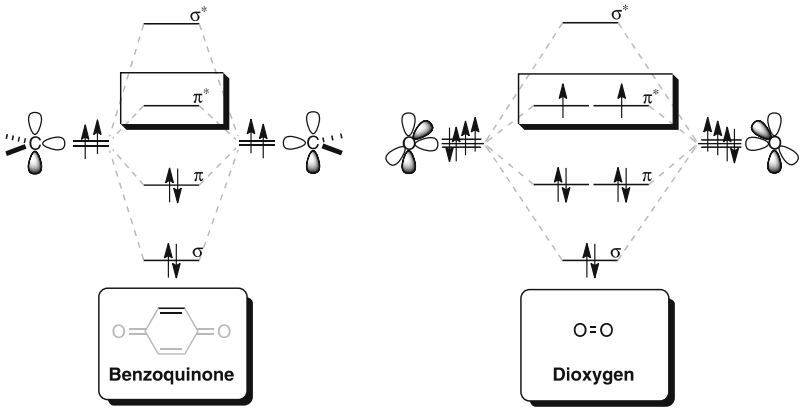

Fig. 1 Qualitative molecular orbital diagrams for the alkene fragment of benzoquinone and dioxygen highlighting the key differences in their respective frontier orbitals

ical overview of palladium oxidation catalysis, we evaluate the fundamental reactivity of dioxygen and benzoquinone with well-defined Pd^0 complexes and the mechanisms by which these reagents oxidize Pd^0 to Pd^{II}. Subsequently, we survey selected classes of Pd-catalyzed oxidation reactions for which both benzoquinone and dioxygen have been used as oxidants. The similarities observed between benzoquinone and dioxygen in both fundamental and catalytic studies suggests that numerous opportunities exist for further development of aerobic oxidation reactions.

2
Historical Perspective on the Use of Benzoquinone and Dioxygen in Palladium-Catalyzed Oxidation Reactions

In 1960, Moiseev and coworkers reported that benzoquinone (BQ) serves as an effective stoichiometric oxidant in the Pd-catalyzed acetoxylation of ethylene (Eq. 2) [19, 20]. This result coincided with the independent development of the Wacker process (Eq. 1, Scheme 1) [1]. Subsequently, BQ was found to be effective in a wide range of Pd-catalyzed oxidation reactions. For example, BQ was used to achieve Wacker-type oxidation of terminal alkenes to methyl ketones in aqueous DMF (Eq. 3 [21]), dehydrogenation of cyclohexanone (Eq. 4 [22]), and alcohol oxidation (Eq. 5 [23]). In the final example, 1,4-naphthoquinone (NQ) was used as the stoichiometric oxidant.

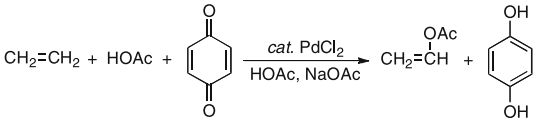

(2)

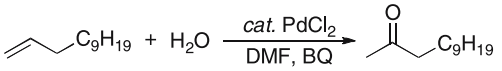

(3)

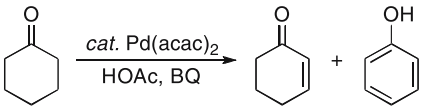

(4)

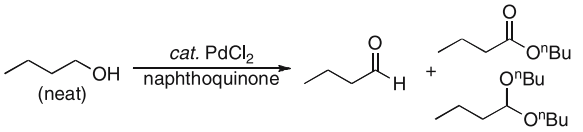

(5)

Despite the utility of BQ as an oxidant, the formation of hydroquinone as a stoichiometric by-product represents an unattractive feature of these

reactions. Bäckvall and coworkers recognized that BQ could be used in catalytic quantities by employing a cocatalyst capable of mediating the in situ oxidation of hydroquinone by a more attractive terminal oxidant [24]. Initial progress in the development of these "multicomponent" or "embedded" catalytic systems featured the use of manganese dioxide [25–27], hydrogen peroxide, or organic peroxides [28, 29] as stoichiometric oxidants.

Subsequently, Bäckvall and coworkers developed "triple-catalysis" systems to enable the use of dioxygen as the stoichiometric oxidant (Scheme 3) [30–32]. Macrocyclic metal complexes (Chart 1) serve as cocatalysts to mediate the dioxygen-coupled oxidation of hydroquinone. Polyoxometallates have also been used as cocatalysts [33]. The researchers propose that the cocatalyst/BQ systems are effective because certain thermodynamically favored redox reactions between reagents in solution (including the reaction of Pd^0 with O_2) possess high kinetic barriers, and the cocatalytic mixture exhibits highly selective kinetic control for the redox couples shown in Scheme 3 [27].

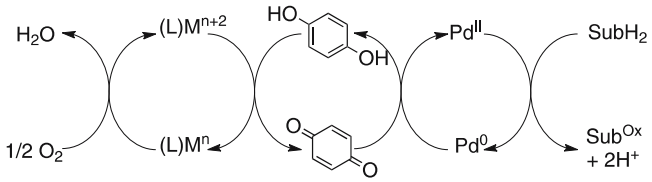

Scheme 3 "Triple-catalysis" strategy for aerobic palladium-catalyzed oxidation reactions

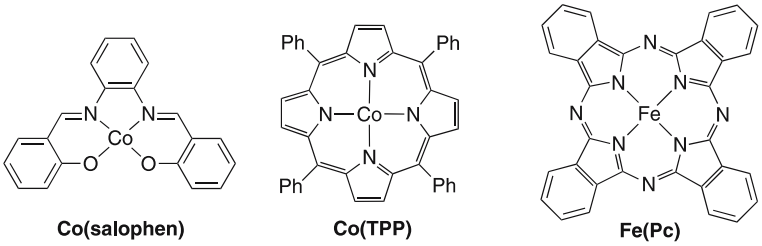

Chart 1 Transition metal cocatalysts used in multicomponent aerobic palladium-catalyzed oxidation reactions

These multicomponent catalyst systems have been employed in a variety of aerobic oxidation reactions [27]. For example, use of the Co(salophen) cocatalyst, **1**, enables selective allylic acetoxylation of cyclic alkenes (Eq. 6). Cyclohexadiene undergoes diacetoxylation under mild conditions with Co(TPP), **2** (Eq. 7), and terminal alkenes are oxidized to the corresponding methyl ketones with Fe(Pc), **3**, as the cocatalyst (Eq. 8).

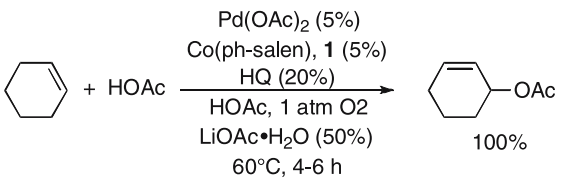

(6)

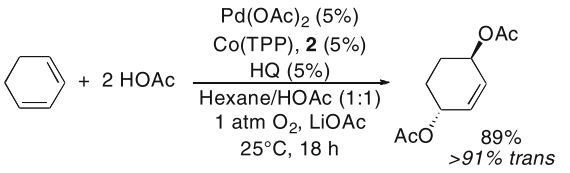

(7)

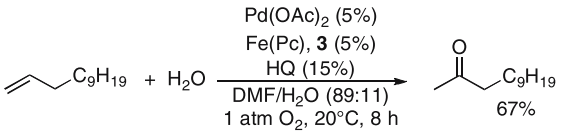

(8)

Although the methods illustrated above describe important steps toward the use of molecular oxygen in selective oxidation reactions, the need for co-catalysts increases the reaction's complexity and decreases the overall atom economy of the reaction [34, 35]. It would be even more attractive if dioxygen could be used as the sole oxidant for Pd^0. Indeed, early examples of direct dioxygen-coupled catalysis had been reported (Eqs. 9–11) [36–39], but prospects for this class of Pd-catalyzed oxidation reactions did not become widely appreciated until recently [12–18].

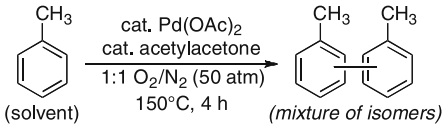

(9)

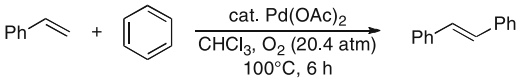

(10)

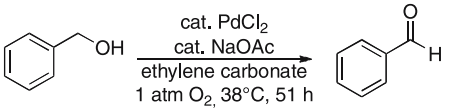

(11)

The recognition that certain organic ligands can promote direct dioxygen-coupled turnover (Scheme 2) prompted a resurgence of interest in Pd-catalyzed oxidation reactions [12–18]. For example, numerous new catalysts have been developed for aerobic alcohol oxidation (Chart 2) [40–56], which

have been the subject of extensive experimental and computational investigation [57–78]. The results of these studies reveal that reactions between Pd^0 and dioxygen are not necessarily slow. In nearly every reaction studied thus far, the rate-limiting step during catalytic turnover is associated with Pd^{II}-mediated oxidation of the substrate (Scheme 2, step A), *not* aerobic oxidation of the catalyst (Scheme 2, step B). Despite these promising recent results, many Pd-catalyzed oxidation reactions still do not undergo effective catalytic turnover with O_2 as the sole oxidant. Ongoing efforts are directed toward understanding the origin of this limitation and developing improved catalytic reactions.

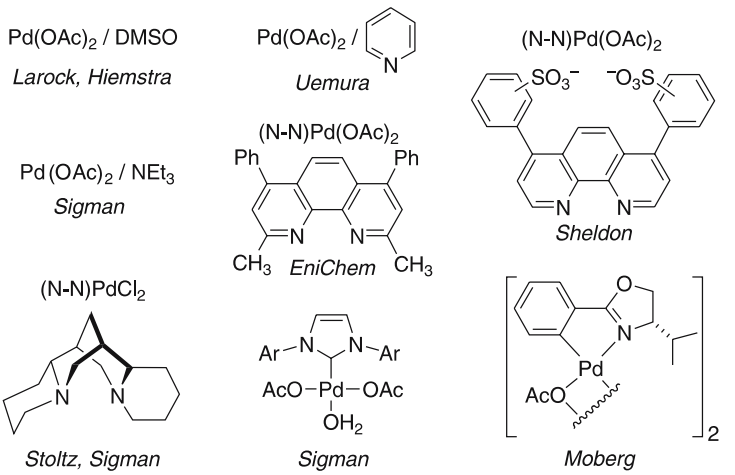

Chart 2 Catalytic systems developed for direct dioxygen-coupled palladium-catalyzed alcohol oxidation

3
Fundamental Studies of Palladium(0) Oxidation by Benzoquinone and Dioxygen

3.1
Palladium(0) Oxidation by Benzoquinone

3.1.1
Palladium–Quinone Complexes

Benzoquinone is widely recognized as a useful oxidant in organic and inorganic chemistry [79, 80]. It often reacts with transition metals by coordination of the electron-deficient alkene fragment to the metal center, forming

an η^2–π complex [81, 82]. The first examples of palladium–quinone complexes were reported by Hagihara and coworkers in 1967 [83]. In benzene, $Pd(PPh_3)_4$, **4**, reacts with BQ or NQ to form the corresponding bis-phosphine palladium–quinone complexes, **5** and **6** (Eq. 12). An X-ray crystal structure of the platinum analog, $(PPh_3)_2Pt(BQ)$, was determined in 1977 [84]. The analogous structure of $(PPh_3)_2Pd(BQ)$, **5**, was reported only recently [85].

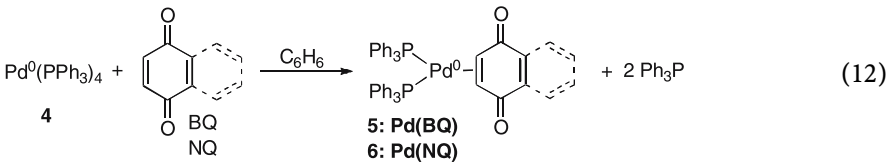

(12)

A number of palladium–quinone complexes have been prepared. Several of these have been characterized by X-ray crystallography [86–91], including other examples of complexes bearing monodentate phosphine ligands [92–94]. Related complexes with bidentate, *cis*-chelating ligands (Chart 3) tend to be more stable. The earliest use of chelating ligands was reported by Ishii, Ibers, and coworkers in 1974 with the preparation of bidentate, nitrogen-ligated Pd(Q) complexes using phen, bpy, and tmeda [95]. Numerous additional examples of stable BQ and NQ complexes of Pd are known [96–98].

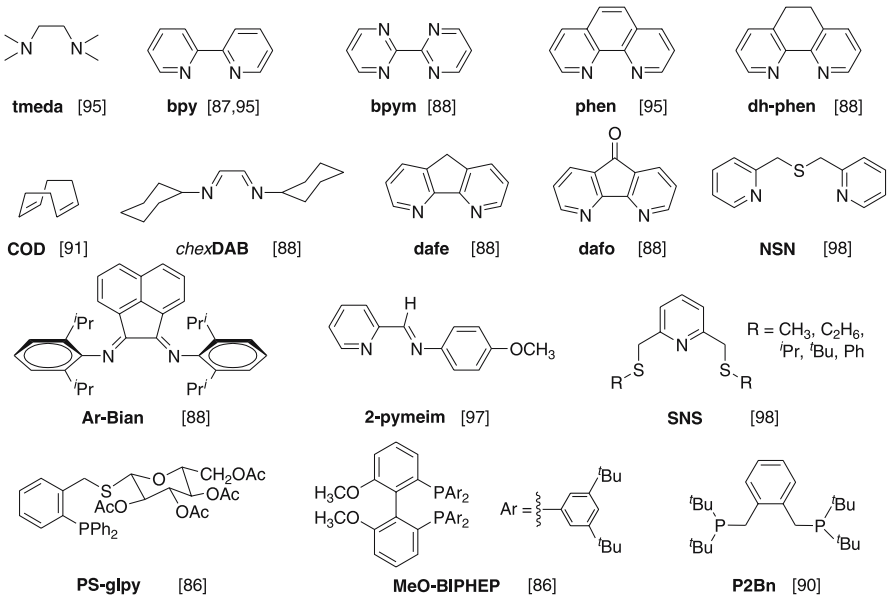

Chart 3 Examples of chelating ligands that form quinone complexes of Pd [references in brackets]

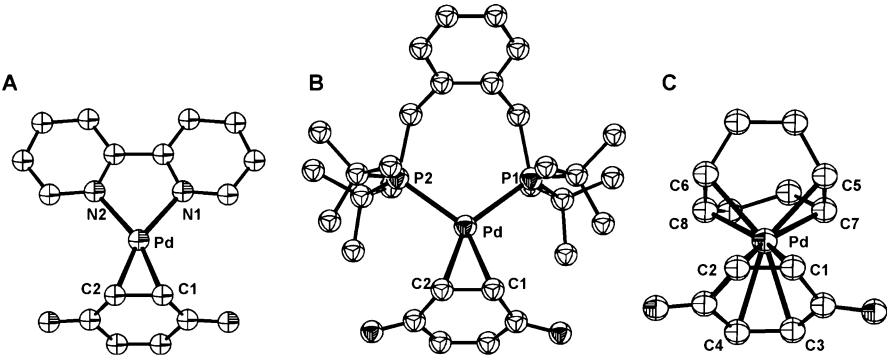

Fig. 2 ORTEP of (bpy)Pd(η^2-BQ) (**9**) (P2Bn)Pd(η^2-BQ) (**10**), and (COD)Pd(BQ) (**11**). Hydrogen atoms have been omitted for clarity

Based on X-ray crystallographic data, the coordination geometry of Pd–quinone complexes can be described as trigonal or square planar, depending on the preferred resonance structure, Pd^0–alkene versus Pd^{II}–metallacyclopropane (Eq. 13). X-ray crystal structures of (bpy)Pd(BQ), **9** [87], and (P2Bn)Pd(BQ), **10** [90] (Fig. 2) reveal that the C = C bond in these complexes is elongated significantly (1.423(6) and 1.425(10) Å for **9** and **10**, respectively) with respect to free BQ (1.33 Å) [99]. This observation is consistent with substantial Pd → alkene back-bonding and a palladium oxidation state that lies between 0 and + 2 (Eq. 13). The crystal structure of (COD)Pd(BQ), **11** [91], reveals a tetrahedral coordination environment in which both alkene fragments of BQ are coordinated to Pd. The cyclooctadiene ligand competes with BQ for π-back-bonding electron density, and, therefore, the C = C bond lengths are considerably shorter (1.373(14) Å) than those in **9** and **10**.

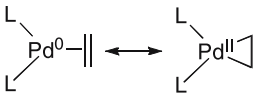

(13)

7 **8**

3.1.2 Mechanism of Palladium(0) Oxidation by Benzoquinone

The oxidation of Pd^0 by BQ to form Pd^{II} and hydroquinone requires two proton equivalents (Scheme 2). In order to probe the BQ-mediated oxidation of Pd^0, Bäckvall and coworkers investigated the reaction of (COD)Pd(BQ), **11**, with different Brønsted acids, including AcOH, CF_3CO_2H (TFAH), and CH_3SO_3H (Eq. 14) [100]. These acidic reagents possess different pK_a values, and only the strongest acid, CH_3SO_3H, is capable of reacting with **11** in

2 : 1 stoichiometry to yield hydroquinone. The reactions with AcOH and TFAH require excess acid (10 equiv) to achieve quantitative formation of hydroquinone and Pd^{II}. Addition of only two equivalents of acetic acid to BQ complex **11** yields the protonated BQ adduct **12** (Scheme 4). Although no direct evidence was obtained for oxallyl intermediates of the type **13a–c** (Scheme 4), these species represent probable intermediates in the conversion of **12** to $Pd^{II}X_2$ and hydroquinone (Scheme 4).

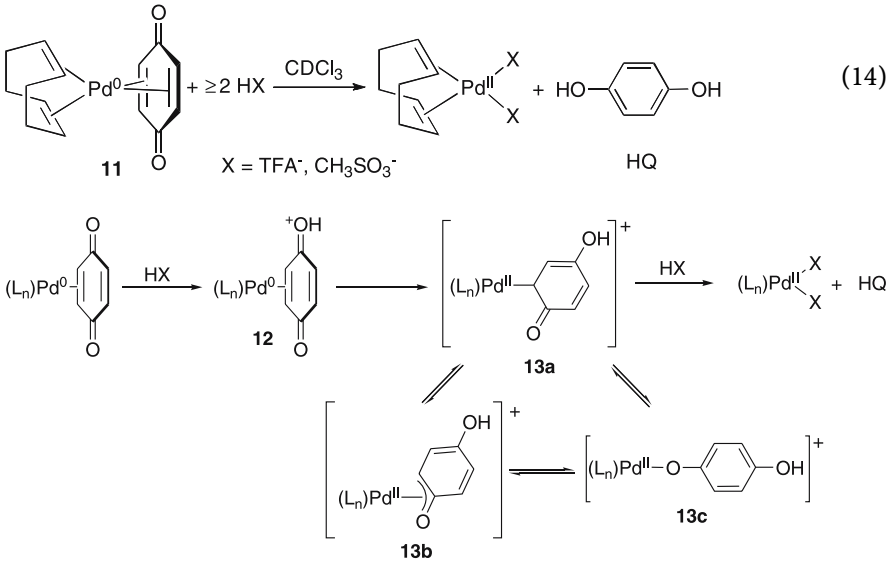

(14)

Scheme 4 Mechanism of benzoquinone/acid-promoted oxidation of palladium(0)

3.2 Palladium(0) Oxidation by Dioxygen

3.2.1 Palladium–Dioxygen Complexes

The reaction of dioxygen with transition metal complexes has stimulated the curiosity of scientists for decades. Seminal studies by Vaska in the 1960s revealed that dioxygen coordinates reversibly to the the Ir^{I} center in $(Ph_3P)_2Ir(CO)Cl$, **14** (Eq. 15) [101–104]. Following this report, numerous groups reported dioxygen adducts of other late transition metals [105].

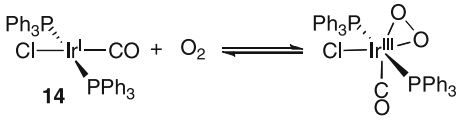

(15)

In 1966, Hagihara and coworkers reported that dioxygen oxidizes the phosphine ligands of $Pd(PPh_3)_4$, **4**, and they proposed the existence of a palladium–dioxygen intermediate [106]. The following year, the groups of Hiembach and Wilkinson independently reported isolation of $(Ph_3P)_2Pd(O_2)$, **15**, as the product of this Pd^0 oxygenation reaction (Eq. 16) [107, 108], although an X-ray crystal structure of **15** was determined only recently (see below) [109]. Chart 4 illustrates additional ligands for which peroxopalladium(II) complexes have been isolated and structurally characterized [110–115].

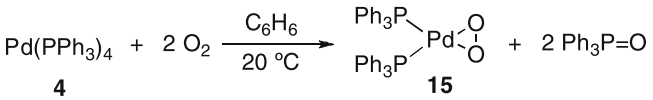

4 **15** (16)

X-ray crystal structures of three representative η^2-peroxopalladium(II) complexes are shown in Fig. 3. Each of these complexes exhibits pseudo-square-planar geometry in which the dioxygen moiety is coplanar with the two donor ligands. The O – O bond lengths in each of the structurally characterized $Pd(\eta^2\text{-}O_2)$ complexes (Table 1) are elongated relative to dioxygen and superoxide (O_2^-) and approach the value for hydrogen peroxide (Table 2). In addition, the O – O vibrational frequencies (Table 1) confirm the highly reduced nature of the O_2 fragment. The O – O bond lengths and vibrational frequencies of transition metal–dioxygen complexes have been shown to correlate with the extent of dioxygen reduction [116]. These characterization data justify the description of these complexes as peroxopalladium(II) species.

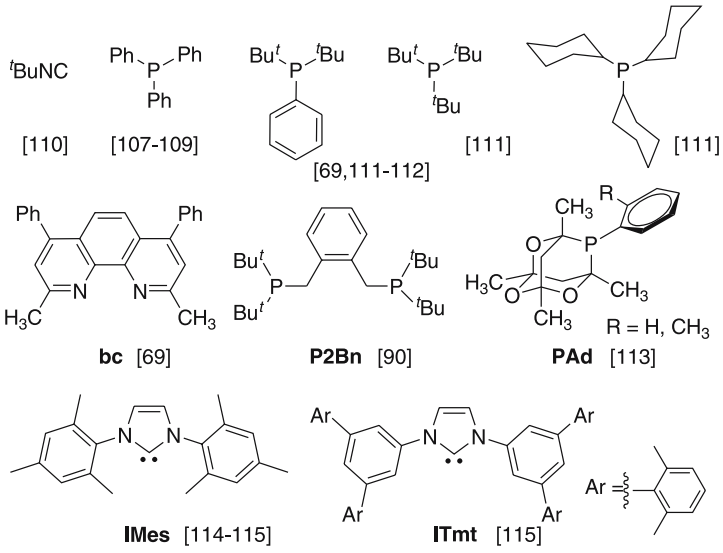

Chart 4 Ligands that form $(L_n)Pd(\eta^2 - O_2)$ complexes [references in brackets]

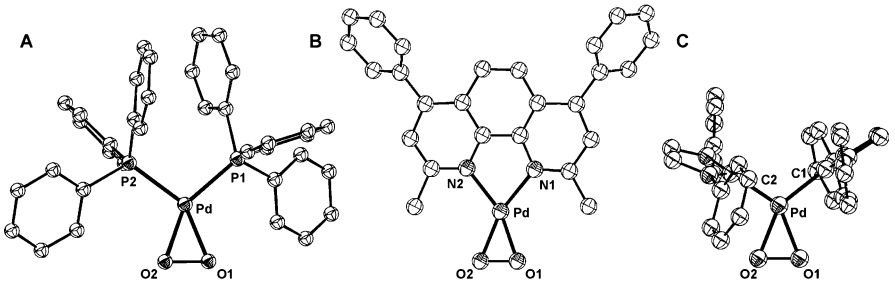

Fig. 3 ORTEP of $(Ph_3P)_2Pd(\eta^2\text{-}O_2)$, **15**, (bc)$Pd(\eta^2\text{-}O_2)$, **16**, and $(IMes)^2Pd(\eta^2\text{-}O_2)$, **17**. Hydrogen atoms have been omitted for clarity

Table 1 Available structural and infrared spectroscopic data for $(L_n)Pd^{II}(\eta^2\text{-}O_2)$ complexes

Complex (ligand[a])	O – O (Å)	$\nu_{O\text{-}O}$ (cm^{-1})	Refs.
18 (^{t}Bu$_2$PhP)	1.37(2)	915	[112]
	1.412(4)		[69]
19 (PAd-*o*Tol)	1.412(2)	–	[113]
20 (PAd-Ph)	1.413(3)	–	[113]
16 (bc)	1.415(15)	891	[69]
15 (PPh_3)	1.422(3)	885	[109]
21 (P2Bn)	1.443(3)	–	[90]
17 (IMes)	1.443(2)	868	[114]
22 (ITmt)	1.479(11)	–	[115]

[a] For abbreviations, see Chart 3

Table 2 Structural and infrared spectroscopic data for dioxygen species [117]

	Bond length (Å)	$\nu_{O\text{-}O}$ (cm^{-1})
O_2	1.21	1580
O_2^-	1.33	1097
O_2^{2-}	1.49	802

Early studies of these complexes focused primarily on the investigation of their oxygen-atom-transfer reactivity. Relatively little success was achieved, however. The peroxo fragments in these complexes exhibit nucleophilic character, and, therefore, they are generally ineffective oxidants for reactions with synthetically interesting electron-rich substrates such as alkenes and sulfides. Most of the known reactivity involves electrophilic substrates that, in many cases, insert into the Pd – O bond of peroxopalladium(II) species (Fig. 4) [105, 118].

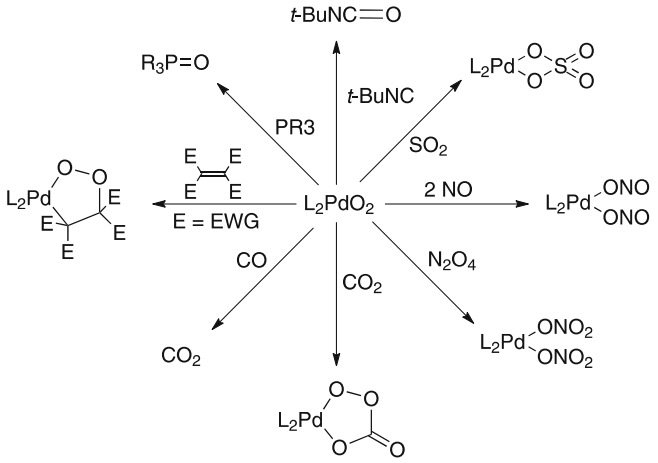

Fig. 4 Known reactions of $(L_n)Pd(\eta^2\text{-}O_2)$ complexes

3.2.2 Mechanism of Palladium(0) Oxidation by Dioxygen

Interest in peroxopalladium(II) complexes has returned in recent years. Research efforts have shifted away from the oxygen-atom-transfer reactivity of these complexes toward their role in "oxidase"-like reactions depicted in Scheme 2. The success of recent Pd-catalyzed aerobic oxidation reactions is linked to the identification of oxidatively robust ancillary ligands that stabilize Pd^0 to prevent catalyst decomposition and promote efficient oxygenation of Pd^0.

Several studies in recent years have provided fundamental insights into the reactions between molecular oxygen and Pd^0 complexes bearing catalytically relevant ligands. *N*-Heterocyclic carbenes (NHCs) represent a promising ligand class for Pd-catalyzed oxidation reactions [52, 54, 71, 73, 119, 120] (see the chapter by T. Strassner, in this volume). The NHC–Pd^0 complex $(IMes)_2Pd^0$, **23**, reacts with molecular oxygen (Eq. 17) very rapidly in solution (within the solution mixing time at – 78 °C) as well as in the solid state [114]. A similar solid-state reaction with dioxygen was subsequently reported for the related Pd^0 complex, $(ITmt)_2Pd^0$, **24** (Chart 4) [115]. These observations suggest that direct addition of O_2 to a Pd^0 center can be extremely facile.

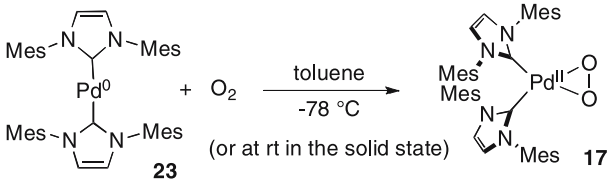

(17)

One of the first fundamental studies of Pd^0 oxygenation focused on the reactivity of (bc)Pd(dba) (bc = bathocuproine, dba = dibenzylideneacetone), **25** [69], a model Pd^0 complex based on catalysts reported earlier by coworkers at Enichem (Eq. 18) [121]. Mechanistic studies reveal that dioxygen reacts via associative displacement of the η^2-bound alkene ligand. The reaction exhibits a simple bimolecular rate law (rate = k[(bc)Pd(dba)]·pO_2) and a large negative entropy of activation ($\Delta S^{\ddagger}$ =– 43 e.u.). In contrast to the fast rate observed for the oxygenation of the *N*-heterocyclic carbene complexes noted above, this reaction requires 30–40 min to reach completion at room temperature ([Pd] = 220 mM, $pO_2 = 1$ atm). The electron-deficient dba ligand reduces electron density at the Pd^0 center and causes it to be less reactive with molecular oxygen.

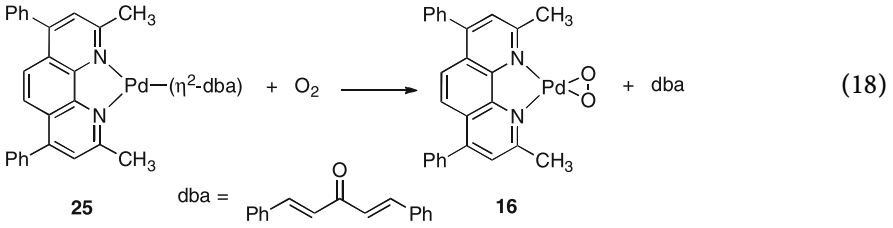

(18)

A study of $Pd(PPh_3)_4$, **4**, reported recently by Roth and coworkers, reveals yet another mechanistic pathway for Pd^0 oxygenation [122]. Complete dissociation of one PPh_3 ligand from Pd^0 occurs in solution to produce a three-coordinate palladium(0) species, **26**. Kinetic studies reveal that **26** reacts with dioxygen via parallel associative and dissociative pathways (Scheme 5). The latter dissociative pathway results in the formation of the two-coordinate complex **27**, which undergoes very rapid reaction with dioxygen in a manner directly analogous to that of the well-defined two-coordinate NHC complexes **23** and **24**.

In order to probe electronic structural issues in the Pd^0 oxygenation reaction, Landis, Stahl, and coworkers performed a computational study on

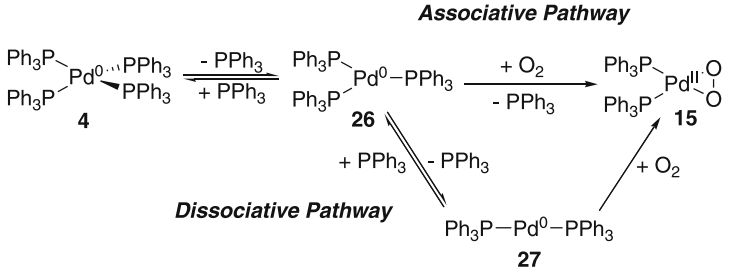

Scheme 5 Mechanism of oxygenation of $Pd(PPh_3)_4$ proceeds by competitive associative and dissociative pathways

the reaction of dioxygen with a singlet Pd^0 fragment bearing the chelating nitrogen ligand, ethylene diamine [123]. The results of this study indicate that triplet dioxygen initially approaches the palladium center with an end-on trajectory. Charge transfer from Pd^0 to O_2 results in formation of a triplet biradical η^1-superoxopalladium(I) species, **28** (Scheme 6) [124]. Coordination of dioxygen to the Pd center reduces the electronic exchange interaction between the unpaired spins, and the energy difference between the triplet and singlet energy surfaces (~ 3 kcal/mol) is significantly smaller than that of free dioxygen (23 kcal/mol). At short Pd – O distances, these surfaces converge (~ 2.2 Å) and triplet–singlet spin crossover occurs to enable formation of the second Pd – O bond. Estimation of the spin-crossover rate based on Pd spin–orbit coupling ($\sim 10^{12}$ s^{-1}) reveals that intersystem crossing will have little influence on the rate of the overall reaction. Once the molecule progresses to the singlet surface, it collapses to the stable η^2-peroxo structure.

Addition of Brønsted acids, HX, to $L_2Pd(O_2)$ complexes forms hydrogen peroxide and L_2PdX_2. This process, which completes the stepwise sequence for dioxygen-promoted oxidation of Pd^0 to Pd^{II} [125], was first observed by Kamiya and coworkers, who investigated the reaction of acetic acid with $(Ph_3P)_2Pd(O_2)$, **15** [126]. Analogous reactivity has been exploited to achieve the Pd-catalyzed synthesis of hydrogen peroxide from dioxygen in the presence of a sacrificial reductant (i.e., CO, RCH_2OH; Scheme 7) [121, 127–132]. Biphasic reaction conditions must be used to achieve significant buildup of H_2O_2 because, under normal reaction conditions, H_2O_2 undergoes rapid disproportionation into dioxygen and water (Eq. 19) [59]. The mechanism of

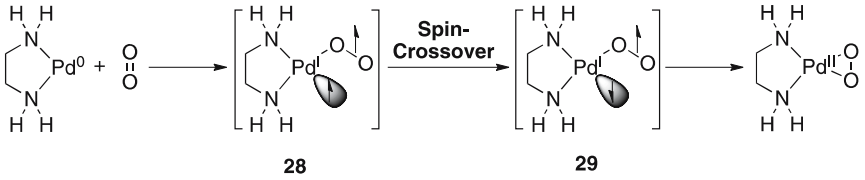

Scheme 6 Mechanistic insight into the reaction of $(en)Pd^0$ with triplet O_2 based on density functional theory (DFT)

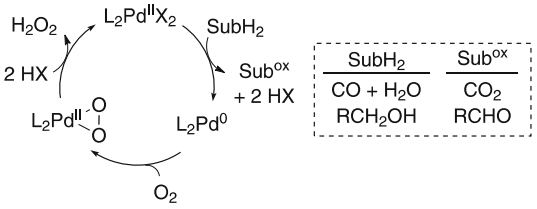

Scheme 7 Catalytic cycle for the synthesis of hydrogen peroxide from dioxygen

this "catalase"-like activity is not presently known; however, this reaction has important practical consequences because it permits all four oxidizing equivalents in dioxygen to be used in substrate oxidation.

$$H_2O_2 \xrightarrow{[Pd]} 1/2\ O_2 + H_2O \qquad (19)$$

In order to gain a better understanding of the overall Pd^0 oxidation sequence, Stahl and coworkers recently investigated the protonolysis of two different peroxo Pd^{II} complexes. In the first study, acetic acid was added to (bc)$Pd(O_2)$, **16** (Scheme 8) [69]. The presumed intermediate hydroperoxo Pd^{II} complex, **30**, does not build up in this reaction. If only one equivalent of acetic acid is added, 0.5 equivalents of the diacetate complex, **31**, is formed together with 0.5 equivalents of unreacted **16**. This result implies that the second protonation step proceeds much more rapidly than the first.

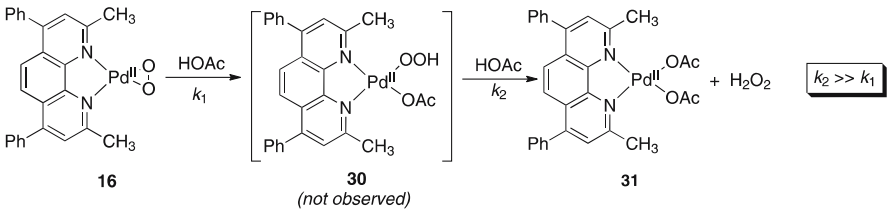

Scheme 8 Protonolysis of (bc)$Pd(O_2)$, **16**, with acetic acid

In a second study, the protonolysis of $(IMes)_2Pd(O_2)$, **17**, was investigated [114]. Addition of one equivalent of acetic acid generates the hydroperoxo-Pd^{II} complex, **32**, which has undergone *cis–trans* isomerization in the protonolysis step (Scheme 9). The ability to isolate and characterize this complex reveals that protonolysis of the second Pd – O bond is much slower than the first. Addition of a second equivalent of acetic acid forms the diacetate complex, **33**, but only after 3 days at room temperature. The systematic studies summarized in Eqs. 17 and 18 and Schemes 8 and 9 reveal the strong influence of ancillary ligands on fundamental rate constants associated with aerobic oxidation of Pd^0 to Pd^{II}. Similar effects undoubtedly will impact the success of Pd-catalyzed aerobic oxidation reactions.

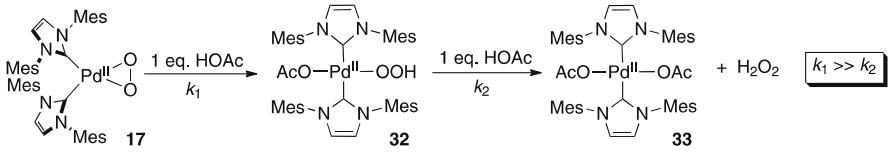

Scheme 9 Model study of the sequential protonation of $(IMe)_2Pd(O_2)$, **17**

3.3 Relationship Between Reactions of Dioxygen and Alkenes (Including Benzoquinone) with Palladium(0)

The results outlined above highlight numerous similarities between dioxygen- and BQ-mediated oxidation of palladium(0). The key steps in the respective pathways appear virtually identical (Scheme 10). Recent studies of the reactivity of dioxygen and electron-deficient alkenes with Pd^0–alkene complexes reinforce these similarities.

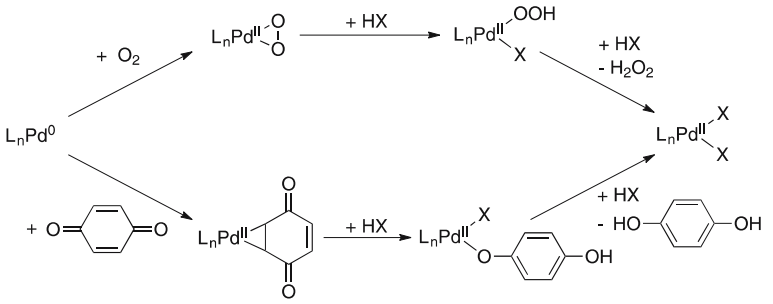

Scheme 10 Mechanistic similarity between the oxidation of Pd^0 by dioxygen and benzoquinone

The oxygenation of (bc)Pd(dba), **25**, to form (bc)Pd(O_2), **16** (Sect. 3.2.2, Eq. 18), was found to proceed by an associative-substitution mechanism that closely resembles alkene exchange reactions at Pd^0 [133–135]. In order to compare these reactions directly, Stahl and coworkers investigated both oxygenation and alkene exchange reactions with a uniform class of Pd^0 complexes, (bc)$Pd^0(ns^X)$, $\mathbf{34}^X$ (ns^X = *para*-substituted *trans*-β-nitrostyrene; X = CH_3O, CH_3, H, Br, CF_3, NO_2) (Eqs. 20 and 21) [70, 136]. Mechanistic data confirm that both reactions proceed via associative pathways (e.g., both reactions exhibit a bimolecular rate law and have large negative entropies of activation).

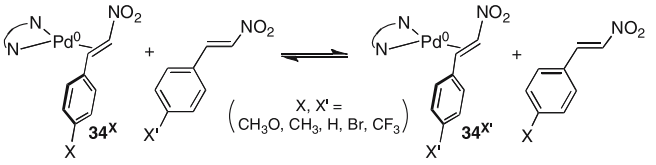

(20)

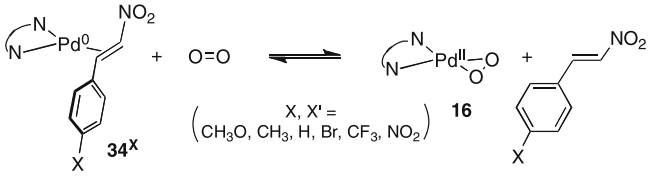

(21)

Hammett studies probing the correlation between the reaction rate and *para* substituents of the nitrostyrene ligand (or substrate) provided key insights into the similarity between these reactions. In the oxygenation reaction (Eq. 21), more-electron-rich nitrostyrene ligands promote faster reaction with O_2 [137]. This result is expected because the Pd^0 center is formally oxidized to Pd^{II} in the reaction, and more-electron-rich metal centers should undergo more facile oxidation. In alkene exchange reactions, the Pd center does not change oxidation state; however, a similar electronic trend is observed. The maximum substitution rate occurs in the reaction between an electron-deficient alkene and a Pd^0 complex bearing an electron-rich nitrostyrene ligand. These results indicate that *both* oxygenation and alkene exchange follow "oxidative" trajectories, in which the Pd^0 center is formally oxidized in the transition state [70, 136]. Density functional theory calculations support this conclusion and reveal the orbital picture shown in Fig. 5 [136]. Both reactions involve charge transfer from the electron-rich Pd^0 center to the π^* orbital of the incoming ligand. A similar analysis should apply to the reaction of Pd^0 with BQ, which is also an electron-deficient alkene.

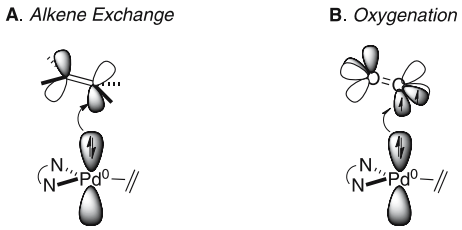

Fig. 5 Illustration of the "oxidative" trajectory for alkene exchange and oxygenation of Pd^0–alkene complexes

Further studies revealed that electron-deficient alkenes are capable of displacing O_2 from a peroxopalladium(II) complex. The reaction of nitrostyrene derivatives with (bc)Pd(O_2) results in quantitative displacement of dioxygen and formation of the (bc)Pd(ns^X) complex (i.e., the reverse reaction in Eq. 21) [138]. Moreover, preliminary results reveal that dioxygen and BQ undergo reversible exchange at a bathocuproine-coordinated Pd center (Eq. 22) (Popp BV, Stahl SS, unpublished results). This observation is the most direct experimental result to date that establishes the similar reactivity of dioxygen and BQ with palladium.

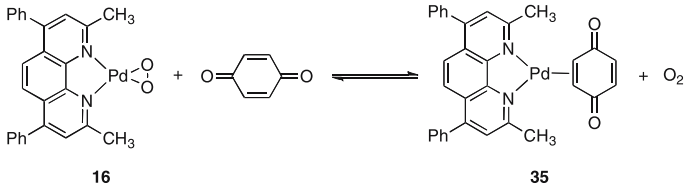

16 35 (22)

4
Palladium-Catalyzed Oxidation Reactions with Benzoquinone and Dioxygen as Stoichiometric Oxidants

The previous sections illustrate the close relationship between the fundamental reactions of molecular oxygen and BQ with well-defined palladium complexes. The insights from these studies complement those obtained from catalytic reactions. The following sections highlight catalytic reactions for which both dioxygen and BQ have been employed as stoichiometric oxidants, and the results suggest these oxidants may be more similar than previously appreciated. Rather than provide a comprehensive review of Pd-catalyzed oxidation reactions, selected examples are presented that highlight the use of both dioxygen and BQ. Reaction classes include oxidative hetero- and carbocyclization reactions of alkenes, intermolecular oxidative functionalization of alkenes (C – N and C – C bond formation), dehydrosilylation of silyl enol ethers (Saegusa oxidation), and allylic C – H acetoxylation.

4.1
Oxidative Hetero- and Carbocyclization Reactions of Alkenes Bearing Tethered Nucleophiles

4.1.1
Heterocyclization Reactions

Palladium-catalyzed, Wacker-type oxidative cyclization of alkenes represents an attractive strategy for the synthesis of heterocycles [139]. Early examples of these reactions typically employed stoichiometric Pd and, later, cocatalytic palladium/copper [140–142]. In the late 1970s, Hegedus and coworkers demonstrated that Pd-catalyzed methods could be used to prepare nitrogen heterocyles from unprotected 2-allylanilines and tosyl-protected amino olefins with BQ as the terminal oxidant (Eqs. 23–24) [143, 144]. Concurrently, Hosokawa and Murahashi reported that the cyclization of allylphenol substrates can be accomplished by using a palladium catalyst with dioxygen as the sole stoichiometric reoxidant (Eq. 25) [145].

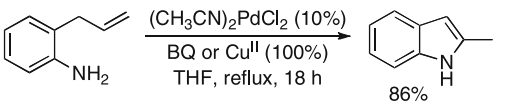

(23)

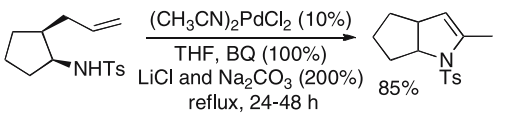

(24)

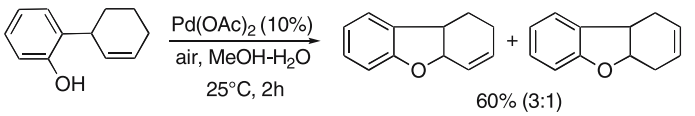

(25)

In the 1990s, the groups of Hiemstra and Larock independently discovered that $Pd(OAc)_2$ in DMSO serves as an effective catalyst for direct dioxygen-coupled catalytic turnover, and this catalyst system was applied widely to oxidative heterocyclization reactions. Examples include the addition of carboxylic acid, phenol, alcohol, formamide, and sulfonamide nucleophiles to pendant olefins (Eq. 26) [146–149].

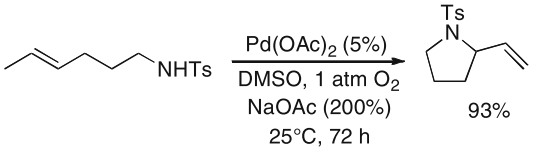

(26)

In a subsequent study of oxygen heterocyclization, Andersson et al. investigated various catalyst reoxidation conditions with the $Pd(OAc)_2$/DMSO catalyst system (Eq. 27, Table 3) [150]. Several conditions result in high substrate conversion to the product, including the use of BQ, BQ with methanesulfonic acid, and molecular oxygen, with and without copper(II) salts as a cooxidant. Only the aerobic methods enable formation of the product **37** with high regioselectivity. The presence of a copper cocatalyst enhances the rate but is not necessary for catalysis.

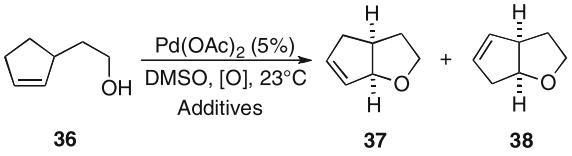

36 **37** **38**

(27)

Table 3 Terminal oxidant and additive screen for Eq. 27

Entry	[O]	Additives	Time (h)	Conversion (%)	**37 : 38**
1	BQ	None	24	> 95	76 : 24
2	BQ	10 mol % $MeSO_3H$	0.5	> 95	66 : 34
3	O_2	10 mol % $Cu(OAc)_2$	5	> 95	> 95 : 5
4	O_2	2 equiv. $Cu(OAc)_2$	2	> 95	> 95 : 5
5	O_2	None	7	> 95	> 95 : 5

The $Pd(OAc)_2$/pyridine catalyst system, initially developed for aerobic alcohol oxidation [41, 42], was shown by Stahl and coworkers to be highly

effective for the oxidative synthesis of nitrogen heterocycles. Molecular oxygen is the sole oxidant for the Pd catalyst in this reaction (Eq. 28) [151]. The nitrogen nucleophile must possess an electron-withdrawing group, and the identity of this group has a significant effect on the reaction time. The tosyl-protected substrate (**39^{Ts}**) proceeds to completion in 2 h, whereas the Cbz substrate requires 48 h under comparable conditions. Stoltz and coworkers subsequently employed $Pd(O_2CR)_2$/pyridine-based catalysts for additional heterocyclization reactions [152, 153]. Several oxygen and nitrogen functional groups undergo cyclization onto tethered alkenes in good to excellent yields (Table 4). Trifluoroacetate is more effective than acetate as an anionic ligand in these reactions.

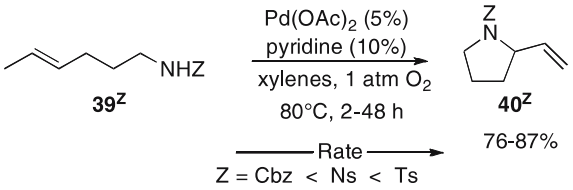

(28)

Table 4 Substrate scope for direct dioxygen-coupled heterocyclization using the Pd/pyridine catalyst system

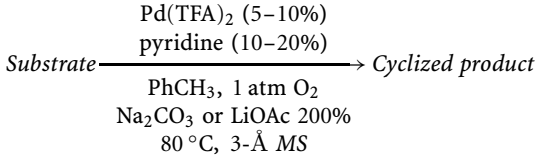

Entry	Substrate	Product		Time	Yield (%)
1	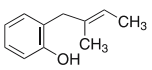	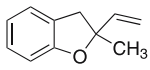		20 min	95
2	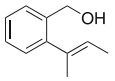	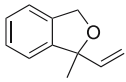		3 h	87
3	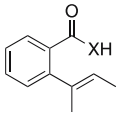	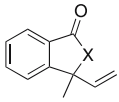	X = O	8 h	90
4			X = NTs	8 h	88
5			X = NOBn	4 h	82
6	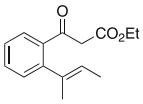	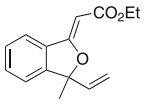		48 h	63

N-Heterocyclic carbenes (NHCs) are also useful ancillary ligands for direct dioxygen-coupled Pd-catalyzed oxidation reactions [119]. Sigman described $(NHC)Pd(O_2CR)_2$ catalysts for aerobic alcohol oxidation [54, 71], and, more recently, related catalysts have been used by the groups of Muñiz and Stahl in the oxidative heterocyclization of alkenyl phenols and tosylamides, respectively (Eqs. 29 and 30) [154, 155]. These results highlight the potential of NHC ligands to facilitate the direct reaction between dioxygen and Pd^0 under catalytic conditions (Eq. 17).

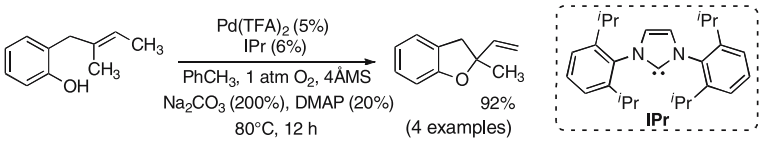

(29)

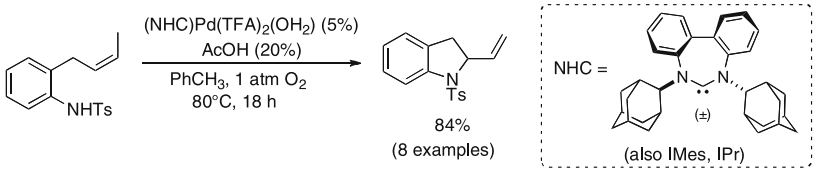

(30)

Gouverneur and coworkers showed that α,β-unsaturated esters can be cyclized in good to excellent yields (Eq. 31) [156]. Optimization of the reaction conditions revealed that four equivalents of BQ were necessary to achieve good yields (73%). Aerobic conditions, without a copper cocatalyst, proved to be superior, resulting in 89% yield over extended reaction times. No cyclization product was observed with the Pd/pyridine catalyst system described above.

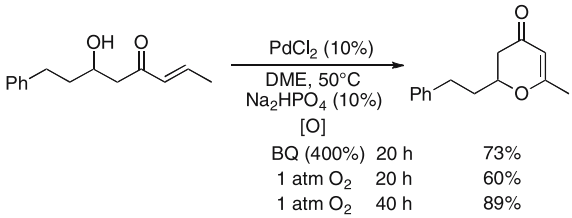

(31)

In addition to the development of new catalysts and reaction conditions for aerobic oxidative heterocyclization, considerable effort has been directed toward asymmetric transformations. Hosokawa and Murahashi reported the first example of asymmetric Pd-catalyzed oxidative heterocyclization reactions of this type [157, 158]. They employed catalytic $[(+)\text{-}(\eta^3\text{-pinene})Pd^{II}(OAc)]_2$ together with cocatalytic $Cu(OAc)_2$ for the cyclization of 2-allylphenol substrates; however, the selectivity was relatively poor ($\leq$ 26% ee).

Highly enantioselective transformations have been achieved recently with the use of chiral chelating nitrogen ligands for Pd^{II}. Both BQ and molecular oxygen have been used as oxidants in these reactions. Uozumi and Hayashi

reported one of the most successful examples, which features C_2-symmetric bis(oxazoline) ligands based on a 1,1′-binaphthyl framework (e.g., (*S*,*S*)-ip-boxax, **41**) (Eq. 32) [159–161]. The use of weakly coordinating anionic ligands, such as trifluoroacetate (TFA) and BF_4^-, benefits both catalytic activity and enantioselectivity. Sasai and coworkers achieved an enantioselective tandem cyclization of alkenyl alcohols by utilizing a similar catalyst system with a spirocyclic bis(isoxazoline) ligand, (*M*,*S*,*S*)-ip-SPRIX **42** (Eq. 33) [162]. Both of these reactions are optimal with methanol as the solvent or cosolvent, and they employ four equivalents of BQ as the oxidant. The yields can be enhanced if the reactions containing BQ are performed under an oxygen atmosphere [161]; however, the use of dioxygen alone was not described.

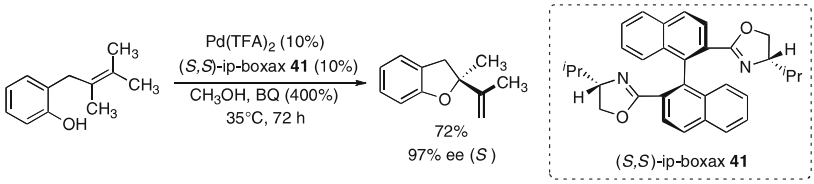

(32)

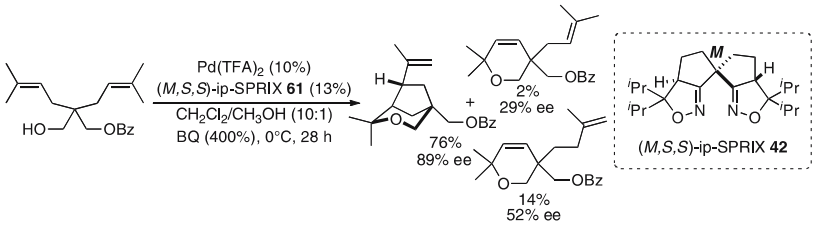

(33)

Analogous reactions have been achieved recently with molecular oxygen as the sole stoichiometric oxidant by employing (–)-sparteine (sp) as the chiral ligand [153, 163]. Stoltz and coworkers demonstrated asymmetric oxidative cyclization of a 2-allylphenol substrate (Eq. 34). A stoichiometric quantity of the sp ligand was necessary, perhaps because it also serves as a base in the reaction. Enantioselective oxidative tandem cyclization of 2-allyl anilides was achieved by Yang and coworkers (Eq. 35). The reactions proceed exclusively to the five-membered exocyclization products.

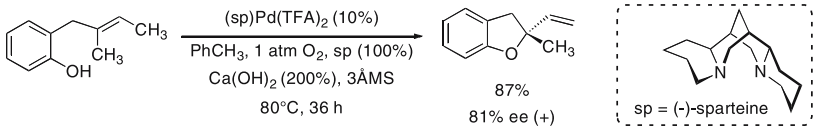

(34)

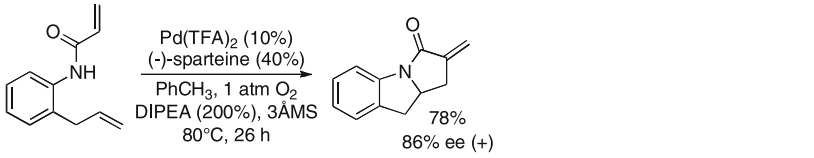

(35)

4.1.2
Carbocyclization Reactions

The intramolecular addition of carbon nucleophiles to alkenes has received comparatively little attention relative to heterocyclization reactions. The first examples of Pd-catalyzed oxidative carbocyclization reactions were described by Bäckvall and coworkers [164–166]. Conjugated dienes with appended allyl silane and stabilized carbanion nucleophiles undergo 1,4-carbochlorination (Eq. 36) and carboacetoxylation (Eq. 37), respectively. The former reaction employs BQ as the stoichiometric oxidant, whereas the latter uses O_2. The authors do not describe efforts to use molecular oxygen in the reaction with allyl silanes; however, BQ was cited as being unsuccessful in the reaction with stabilized carbanions. Benzoquinone is known to activate π-allyl-Pd^{II} intermediates toward nucleophilic attack (see below, Sect. 4.4). In the absence of BQ, β-hydride elimination occurs to form diene **43** in competition with attack of acetate on the intermediate π-allyl-Pd^{II} species to form the 1,4-addition product **44**.

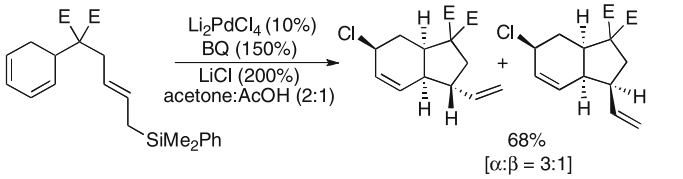

(36)

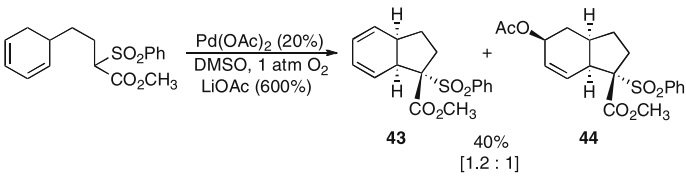

(37)

Toyota, Ihara, and coworkers demonstrated that silyl enol ethers undergo Pd^{II}-promoted intramolecular nucleophilic attack on alkenes [18]. Although early examples required stoichiometric Pd^{II} [167], they have also shown that $Pd(OAc)_2$ in DMSO is an effective catalyst in the presence of an aerobic atmosphere (Eq. 38) [168–170]. The reaction is proposed to proceed through an oxo-π-allyl intermediate that can undergo competitive alkene insertion or β-hydride elimination (Scheme 11). The latter reaction is the basis for the synthetically useful conversion of silyl enol ethers to α,β-unsaturated carbonyl compounds (see below). Efforts to use BQ as an oxidant were not described.

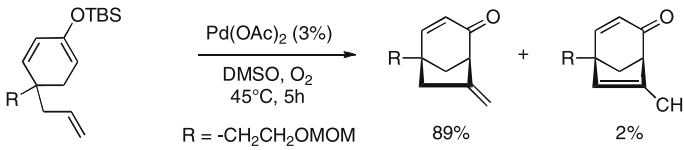

(38)

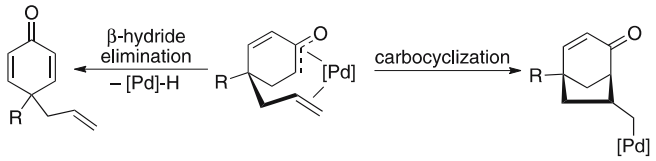

Scheme 11 Alternative fates of the oxo-π-allylpalladium(II) intermediate in the oxidative carbocyclization of silyl enol ether substrates

Widenhoefer has developed methods for Pd-catalyzed addition of 1,3-dicarbonyl nucleophiles to alkenes [171–173]. Most of these reactions employ stoichiometric copper as the oxidant; however, Yang and coworkers recently reported a modified procedure that employs cocatalytic lanthanide Lewis acids to achieve direct dioxygen-coupled turnover (Eq. 39) [174]. The Lewis acid is thought to activate the carbon nucleophile, β-keto amide, toward attack on the tethered alkene.

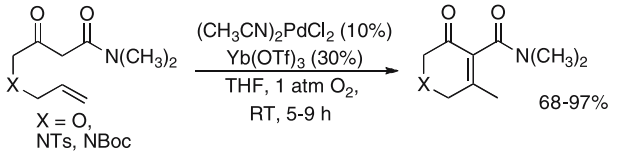

(39)

Oxidative carbocyclization reactions can also be achieved by an oxidative Heck strategy in which an alkene inserts into an intermediate Pd–aryl bond formed by direct palladation of an arene. Stoltz and coworkers recently demonstrated such reactions with electron-rich arenes that possess tethered alkenes. Successful substrates include indoles and oxygen-substituted arenes (Eqs. 40 and 41) [175, 176]. The catalyst is a variant of the $Pd(OAc)_2$/pyridine system in which pyridine is replaced by the electron-deficient analog ethyl nicotinate. Molecular oxygen was the only oxidant used for the indole reactions; however, both BQ and dioxygen were successful in the reactions with oxygenated arenes (Eq. 41). Subsequent optimization of the latter reactions permitted yields as high as 80% by using BQ as the oxidant with cocatalytic NaOAc.

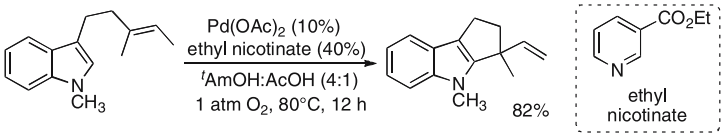

(40)

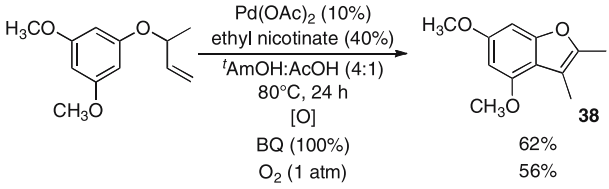

(41)

4.2
Intermolecular Oxidative Functionalization of Alkenes

4.2.1
Carbon–Nitrogen Bond Formation

Palladium-catalyzed addition of oxygen nucleophiles to alkenes dates back to the Wacker process and acetoxylation of ethylene (Sects. 1 and 2). In contrast, catalytic methods for intermolecular oxidative amination of alkenes (i.e., "aza-Wacker" reactions) have been identified only recently. Both O_2 and BQ have been used as oxidants in these reactions.

Hosokawa, Murahashi, and coworkers demonstrated the ability of Pd^{II} to catalyze the oxidative conjugate addition of amide and carbamate nucleophiles to electron-deficient alkenes (Eq. 42) [177]. Approximately 10 years later, Stahl and coworkers discovered that Pd-catalyzed oxidative amination of styrene proceeds with either Markovnikov or anti-Markovnikov regioselectivity. The preferred isomer is dictated by the presence or absence of a Brønsted base (e.g., triethylamine or acetate), respectively (Scheme 12) [178, 179]. Both of these reaction classes employ O_2 as the stoichiometric oxidant, but optimal conditions include a copper cocatalyst. More recently, Stahl and coworkers found that the oxidative amination of unactivated alkyl olefins proceeds most effectively in the absence of a copper cocatalyst (Eq. 43) [180]. In the presence of 5 mol % $CuCl_2$, significant alkene amination is observed, but the product consists of a complicated isomeric mixture arising from migration of the double bond into thermodynamically more stable internal positions.

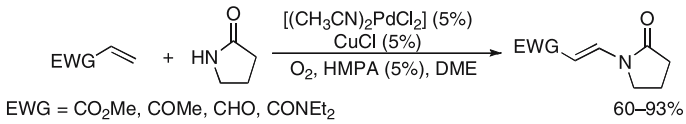

(42)

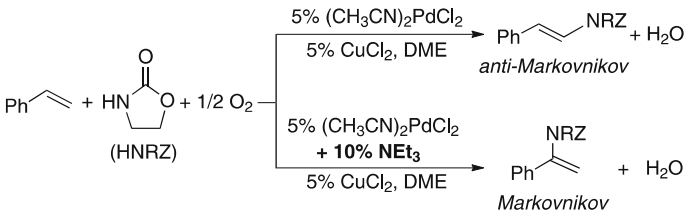

Scheme 12 Regioselective Pd-catalyzed oxidative amination of styrene

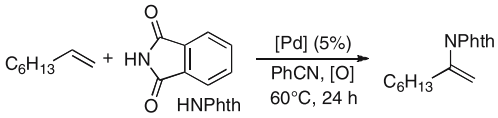

(43)

[Pd]	[O]	Yield (%)
$PdCl_2$	O_2 (1 atm)	17
	BQ (200%)	10
$Pd(OAc)_2$	**O_2 (1 atm)**	**81**
	BQ (200%)	10
$Pd(TFA)_2$	O_2 (1 atm)	4

Catalyst conditions very similar to those employed in Eq. 42 and Scheme 12 were used recently by Lloyd-Jones, Booker-Milburn, and coworkers to achieve Pd-catalyzed diamination of conjugated dienes with urea nucleophiles (Eq. 44) [181]. Both dioxygen and BQ were evaluated as oxidants, and BQ proved to be significantly more effective (Eq. 44). The beneficial effect of BQ probably arises from its ability to promote nucleophilic attack on the intermediate π-allyl palladium complex (see below, Sect. 4.4). This hypothesis is supported by the observation that the oxidative amination of styrene with urea, which does not undergo the second nucleophilic attack, proceeds equally effectively with both O_2 and BQ as the oxidant (Eq. 45).

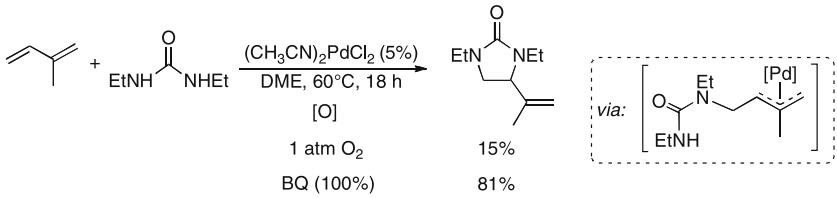

(44)

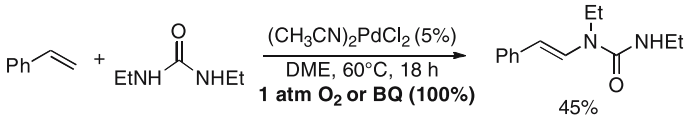

(45)

4.2.2 Carbon–Carbon Bond Formation

Palladium(0)-catalyzed cross-coupling of aryl halides and alkenes (i.e., the Heck reaction) is widely used in organic chemistry. "Oxidative Heck" reactions can be achieved by forming the Pd^{II}-aryl intermediate via direct palladation of an arene C – H bond. Intramolecular reactions of this type were described in Sect. 4.1.2, but considerable effort has also been directed toward the development of intermolecular reactions. Early examples by Fujiwara and others used organic peroxides and related oxidants to promote catalytic turnover [182–184]. This section will highlight several recent examples that use BQ or dioxygen as the stoichiometric oxidant.

Palladium(II) effects orthometalation of acetanilides to form the corresponding palladacycles [185]. De Vries, van Leeuwen, and coworkers exploited this reactivity to achieve regioselective oxidative coupling of acetanilides and *n*-butyl acrylate that proceeds efficiently with BQ as the stoichiometric oxidant (Eq. 46) [186]. The use of TsOH as an additive and acetic acid as a cosolvent significantly improves the results. Inferior results are observed with hydrogen peroxide or copper(II) acetate as the stoichiometric oxidant, but efforts to use molecular oxygen were not described.

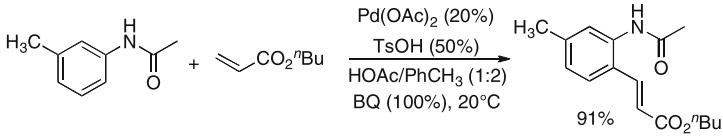

(46)

Jacobs and coworkers subsequently reported an aerobic method to achieve arene–alkene coupling in the absence of directing groups [187]. $Pd(OAc)_2$, dissolved in neat aromatic solvents (e.g., benzene, toluene, anisole), undergoes electrophilic activation of an aromatic C – H bond. Reaction of the aryl-Pd^{II} intermediate with electron-deficient alkenes yields Heck-type products. Various redox-active cocatalysts were investigated to promote dioxygen-coupled turnover, including $Mn(OAc)_3$, $Mn(acac)_2$, and $Co(OAc)_2$; however, the most effective condition simply features benzoic acid as a cocatalyst, allowing subsequent alkene insertion to yield Heck-type products. The use of 0.1 mol % $Pd(OAc)_2$ and 20 mol % benzoic acid results in 762 turnovers and a turnover frequency of 73 h^{-1} for the reaction in Eq. 47. The reactions proceed in high yield (typically > 90%) with respect to the alkene as the limiting reagent; however, all three regioisomers are generated.

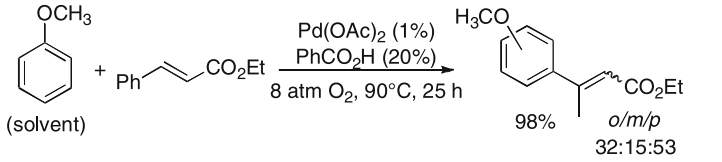

(47)

A regioselective example of aerobic oxidative coupling has been achieved by Gaunt and coworkers in the reaction of pyrroles with electron-deficient alkenes [188]. Selective functionalization of the C-2 or C-3 position of pyrroles is controlled by the identity of the nitrogen-protecting group. Groups with minimal steric bulk (e.g., BOC, Ts, Bn) lead to selective alkenylation at the C-2 position, whereas the sterically bulky group, TIPS, results in selective functionalization of the C-3 position (Eq. 48). The reactions proceed with air, pure O_2, or *t*BuOOBz as the oxidant.

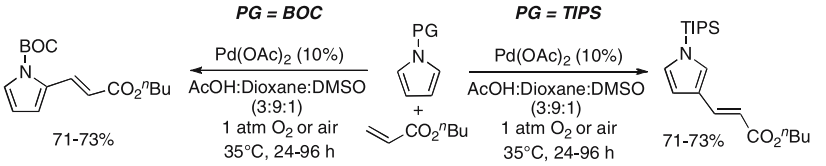

(48)

Regioselective oxidative Heck coupling can also be accomplished by forming aryl-Pd^{II} species via transmetalation from arylboronic acids. This method was first developed by Jung and coworkers (Eq. 49) [189]. The aerobic reaction conditions are compatible with a range of electron-deficient alkenes and aryl boron sources. Subsequently, Larhed and coworkers employed a catalyst system featuring a bidentate nitrogen ligand (dmphen) and *N*-methyl morpholine (NMM), which exhibits higher turnover numbers (1% Pd^{II} catalyst) and generally improved yields (Eq. 50) [190–192].

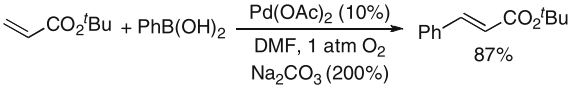

(49)

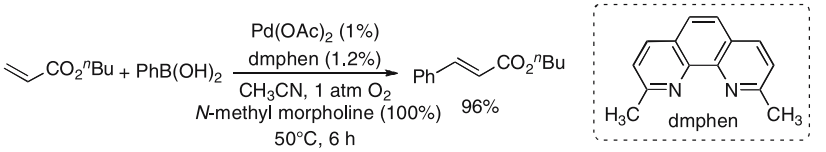

(50)

4.3
Dehydrosilylation of Silyl Enol Ethers

In 1978, Saegusa and coworkers discovered that silyl enol ethers can be converted into α,β-unsaturated ketones and aldehydes by Pd^{II} [193]. In the presence of 0.5 equivalents of BQ, substoichiometric $Pd(OAc)_2$ (0.5 equiv) effects nearly quantitative conversion of the substrate into product in acetonitrile (Eq. 51). Attempts to lower the catalyst loading further results in longer reaction times as well as increased yields of saturated carbonyl by-product, **47**.

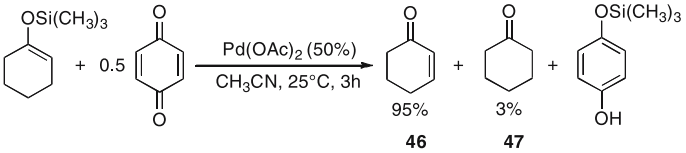

(51)

By using $Pd(OAc)_2$ in DMSO, Kraus, Larock, and coworkers developed a dioxygen-coupled catalytic procedure for this class of reactions (Eq. 52) [194]. Additives (e.g., exogenous base) were not beneficial in this reaction. Attempts to conduct the reaction in a solvent mixture of DMSO and H_2O (9 : 1) leads

to an equal ratio of the desired α,β-unsaturated ketone **48** and the saturated ketone by-product **49**. A number of other silyl enol ethers were shown to undergo catalytic dehydrosilylation under these reaction conditions.

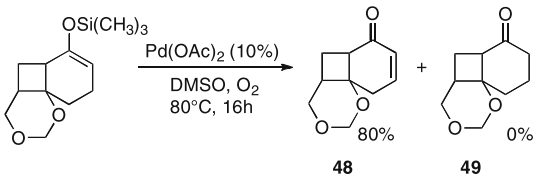

(52)

The Saegusa oxidation is believed to proceed through the mechanism shown in Scheme 13. An oxo-π-allyl intermediate can undergo β-hydride elimination to form a Pd^{II} hydride and the α,β-unsaturated product. Loss of H^+ from the Pd^{II} hydride will form Pd^0 that can be reoxidized by BQ or O_2. The difficulty in achieving efficient reoxidation of the Pd^0 catalyst might arise from strong coordination of the α,β-unsaturated product to the reduced metal center. Indeed, Mulzer et al. have isolated and crystallographically characterized a tetraolefin Pd^0 complex obtained from a Saegusa oxidation reaction [195]. Equilibrium reactions between the Pd^0–alkene complex **50** and BQ (Eq. 53) or dioxygen are reminiscent of the fundamental oxygenation reactions described above in Sect. 3.3.

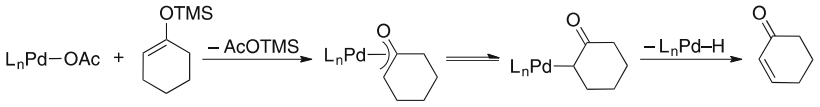

Scheme 13 Mechanism for the Saegusa oxidation reaction

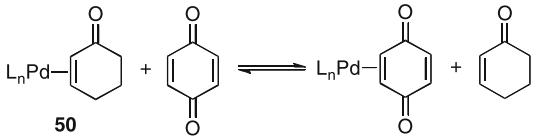

(53)

4.4
Acetoxylation of Allylic C–H Bonds

The formation of vinyl acetate via the oxidative coupling of ethylene and acetic acid was among the earliest Pd-catalyzed reactions developed (Sect. 2) [19, 20]. Subsequent study of this reaction with higher olefins revealed that, in addition to C-2 acetoxylation, allylic acetoxylation occurs to generate products with the acetoxy group at the C-1 and C-3 positions (Scheme 14). The synthetic utility of these products underlies the substantial historical interest in these reactions, and both BQ and dioxygen have been used as oxidants.

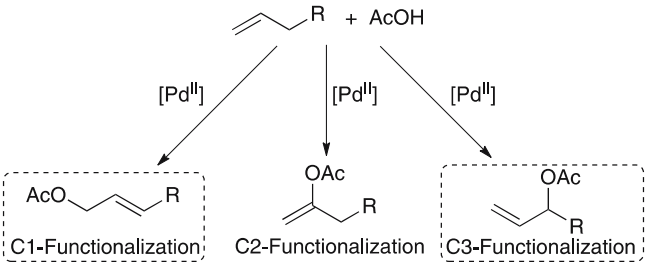

Scheme 14 Possible outcomes for the palladium-catalyzed oxidative acetoxylation of alkenes

Historically, cyclohexene has been a benchmark substrate for Pd-catalyzed allylic acetoxylation reactions. 2-Cyclohexenyl-1-acetate, **51**, is the desired product; however, in many cases, the homoallylic acetoxylation product **52** is also observed. Early efforts employed $Cu^{II}Cl_2$ and BQ to promote catalytic turnover (Table 5, entries 1 and 2) [196]. Unfortunately, these early methods proved to be rather unselective, including the formation of chlorinated products [197]. In 1984, two groups reported methods that achieved higher selectivity. McMurray employed a more electrophilic Pd^{II} catalyst, $Pd(O_2CCF_3)_2$, together with *o*-methoxyacetophenone and stoichiometric BQ at room temperature (Table 5, entry 3) [198]. Heumann and Åkermark used $Pd(OAc)_2$ and cocatalytic BQ with MnO_2 as the stoichiometric oxidant (Table 5, entries 4 and 5) [199, 200]. In both cases, selective allylic acetoxylation to form **51** occurs in good yield. The allylic acetoxylation of other cyclic and acyclic alkenes was described in these studies based on similar protocols. In subsequent years, Åkermark and Bäckvall developed multicomponent catalytic systems that use cocatalytic BQ with more environmentally benign terminal oxidants, including O_2 and H_2O_2, to carry out selective alkene acetoxylation (Table 5, entries 6–9) [27, 28, 201].

The proposed mechanism for allylic acetoxylation of cyclohexene is illustrated in Scheme 15. Pd^{II}-mediated activation of the allylic C – H bond generates a π-allyl Pd^{II} intermediate. Coordination of BQ to the Pd^{II} center promotes nucleophilic attack by acetate on the coordinated allyl ligand, which yields cyclohexenyl acetate and a Pd^0–BQ complex. The latter species reacts with two equivalents of acetic acid to complete the cycle, forming $Pd(OAc)_2$ and hydroquinone. The HQ product can be recycled to BQ if a suitable cocatalyst and/or stoichiometric oxidant are present in the reaction. This mechanism reveals that BQ is more than a reoxidant for the Pd catalyst. Mechanistic studies reveal that BQ is required to promote nucleophilic attack on the π-allyl fragment [25, 204–206].

Two important extensions of this chemistry have been reported in recent years. White and coworkers demonstrated that terminal alkenes undergo regioselective acetoxylation at the C-1 or C-3 position, depending on the re-

Table 5 Methods for the selective generation of functionalized cyclohexene

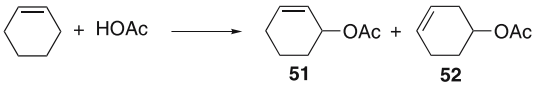

Entry	Catalyst	Cocatalyst	[O]	Additive	Temp. (°C)	Time (h)	**51** (%)	**52** (%)	Refs.
1	$PdCl_2$	None	$CuCl_2$ (unspecified loading)	NaOAc	20	NA	73	27	[196]
2	$PdCl_2$	None	BQ (unspecified loading)	NaOAc	20	NA	76	24	[196]
3	$Pd(TFA)_2$ (5%)	None	BQ (100%)	 40%	20	24	80	–	[198]
4	$Pd(OAc)_2$ (0.5%)	BQ (10%)	MnO_2 (110–200%)	None	60	50	77	–	[200]
5	$Pd(OAc)_2$ (5%)	BQ (20%)	MnO_2 (110–200%)	None	20	75	82	–	[200]
6	$Pd(OAc)_2$ (5%)	BQ (10%)	H_2O_2 (150%)	None	50	2	77	–	[28]
7	$Pd(OAc)_2$ (5%)	$Cu(OAc)_2$ (5%) HQ (10%)	1 atm O_2	None	50	22	> 85	–	[201]
8	$Pd(OAc)_2$ (5%)	Fe(Pc), **3** (5%) HQ (20%)	1 atm O_2	$LiOAc{\cdot}H_2O$ (50%)	60	4–6	90	–	[27]
9	$Pd(OAc)_2$ (5%)	Co(salophen), **1** (5%) HQ (20%)	1 atm O_2	$LiOAc{\cdot}H_2O$ (50%)	60	4–6	100	–	[27]

action conditions (Eq. 54). Very little formation of Wacker/Moiseev-like vinyl acetate by-product (i.e., C-2 acetoxylation) is observed. Preliminary mechanistic studies of the reaction under conditions B (Eq. 54) [207, 208] reveal that the vinyl sulfoxide promotes allylic C – H activitation of the terminal alkene by Pd^{II} to form a π-allyl species. As noted in the earlier studies, benzoquinone is required to promote nucleophilic attack by acetate on the π-allyl fragment.

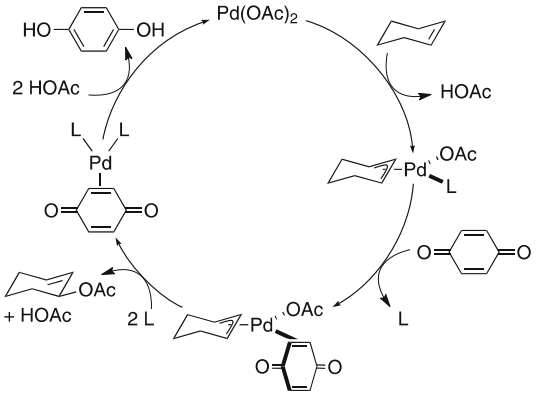

Scheme 15 Proposed mechanism for the allylic acetoxylation of cyclohexene

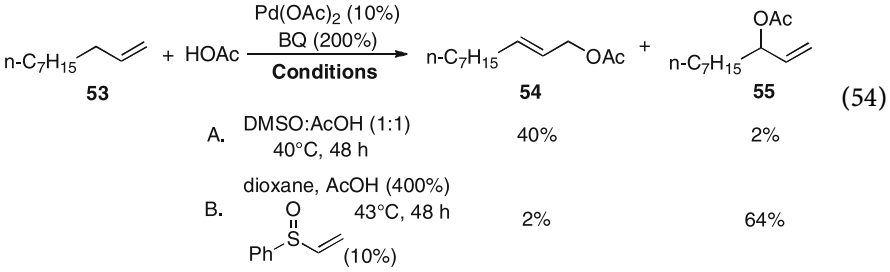

(54)

The mechanistic role of BQ in the allylic acetoxylation of alkenes suggests that it may not be possible to achieve direct dioxygen-coupled turnover. Recently, however, Kaneda and coworkers reported BQ-free conditions for aerobic allylic acetoxylation that feature a solvent mixture of acetic acid and *N*,*N*-dimethylacetamide (DMA) and O_2 as the sole oxidant for the Pd catalyst (Eq. 55) [209]. The reactions are highly selective for C-1 acetoxylation (C-1 : C-3 = 7–45 : 1). High pressures of O_2 (6 atm) are required to achieve these results.

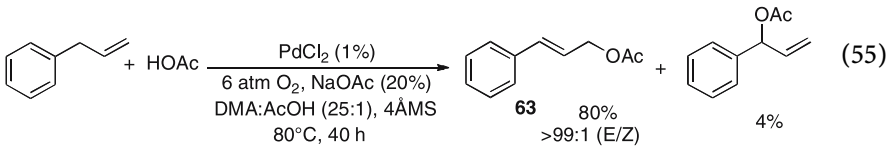

(55)

The results of Kaneda are mechanistically interesting because they reveal that BQ is not required for functionalization of the intermediate π-allyl Pd^{II} species (Scheme 15). In Sect. 3, we outlined the fundamental similarities between BQ and dioxygen in their reactions with Pd^0. The allylic acetoxylation results described above suggest that similarities also exist between the reactions of BQ and O_2 with Pd^{II}. Because little is known about the coordination

properties of BQ and O_2 to Pd^{II}, further study will be necessary to elucidate this relationship.

5 Conclusion

Palladium-catalyzed oxidation reactions are attractive methods for the selective oxidation of organic molecules, and their utility could be further enhanced by the development of more effective ways to use molecular oxygen (or air) to promote catalyst oxidation. The results outlined in this chapter reveal significant similarities between the reaction of dioxygen and BQ, both in fundamental reactions with palladium and in catalysis. These observations imply that BQ-based Pd-catalyzed oxidation reactions represent an important starting point for the development of new aerobic oxidation reactions. The results further suggest that complex, multicomponent, coupled catalyst systems for the in situ oxidation of hydroquinone may not be required to achieve efficient dioxygen-coupled catalytic turnover. Rather, dioxygen alone can be an effective oxidant in Pd-catalyzed reactions. Despite this optimistic outlook, dioxygen and BQ do not perform identically in catalytic reactions, and further studies will be necessary to elucidate the mechanistic origin of these differences. Such studies will play an important role in the ongoing development of Pd-catalyzed aerobic oxidation reactions.

References

1. Smidt J, Hafner W, Jira R, Sedlmeier J, Sieber R, Rüttinger R, Kojer H (1959) Angew Chem 71:176
2. Smidt J (1962) Chem Ind London 54
3. Smidt J, Hafner W, Jira R, Sieber R, Sedlmeier J, Sabel A (1962) Angew Chem Int Ed Engl 1:80
4. Punniyamurthy T, Velusamy S, Iqbal J (2005) Chem Rev 105:2329
5. Monflier E, Mortreux A (2004) In: Cornils B, Herrmann WA (eds) Aqueous-phase organometallic catalysis: concepts and applications. Wiley, Weinheim, p 481
6. Hintermann L (2004) In: Beller M, Bolm C (eds) Transition metals for organic synthesis, 2nd edn, vol 2. Wiley, Chichester, p 379
7. Takacs JM, Jiang X (2003) Curr Org Chem 7:369
8. Jira R (2002) In: Cornils B, Herrmann WA (eds) Applied homogeneous catalysis with organometallic compounds, vol 1. Wiley, Weinheim, p 386
9. Feringa BL (1998) In: Beller M, Bolm C (eds) Transition metals for organic synthesis, vol 2. Wiley, Chichester, p 307
10. de Meijere A, Diederich F (2004) Metal-catalyzed cross-coupling reactions, vols 1 and 2. Wiley, Chichester
11. Heumann A, Jens K-J, Réglier M (1994) Prog Inorg Chem 42:483
12. Stahl SS (2005) Science 309:1824

13. Stahl SS (2004) Angew Chem Int Ed 43:3400
14. Sigman MS, Schultz MJ (2004) Org Biomol Chem 2:2551
15. Stoltz BM (2004) Chem Lett 33:362
16. Nishimura T, Uemura S (2004) Synlett 201
17. Sheldon RA, Arends IWCE, ten Brink G-J, Dijksman A (2002) Acc Chem Res 35:774
18. Toyota M, Ihara M (2002) Synlett 1211
19. Moiseev II, Vargaftik MN, Syrkin YK (1960) Dokl Akad Nauk SSSR 133:377
20. Moiseev II, Vargaftik MN (2004) Coord Chem Rev 248:2381
21. Clement WH, Selwitz CM (1964) J Org Chem 29:241
22. Theissen RJ (1971) J Org Chem 36:752
23. Lloyd WG (1967) J Org Chem 32:2816
24. Bäckvall J-E (2004) In: de Meijere A, Diederich F (eds) Metal-catalyzed cross-coupling reactions, vol 2. Wiley, Chichester, p 479
25. Bäckvall J-E, Byström SE, Nordberg RE (1984) J Org Chem 49:4619
26. Bäckvall J-E, Vågberg J, Nordberg RE (1984) Tetradedron Lett 25:2717
27. Bäckvall J-E, Hopkins RB, Grennberg H, Mader MM, Awasthi AK (1990) J Am Chem Soc 112:5160
28. Åkermark B, Larsson EM, Oslob JD (1994) J Org Chem 59:5729
29. Jia CG, Müller P, Mimoun H (1995) J Mol Catal A 101:127
30. Bäckvall J-E, Awasthi AK, Renko ZD (1987) J Am Chem Soc 109:4750
31. Grennberg H, Faizon S, Bäckvall J-E (1993) Angew Chem Int Ed Engl 32:263
32. Verboom RC, Slagt VF, Bäckvall J-E (2005) Chem Commun 1282
33. Bergstad K, Grennberg H, Bäckvall J-E (1998) Organometallics 17:45
34. Trost BM (1992) Pure Appl Chem 64:315
35. Trost BM (1995) Angew Chem Int Ed Engl 34:259
36. Davidson JM, Triggs C (1968) J Chem Soc A 1324
37. Shue RS (1971) J Chem Soc Chem Commun 1510
38. Iataaki H, Yoshimoto H (1973) J Org Chem 38:76
39. Blackburn TF, Schwartz J (1977) J Chem Soc Chem Commun 157
40. Peterson KP, Larock RC (1998) J Org Chem 63:3185
41. Nishimura T, Onoue T, Ohe K, Uemura S (1998) Tetrahedron Lett 39:6011
42. Nishimura T, Onoue T, Ohe K, Uemura S (1999) J Org Chem 64:6750
43. Nishimura T, Maeda Y, Kakiuchi N, Uemura S (2000) J Chem Soc Perkin Trans I 4301
44. Jensen DR, Pugsley JS, Sigman MS (2001) J Am Chem Soc 123:7475
45. Ferreira EM, Stoltz BM (2001) J Am Chem Soc 123:7725
46. Mandal SK, Jensen DR, Pugsley JS, Sigman MS (2003) J Org Chem 68:4600
47. Mandal SK, Sigman MS (2003) J Org Chem 68:7535
48. Bagdanoff JT, Ferreira EM, Stoltz BM (2003) Org Lett 5:835
49. Bagdanoff JT, Stoltz BM (2004) Angew Chem Int Ed 43:353
50. Caspi DD, Ebner DC, Bagdanoff JT, Stoltz BM (2004) Adv Synth Catal 346:185
51. Schultz MJ, Park CC, Sigman MS (2002) Chem Commun 3034
52. Schultz MJ, Hamilton SS, Jensen DR, Sigman MS (2005) J Org Chem 70:3343
53. Bortolo R, Bianchi D, D'Aloisio R, Querci C, Ricci M (2000) J Mol Catal A 153:25
54. Jensen DR, Schultz MJ, Mueller JA, Sigman MS (2003) Angew Chem Int Ed 42:3810
55. ten Brink G-J, Arends IWCE, Sheldon RA (2000) Science 287:1636
56. Hallman K, Moberg C (2001) Adv Synth Catal 343:260
57. Steinhoff BA, Fix SR, Stahl SS (2002) J Am Chem Soc 124:766
58. Zierkiewicz W, Privalov T (2005) Organometallics 24:6019
59. Steinhoff BA, Stahl SS (2006) J Am Chem Soc 128:4348
60. Steinhoff BA, Stahl SS (2002) Org Lett 4:4179

61. Steinhoff BA, Guzei IA, Stahl SS (2004) J Am Chem Soc 126:11268
62. Steinhoff BA, King AE, Stahl SS (2006) J Org Chem 71:1861
63. Mueller JA, Jensen DR, Sigman MS (2002) J Am Chem Soc 124:8202
64. Mueller JA, Sigman MS (2003) J Am Chem Soc 125:7005
65. Trend RM, Stoltz BM (2004) J Am Chem Soc 126:4482
66. Nielsen RJ, Keith JM, Stoltz BM, Goddard III WA (2004) J Am Chem Soc 126:7967
67. Mueller JA, Cowell A, Chandler BD, Sigman MS (2005) J Am Chem Soc 127:14817
68. Schultz MJ, Adler RS, Zierkiewicz W, Privalov T, Sigman MS (2005) J Am Chem Soc 127:8499
69. Stahl SS, Thorman JL, Nelson RC, Kozee MA (2001) J Am Chem Soc 123:7188
70. Stahl SS, Thorman JL, de Silva N, Guzei IA, Clark RW (2003) J Am Chem Soc 125:12
71. Mueller JA, Goller CP, Sigman MS (2004) J Am Chem Soc 126:9724
72. Privalov T, Linde C, Zetterberg K, Moberg C (2005) Organometallics 24:885
73. Sigman MS, Jensen DR (2006) Acc Chem Res 39:221
74. ten Brink G-J, Arends IWCE, Papadogianakis G, Sheldon RA (2000) Appl Catal A 194:435
75. ten Brink G-J, Arends IWCE, Sheldon RA (2002) Adv Synth Catal 344:355
76. ten Brink G-J, Arends IWCE, Hoogenraad M, Verspui G, Sheldon RA (2003) Adv Synth Catal 345:497
77. ten Brink G-J, Arends IWCE, Hoogenraad M, Verspui G, Sheldon RA (2003) Adv Synth Catal 345:1341
78. Paavola S, Zetterberg K, Privalov T, Csöregh I, Moberg C (2004) Adv Synth Catal 346:237
79. Patai S (1974) The chemistry of the quinonoid compounds, vol 1. Wiley, New York, p 335
80. Patai S, Rappoport Z (1988) The chemistry of the quinonoid compounds, vol 2. Wiley, New York, p 1351
81. Fischer EO, Werner H (1966) Metal π-complexes. Elsevier, New York
82. Herberhold M (1972) Metal π-complexes. Elsevier, New York
83. Takahashi S, Hagihara N (1967) Nippon Kagaku Zasshi 88:1306
84. Vagg RS (1977) Acta Crystallogr B33:3708
85. Kulik AV, Bruk LG, Temkin ON, Khabibulin VR, Belsky VK, Zavodnik VE (2002) Mendeleev Commun 47
86. Tschoerner M, Trabesinger G, Albinati A, Pregosin PS (1997) Organometallics 16:3447
87. Milani B, Anzilutti A, Vicentini L, Sessanta o Santi A, Zangrando E, Geremia S, Mestroni G (1997) Organometallics 16:5064
88. Klein RA, Witte P, van Belzen R, Fraanje J, Goubitz K, Numan M, Schenk H, Ernsting JM, Elsevier CJ (1998) Eur J Inorg Chem 319
89. Milani B, Mestroni G, Zangrando E (2001) Croat Chem Acta 74:851
90. Clegg W, Eastham GR, Elsegood MRJ, Heaton BT, Iggo JA, Tooze RP, Whyman R, Zacchini S (2002) J Chem Soc Dalton Trans 3300
91. Yamamoto Y, Ohno T, Itoh K (2003) Organometallics 22:2267
92. Minematsu H, Takahashi S, Hagihara N (1975) J Organomet Chem 91:389
93. Hiramatsu M, Fujinami T, Sakai S (1981) J Organomet Chem 218:409
94. Hiramatsu M, Nakano H, Fujinami T, Sakai S (1982) J Organomet Chem 236:131
95. Ukai T, Kawazura H, Ishii Y, Bonnet JJ, Ibers JA (1974) J Organomet Chem 65:253
96. Hiramatsu M, Shiozaki K, Fujinami T, Sakai S (1983) J Organomet Chem 246:203
97. Canovese L, Visentin F, Uguagliati P, Crociani B (1996) J Chem Soc Dalton Trans 1921

98. Canovese L, Visentin F, Chessa G, Gardenal G, Uguagliati P (2001) J Organomet Chem 622:155
99. Trotter J (1960) Acta Crystallogr 13:86
100. Grennberg H, Gogoll A, Bäckvall J-E (1993) Organometallics 12:1790
101. Vaska L (1963) Science 140:809
102. Vaska L (1968) Acc Chem Res 1:335
103. Vaska L, Chen LS, Senoff CV (1971) Science 174:587
104. Vaska L (1976) Acc Chem Res 9:175
105. Valentine JS (1973) Chem Rev 73:235
106. Takahashi S, Sonogashira K, Hagihara N (1966) Nippon Kagaku Zasshi 87:610
107. Wilke G, Schott H, Heimbach P (1967) Angew Chem Int Ed Engl 6:92
108. Nyman CJ, Wymore CE, Wilkinson G (1968) J Chem Soc A 561
109. Aboelella NW, York JT, Reynolds AM, Fujita K, Kinsinger CR, Cramer CJ, Riordan CG, Tolman WB (2004) Chem Commun 1716
110. Otsuka S, Nakamura A, Tatsuno Y (1969) J Am Chem Soc 91:6994
111. Yoshida T, Otsuka S (1977) J Am Chem Soc 99:2134
112. Yoshida T, Tatsumi K, Matsumoto M, Nakatsu K, Nakamura A, Fueno T, Otsuka S (1979) Nouv J Chim 3:761
113. Adjabeng G, Brenstrum T, Frampton CS, Robertson AJ, Hillhouse J, McNulty J, Capretta A (2004) J Org Chem 69:5082
114. Konnick MM, Guzei IA, Stahl SS (2004) J Am Chem Soc 126:10212
115. Yamashita M, Goto K, Kawashima T (2005) J Am Chem Soc 127:7294
116. Cramer CJ, Tolman WB, Theopold KH, Rheingold AL (2003) Proc Natl Acad Sci USA 100:3635
117. Cotton FA, Wilkinson G, Murillo CA, Bochmann M (1999) Advanced inorganic chemistry, 6th edn. Wiley, New York, p 450
118. Sheldon RA, Kochi JK (1981) Metal-catalyzed oxidations of organic compounds. Academic Press, New York
119. Rogers MM, Stahl SS (2006) Top Organomet Chem 21 (in press)
120. Strasser T (2006) (in this volume) Springer, Berlin
121. Bianchi D, Bortolo R, D'Aloisio R, Ricci M (1999) Angew Chem Int Ed 38:706
122. Lanci MP, Brinkley DW, Stone KL, Smirnov VV, Roth JP (2005) Angew Chem Int Ed 44:7273
123. Landis CR, Morales CM, Stahl SS (2004) J Am Chem Soc 126:16302
124. Keith JM, Nielsen RJ, Oxgaard J, Goddard WA (2005) J Am Chem Soc 127:13172
125. Thiel WR (1999) Angew Chem Int Ed 38:3157
126. Muto S, Ogata H, Kamiya Y (1975) Chem Lett 809
127. Zudin VN, Likholobov VA, Ermakov YI (1979) Kinet Katal 20:1324
128. Jacobson SE (1987) US Patent 4,711,772
129. Bortolo R, D'Aloisio R, Bianchi D (1997) EU Patent EP 0 788 998 A1
130. Bianchi D, Bortolo R, D'Aloisio R, Ricci M, Soattini S (1997) EU Patent EP 0 808 796 A1
131. Bianchi D, Bortolo R, D'Aloisio R, Ricci M (1999) J Mol Catal A 150:87
132. Bianchi D, Bortolo R, D'Aloisio R, Querci C, Ricci M (1999) Stud Surf Sci Catal 126:481
133. Ozawa F, Ito T, Nakamura Y, Yamamoto A (1979) J Organomet Chem 168:375
134. van Asselt R, Elsevier CJ, Smeets WJJ, Spek AL (1994) Inorg Chem 33:1521
135. Canovese L, Visentin F, Chessa G, Uguagliati P, Dolmella A (2000) J Organomet Chem 601:1

136. Popp BV, Thorman JL, Morales CM, Landis CR, Stahl SS (2004) J Am Chem Soc 126:14832
137. Popp BV, Thorman JL, Stahl SS (2006) J Mol Catal A 251:2
138. Popp BV, Stahl SS (2006) J Am Chem Soc 128:2804
139. Zeni G, Larock RC (2004) Chem Rev 104:2285
140. Hosokawa T, Ohkata H, Moritani I (1975) Bull Chem Soc Jpn 48:1533
141. Hosokawa T, Yamashita S, Murahashi S-I, Sonoda A (1976) Bull Chem Soc Jpn 49:3662
142. Hegedus LS, Allen GF, Waterman EL (1976) J Am Chem Soc 98:2674
143. Hegedus LS, Allen GF, Bozell JJ, Waterman EL (1978) J Am Chem Soc 100:5800
144. Hegedus LS, McKearin JM (1982) J Am Chem Soc 104:2444
145. Hosokawa T, Miyagi S, Murahashi S-I, Sonoda A (1978) J Org Chem 43:2752
146. Larock RC, Hightower TR (1993) J Org Chem 58:5298
147. Larock RC, Hightower TR, Hasvold LA, Peterson KP (1996) J Org Chem 61:3584
148. van Benthem RATM, Hiemstra H, Longarela GR, Speckamp WN (1994) Tetrahedron Lett 35:9281
149. van Benthem RATM, Hiemstra H, Michels JJ, Speckamp WN (1994) J Chem Soc Chem Commun 357
150. Rönn M, Bäckvall J-E, Andersson PG (1995) Tetrahedron Lett 36:7749
151. Fix SR, Brice JL, Stahl SS (2002) Angew Chem Int Ed 41:164
152. Trend RM, Ramtohul YK, Ferreira EM, Stoltz BM (2003) Angew Chem Int Ed 42:2892
153. Trend RM, Ramtohul YK, Stoltz BM (2005) J Am Chem Soc 127:17778
154. Muñiz K (2004) Adv Synth Catal 346:1425
155. Rodgers MM, Wendlandt JE, Guzei IA, Stahl SS (2006) Org Lett 8:2257
156. Reiter M, Ropp S, Gouverneur V (2004) Org Lett 6:91
157. Hosokawa T, Uno T, Inui S, Murahashi S-I (1981) J Am Chem Soc 103:2318
158. Hosokawa T, Okuda C, Murahashi S-I (1985) J Org Chem 50:1282
159. Uozumi Y, Kato K, Hayashi T (1997) J Am Chem Soc 119:5063
160. Uozumi Y, Kato K, Hayashi T (1998) J Org Chem 63:5071
161. Uozumi Y, Kyota H, Kato K, Ogasawara M, Hayashi T (1999) J Org Chem 64:1620
162. Arai MA, Kuraishi M, Arai T, Sasai H (2001) J Am Chem Soc 123:2907
163. Yip K-T, Yang M, Law K-L, Zhu N-Y, Yang D (2006) J Am Chem Soc 128:3130
164. Castaño AM, Bäckvall J-E (1995) J Am Chem Soc 117:560
165. Castaño AM, Persson BA, Bäckvall J-E (1997) Chem Eur J 3:482
166. Rönn M, Andersson PG, Bäckvall J-E (1997) Tetrahedron Lett 38:3603
167. Ito Y, Aoyama H, Hirao T, Mochizuki A, Saegusa T (1979) J Am Chem Soc 101:494
168. Toyota M, Wada T, Fukumoto K, Ihara M (1998) J Am Chem Soc 120:4916
169. Toyota M, Odashima T, Wada T, Ihara M (2000) J Am Chem Soc 122:9036
170. Toyota M, Wada T, Ihara M (2000) J Org Chem 65:4565
171. Pei T, Wang X, Widenhoefer RA (2003) J Am Chem Soc 125:648
172. Liu C, Wang X, Pei T, Widenhoefer RA (2004) Chem Eur J 10:6343
173. Wang X, Widenhoefer RA (2004) Chem Commun 660
174. Yip K-T, Li J-H, Lee O-Y, Yang D (2005) Org Lett 7:5717
175. Ferreira EM, Stoltz BM (2003) J Am Chem Soc 125:9578
176. Zhang H, Ferreira EM, Stoltz BM (2004) Angew Chem Int Ed 43:6144
177. Hosokawa T, Takano M, Kuroki Y, Murahashi S-I (1992) Tetrahedron Lett 33:6643
178. Timokhin VI, Anastasi NR, Stahl SS (2003) J Am Chem Soc 125:12996
179. Timokhin VI, Stahl SS (2005) J Am Chem Soc 127:17888
180. Brice JL, Harang JE, Timokhin VI, Anastasi NR, Stahl SS (2005) J Am Chem Soc 127:2868

181. Bar GLJ, Lloyd-Jones GC, Booker-Milburn KI (2005) J Am Chem Soc 127:7308
182. Jia C, Kitamura T, Fujiwara Y (2001) Acc Chem Res 34:633
183. Fujiwara Y, Jia C (2001) Pure Appl Chem 73:319
184. Tsuji J, Nagashima H (1984) Tetrahedron 40:2699
185. Horino H, Inoue N (1981) J Org Chem 46:4416
186. Boele MDK, van Strijdonck GPF, de Vries AHM, Kamer PCJ, de Vries JG, van Leeuwen PWNM (2002) J Am Chem Soc 124:1586
187. Dams M, De Vos DE, Celen S, Jacobs PA (2003) Angew Chem Int Ed 42:3512
188. Beck EM, Grimster NP, Hatley R, Gaunt MJ (2006) J Am Chem Soc 128:2528
189. Jung YC, Mishra RK, Yoon CH, Jung KW (2003) Org Lett 5:2231
190. Andappan MMS, Nilsson P, Larhed M (2004) Chem Commun 218
191. Andappan MMS, Nilsson P, von Schenck H, Larhed M (2004) J Org Chem 69:5212
192. Enquist P-A, Lindh J, Nilsson P, Larhed M (2006) Green Chem 8:338
193. Ito Y, Hirao T, Saegusa T (1978) J Org Chem 43:1011
194. Larock RC, Hightower TR, Kraus GA, Hahn P, Zheng D (1995) Tetrahedron Lett 36:2423
195. Porth S, Bats JW, Trauner D, Giester G, Mulzer J (1999) Angew Chem Int Ed 38:2015
196. Green M, Haszeldine RN, Lindley J (1966) J Organomet Chem 6:107
197. Henry PM (1980) Palladium-catalyzed oxidation of hydrocarbons. Reidel, Boston
198. McMurry JE, Kočovský P (1984) Tetrahedron Lett 25:4187
199. Heumann A, Åkermark B (1984) Angew Chem Int Ed Engl 23:453
200. Hansson S, Heumann A, Rein T, Åkermark B (1990) J Org Chem 55:975
201. Byström SE, Larsson EM, Åkermark B (1990) J Org Chem 55:5674
202. Bäckvall JE, Gogoll A (1988) Tetrahedron Lett 29:2243
203. Szabó KJ (1998) Organometallics 17:1677
204. Bäckvall J-E, Nordberg RE, Bjorkman EE, Moberg C (1980) J Chem Soc Chem Commun 943
205. Bäckvall J-E, Nordberg RE (1981) J Am Chem Soc 103:4959
206. Bäckvall J-E, Nordberg RE, Nyström J-E (1982) Tetrahedron Lett 23:1617
207. Chen MS, White MC (2004) J Am Chem Soc 126:1346
208. Chen MS, Prabagaran N, Labenz NA, White MC (2005) J Am Chem Soc 127:6970
209. Mitsudome T, Umetani T, Nosaka N, Mori K, Mizugaki T, Ebitani K, Kaneda K (2006) Angew Chem Int Ed 45:481

Top Organomet Chem (2007) 22: 191–240
DOI 10.1007/3418_2006_060

Published online: 13 January 2007

Homogeneous Copper-Catalyzed Oxidations

Jarl Ivar van der Vlugt · Franc Meyer (✉)

Institut für Anorganische Chemie, Georg-August-Universität Göttingen,
Tammanstrasse 4, 37077 Göttingen, Germany
franc.meyer@chemie.uni-goettingen.de

Abstract The bioinorganic chemistry of copper has provided a stimulating background for exciting research on homogeneous copper-catalyzed reactions in recent years, and this review starts with a brief and concise overview of the role of copper containing active sites in metalloproteins that catalyze oxidation or oxygenation reactions in nature. Efficient bio-inspired Cu-based catalysts for a variety of chemical oxidative transformations have been developed over the last decade, with oxygen as the prime oxidant of choice, and several prominent examples are presented in this review. Selected contributions with (organic) peroxides or other oxygen-transfer agents are described as well. Key themes discussed in this review include the oxidation of alkanes, alcohols, amines and phenols

as well as oxidative coupling or polymerization reactions with phenols. Focus is placed on the results obtained in catalysis and the mechanistic studies undertaken to support these results; therefore, less emphasis is given to more fundamental coordination chemistry aspects of the Cu-complexes described as well as their spectroscopic characteristics.

Keywords Biomimetic dioxygen reactivity · Copper · Coupling reactions · Homogeneous catalysis · Oxidation chemistry

Abbreviations

BHT	butylated hydroxytoluene (2,6-di-*t*-butyl-4-methylphenol)
*t*BuOOH	*tert*-butylhydroperoxide
CDC	cross-dehydrogenative coupling
DACH	1,2-diaminocyclohexane
DAPHEN	9,10-diaminophenanthrene
DBAD	di-*tert*-butyl azodicarboxylate
DMAP	dimethylaminopyridine
bmpy	1-butyl-4-methylpyridinium
DPQ	diphenoquinone
DTBC	3,5-di-*tert*-butylcatechol
ESR	electron spin resonance spectroscopy
HDB	3,5-dimethyl-4-hydroxybenzaldehyde
LMCT	ligand-to-metal charge transfer
MDP	4-(methoxymethyl)-2,6-dimethylphenol
NMI	*N*-methylimidazole
pMMO	particulate methane monooxygenase
PAM	peptidyl-α-amidating monoxygenase
PHM	peptidylglycine-α-hydroxylating monoxygenase
PPE	poly(2,6-dimethylphenylene ether)
tacn	1,4,7-*tri*isopropyl-1,4,7-triazacyclononane
TEMPO	2,2,6,6-Tetramethylpiperidine-1-oxyl
TMAO	trimethylamine-*N*-oxide
TMEDA	*N*,*N*,*N*′,*N*′-tetramethylethylenediamine
TMP	2,4,6-trimethylphenol
TMQ	trimethyl-1,4-benzoquinone
tpb	tris(pyrazolyl)borate
tpm	tris(pyrazolyl)methane
TON	turnover number
TOF	turnover frequency

1 Introduction

Although organocopper compounds are established for various organosynthetic transformations and simple Cu^{II} salts are widely applied in organic syntheses [1, 2], conventional applications of Cu in oxidation or oxygenation catalysis have largely been limited to a co-catalytic role. The most promi-

nent examples are the Wacker-type oxidations of alkenes, where Cu salts mediate the in situ reoxidation of Pd^{II} by molecular oxygen [3–5]. Other well-known applications of Cu include the oxychlorination of ethylene to yield 1,2-dichloroethane (catalyzed by organometallic complexes based on mixed cupric and cuprous chlorides) [6, 7] and oxidative carbonylations (with Cu^{II} as a reoxidant that renders the reactions catalytic) [8], just to mention a few. As has been recognized during the last decades, however, the high reactivity of many Cu^{I} compounds towards O_2 is a key feature observed in many natural systems, and Cu is abundantly found in the active sites of metalloproteins that play vital roles in biological processes [9–17]. Cu also is the third most abundant trace element found in the human body, after iron and zinc. Its biological roles mainly center around redox-chemistry, either electron transfer or oxidation/oxygenation of organic substrates, although some non-redox copper containing active sites are known [14–17]. The controlled activation of aerial dioxygen by diverse classes of Cu-containing metalloenzymes has stimulated manifold studies directed towards the design and synthetic use of biomimetic or bioinspired molecular Cu complexes for the selective oxidative transformation of substrates [18, 19]. It should be noted that such systems in general do not involve direct Cu – C bonds and strictly speaking are not organometallic. However, due to the increasing importance of Cu (as well as Fe) in homogeneous oxidation reactions this review has been included in the volume on Organometallic Oxidation Catalysis in order to highlight some recent developments in the field. In view of the volume of work that appeared over the last few years this review does not intend to be exhaustive, and we apologize if our selection does not match the preference of all readers.

2
Bioinorganic Background

Active sites of the Cu metalloproteins may take part in either of four major functions: (i) metal ion uptake, storage and transport, (ii) dioxygen uptake, storage and transport, (iii) electron transfer, and (iv) catalytic conversions [14–17, 20]. Recent discoveries of various novel Cu-containing protein active sites and spectacular advances in protein X-ray crystallography have led to the need to expand the traditional classification of biological Cu centers, which were originally grouped into three classes distinguished by their spectroscopic features. The currently known biological Cu systems can now be categorized into seven classes [21], of which type 2, type 3 and type 4 are involved in oxidation catalysis, while the Cu_B and Cu_Z type active sites are involved in reduction catalysis (of O_2 to H_2O and N_2O to N_2, respectively). Some selected examples are briefly introduced here to illustrate the scope and diversity of Cu-mediated biological oxidations and oxygenations.

2.1
Type 2 Copper Sites

These systems are also described as "normal" copper proteins due to their conventional ESR features. In the oxidized state, their color is light blue (almost undetectable) due to weak *d–d* transitions of the single Cu^{II} ion. The coordination sphere around Cu, which has either square planar or distorted tetrahedral geometry, contains four ligands with N and/or O donor atoms [12, 22]. Representative examples of proteins with this active site structure (see Fig. 1) and their respective catalytic function include galactose oxidase (**1**) (oxidation of primary alcohols) [23, 24], phenylalanine hydroxylase (hydroxylation of aromatic substrates) [25, 26], dopamine-β-hydroxylase (C – H bond activation of benzylic substrates) [27] and CuZn superoxide dismutase (disproportionation of O_2^- superoxide anion) [28, 29].

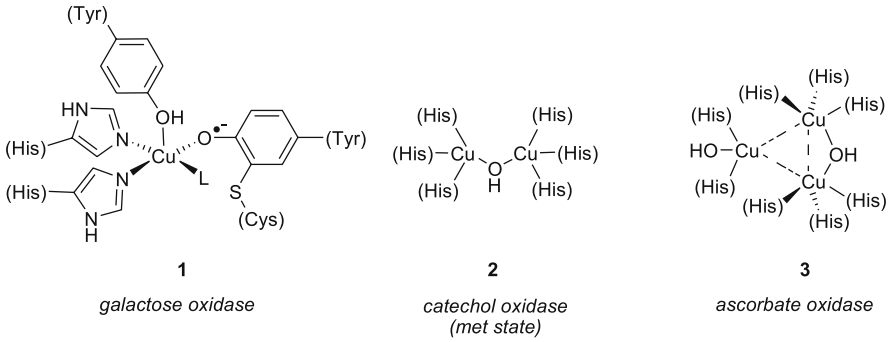

Fig. 1 Structures of the active sites of galactose oxidase, catechol oxidase, and ascorbate oxidase metalloenzymes

2.2
Type 3 Copper Sites

Hemocyanin [30, 31], tyrosinase [32] and catechol oxidase (**2**) [33] comprise this class of proteins. Their active sites are very similar and contain a dicopper core in which both Cu ions are ligated by three N-bound histidine residues. All three proteins are capable of binding dioxygen reversibly at ambient conditions. However, whereas hemocyanin is responsible for O_2 transport in certain mollusks and arthropods, catechol oxidase and tyrosinase are enzymes that have vital *catalytic* functions in a variety of natural systems, namely the oxidation of phenolic substrates to catechols (Scheme 1) (tyrosinase) and the oxidation of catechols to *o*-quinones (tyrosinase and catechol oxidase). Antiferromagnetic coupling of the two Cu^{II} ions in the *oxy* state of these metalloproteins leads to ESR-silent behavior. Structural insight from X-ray crystallography is now available for all three enzymes, but details

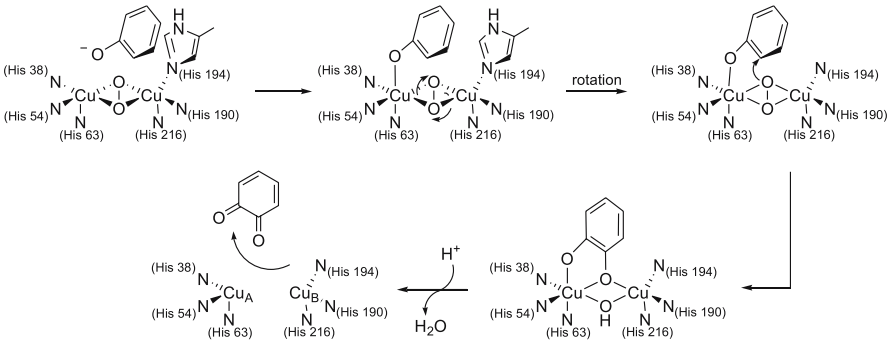

Scheme 1 Proposed catalytic cycle for the oxidation of phenol to catechol in tyrosinase [37]

of the catalytic mechanisms for both catechol oxidase and tyrosinase are still under debate [34–37].

2.3 Type 4 Copper Sites

Usually, these metalloproteins contain both type 2 and type 3 copper centers, together forming a triangular-shaped trinuclear active site, such as found in laccase (polyphenol oxidase) [38–41] and ascorbate oxidase (**3**) [42]. Recent evidence for a related arrangement has been reported for the enzyme particulate methane monooxygenase as well [43], but in this case the Cu···Cu distance of the type 2 subunit (2.6 Å) appears to be unusually short and the third Cu ion is located far from the dinuclear site.

2.4 Oxygenases

Tyrosinase, peptidylglycine-α-hydroxylating monooxygenase (PHM) and dopamine-β-hydroxylase are examples of monooxygenase enzymes, whereby only one O-atom, originating from O_2, is transferred to a substrate molecule. In the case of tyrosinase, very recent crystallographic information has allowed a rather detailed mechanistic picture of the catalytic cycle [32, 37] (Scheme 1). It starts with a Cu^ICu^I species (the *deoxy* form)—the two Cu centers are denoted Cu^A and Cu^B—which reversibly binds O_2 to form the common $Cu^{II}(\mu\text{-}\eta^2 : \eta^2\text{-peroxo})Cu^{II}$ species (*oxy* form) that is pivotal to all type 3 dicopper sites. The substrate then docks to one of the metal ions of the *oxy* state (most likely Cu^A) and is properly oriented through interactions with histidine residues to enable hydroxylation of the aromatic ring. To this end, the O – O axis of the peroxo ligand has been suggested to rotate in order to point towards the phenolic ring, leading to electrophilic attack of the Cu(μ–

O_2)Cu moiety on the ring with concomitant cleavage of the O – O bond [37]. The diphenolic intermediate ends up bound in a bidentate fashion and is subsequently released as the *o*-chinone to regenerate the deoxy form of the dicopper center. It should be noted though that alternative mechanistic proposals are being discussed [44–47], and even the site of substrate binding (Cu^A or Cu^B) is not yet fully clarified. Similar considerations apply to catechol oxidase, where important open questions comprise the exact mode of substrate and product binding (to one or two Cu ions), and where several scenarios have been proposed for the catalytic cycle [34–36].

PHM, an ascorbate-dependent enzyme, constitutes one domain of peptidyl-α-amidating monoxygenase (PAM) which cleaves the C – N bond of a glycine-extended peptide chain to yield an amide-terminated peptide chain and glyoxylic acid as the oxidized fragment [48, 49]. PHM performs the first part of that sequence, i.e. the hydroxylation of the C_α of a C-terminal glycine via a glycyl radical intermediate (Eq. 1) [50]. The reaction proceeds through initial abstraction of the glycine *pro-S* hydrogen by a Cu-oxygen species, presumably by an *end-on* Cu^{II} superoxide, as it has been trapped and characterized crystallographically for the protein [51, 52]. The reactivity of dopamine-β-hydroxylase is related to that of PHM: this enzyme converts dopamine [4-(2-aminoethyl)benzene-1,2-diol] into the neurotransmitter noradrenaline (Eq. 2) by selective benzylic C – H bond activation, thereby installing an OH-group at the α-carbon [27]. This chemistry has been extended to other benzylic amino substrates, such as 2-aminoindane, by Réglier (Eq. 3) [53]. Use of synthetic Cu complexes in which the target has been attached to the ligand backbone elucidated the stereospecificity of the latter reaction.

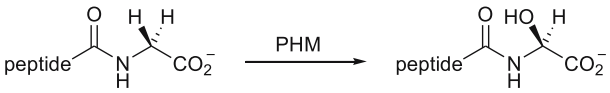

(1)

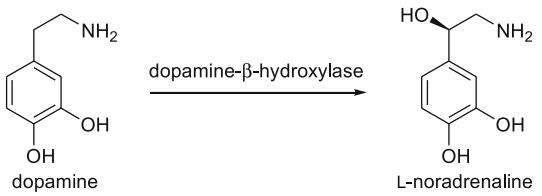

(2)

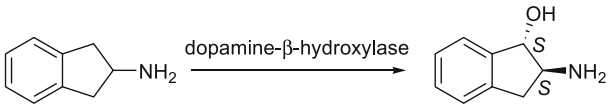

(3)

Some dioxygenase enzymes are known that incorporate both atoms of O_2 into one substrate molecule, as seen in 2,3-dioxygenases, which catalyze the

1,2-cleavage of arene-1,2-diols or semiquinones, presumably via formation of an organic peroxide fragment [54, 55].

2.5 Oxidases

So-called "blue" multinuclear copper oxidase enzymes, such as laccase and ascorbate oxidase, catalyze the stepwise oxidation of organic substrates (most likely in successive one-electron steps) in tandem with the four-electron reduction of O_2 to water, i.e. no oxygen atom(s) from O_2 are incorporated into the substrate (Eq. 4) [15]. Catechol oxidase, containing a type 3 center, mediates a two-electron substrate oxidation (*o*-diphenols to *o*-chinones), and turnover of two substrate molecules is coupled to the reduction of O_2 to water [34, 35]. The "non-blue" copper oxidases, e.g. galactose oxidase and amine oxidases [27, 56–59], perform similar oxidation catalysis at a mononuclear type 2 Cu site, but H_2O_2 is produced from O_2 instead of H_2O, in a two-electron reduction.

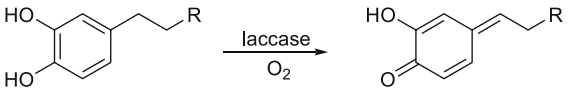

(4)

Galactose oxidase represents a textbook example for a free radical metalloenzyme, defining the broader class of radical-copper oxidases [60, 61]. The combination of a single Cu (shuttling between the Cu^{I} and Cu^{II} states) and a modified tyrosine residue (that generates a Cu-bound tyrosyl radical as the second redox center) accomplishes the overall two-electron, two-proton oxidation of primary alcohols to the corresponding aldehydes (Eq. 5) [62, 63]. An active site semiquinone is involved in copper amine oxidase, which catalyzes the two-electron oxidative deamination of primary amines coupled to the two-electron reduction of dioxygen to hydrogen peroxide (Eq. 6) [64–66]. The enormous synthetic potential and industrial interest in these fundamental catalytic conversions has inspired a number of groups to mimic the enzymatic functional principles by means of small bioinspired complexes, aiming at molecular systems of inexpensive Cu that mediate the selective oxidation of organic substrates [67–69].

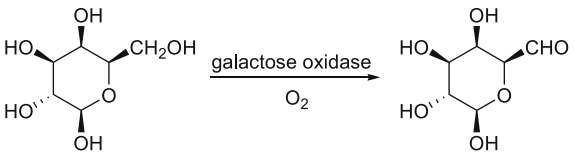

(5)

$$RCH_2NH_2 + O_2 + H_2O \xrightarrow{\text{amine oxidase}} RCHO + H_2O_2 + NH_3 \qquad (6)$$

3
Dioxygen Binding and Cleavage

Fueled by the biological relevance, the initial steps of Cu-based O_2 activation have attracted much interest in the last decades. Various, very different Cu_x/O_2 species that result from the reaction of dioxygen with Cu^I complexes have meanwhile been identified (Fig. 2) [70–90], where mononuclear species **A** and **B** as well as dinuclear type **E** and **F** species (and some tricopper systems as in, for example, laccase) are considered the most relevant in nature.

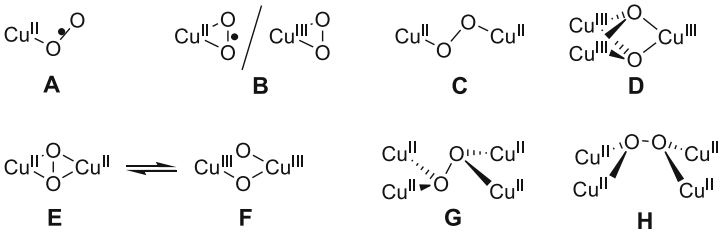

Fig. 2 Structurally characterized Cu_x/O_2 species

The elucidation of structural and spectroscopic details of these Cu_x/O_2 species as well as the mechanism of their formation and their subsequent reactivity remains a topic of intense research [88–93]. Bis(μ-peroxo)$Cu^{II}{}_2$ systems **E** have been shown to reversibly convert to the bis(μ-oxo)$Cu^{III}{}_2$ isomers **F** under suitable conditions, and it is still a debated question which of the two species is the actual oxidant in subsequent attack of a substrate [94–98].

Many of the studies today are focussed on understanding the controlling factors behind Cu-dioxygen chemistry, as well as on the use of bioinspired Cu complexes for catalytic applications in substrate oxidation or oxygenation. Excellent reviews dealing with fundamental aspects of bioinorganic Cu/O_2 chemistry have appeared. Although of some relevance to the type of oxidations described here, the chemistry behind the research of Cu^I species and their reactivity towards dioxygen is beyond the scope of this review and the interested reader is referred to recent literature for an up-to-date overview [88–90, 99–108].

4
Homogeneous Copper-Catalyzed Oxidations

4.1
C – H Bond Activation

4.1.1
Oxidation of Alkanes

Somewhat related to the chemistry observed with the peptidylglycine-α-hydroxylating monoxygenase (PHM), the aerobic oxidation of cyclohexane has been studied by several groups. Murahashi et al. have reported that with $CuCl_2$ and acetaldehyde and in the presence of 18-crown-6, cyclohexanone was obtained as the major product (cyclohexanol was formed as the major by-product) under relatively mild conditions (70 °C) [109, 110]. Turnover numbers of up to 1600 were achieved with 61% yield of cyclohexanone at 1 atm of O_2, but the precise mechanism has not been elucidated (Eq. 7).

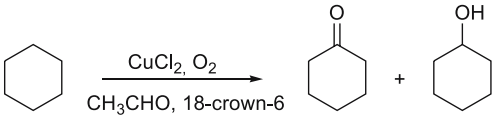

(7)

Itoh et al. used Cu^{II} β-diketiminato complexes with general formula **4**, and their reactivity has been described as a functional model for pMMO (particulate methane monooxygenase). Initially, the ligands were reacted with both Cu^{I} and Cu^{II} precursors, with a variety of species formed, depending on the specific conditions employed [111, 112]. It was then shown that both Cu^{I} and Cu^{II} complexes ultimately led to bis(μ-oxo)$(Cu^{III})_2$ species upon reaction with O_2 and H_2O_2, respectively. Use of these Cu^{II} complexes as the pre-catalysts for the oxidation of alkanes (cyclohexane and adamantane) in the presence of H_2O_2 resulted in low yields ($\sim$ 20%).

Cyclohexane and various alkylbenzenes are oxidized to the corresponding ketones with the Cu^{II} complex **5a** in the presence of 30% H_2O_2 [113]. For in-

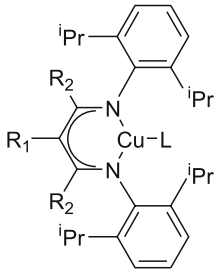

4

stance, oxidation of diphenylmethane with 0.1 mol % **5a** and 10 equiv. of 30% H_2O_2 under ambient conditions afforded a 1 : 1 mixture of diphenylmethanol and benzophenone in 34% yield after 16 h. When heated to 80 °C for 5 h, the reaction is driven to the formation of benzoquinone in 87% yield. $Cu(OAc)_2$ and Cu^{II}(salen) also afforded benzoquinone under identical conditions, but were found to be less effective than **5a**.

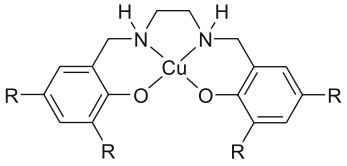

5a (R = H)
5b (R = tBu)

Even simple Cu^I systems prepared from $[Cu^I(NCMe)_4]ClO_4$ and various N-donor ligands such as pyridine, bipyridine, terpyridine, tris(pyrazolyl)-borate (tpb), and tris(pyrazolyl)methane (tpm) have been reported to be capable of oxidizing alkanes, alkenes, and alcohol under appropriate conditions, using *t*BuOOH and one atmosphere oxygen pressure. For instance, the combination of $[Cu^I(py)(tpb)]$ (5 mM), *t*BuOOH (10 mM), and ethylbenzene (1 M) under 1 atm of O_2 forms 57.7 mM acetophenone as basically the only product. No products that might result from free *t*BuO· radicals were observed. In close analogy to previous ideas [114], initial intermediates $[LCu^I - OOtBu]$ are proposed that react with O_2 to give active superoxide species $[LCu^{II}(OOtBu)(OO\cdot)]$.

The most active system to date for the Cu-catalyzed oxidation of cyclohexane has only recently been reported. Reaction of triethanolamine with $Cu(NO_3)_2$ in the presence of NaOH and different types of aromatic carboxylates, NaN_3 or $NaBF_4$ yielded a family of multinuclear copper complexes with different structural characteristics, including **6** and **7**. These systems showed

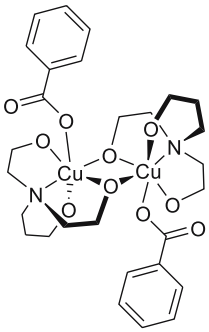

6

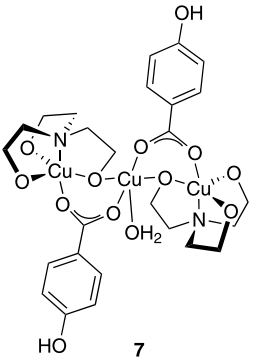

7

excellent activities for the oxidation of cyclohexane in MeCN, using H_2O_2 as oxidant, effectively creating a liquid biphasic, acidic system [115, 116].

Screening experiments revealed an optimal molar ratio of peroxide to catalyst of 200 : 1 to 400 : 1. Total conversions (cyclohexanol and cyclohexanone combined) of up to 32% and turnover numbers of $\sim$ 380 at high alkane to catalyst ratios after 72 h at room temperature were achieved, with the selectivity and conversion being dependent on the molar ratio of peroxide to catalyst as well as the acid concentration. The oxidation of ethane and methane gave around 2% conversion in both cases, with TON's of 47 and 23, respectively, at 40 °C and 30 atm alkane pressure. The rates achieved appear to rival those for the native enzyme pMMO. Those Cu complexes that contain labile sites (Cu – N_3, Cu – OH_2 or Cu–(μ_4–O) fragments) showed the highest activities. Simple recycling tests indicated little loss of activity within five cycles. Though no mechanistic studies were reported, it was proposed that carbon- and oxygen-centered radicals were involved in the reaction. This was supported by a marked decrease in catalyst activity upon addition of the radical-traps TEMPO or $CBrCl_3$ or the oxygen-traps Ph_2NH or BHT [115, 116].

The selective oxidation of methane by a bis(μ-oxo)(Cu^{III})$_2$ species, stabilized on various zeolites, was reported to proceed at high temperatures. Selective oxidation to methanol was observed [117].

Non-catalytic intermolecular oxidation of C – H and O – H bonds, i.e. 9,10-dihydroanthracene or xanthene and 2,4-di-*tert*-butylphenol, respectively, by molecularly defined Cu^{III} complexes was reported [118].

The Cu-catalyzed cross-dehydrogenative coupling (CDC) between two C – H sp^3 bonds—from a tertiary amine and a nitroalkane—using CuBr and in the presence of stoichiometric amounts of *tert*-butylhydroperoxide was described recently (Eq. 8) [119]. The mechanism is not understood at present, but coordination of both an iminium and a nitrite fragment to the copper center, followed by intramolecular coupling, has been suggested, although interaction of the organic peroxide with either substrate or metal complex can

not be ruled out. Cu(OTf) and $Cu(OTf)_2$ were less effective. A similar CuBr-catalyzed alkynylation of sp^3 C – H bonds adjacent to an N atom had been reported previously, also using *tert*-butylhydroperoxide [120].

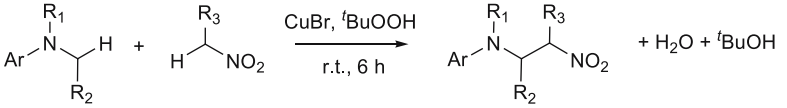

(8)

The same catalytic system as described for the CDC of amines and nitroalkanes, complemented with $CoCl_2$ as a co-catalyst, also proved efficient for the allylic alkylation via cross-dehydrogenative coupling between various cycloalkenes and diketones (Eq. 9). Again, the exact mechanism or role of the organic peroxide are not known to date, but the formation of water probably provides the thermodynamic driving force for these reactions [121, 122].

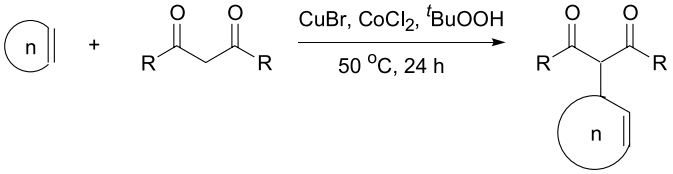

(9)

It should be noted at this point that several Cu_x/O_2 species of either type **E** or type **F** (compare Fig. 2) have been shown to oxidatively *N*-dealkylate specific substituents of the ancillary ligands. Mechanistic studies implicate an initial hydroxylation at the activated position α to the N atom by a rate-controlling C – H bond scission to yield a carbinolamine intermediate, which then decomposes to the product aldehyde and secondary amine [123]. By using the supporting ligand L^H (Scheme 2) clean generation of a bis(μ-oxo) core of type **F** was observed, which upon warming to ambient temperature gave the product from ligand hydroxylation at the benzylic position [124, 125]. The origin of the O atom was molecular oxygen, as confirmed by an $^{18}O_2$ labeling experiment. Using L^D a kinetic deuterium isotope effect of 35.4 at – 80 °C was measured, which together with the Hammett parameter from changes of the X substituent suggested H atom abstraction (or a concerted reaction variant) as the rate-determining step. Selective oxidation of relatively weak benzylic C – H bonds has also been achieved with external substrates, as described for selected examples in the following section.

4.1.2
Oxidation of Benzylic C – H Bonds

2,4,6-Trimethylphenol (TMP) can not undergo C – O polymerization (vide infra, Sect. 4.7). The selective oxidation of the *para*-methyl group by molecular oxygen to yield 3,5-dimethyl-4-hydroxybenzaldehyde (HDB) has been

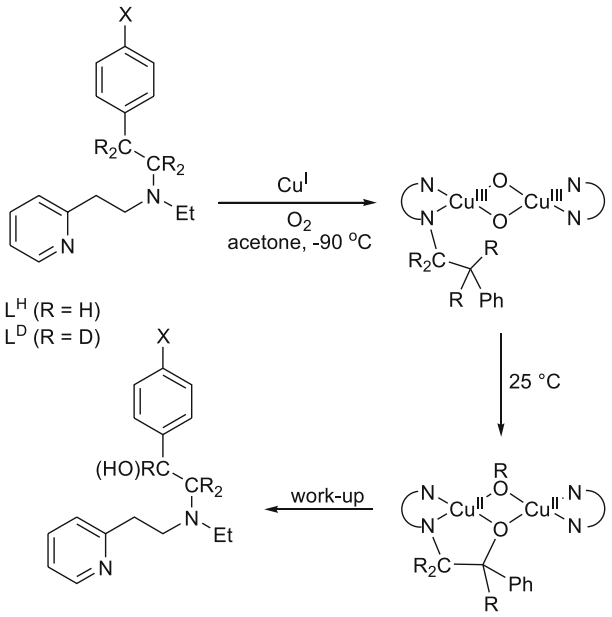

Scheme 2 Aliphatic hydroxylation in benzylic position of an ancillary ligand by a bis(μ-oxo)dicopper(III) core [124]

achieved, using $CuCl_2$ in the presence of amine or oxime ligands and alcohol [126–128]. This transformation bears distant resemblance to the enzymatic oxygenation of aromatic CH_3-groups into the corresponding aldehyde functionality, as observed in laccase or vanillyl alcohol oxidase [129]. It has been assumed that the product is formed via a phenoxyl radical (that reacts with O_2) and a benzoquinone methide intermediate, followed by repeated 1,6-addition of alcohol to sequentially form 4-(alkoxymethyl)-2,6-dimethylphenol and 3,5-dimethyl-4-hydroxybenzaldehyde dialkyl acetal, which is then hydrolyzed to give HDB. More recently novel well-defined Cu complexes have been discovered that mediate this reaction [130, 131]. Four equivalents of a Cu^{II}-based system [$CuCl_2$(neocuproine)/NaOMe] (neocuproine = 2,9-dimethylphenanthroline) were shown to oxidize TMP selectively to HDB at room temperature in MeOH, which is in accord with the four-electron process for this oxidation (Eq. 10). The catalytic conversion of TMP to HDB in the presence of H_2O_2 in refluxing MeOH was observed under an Ar-atmosphere, indicating that O_2 does not play any role in this oxidation. A decrease in the stoichiometry NaOMe : TMP led to selective isolation of the intermediate product 4-(methoxymethyl)-2,6-dimethylphenol (MDP). The catalytic activity of the $CuCl_2$(neocuproine) system is rather low, however, as one equiv. TMP is converted within 6 h using 0.13 equiv. of the Cu-catalyst and 0.105 equiv. of the co-catalyst NaOMe, corresponding to a turnover fre-

quency of $\sim 1.4\,h^{-1}$. Use of the model substrate pentafluorophenol C_6F_5OH together with the ligand neocuproine in the presence of NaOMe led to clean formation of a dinuclear $Cu^{II}Cu^{II}$ core, bridged by a methoxide and a phenoxide (**8**), as shown by X-ray crystallography, suggesting a bimetallic reaction pathway for the observed catalysis.

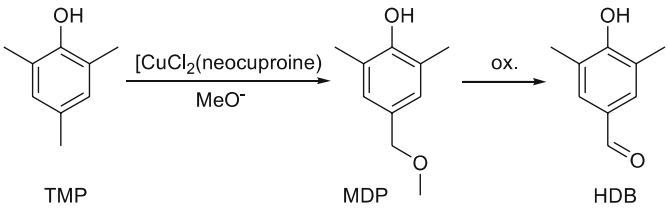

(10)

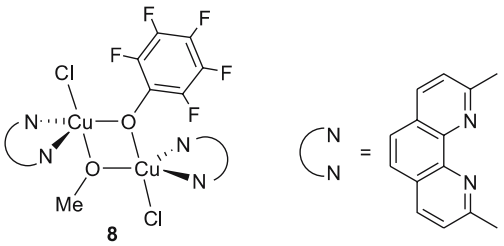

8

In line with the idea of a bimetallic reaction mechanism, the same product HDB could be obtained using a bioinspired pyrazolate-based dinuclear Cu^{II} complex [131]. Compartmental pyrazolate ligands with chelating side arms in the 3- and 5-positions of the heterocycle have proven valuable scaffolds to achieve cooperative two-center reactivity [132], also in Cu chemistry [133–135]. Variations of the chelate arms (side arm chain length, donor atoms, bulkiness) allow control over crucial parameters of the bimetallic core, such as the Cu···Cu separation or redox potentials. The labile MeO···HOMe bridge in **9** forms due to the large Cu···Cu distance that is enforced by the rather short side arms of the particular pyrazolate/bis-imidazole ligand [136]. At low substrate to complex ratios, TMP is oxygenated to give HDB, while in the presence of an excess of TMP regioselective para C – C coupling occurs to catalytically produce stilbenequinone (Eq. 11) [131].

Upon addition of the substrate to a solution of **9** in MeCN or CH_2Cl_2, the green solution turned red instantaneously. UV/Vis spectroscopy suggested coordination of a phenolate ligand to one Cu ion, with an LMCT band occurring at $495\,cm^{-1}$ (2 : 3 mixture of MeCN : CH_2Cl_2), as is also observed in the molecular structure of **10** that results from addition of the substrate analogue C_6F_5OH. Under exclusion of O_2 in a glove-box, this red putative adduct from **9** and TMP gradually reacts further, and 1,2-bis(4-hydroxy-3,5-dimethylphenyl)ethane, originating from an oxidative 4,4′-addition of two phenolate moieties, could be isolated as the initial product. This slowly un-

derwent further oxidation only in the presence of reoxidized dicopper catalyst and air, yielding the final product stilbenequinone as a red crystalline material. Further details of the reaction mechanism still have to be elucidated. The same C – C coupled product stilbenequinone had also been obtained from TMP and (tacn)$CuCl_2$ in CH_2Cl_2 (tacn = triazacyclononane) [137].

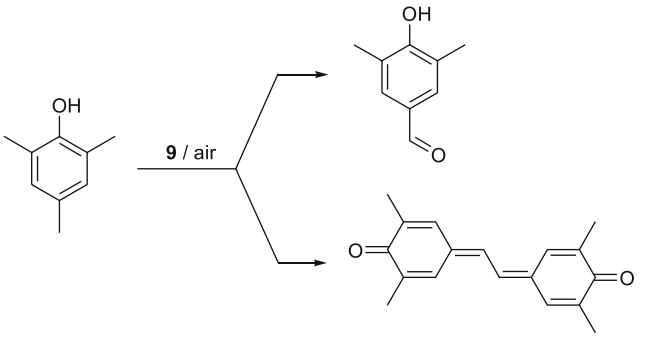

(11)

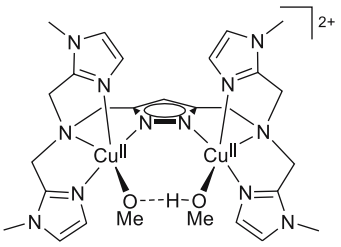

9

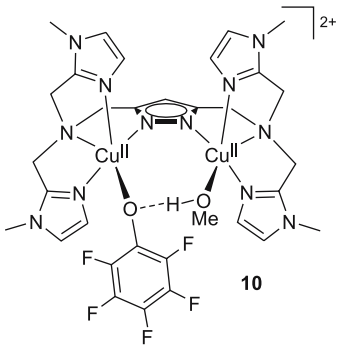

10

Using the same [$CuCl_2$(neocuproine)] pre-catalyst system mentioned above, Reedijk et al. have also reported other oxidative coupling reactions of TMP with various nucleophiles, proposedly via the in situ formation of a benzoquinone methide [138]. Typically, reactions were carried out in DMF as a non-nucleophilic solvent, and with NaH as the base for deprotonation of the *para*-CH_3 group of TMP to form the proposed reactive benzoquinone methide intermediate. Nucleophiles used included 1,2-ethanediol, 2,2′-dipyridylamine and 2,4-pentanedione. As no oxidative coupling was observed without neocuproine present in the system, it was argued that this rigid, bulky bidentate ligand, known to stabilize the Cu^{I}-oxidation state, probably effects the Cu^{II}/Cu^{I} redox-couple, in favor of reduction of Cu^{II} to Cu^{I}, concomitant with formation of the benzoquinone methide fragment. Further indication for this hypothesis was the absence of any activity for TMP-conversion when 2,2-bipyridine was used instead of neocuproine, since the Cu^{II} complexes of the latter ligand are

more difficult to reduce ($E = 0.18$ V versus $E = 0.37$ V vs. Ag^+/Ag). Copper-catalyzed oxidation of 2,6-disubstituted-4-methylphenols to yield the corresponding 4-hydroxybenzaldehydes in good yields was also reported with poly(pyridine-2,5-diyl) and poly(2,2′-bipyridine-5,5′-diyl) ligands, although the catalyst systems were rather undefined [139].

Various UV/Vis spectroscopic studies have been described by Reedijk and co-workers, aimed at identifying the proposed dicopper species with bridging methoxide and phenoxide ligands (compare **8**) in the absence of neocuproine. Notion is made of two bands, appearing at 420 and 450 cm^{-1}, which were attributed to the formation of μ-OMe and μ-phenoxo bridges, respectively.

It should be noted that dihydroanthracene, due to its weak benzylic C – H bonds, is often used as a test substrate to demonstrate the H atom abstraction capability of Cu_x/O_2 species, usually in a stoichiometric fashion [140].

4.2 Oxidation of Alcohols

The selective oxidation of alcohols to the corresponding aldehydes and ketones is of prime importance for organic synthesis, and various types of reagents have been described that achieve this transformation selectively and efficiently [141, 142]. However, the number of sub-stoichiometric, non-toxic, non-hazardous oxidation systems has been relatively limited. As copper enzymes such as galactose oxidase are known to catalyze this oxidation reaction, bioinspired homogeneous catalysts based on copper species have also been developed in recent years.

4.2.1 TEMPO as Co-Catalyst

TEMPO (2,2,6,6-tetramethylpiperidine-1-oxyl) has been widely used as an oxidant in metal-mediated catalytic oxidations [143]. A combined effort of the Reedijk and Sheldon groups established the $CuBr_2$/bipyridine-catalyzed aerobic oxidation of primary alcohols to their corresponding aldehydes, using TEMPO and KO^tBu as the co-catalysts in air at room temperature [144]. TEMPO is believed to act as H-atom abstractor during the catalytic cycle, while the deprotonated alcohol is coordinated to the Cu center. Optimized activity was around 14 h^{-1} and a marked decrease in activity was seen when no additional base was used. Secondary alcohols did not react, presumably due to either steric hindrance or the absence of a stabilizing H-bonding interaction between the protonated TEMPO-species and the β-hydrogen of a primary alcohol fragment. In a succeeding study, $Cu(ClO_4)_2$ was shown to yield a more active catalyst than $CuBr_2$, while $CuCl_2$ and $Cu(NO_3)_2$ provided less active catalysts, likely related to the propensity of the anionic ligand to dissociate [145]. Furthermore, the choice of solvent mixture had a dramatic

effect on the catalytic results: MeCN proved advantageous, presumably because it can act as a weak ligand for stabilization of Cu^{I} species in solution, but H_2O was needed in addition to boost catalyst performance, attributed to increasing the required solubility of the base added and the products formed.

A copper-centered mechanism for the Cu-TEMPO-catalyzed aerobic oxidation of alcohols was proposed by Sheldon and co-workers, wherein the active catalytic Cu^{II} species is generated by oxidation of a Cu^{I} species with TEMPO, in the presence of alcohol, with formation of TEMPOH (Scheme 3) [146]. The resulting Cu^{II} species is then capable of oxidizing the alcoholate to the aldehyde or ketone species. Regeneration of the TEMPO radical species was achieved by rapid oxidation of TEMPOH with O_2.

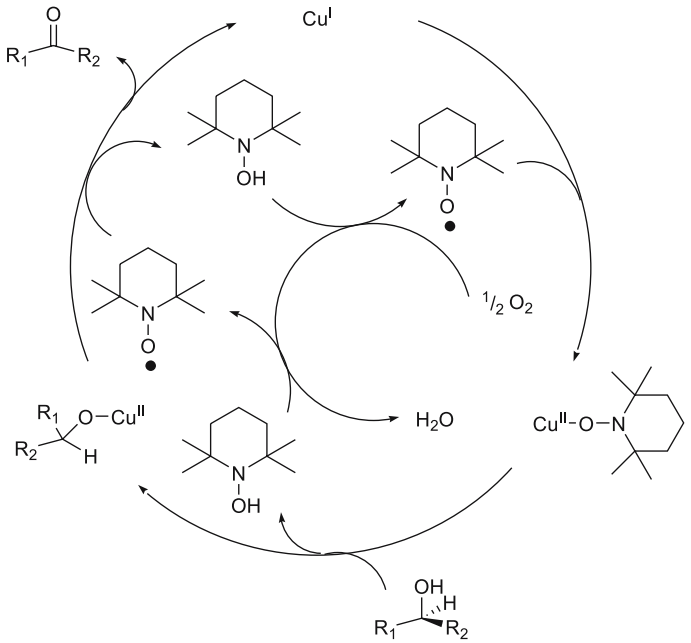

Scheme 3 Proposed catalytic mechanism for the copper catalyzed oxidation of alcohols with TEMPO as oxidant

Oxidation of Cu^{I} with O_2 is markedly slower than the analogous oxidation by TEMPO. The existence of a copper-centered dehydrogenation step was supported by investigating kinetic isotope effects and Hammett correlation studies using different substituted benzylic alcohols. The β-hydrogen abstraction was postulated to occur in a concerted mechanism with an η^2-coordinated TEMPO radical ligand (Scheme 4). As such, this TEMPO-mediated copper-catalyzed oxidation of alcohols bears resemblance

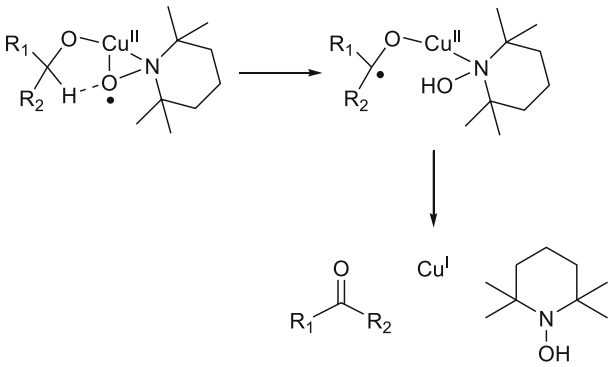

Scheme 4 Postulated concerted mechanism for the β-hydrogen abstraction during oxidation of alcohols with TEMPO

to the catalysis observed with galactose oxidase and its biomimetic model systems.

Knochel et al. reported on the use of an in situ generated Cu catalyst, formed from $CuBr \cdot SMe_2$ and a perfluorinated bipyridine, in a mixture of perfluorooctane and chlorobenzene for the oxidation of 4-nitrobenzylalcohol to the corresponding 4-nitrobenzaldehyde, with TEMPO as the co-catalyst [147, 148]. Rather than applying a perfluorinated N-donor ligand, the groups of Vincent and Fish have demonstrated the use of a perfluorinated copper precursor ($Cu(OAc^F)_2$, $OAc^F = (C_8F_{17}(CH_2)_2)_2CHCO_2$) for the oxidation of alkenols and alcohols in the presence of TEMPO under fluorous biphasic conditions, partly also using the thermomorphic property of the catalyst system for recycling purposes [149].

The application of ionic liquids as a reaction medium for the copper-catalyzed aerobic oxidation of primary alcohols was reported recently by various groups, in attempts to recycle the relatively expensive oxidant TEMPO [150, 151]. A TEMPO/CuCl-based system was employed using $[bmim]PF_6$ (bmim = 1-butyl-3-methylimodazolium) as the ionic liquid. At 65 °C a variety of allylic, benzylic, aliphatic primary and secondary alcohols were converted to the respective aldehydes or ketones, with good selectivities [150]. A three-component catalytic system comprised of $Cu(ClO_4)_2$, dimethylaminopyridine (DMAP) and acetamido-TEMPO in the ionic liquid $[bmpy]PF_6$ (bmpy = 1-butyl-4-methylpyridinium) was also applied for the oxidation of benzylic and allylic alcohols as well as selected primary alcohols. Possible recycling of the catalyst system for up to five runs was demonstrated, albeit with significant loss of activity and yields. No reactivity was observed with 1-phenylethanol and cyclohexanol [151].

4.2.2
H_2O_2 as Oxidant

The salen-Cu^{II} complex **5a** was shown to oxidize a selected number of secondary alcohols (e.g. 1-phenylethanol) to the corresponding ketones, with a wider range of primary alcohols being further oxidized to the analogous carboxylic acids, in the presence of ~ 5–15 equiv. of H_2O_2 as oxidant, while molecular oxygen proved inefficient as oxidant [152]. The derivative **5b** has been reported to catalyze the electrochemical oxidation of primary alcohols (but not secondary alcohols) into the corresponding aldehydes, with turnovers > 30 [153].

4.2.3
Molecular Oxygen as the Oxidant

Functional models for the catalytic activity observed in galactose oxidase have attracted considerable attention. An elegant copper system with a binaphthol-derived salen ligand has been developed by Stack et al. (Scheme 5) [154]. The resulting Cu^{II} complex **11** showed significant deviation from square-planar geometry, mimicking the coordination observed around the Cu center in the native enzyme. Efficient oxidation of benzylic and allylic alcohols to the corresponding aldehydes and ketones was observed at r.t. employing 1 atm of O_2 with total turnovers of over 1000, but secondary aliphatic alcohols proved unreactive. Kinetic and spectroscopic measurements pointed

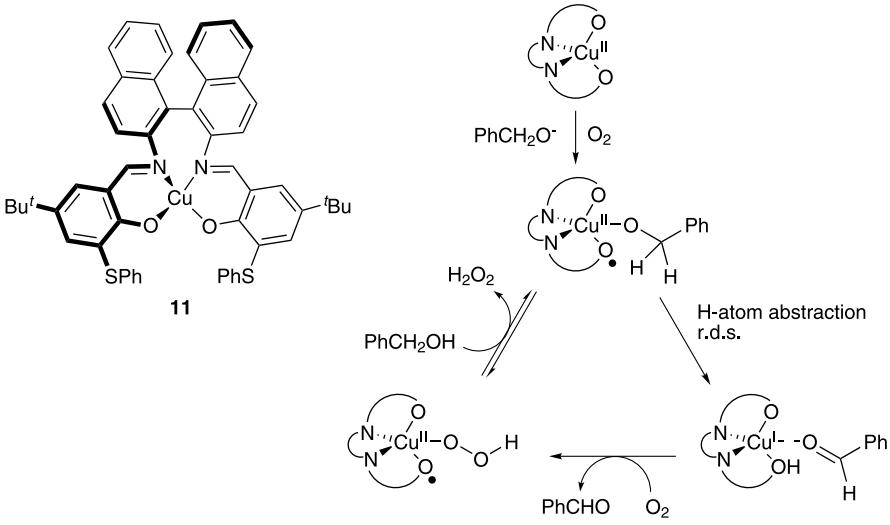

Scheme 5 Complex **11** and its proposed catalytic mechanism in the oxidation of benzylic alcohols

towards a mechanism where benzylic C – H bond cleavage within the coordinated alcoholate fragment is involved in the rate-determining step. The proposed peroxide intermediate, formed after replacement of the formed product by O_2, concomitant with H-atom transfer, has not been observed spectroscopically, but its formation is inferred from the measured 1 : 1 ratio of O_2 uptake to product formation at initial stages of the catalysis.

Using an aminobisphenol ligand HL^N or a selenobisphenol ligand HL^{Se} in the presence of a Cu^{II} salt, and with NEt_3 as an additional amine ligand, Chaudhuri and co-workers prepared the mononuclear complexes **12** and **13** [155–157], which proved to be efficient catalysts for the oxidation of primary alcohols (Eq. 12). The rate of aldehyde formation increases with increasing NEt_3 concentration until a maximum is reached and then starts to decrease, indicating that the NEt_3 ligand is required for catalytic activity while the five-coordinate species with two NEt_3 ligands (which forms at larger excess of NEt_3) is inactive.

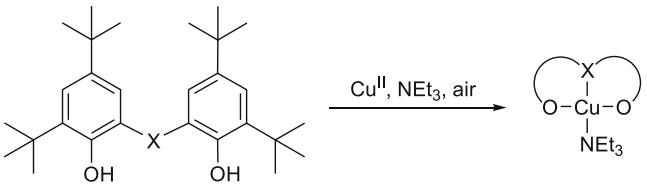

HL^N (X = NH)
HL^{Se} (X = Se)

12 (X = NH)
13 (X = Se)

(12)

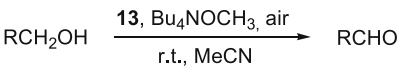

Kinetic measurements, comparing conversion rates of $C_6H_5CD_2OH$ vs. $C_6H_5CH_2OH$, revealed a kinetic isotope effect of 8.0 or 8.5 for **12** and **13**, respectively, which suggests H-atom abstraction from the α-carbon of the ligated benzyl alcohol to be rate determining. A mechanism shown in Scheme 6 was proposed for **13**, similar to that for galactose oxidase and respective functional model systems, in which a deprotonated alcohol molecule first coordinates to the mononuclear Cu^{II} complex, concomitant with formation of a phenoxyl radical on the tridentate {O,Se,O} ligand system. Upon H-atom abstraction a bound ketyl radical anion is formed, which undergoes internal electron transfer to yield the Cu^I species with a weakly bound aldehyde fragment. Replacement by O_2 leads to dissociation of the oxidized substrate with formation of the Cu^{II} hydroperoxo species. Protonation of the latter by another molecule of benzylalcohol yields H_2O_2 and the regenerated phenoxyl radical species [156].

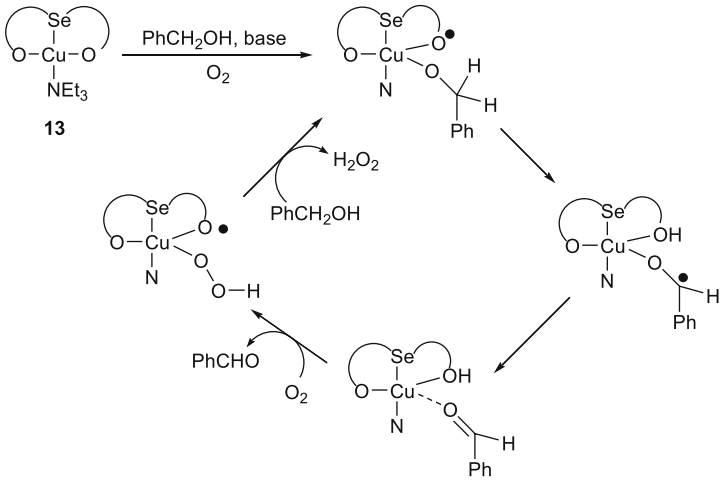

Scheme 6 Proposed catalytic mechanism with pre-catalyst **13** in the oxidation of benzyl alcohol

Closely related behavior had previously been observed with the Cu complex **14**, prepared from the corresponding thiobisphenol ligand (HL^S) (Scheme 7) [158]. The species formed upon oxidation was proposed at the time to be a dinuclear diphenoxyl radical dication **15**. The catalytic behav-

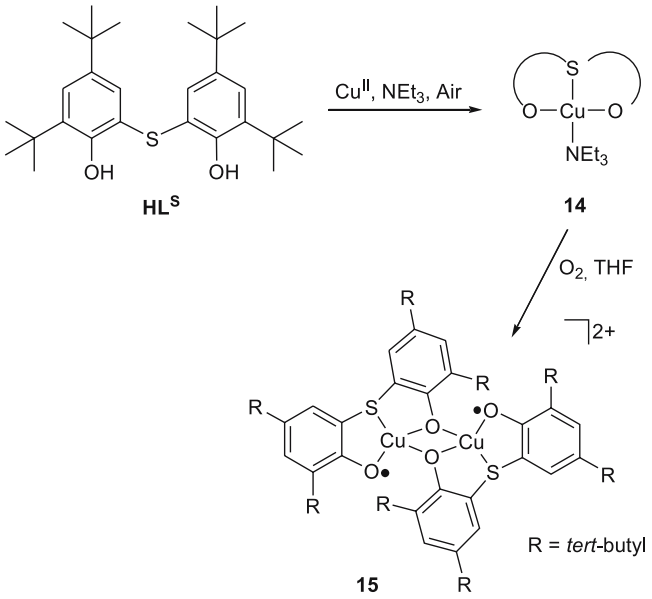

Scheme 7 Synthesis of the dicopper diphenoxyl diradical dication **15**

ior of **15** was studied as extensively as for **13**, and it was shown that ethanol, benzylalcohol and 2-butanol could be selectively converted to the analogous ketones in moderate to excellent yields, with concomitant formation of H_2O_2. However, use of either 2-propanol or diphenylcarbinol gave the 1,2-glycol derivatives as major products. These latter compounds were shown by kinetic measurements to originate from oxidative coupling of the alcohol substrates.

In contrast to the active site of galactose oxidase, to pre-catalyst **13**, and to the system reported by Stack et al., the proposed catalytic species **15** does not undergo reduction to Cu^I intermediates, as the oxidation equivalents needed for the catalysis are provided for solely by the phenoxyl radical ligands. Since the conversion of alcohols into aldehydes is a two-electron oxidation process, only a dinuclear Cu species with two phenoxyl ligands is thought to be active. Furthermore, concentrated H_2O_2 is formed as byproduct in the reaction instead of H_2O, as in the system described by Markó et al. [159].

A similar biradical process has also been established for some mononuclear Cu complexes **17** (derived from ligand **16**) and **18** that contain two iminosemiquinone radicals [156, 160]. Complex **17** proved to be a good catalyst for the aerial oxidation of benzyl alcohol to benzaldehyde, while **18** even oxidizes ethanol and methanol. Primary kinetic isotope effects again confirm that H-atom abstraction from the substrate is the rate-determining step.

In a combinatorial approach, 3,4-dimethoxybenzylalcohol (veratryl alcohol) was oxidized with $Cu(SO_4)_2$ and a series of 22 amine ligands in order to screen catalytic activity for the selective oxidation towards veratryl alde-

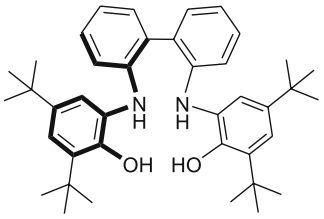

16

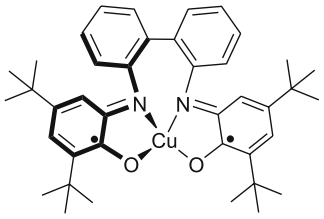

17

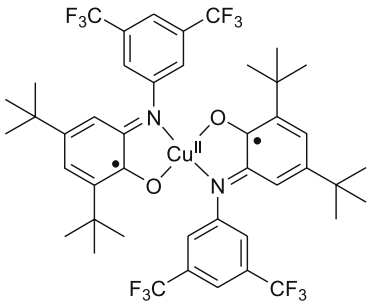

18

hyde [161]. The most active catalysts were found to incorporate TMEDA, 1,2-diaminocyclohexane (DACH) or 9,10-diaminophenanthrene (DAPHEN). Further screening revealed that the counterion did not have a significant effect on the catalytic results, while ligand-dependent optimization of the pH had great influence on the outcome. Also, different optimal ligand-to-metal ratios were found in all three cases, dependent on ligand solubility in the aqueous media (DAPHEN) and chelating strength of the ligands. Peptidic ligand libraries with natural and non-natural amino acids have been generated via combinatorial methods and their Cu complexes were tested for catalytic activity in the air oxidation of benzyl alcohol and 3-methoxybenzyl alcohol [162]. Pronounced sequence dependence of the catalytic activity was observed, with the best systems (up to 6 turnovers after 24 h at ambient temperature) containing a TEMPO-derived radical α-amino acid.

The use of a novel $\{N_3O_2\}$ ligand set provided an unsaturated five-coordinated Cu^{II} complex (**19**), capable of performing the aerobic oxidation of benzyl alcohol to benzaldehyde in the presence of $Cu(CF_3SO_3)_2$ as initial oxidant, with $\sim$ 44 turnovers in 24 h [163]. The initial step produces the active bis-phenoxy radical species **20** (Eq. 13). Under exclusion of air, greatly reduced catalytic activity was observed, indicative of reoxidation of the active catalyst by O_2, although the possibility for H_2O_2 (which is a likely side-product) to act as oxidant could not be ruled out.

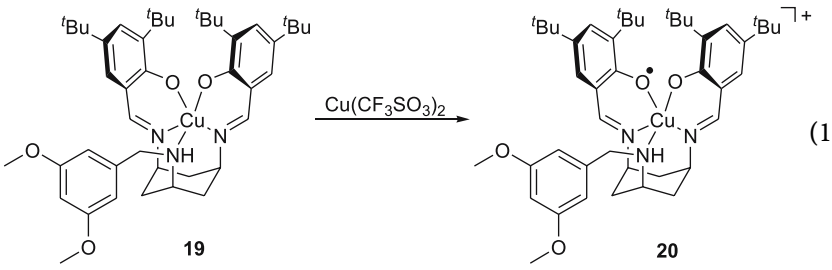

19 **20** (13)

A very powerful catalytic system, capable of oxidizing a wide range of primary, secondary, allylic and benzylic alcohols, was developed by Markó and co-workers [159]. The basic ingredients were shown to be CuCl, phenanthroline, DBAD (di-*tert*-butyl azodicarboxylate), base (K_2CO_3) and air or molecular O_2, with further improvements achieved when a Ru co-catalyst [164] or neutral conditions were employed [165]. However, these catalytic systems proved incapable of converting primary *aliphatic* alcohols under all tested conditions. Very recently, a simple but significant optimization step was reported, applying a nitrogen-derived additive, most notably 10 mol % dimethylaminopyridine (DMAP) or 7 mol % *N*-methylimidazole (NMI) to the aforementioned Cu-based system (Scheme 8) [166]. The additional amine is believed to act as a pseudo-protecting agent; after dissociation of the aldehyde, formed via intramolecular hydrogen-transfer from the alcoholate to the hydrazine ligand, a vacant site is generated. Despite fast reactivity of this unsaturated copper species with dioxygen, yielding a proposed dimeric peroxide, occasional coordination of free alcohol would ultimately lead to inactive copper alkoxide. The reversible binding of the amine suppresses this latter deactivation route, thereby ensuring long catalyst lifetime.

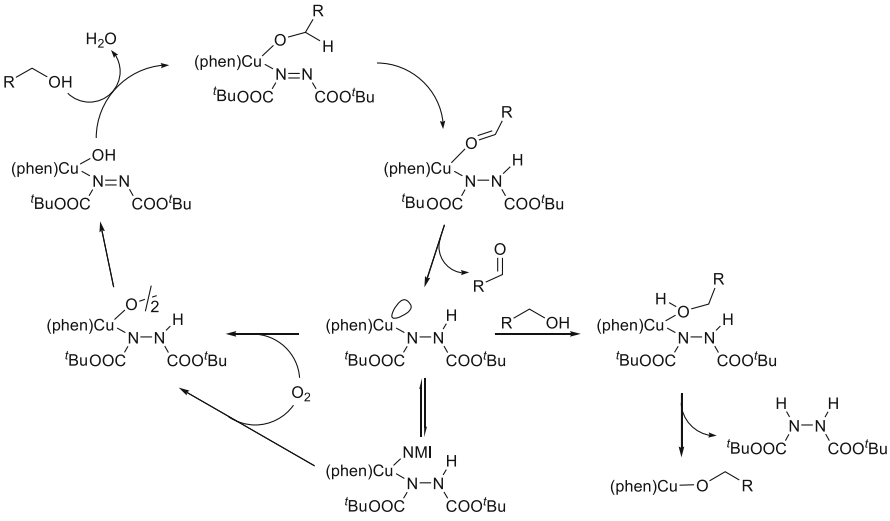

Scheme 8 Catalytic cycle for the oxidation of alcohols using Markó's catalyst, including the beneficial use of NMI

The stoichiometric selective oxidation of the benzylic alcohol function in (di)hydroxy-substituted benzylalcohols (Eq. 14) has been demonstrated by Nolte et al., using host-guest chemistry to steer the regiospecificity in the reaction [167–170]. The host-receptor used to construct dicopper complex **21** is based on the building block diphenylglycoluril, which was functionalized

with two bis(pyrazolyl)amine fragments, to provide the necessary coordination for a bimetallic active site.

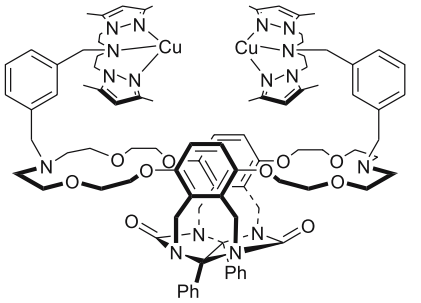

(14)

4.3 Oxidation of Amines

Using the selenobiphenol ligand HL^{Se} mentioned in the previous paragraph, Chaudhuri and co-workers also isolated the trinuclear complex **22** and the dinuclear complex **23** (Scheme 9) [155]. The latter was shown to catalyze the selective aerial oxidation of primary amines with at least one

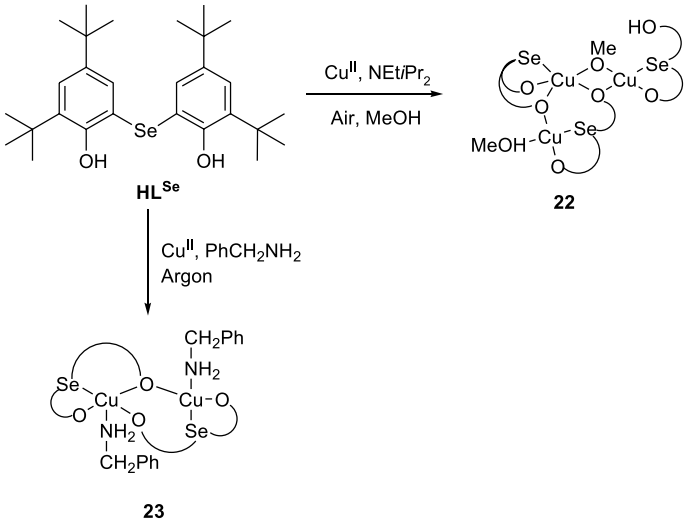

Scheme 9 Dinuclear and trinuclear Cu complexes **22** and **23** from HL^{Se}

α-H atom, which represents a functional model for copper amine oxidase. Although H_2O_2 could not be detected by GC-MS spectrometry, which may point to some catalase activity by the Cu species, NH_3 was qualitatively detected. With benzylamine as a substrate, only benzylidinebenzylamine (the Schiff base condensation product of benzaldehyde and benzylamine) was obtained, with 17 turnovers. Similar Schiff base products were observed for α-phenylbenzylamine and cyclohexylamine, while acetophenone was detected as the only oxidation product of α-methylbenzylamine, with 10 turnovers. Applying benzylamine with selective deuteration of the α-carbon resulted in a kinetic isotope effect of 4, implying that H atom abstraction from a coordinated benzylamine ligand is the rate-limiting step for this process (Scheme 10).

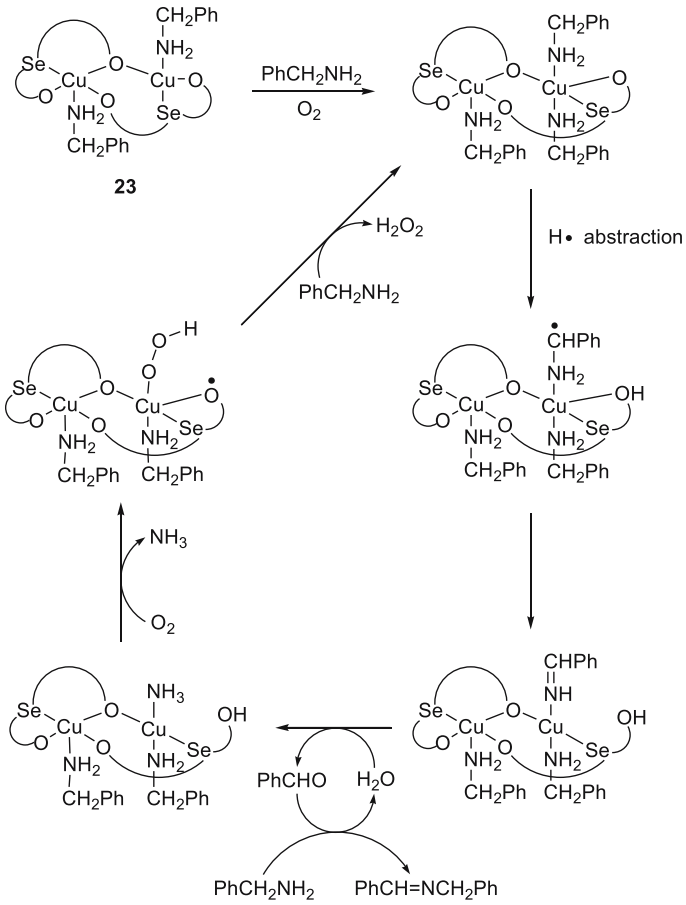

Scheme 10 Catalytic mechanism for the oxidation of benzylamine to benzylidinebenzylamine using **23**

An unusual oxo-transfer to an amine has been observed, besides other products that originate from oxidative N-dealkylation chemistry, when the dicopper(I) complex of ligand **24** was reacted with O_2 at 0 °C (Scheme 11) [169]. A labeling experiment showed that the O atom in **25** is derived from molecular dioxygen.

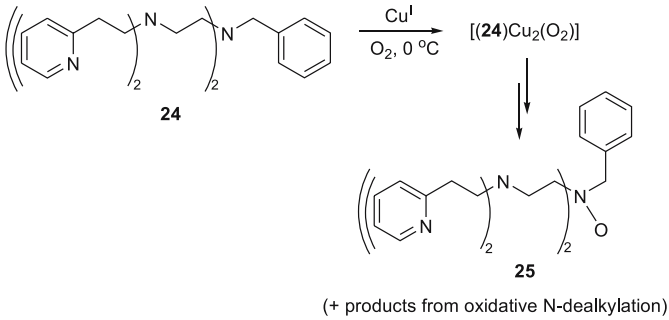

Scheme 11 Intramolecular oxo-transfer to an amine with a dicopper complex [171]

4.4 Hydroxylation of Phenols

The first of two conversions catalyzed by the metalloenzyme tyrosinase is the selective *ortho*-hydroxylation of a phenol moiety, yielding catechol. Few synthetic systems exist that are capable of selectively performing the same monooxygenase reaction [172–178]. The group of Casella has studied a series of dicopper complexes based on 2,6-disubstituted benzene ligands providing two $\{N_3\}$ compartments [179–181] (**26a**,**b**) as well as the asymmetrically substituted tripodal amine-based ligand (**27**) [182].

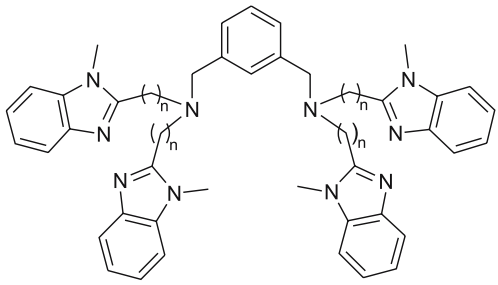

With respect to the oxygenation of methyl 4-hydroxybenzoate (as its *tetra-n*-butylammonium salt) to methyl 3,5-dihydroxybenzoate, remarkable differences in activity for this test reaction were observed with the three ligand sys-

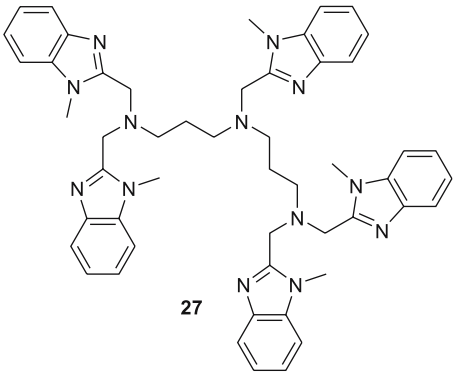

27

tems. It should be noted here that the electron-withdrawing ester-group aids in stabilizing the dicopper(II)-catecholate product against internal electron transfer to yield the dicopper(I) species and quinone; this effectively increases the selectivity by preventing further redox and condensation chemistry.

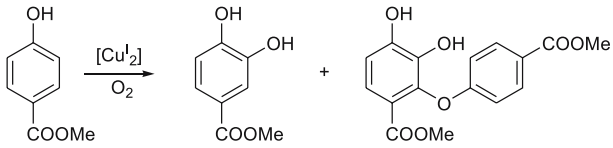

(15)

With the benzene-derived ligands **26a**,**b** the Cu-catalyzed *ortho*-hydroxylation of methyl-4-hydroxybenzoate was only highly selective at low temperature, as at room temperature bound catecholate was shown to undergo a formal Michael addition with unreacted phenolate to yield methyl 2-[4-(carbomethoxy)phenoxy]-3,4-dihydroxybenzoate [181, 270]. With the amine-based ligand **27**, no such reactivity was observed and the catechol product methyl 3,4-dihydroxybenzoate was formed selectively. Interestingly, this latter ligand system also displayed some selective reactivity with the neutral 4-hydroxybenzoic acid substrate.

Besides hydroxylation of exogeneous phenol to the corresponding catechol, some imine and xylene-based ligand systems have been shown to undergo (partial) hydroxylation of a central benzene-ring to yield a phenolate fragment in an intramolecular hydroxylation reaction [179, 183–189]. Somewhat related reactivity was observed in the intramolecular hydroxylation at a benzylic position of a sidearm on a specific aminopyridine ligand (compare Sect. 4.1).

Fukuzumi and Itoh have jointly reported on a μ-$\eta^2:\eta^2$-peroxo dicopper(II) complex that acts as a functional model for the phenolase activity of tyrosinase. Lithium salts of *para*-substituted phenols were used as substrates, reaching yields between 60 and 90% with only the catechol product formed

(Scheme 12) [178]. Isotope labeling experiments using $^{18}O_2$ confirmed that the origin of one of the O atoms of the catechol product is molecular oxygen. Deprotonation of the substrate is essential, since only the C – C coupling

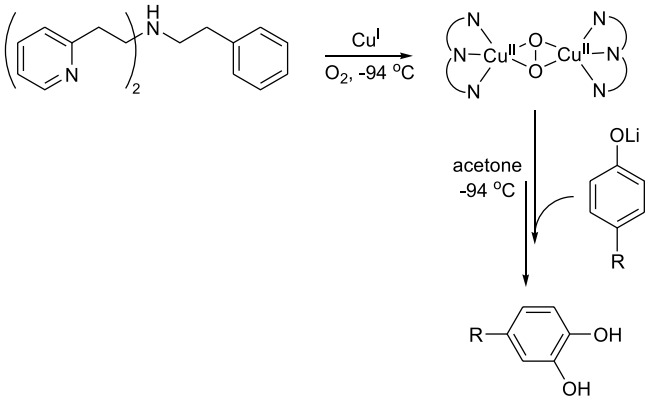

Scheme 12 Ortho-hydroxylation by peroxo (or bis(μ-oxo)) dicopper intermediates derived from tridentate amine ligands [178]

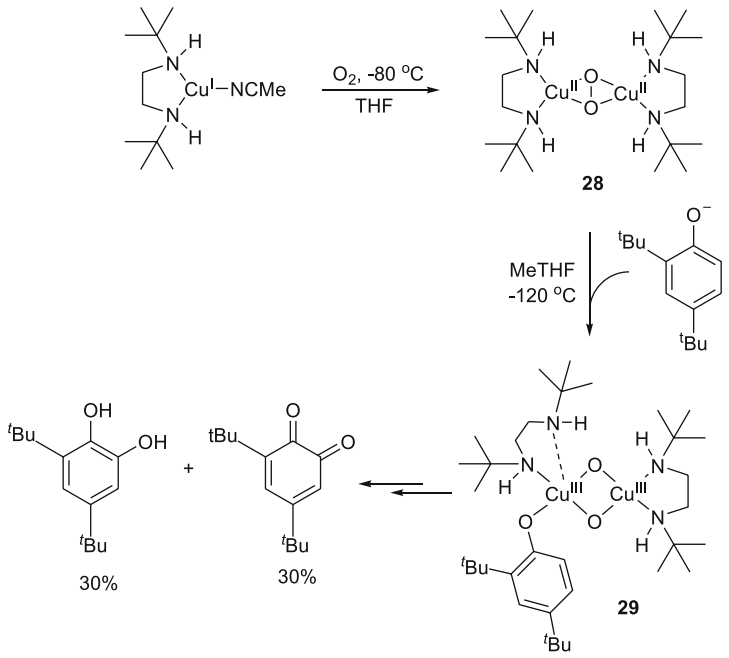

Scheme 13 Pathway for the oxidation of 3,5-di-tert-butylphenolate to the corresponding catechol and quinone products using dicopper species **28**, via the spectroscopically observed bis(μ-oxo)phenolate intermediate **29** [190]

dimer was obtained when the phenol itself was used instead of the phenolate as the exogenous substrate, and kinetic data indicated formation of a complex between the substrate and the peroxo intermediate prior to the oxygenation step.

Stack and co-workers recently reported a related μ-η^2 : η^2-peroxodicopper(II) complex **28** with a bulky bidentate amine ligand capable of hydroxylating phenolates at – 80 °C. At – 120 °C, a bis(μ-oxo)dicopper(III) phenolate complex **29** with a fully cleaved O – O bond was spectroscopically detected (Scheme 13) [190]. These observations imply an alternative mechanism for the catalytic hydroxylation of phenols, as carried out by the tyrosinase metalloenzyme, in which O – O bond scission precedes C – O bond formation. Hence, the hydroxylation of 2,4-di-*tert*-butylphenolate would proceed via an electrophilic aromatic substitution reaction.

An efficient and selective Cu-assisted *ortho*-hydroxylation procedure for the conversion of benzoate to salicylate has been described, involving trimethylamine N-oxide (TMAO) as the oxidant [191, 192]. The reaction was assumed to proceed via oxidation of a Cu^{II} carboxylate complex by TMAO to produce the active species (postulated to be a Cu^{II} hydroxo complex, but with only circumstantial evidence), followed by oxygen transfer to the benzoate group (Scheme 14). Using a set of different amide derivatives of benzoic acid, Comba and co-workers gained additional mechanistic hints in support of a reactive Cu-oxo or Cu-hydroxo intermediate that is stabilized by a five-membered chelate [193]. A pre-equilibrium involving Cu^{II}, the ligand, and TMAO was proposed, but details of the reaction are far from clear.

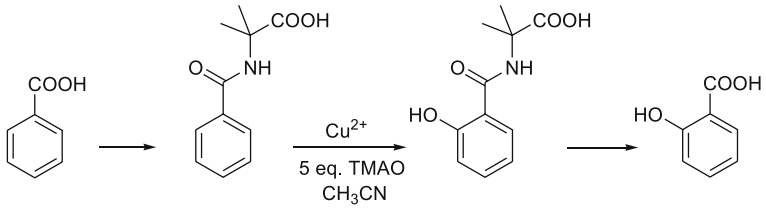

Scheme 14 Cu-assisted ortho-hydroxylation of benzoate to salicylate with TMAO

4.5 Oxidation of Phenols and Catechols

While only tyrosinase catalyzes the *ortho*-hydroxylation of phenol moieties, both tyrosinase and catechol oxidase mediate the subsequent oxidation of the resulting catechols to the corresponding quinones. Various mono- and dinuclear copper coordination compounds have been investigated as biomimetic catalysts for catechol oxidation [21, 194], in most cases using 3,5-di-*tert*-butylcatechol (DTBC) as the substrate (Eq. 16). The low redox potential of DTBC makes it easy to oxidize, and its bulky *tert*-butyl groups prevent un-

wanted side reactions such as ring opening or polymerization of the resulting 3,5-di-*tert*-butylquinone (DTBQ). Either H_2O_2 or H_2O may result as the reduction product, depending on the particular Cu catalyst used. Curiously, in some cases the formation of H_2O_2 goes along with the detection of a semiquinone species in the catalytic reaction, and it has been proposed that H_2O_2 may form upon oxidation of a Cu^I-semiquinone intermediate.

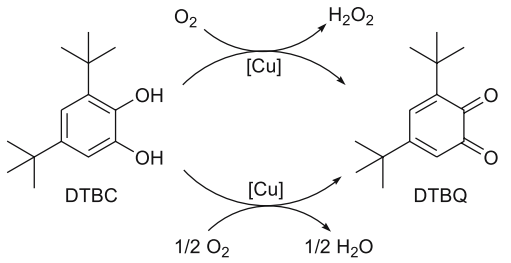

(16)

For dinuclear Cu complexes, several pathways are possible as summarized in Scheme 15 [182]. In addition, plausible alternatives involve mixed-valent Cu^ICu^{II} species where only one of the Cu ions is directly involved in the electron transfer. The latter seems most likely in cases where the substrate binds to only one of the two copper ions, and H_2O_2 may then form upon oxidation of the Cu^ICu^{II}-semiquinone intermediate [195]. Different coordination modes of the DTBC substrate appear to be indeed possible, depending on the particular dicopper scaffold [133, 196, 197]. Unfortunately, detailed mechanistic studies are still quite scarce [198–203] and most proposed catalytic pathways are rather speculative.

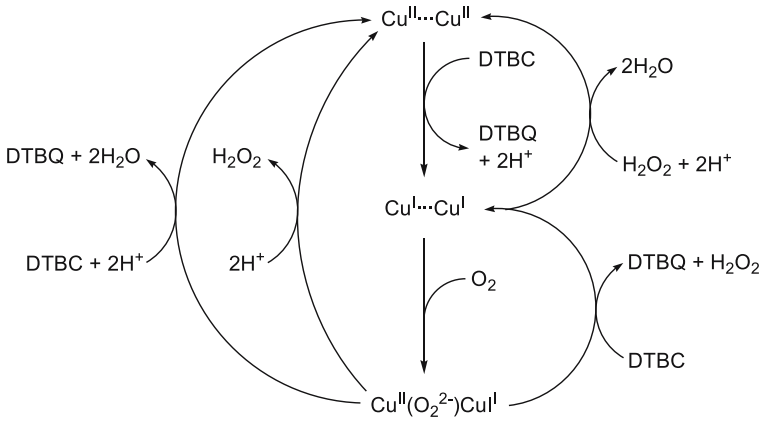

Scheme 15 Possible reaction pathways in the catalytic cycle of dicopper(II) catechol oxidase model systems [182]

Much of the recent interest in catechol oxidase model systems has focussed on the elucidation of structure-activity relationships (for a recent review see [21]). Dinuclear copper complexes are generally found to be more reactive than mononuclear compounds, and a steric match between the dicopper site and the substrate is assumed to be advantageous [133, 204, 207]. Parameters that determine the activity of synthetic dicopper enzyme analogues comprise, inter alia, the metal-metal separation [133, 135, 205–207], the redox properties [135, 208–211], the identity of exogeneous bridging ligands [212, 213], the structure of the dinucleating ligand scaffold [133, 210, 211, 214, 215], and the pH [208, 209, 216–219]. In most cases, however, no clear relation between the catalytic activity and the redox potential of the copper species has been discernible, which may be explained by the manifold steps that are involved in the overall catalytic cycle. Using dicopper complexes of dinucleating ligands **26a**,**b** and **30**, Casella and co-workers succeeded in determining the reaction rates for the two successive steps of the catalytic cycle, i.e. a fast stoichiometric reaction between the dicopper(II) complex and a catechol and slower subsequent reactions that comprise oxygenation of the dicopper(I) species, binding of a second catechol to the $\{Cu_2O_2\}$ intermediate, and electron transfer from the catechol anion to the dioxygen moiety. They showed a clear dependence of the reaction rate in the first stoichiometric step on the Cu^{II}/Cu^{I} reduction potential, while the rate-determining step among the following sequence of events may vary depending on the particular ligand scaffold. In methanol/aqueous buffer at pH 5.1, O_2 is reduced to water, with no formation of H_2O_2 observed [198].

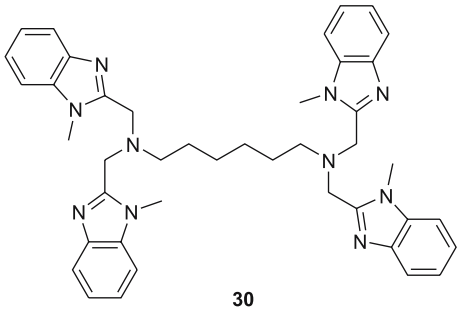

30

Pyrazolate-based dinucleating ligands have proven useful to control crucial characteristics of the dicopper core, such as the Cu···Cu separation and the electronic properties of the metal ions, by variation of the chelate side arms attached to the heterocycle (**31**). This leads to greatly differing activities in the catalytic oxidation of DTBC mediated by those dicopper complexes [133, 135]. While most of the pyrazolate-derived complexes **31** display an enzyme-like Michaelis–Menten type kinetic behavior, it is apparent that both the Cu···Cu separation as well as the redox potential play an important

role: the shortest Cu···Cu distance accessible with the available set of systems (~ 3.5 Å) is clearly advantageous for high activity (which decreases with larger Cu···Cu separation), and activity is greatly diminished when the dicopper complex has a redox potential below a certain threshold value [135]. However, both parameters have to be considered simultaneously, and it is likely that additional factors play a role as well.

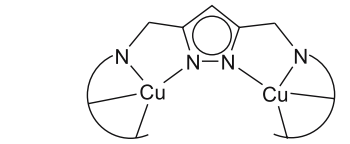

31

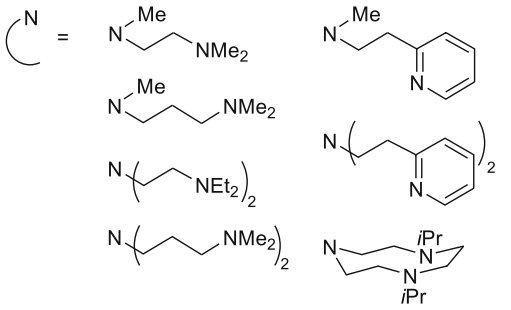

Within a series of O-atom-bridged dicopper(II) complexes, those complexes with a metal-metal distance closest to the *met* form of the enzyme (2.9 Å) displayed the best catalytic performance [207].

Some correlations between the observed rates of reactivity and ligand architecture, copper coordination environment or preorganization of the metal ions have been observed for particular classes of complexes [21]. Within a series of dicopper(II) complexes of generic type **32** with bridging phenoxo ligands, only those bearing at least one coordinating piperazine side arm (**33**) showed activity [210, 211]. This was attributed to the strong distortion of the tetragonal Cu coordination enforced by this particular side arm unit, resulting in strained structures. Further elaboration revealed that an adjacent thioether group in **33c** increases the catecholase activity, possibly because the potentially coordinating thioether helps to remove additional bridging groups (such as acetate) from the bimetallic pocket and thus enhances generation of free binding sites for the substrate [214]. For an assortment of dicopper complexes **34** derived from reduced Schiff base ligands it was found that activity was reduced by electron-withdrawing substituents X but enhanced by electron-donating substituents [220].

Dinuclear copper complexes with aliphatic tripodal amino alcohol ligands were tested in the oxidation of DTBC (Eq. 17) [221]. It was shown that

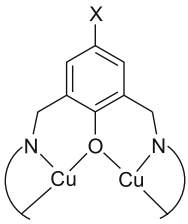

32

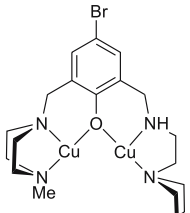

33a (X = CH_2)
33b (X = O)
33c (X = S)

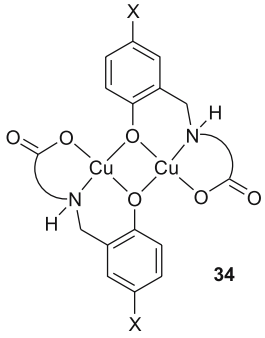

34

a nitrogen-rich coordination environment had a positive influence on the catalytic activity, although under the basic conditions used, the stability of the most active catalyst system was poor. Turnover frequencies of up to 500 h^{-1} were achieved with complex **35** after optimization of, for example, the order of reagent addition.

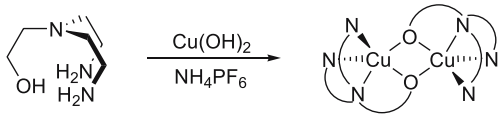

(17)

35

Particularly high efficiency in catechol oxidation was achieved with some Cu^{II} complexes based on aminocarbohydrate ligands [222, 223].

Fukuzumi and co-workers described spectroscopic evidence for a μ-η^2 : η^2-peroxo-$(Cu^{II})_2$ species stabilized with a *bi*dentate nitrogen ligand, but no (catalytic) oxidation behavior towards catechol was noted (a related trinuclear copper species converted 2,4-di-*tert*-butylphenol stoichiometrically towards the biphenol derivative) [224]. Stack et al. have described a similar μ-η^2 : η^2-peroxo-$(Cu^{II})_2$ species (**28**, vide supra) that could be considered a structural and functional model for tyrosinase-activity, as it efficiently reacted with catechol, benzyl alcohol and benzylamine to yield quinone (95%), benzaldehyde (80%) and benzonitrile (70%) [172, 173]. This dinuclear peroxo species is generated by association of two monomeric copper centers, in contrast to the systems based on dinucleating ligand scaffolds described above.

Proposed tetranuclear Cu^I complexes with piperidine and bridging halide ligands were shown to facilitate reduction of O_2 to the corresponding bridging dioxo ligands. The resulting Cu^{II}-based tetranuclear complexes were active in the oxidative coupling of 2,6-dimethylphenol to 3,3′,5,5′-tetramethyl-4,4′-diphenoquinone (DPQ), presumably because of the presence of basic oxo-sites within the tetranuclear framework [225]. More recently, L-/D-DOPA and their methyl esters have become substrates for enantioselective catechol oxidation using chiral copper complexes based on binaphthol [226, 227] or histidine [228].

Trimethyl-1,4-benzoquinone (TMQ) is a key intermediate in the industrial production of vitamin E, and it is currently obtained by *para*-sulfonation of 2,3,6-trimethylphenol, followed by oxidation with MnO_2. A one-step oxidation of 2,3,6-trimethylphenol would be a very attractive alternative. Copper-based biphasic alcohol/water processes have been developed, but almost stoichiometric amounts of the Cu salt (or even more than that) are required, and hence these systems hardly qualify as being catalytic [229–231]. The amount of catalyst could be significantly reduced by adding N-containing co-catalysts [232, 233]. More recently, the aerobic oxidation of 2,3,6-trimethylphenol was reported in an ionic liquid medium, with $CuCl_2$ as the (pre-)catalyst and an oxotetracuprate $[Cu_4(\mu_4\text{-}O)Cl_{10}]^{4-}$ as the proposed active catalyst [234]. With 2.5 mol % of $CuCl_2$ a yield of 86% TMQ (at 100% conversion) could be obtained, the only other product being 2,2′,3,3′,5,5′-hexamethyl-4,4′-dihydroxybiphenyl. The mechanism is proposed to involve a phenolate radical that is attacked by dioxygen in the *para* position, as outlined in Scheme 16.

The copper-mediated stoichiometric enantioselective oxidative dearomatization of pyronoquinone (Eq. 18) was achieved with a Cu^I species and (–)-sparteine as the chiral auxiliary ligand [235].

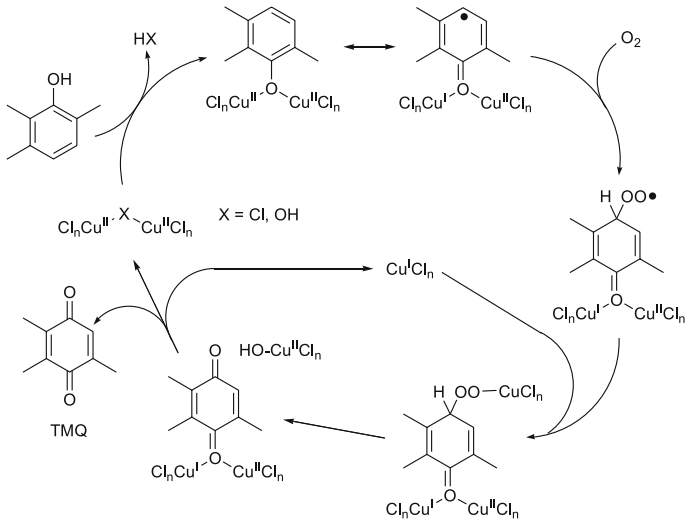

Scheme 16 Proposed mechanism for the aerobic oxidation of 2,3,6-trimethylphenol to TMQ [223]

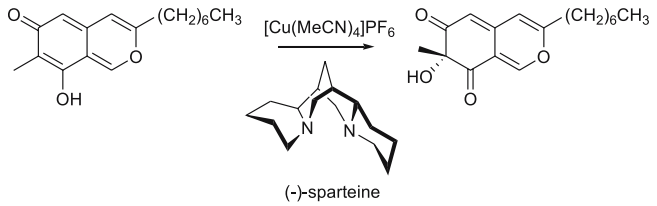

(18)

4.6 Oxidation of Sulfides

Recently, Punniyamurthy and co-workers applied the same catalyst **5a** as used for the oxidation of alkanes [152] (Sect. 4.2) for the selective oxidation of aromatic sulfides to the corresponding sulfoxides with H_2O_2 (Eq. 19) [236]. Addition of 5 mol % TEMPO dramatically improved the selectivity and conversion; with methylphenylsulfide as the substrate, only traces of sulfone were observed.

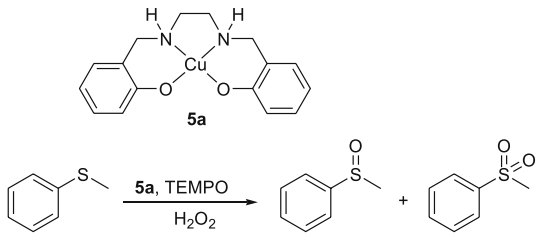

(19)

A square-planar Cu^{II}-hydroperoxo species **36** was reported to act as a catalyst for the selective oxidation of dimethylsulfide to dimethylsulfoxide (Eq. 20), with no trace of higher oxidation products formed and TON's of up to 300. Also thioanisole could be converted on a catalytic basis [237].

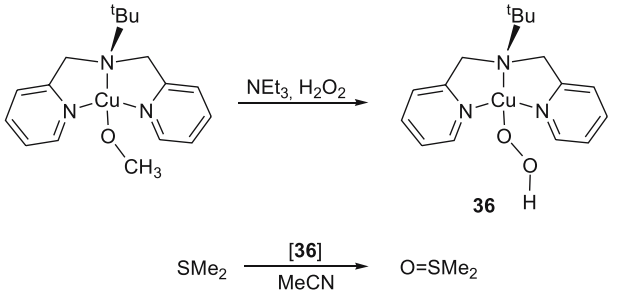

$$SMe_2 \xrightarrow[MeCN]{[\mathbf{36}]} O{=}SMe_2 \qquad (20)$$

4.7 Oxidative Polymerization of Phenols

The aerobic copper-catalyzed oxidative coupling of phenols was first discovered in the laboratories of General Electric in 1959, employing a Cu^{I}-pyridine complex [247]. It was later found that the presence and nature of *ortho*-groups on the phenol-ring greatly influence the reactivity. Phenol or mono-substituted derivatives thereof yield branched products with no added value, while two small *ortho*-groups tend to favor polymerization. Larger substituents shift the selectivity towards the formation of diphenoquinone (DPQ) [238]. Therefore, 2,6-dimethylphenol is often the monomer of choice. Poly(2,6-dimethylphenylene ether) (PPE) is a key ingredient of high-performance engineering plastics. It is a thermoplastic polymer that exhibits unusually low moisture absorption, due to its inherent chemical composition, leading to good electrical insulating properties over a wide range of humidities and temperatures. It is also very resistant to a variety of chemicals, water, most salt solutions, acids and bases. The main applications for this material include computer and television housing, keyboard frames and interface boxes. Production of this polymer, via oxidative C – O coupling of the monomer 2,6-dimethylphenol, is often hampered by co-formation of the undesired C – C coupled product DPQ.

An early mechanism proposed by the group of Challa [239, 240] considered the formation of a dinuclear bis-phenolate bridged Cu^{II} species, that underwent two one-electron transfer steps (centered on one of the bridging phenolate fragments) to yield the corresponding Cu^{I} phenoxonium cation. Subsequent coupling with another phenol "monomer" and reoxidation of the copper atoms regenerated the phenolate-bridged Cu^{II} dimer. The oxygen atoms from molecular oxygen did not end up in the product in this mechanism, as O_2 is reduced to form H_2O.

Reedijk and co-workers have reported a kinetic and spectroscopic study aimed at clarifying the role of the ligand (*N*-methylimidazole) to copper ratio, the choice of base added as well as the effect of water [238]. A fractional order $1 < n < 2$ in copper for the rate law was observed for all ligand/Cu ratios (varied from 1 to 40). From these studies it was concluded that (at least) two competing rate-limiting steps with comparable rates are present in the mechanism. It was argued that both the phenol oxidation on a dinuclear copper center (n would be ~ 1 for a Cu_2 species) and the formation of this dinuclear Cu^{II} species ($n \sim 2$) are likely candidates for these rate-determining steps. At higher ligand to copper ratios a higher fractional order in Cu is observed, which agrees with a disfavoring of the formation of the dinuclear Cu species. Optimal base to copper ratios were found to be around 2. Dioxygen was determined to be necessary only for the previously postulated re-oxidation of the Cu^{I}–Cu^{I} species to Cu^{II}–Cu^{II}, as determined by ESR spectroscopy with and without oxygen present. H_2O was shown to have a detrimental effect on the polymerization, as fast decolorization of a solution containing the Cu^{II}-phenolate complex was observed concomitant with formation of DPQ (Eq. 21). Water did, however, have a beneficial role at the start of the reaction, as it facilitates the actual phenol oxidation. More basic ligands led to higher activities, and monodentate ligands proved better than bidentate analogues. Weakly coordinating solvents such as acetonitrile greatly improved the activity as well [241, 242]. The authors therefore argued against the proposed formation of a bis-phenolate-bridged species (Challa mechanism) and formulated a monophenolate-hydroxo species to be the active catalyst. This would also substantiate the claim that two one-electron transfer steps occur on one phenolate fragment, which is highly unlikely in a symmetric bis-phenolate complex. These observations have led to a modified mechanism for the polymerization of 2,6-dimethylphenol (Scheme 17) [238]. A quinone ketal intermediate is formed, that can either undergo redistribution by nucleophilic attack from another phenolate-functionalized species (monomeric or polymeric) whilst coordinated to the dicopper center, or dissociation from the dicopper complex followed by rearrangement of the quinone ketal into the polymeric, phenol end-capped, C – O coupling product [243, 244]. Similar conclusions were later drawn by Gao et al. [245, 246].

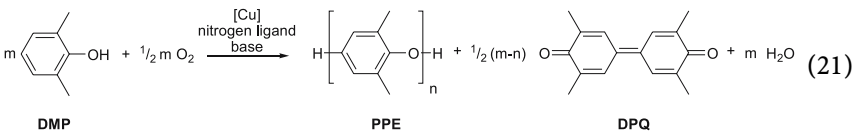

(21)

A series of eight closely related N,O-based ligands was used to unravel possible steric and electronic influences in the copper-catalyzed polymerization of 2,6-dimethylphenol [248]. Applying a biphasic toluene/water emulsion, with an in situ prepared Cu(MeIm)-catalyst (MeIm = 1-methylimidazole),

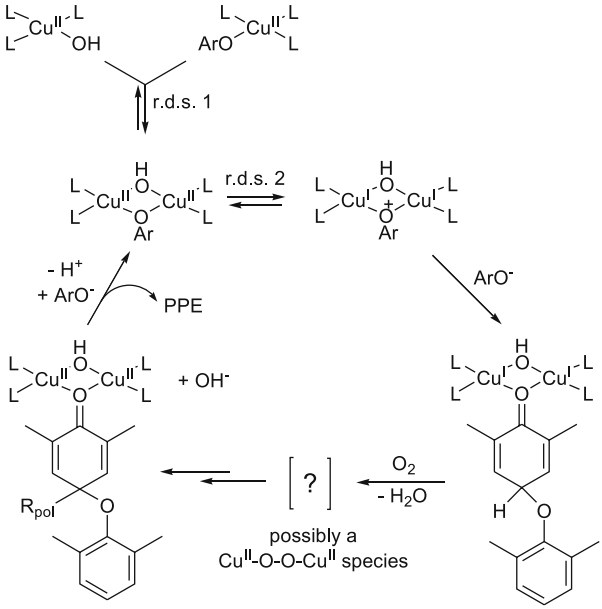

Scheme 17 Postulated mechanism for the oxidative polymerization of dimethylphenol [238]

Reedijk and co-workers were able to selectively obtain PPE with a molecular weight M_w of up to ~ 86 000 Da. The catalytic results were highly dependent on the ligand : metal stoichiometry used, which implied an additional advantageous influence of the MeIm ligand in obtaining a stable emulsion [249]. New pyrazole-containing macrocyclic ligands were developed for the selective polymerization of 2,6-dimethylphenol, but catalytic activities and selectivities were found to be moderate, and catalyst decomposition by way of interference with H_2O formed during reaction was observed, although addition of excess N-methylimidazole circumvented this problem [250].

The oxidative polymerization of DMP to PPE could also be carried out in aqueous NaOH solution (pH ~ 13.5) at 50 °C under vigorous stirring using (tmeda)$CuCl_2$ as the catalyst, resulting in the precipitation of a polymer with an M_n of 2900 g/mol and only traces of the undesired side-product DPQ [252].

(tacn)CuX_2 complexes (where tacn = 1,4,7-*tri*isopropyl-1,4,7-triazacyclononane and X is a halide) were thoroughly tested and compared for their regioselective oxidative polymerization of 4-phenoxyphenol to yield poly(1,4-phenylene oxide) (PPO) [251].

The oxidative coupling of fluorophenols is usually impeded by their high oxidation potential due to the electron-withdrawing nature of the fluorine substituents. Using catalysts composed of $CuCl_2$ and peralkylated amines such as *N*,*N*,*N*′,*N*′-tetramethylethylenediamine (tmeda), *N*,*N*′-bis[2-(dimethylamino)ethyl]methylalkylenediamine ($C_n$tmeda$_2$), or 1,4,7-

triisopropoyl-1,4,7-triazacyclononane (iPr_3tacn), however, the oxidative polymerization of 2,6-difluorophenol could be achieved to give a high molecular weight material with M_w up to 66 000 [253]. The amount of O_2 uptake with respect to the polymer yield was in accordance with a $4e^-$ reduction of O_2, and highly oxidizing species containing the $[Cu^{III}(\mu\text{-}O)_2Cu^{III}]^{2+}$ core were implicated in the reaction, albeit without proof.

4.8 Oxidative Coupling of Phenols

The Ullmann coupling is the classical example of Cu-catalyzed biaryl coupling, wherein (a) a phenol and arylhalide substrate are converted to a bis-arylether or (b) two arenes are coupled to form a bis-arene species. These coupling reactions are of great importance for general organic synthesis as well as pharmaceutical and fine chemicals. The copper-catalyzed phenol coupling to arrive at chiral biphenol derivatives is used extensively as a test reaction for the catalytic activity of new copper complexes [254, 255].

The dicopper(I) complex with dinucleating bisamino-bispyridine ligand **37** as well as the dicopper complex **38** were shown to couple 2,4-di-*tert*-butylphenol to the corresponding bisphenol derivative (Eq. 22), while with 2,6-substituted phenols, oxidative coupling at the *para*-position was observed to yield the diphenoquinone derivatives (Eq. 23) [256, 257]. Similar reactivity is observed for various other dicopper systems.

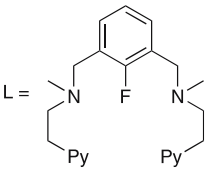

37

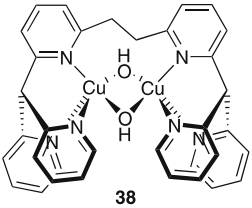

38

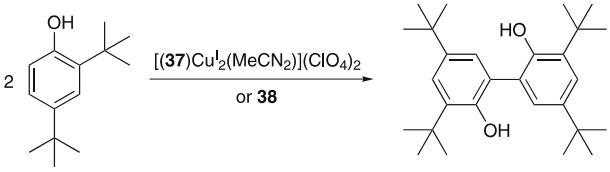

(22)

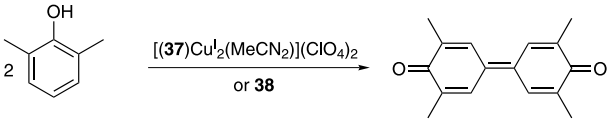

(23)

Chiral dinucleating salen and aminoalcohol-derived ligands **39** and **40** were used to prepare dicopper species that showed moderate to good enantioselectivities of up to 88% in the oxidative coupling of 2-naphthol to 2,2′-binaphthol (Eq. 24). The same reaction with a monomeric analogue of either complex showed dramatically lower selectivity. The precise interaction of the substrate with both copper centers is unknown, as is the actual coupling mechanism, which could proceed intra- as well as intermolecularly [258]. Mononuclear achiral imino-alcohol-derived copper complexes were applied for the same coupling reaction as well as for the coupling of 2,4-dimethylphenol. Low activities but high selectivities were found [259].

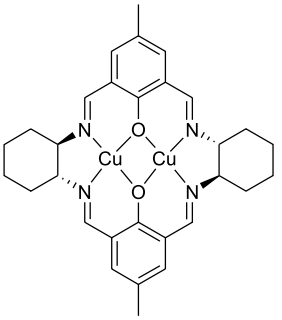

39

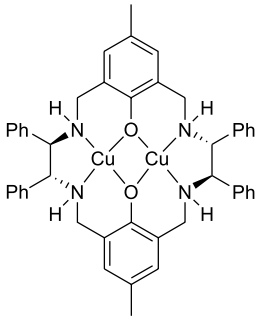

40

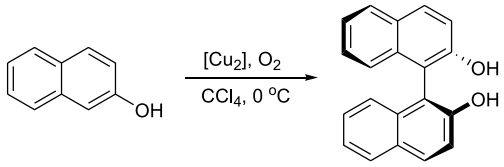

(24)

With the bisoxazoline ligand (*S*)-Phbox and CuCl, the asymmetric oxidative coupling of 2-naphthol and hydroxy-2-naphthoates resulted in an asymmetrically substituted 2,2′-binaphthol with ee's of up to 65% [260]. On the basis of the previous results obtained with this catalyst system, the asymmetric oxidative cross-coupling polymerization of 2,3-dihydroxynaphthalene [261] and methyl 6,6′-dihydroxy-2,2′-binaphthalene-7,7′-dicarboxylate [262] as well as the copolymerization of 6,6′-dihydroxy-2,2′-binaphthalene and dihexyl 6,6′-dihydroxy-2,2′-binaphthalene-7,7′-dicarboxylate with Cu^{I} diamine catalysts were carried out under aerobic conditions, using O_2 as the oxidant, and a cross-coupling selectivity of 99% was achieved [263].

4.9 Miscellaneous

To round off the overview of Cu-mediated oxygenation and oxidation reactions and to give a glance at the broader usefulness of Cu, a few examples of

closely related chemistry are briefly mentioned here. A recent application of bioinspired Cu chemistry is the oxygenation of acetone into lactate that was observed with a monomeric Cu^{I} complex stabilized by a fluorinated trispyrazolyl borate ligand, most likely via a Cu^{II} intermediate [264]. The oxidative homocoupling of acetylenes and the arylhalide-acetylene heterocoupling are both of prime importance in organic synthesis, with applications ranging from polymer chemistry to biochemistry. The aerobic oxidative coupling of acetylenes is catalyzed by simple Cu^{II} salts, with simple amines or pyridine additives as ligands [265–269].

5 Concluding Remarks

The bioinorganic chemistry involving copper and dioxygen, as displayed by a range of metalloenzymes, has not only spurred exciting research in the realm of coordination chemistry with small molecule model complexes, resulting in a plethora of fascinating Cu_x/O_2-species being identified, but has also provided a valuable platform for the development of copper-based homogeneous catalysts, able to oxidize a variety of organic substrates. Of particular current industrial importance are the selective C – O coupled polymerization of disubstituted phenols and the oxidation of alcohols, whilst also the cheap generation of H_2O_2 as a (by)-product from aerobic copper-catalyzed oxidation has attracted attention. Future research might see breakthroughs in, for example, the applicability of the Cu-based oxidation of alkanes. The applicability of reactivity patterns that at first glance appear exotic might become well established within due time.

Acknowledgements We would like to thank the Alexander-von-Humboldt Foundation for a postdoctoral fellowship (to J.I.v.d.V.), and Ms. Angelina Prokofieva for scientific discussions.

References

1. Omae I (1998) Applications of Organometallic Compounds. Wiley, Chichester, p 489
2. Csende F, Geza S (2005) Curr Org Chem 9:1737
3. Smidt J, Hafner W, Sedlmeier J, Jira R, Rüttinger R (1959) Consortium für Elektrochemische Industrie. DE Patent 1 049 845
4. Jira R, Blau W, Grimm D (1975) Hydrocarbon Processing 55:97
5. Jira R (1996) In: Cornils R, Herrmann WA (eds) Applied Homogeneous Catalysis with Organometallic Compounds. Wiley, Weinheim, p 374, ibid (2002) 2nd edn 1:386
6. Naworski JS, Velez ES (1983) In: Leach BA (ed) Applied Industrial Catalysis. Academic Press, New York, p 239
7. Spector ML, Heinemann H, Miller KD (1967) Ind Eng Chem Process Res Dev 6:327

8. Klausener A, Jentsch JD (1996) In: Cornils B, Herrmann WA (eds) Applied Homogeneous Catalysis with Organometallic Compounds. Wiley, Weinheim, 1:169
9. Kaim W, Rall J (1996) Angew Chem Int Ed Engl 35:43
10. Malmström BG, Leckner J (1998) Curr Opin Chem Biol 2:286
11. Pascaly M, Jolk I, Krebs B (1999) Chemie i u Zeit 33:334
12. Solomon EI, Sundaram UM, Machonkin TE (1996) Chem Rev 96:2563
13. McGuirl MA, Dooley DM (1999) Curr Opin Chem Biol 3:138
14. Halcrow MA, Knowles PF, Phillips SEV (2001) In: Bertini I, Sigel A, Sigel H (eds) Handbook on Metalloproteins. Marcel Dekker, New York, p 709
15. Lindley PF (2001) In: Bertini I, Sigel A, Sigel H (eds) Handbook on Metalloproteins. Marcel Dekker, New York, p 763
16. Vila AJ, Fernandez CO (2001) In: Bertini I, Sigel A, Sigel H (eds) Handbook on Metalloproteins. Marcel Dekker, New York, p 813
17. Lindley PF (2001) In: Bertini I Sigel A, Sigel H (eds) Handbook on Metalloproteins. Marcel Dekker, New York, p 857
18. Gamez P, Aubel PG, Driessen WL, Reedijk J (2001) Chem Soc Rev 30:376
19. Fontecave M, Pierre JL (1998) Coord Chem Rev 170:125
20. Bento I, Armenia Carrondo M, Lindley PF (2006) J Biol Inorg Chem 11:539
21. Koval IA, Gamez P, Belle C, Selmeczi K, Reedijk J (2006) Chem Soc Rev 35:814
22. Solomon EI, Baldwin MJ, Lowery MD (1992) Chem Rev 92:521
23. Ito N, Phillips SEV, Stevens C, Ogel ZB, McPherson MJ, Keen JN, Yadav KDS, Knowles PF (1991) Nature 350:87
24. Ito N, Phillips SEV, Yadav KDS, Knowles PFJ (1994) Mol Biol 238:794
25. Eisensmith RC, Woo SLC (1991) Mol Biol Med 8:3
26. Fitzpatrick PF (2003) Biochemistry 42:14083
27. Klinman JP (1996) Chem Rev 96:2541
28. Tainer JA, Getzoff ED, Beem KM, Richardson JS, Richardson DC (1982) J Mol Biol 160:181
29. Tainer JA, Getzoff ED, Richardson JS, Richardson DC (1983) Nature 306:284
30. Volbeda A, Hol WG (1989) J Mol Biol 206:531
31. Volbeda A, Hol WG (1989) J Mol Biol 209:249
32. Matoba Y, Kumagai T, Yamamoto A, Yoshitsu H, Sugiyama MJ (2006) Biol Chem 31:8981
33. Klabunde T, Eicken C, Sacchettini JC, Krebs B (1998) Nat Struct Biol 5:1084
34. Eicken C, Krebs B, Sacchettini JC (1999) Curr Opin Struct Biol 9:677
35. Gerdemann C, Eicken C, Krebs B (2002) Acc Chem Res 35:183
36. Siegbahn PEM (2004) J Biol Inorg Chem 9:577
37. Decker H, Schweikardt T, Tuczek F (2006) Angew Chem Int Ed 45:4546
38. Bertrand T, Jolivalt C, Briozzo P, Caminade E, Joly N, Madzak C, Mougin C (2002) Biochemistry 41:7325
39. Piontec K, Antorini M, Choinowski T (2002) J Biol Chem 277:37663
40. Claus H (2004) Micron 35:93
41. Hakulinen N, Kiiskinen LL, Kruus K, Saloheimo M, Paananen A, Koivula A, Rouvinen (2002) J Nat Struct Biol 9:601
42. Messerschmidt A, Rossi A, Ladenstein R, Huber R, Bolognesi M, Gatti G, Machesini A, Petruzzelli R, Finazzi-Agró A (1989) J Mol Biol 206:513
43. Lieberman RL, Rosenzweig AC (2005) Nature 434:177
44. Decker H, Dillinger R, Tuczek F (2000) Angew Chem Int Ed 39:1591
45. Siegbahn PEM (2003) J Biol Inorg Chem 8:567
46. Granata A, Monzani E, Bubacco L, Casella L (2006) Chem Eur J 12:2504

47. Cramer CJ, Wloch M, Piecuch P, Puzzarini C, Gagliardi L (2006) J Phys Chem A 110:1991
48. Bradbury AF, Finnie MD, Smyth DG (1982) Nature 298:686
49. Eipper BA, Milgram SL, Husten EJ, Yun HY, Mains RE (1993) Protein Sci 2:489
50. Prigge ST, Kolhekar AS, Eipper BA, Mains RE, Amzel LM (1997) Science 278:1300
51. Prigge ST, Eipper BA, Mains RE, Amzel LM (2004) Science 304:864
52. Aboelella NW, Reynolds AM, Tolman WB (2004) Science 304:836
53. Blain I, Giorgi M, de Riggi I, Réglier M (2001) Eur J Inorg Chem p 205
54. Keevil T, Mason HS (1978) Methods Enzymol 52:3
55. Balogh-Hergovich E, Kaizer J, Speier G (2000) J Mol Cat A: Chem 159:215
56. See [20] and Whittaker JW (1994) In: Sigel H, Sigel A (eds) Metal Ions in Biologic Systems. Marcel Dekker, New York, 30:315
57. Stubbe J, van der Donk WA (1998) Chem Rev 98:705
58. Murray JM, Saysell CG, Wilmot CM, Tambyrajan WS, Jaeger J, Knowles PF, Phillips SEV, McPherson MJ (1999) Biochemistry 38:8217
59. Knowles PF, Dooley DM (1994) In: Sigel H, Sigel A (eds) Metal Ions in Biological Systems. Marcel Dekker, New York 30:361
60. Kaim W (2003) Dalton Trans, p 761
61. Rogers MS, Dooley DM (2003) Curr Opin Chem Biol 7:189
62. McPherson JJ, Parsons MR, Spooner RK, Wilmot CM (2001) In: Messerschmidt A, Huber R, Poulos T, Wieghardt K (eds) Handbook of Metalloproteins. Wiley, Chichester, p 1272
63. Whittaker JW (2005) Arch Biochem Biophys 433:227
64. Knowles PF, Dooley DM (1993) In: Sigel H, Sigel A (eds) Metalloenzymes Involving Amino Acid-Residue and Related Radicals. Marcel Dekker, New York, Basel, 30:361
65. Kumar V, Dooley DM, Freeman HC, Guss JM, Harvey I, McGuirl MA, Wilce MCJ, Zubak VM (1996) Structure 4:943
66. Li R, Klinman JP, Mathews FS (1998) Structure 6:293
67. Jazdzewski BA, Tolman WB (2000) Coord Chem Rev 200–202:633
68. Itoh S, Taki M, Fukuzumi S (2000) Coord Chem Rev 198:3
69. Krüger HJ (1999) Angew Chem Int Ed 38:627
70. Würtele C, Gaoutchenova E, Harms K, Holthausen MC, Sundermeyer J, Schindler S (2006) Angew Chem Int Ed 45:3867 (Mode A)
71. Fujisawa K, Tanaka M, Moro-Oka Y, Kitajima N (1994) J Am Chem Soc 116:12079 (Mode B)
72. Aboelella N W, Lewis EA, Reynolds AM, Brennessel WW, Cramer CJ, Tolman WB (2002) J Am Chem Soc 124:10660 (Mode B)
73. Sarangi R, Aboelella NW, Fujisawa K, Tolman WB, Hedman B, Hodgson KO, Solomon EI (2006) J Am Chem Soc 128:8286 (Mode B)
74. Jacobsen RR, Tyeklár Z, Farooq A, Karlin KD, Liu S, Zubieta J (1988) J Am Chem Soc 110:3690 (Mode C)
75. Cole AP, Root DE, Mukherjee P, Solomon EI, Stack TDP (1996) Science 273:1848 (Mode D)
76. Kitajima N, Fuisawa K, Moro-Oka Y, Toriumi K (1989) J Am Chem Soc 111:8975 (Mode E)
77. Kitajima N, Fujisawa K, Fujimoto C, Moro-Oka Y, Hashimoto S, Kitagawa T, Toriumi K, Tatsumi K, Nakamura A (1992) J Am Chem Soc 114:1277 (Mode E)
78. Halfen JA, Mahapatra S, Wilkinson EC, Kaderlin S, Young VG Jr, Que L Jr, Zuberbühler AD, Tolman WB (1996) Science 271:1397 (Mode E/F)

79. Mahapatra S, Halfen JA, Wilkinson EC, Pan G, Wang X, Young VG Jr, Cramer CJ, Que L Jr, Tolman WB (1996) J Am Chem Soc 118:11555 (Mode F)
80. Mahapatra S, Young VG Jr, Kaderli S, Zuberbühler AD, Tolman WB (1997) Angew Chem Int Ed Engl 36:130 (Mode F)
81. Kodera M, Katayama K, Tachi Y, Kano K, Hirota S, Fujinami S, Suzuki M (1999) J Am Chem Soc 121:11006 (Mode E)
82. Straub BF, Rominger F, Hofmann P (2000) Chem Commun 1611 (Mode F)
83. Hu Z, George GN, Gorun SM (2001) Inorg Chem 40:4812 (Mode F)
84. Kodera M, Kaita Y, Tachi Y, Katayama K, Kano K, Hirota S, Fujinami S, Suzuki M (2004) Angew Chem Int Ed 43:334 (Mode F)
85. Meyer F, Pritzkow H (2000) Angew Chem Int Ed 39:2112 (Mode G)
86. Reim J, Krebs B (1994) Angew Chem Int Ed Engl 33:1969 (Mode H)
87. Reim J, Werner R, Haase W, Krebs B (1998) Chem Eur J 4:289 (Mode H)
88. Blackman AG, Tolman WB (2000) Struct Bonding 97:179
89. Solomon EI, Chen P, Metz M, Lee SK, Palmer AE (2001) Angew Chem Int Ed 40:4570
90. Schindler S (2000) Eur J Inorg Chem p 2311
91. Kitajima N, Moro-oka Y (1994) Chem Rev 94:737
92. Karlin KD, Kaderli S, Zuberbühler AD (1997) Acc Chem Res 30:139
93. Liang HC, Dahan M, Karlin KD (1999) Curr Opin Chem Biol 3:168
94. Tolman WB (1997) Acc Chem Res 30:227
95. Holland PL, Tolman WB (1999) Coord Chem Rev 190–192:855
96. Holland PL, Rodgers KR, Tolman WB (1999) Angew Chem Int Ed 38:1139
97. Mahadevan V, Henson MJ, Solomon EI, Stack TDP (2000) J Am Chem Soc 122: 10249
98. Siegbahn PEM, Wirstam M (2001) J Am Chem Soc 123:11819
99. Que L Jr, Tolman WB (2002) Angew Chem Int Ed 41:1114
100. Mizuno M, Hayashi H, Fujinami S, Furutachi H, Nagatomo S, Otake S, Uozumi K, Suzuki M, Kitagawa T (2003) Inorg Chem 42:8534
101. Mirica LM, Ottenwaelder X, Stack TDP (2004) Chem Rev 104:1013
102. Lewis EA, Tolman WB (2004) Chem Rev 104:1047
103. Hatcher LQ, Karlin KD (2004) J Biol Inorg Chem 9:669
104. Liang HC, Henson MJ, Hatcher LQ, Vance MA, Zhang CX, Lahti D, Kaderli S, Sommer RD, Rheingold AL, Zuberbühler AD, Solomon EI, Karlin KD (2004) Inorg Chem 43:4115
105. Kuzelka J, Mukhopadhyay S, Spingler B, Lippard SJ (2004) Inorg Chem 43:1751
106. Komiyama K, Furutachi H, Nagatomo S, Hashimoto A, Hayashi H, Fujinami S, Suzuki M, Kitagawa T (2004) Bull Chem Soc Jpn 77:59
107. Shearer J, Zhang CX, Zakharov LN, Rheingold AL, Karlin KD (2005) J Am Chem Soc 127:5469
108. Hatcher LQ, Vance MA, Narducci Sarjeant AA, Solomon EI, Karlin KD (2006) Inorg Chem 45:3004
109. Murahashi SI, Oda Y, Naota T, Komiya N (1993) J Chem Soc Chem Commun, p 139
110. Komiya N, Naota T, Murahashi SI (1996) Tetrahedron Lett 37:1633
111. Shimokawa C, Yokota S, Tachi Y, Nishiwaki N, Ariga M, Itoh S (2003) Inorg Chem 42:8395
112. Shimokawa C, Teraoka J, Tachi Y, Itoh S (2006) J Inorg Biochem 100:1118
113. Velusamy S, Punniyamurthy T (2003) Tetrahedron Lett 44:8955
114. Sawyer DT, Sobkowiak A, Matsushita T (1996) Acc Chem Res 29:409
115. Kirillov AM, Kopylovich MN, Kirillova MV, Haukka M, Guedes da Silva MFC, Pombeiro AJL (2005) Angew Chem Int Ed 44:4345

116. Kirillov AM, Kopylovich MN, Kirillova MV, Karabach EY, Haukka M, Guedes da Silva MFC, Pombeiro AJL (2006) Adv Synth Catal 348:159
117. Groothaert MH, Smeets PJ, Sels BF, Jacobs PA, Schoonheydt RA (2005) J Am Chem Soc 127:1394
118. Lockwood MA, Blubaugh TJ, Collier AM, Lovell S, Mayer JM (1999) Angew Chem Int Ed 38:225
119. Li Z, Li CJ (2005) J Am Chem Soc 127:3672
120. Li Z, Li CJ (2004) Org Lett 6:4997
121. Li Z, Li CJ (2006) J Am Chem Soc 128:56
122. Li Y, Bohle S, Li CJ (2006) Proc Natl Acad Sci USA 103:8928
123. Mahapatra S, Halfen JA, Tolman WB (1996) J Am Chem Soc 118:11575
124. Itoh S, Taki M, Nakao H, Holland PL, Tolman WB, Que L Jr, Fukuzumi S (2000) Angew Chem Int Ed 39:398
125. Itoh S, Kondo T, Komatsu M, Ohshiro Y, Li C, Kanehisa N, Kai Y, Fukuzumi S (1995) J Am Chem Soc 117:4714
126. Takehira K, Shimizu M, Watanabe Y, Orita H, Hayakawa T (1990) Tetrahedron Lett 31:2607
127. Shimizu M, Watanabe Y, Orita H, Hayakawa T, Takehira K (1991) Tetrahedron Lett 32:2053
128. Shimizu M, Watanabe Y, Orita H, Hayakawa T (1993) Bull Chem Soc Jpn 66:251
129. van den Heuvel RHH, Fraaije MW, Ferrer M, Mattevi A, van Berkel WJH (2000) Proc Natl Acad Sci USA 97:9455
130. Boldron C, Gamez P, Tooke DM, Spek AL, Reedijk J (2005) Angew Chem Int Ed 44:3585
131. Prokofieva A, Prikhod'ko AI, Dechert S, Meyer F (submitted for publication)
132. Klingele J, Dechert S, Meyer F (2007) Coord Chem Rev (submitted for publication)
133. Ackermann J, Meyer F, Kaifer E, Pritzkow H (2002) Chem Eur J 8:247
134. Ackermann J, Meyer F, Pritzkow H (2004) Inorg Chim Acta 357:3703
135. Ackermann J, Buchler S, Meyer F (2007) CR Chimie, in press
136. Prokofieva A, Prikhod'ko AI, Enyedy EA, Farkas E, Maringgele W, Demeshko S, Dechert S, Meyer F (submitted for publication)
137. Oyaizu K, Saito K, Tsuchida E (2000) Chem Lett 1318
138. Boldron C, Özalp-Yaman S, Gamez P, Tooke DM, Spek AL, Reedijk J (2005) Dalton Trans p 3535
139. Takaki K, Shimasaki Y, Shishido T, Takehira K (2002) Bull Chem Soc Jpn 75:311
140. Obias HV, Lin Y, Murthy NN, Pidcock E, Solomon EI, Ralle M, Blackburn NJ, Neobold YM, Zuberbühler AD, Karlin KD (1998) J Am Chem Soc 120:12960
141. Parshall GW, Ittel SD (1992) Homogeneous Catalysis. Wiley, New York
142. Sheldon RA, Kochi JK (1981) Metal-Catalyzed Oxidation of Organic Compounds. Academic Press, New York
143. Sheldon RA, Arends IWCE (2006) J Mol Cat A: Chem 251:200
144. Gamez P, Arends IWCE, Reedijk J, Sheldon RA (2003) Chem Commun, p 2414
145. Gamez P, Arends IWCE, Reedijk J, Sheldon RA (2004) Adv Synth Catal 346:805
146. Dijksman A, Arends IWCE, Sheldon RA (2003) Org Biomol Chem 1:3232
147. Betzemeir B, Cavazzini M, Quici S, Knochel P (2000) Tetrahedron Lett 41:4343
148. Ragagnin G, Betzemeier B, Zuici S, Knochel P (2002) Tetrahedron 58:3985
149. Contel M, Villuendas PR, Fernández-Gallardo J, Alonso PJ, Vincent JM, Fish RH (2005) Inorg Chem 44:9771
150. Ansari IA, Gree R (2002) Org Lett 4:1507
151. Jiang N, Ragauskas AJ (2005) Org Lett 7:3689

152. Velusamy S, Punniyamurthy T (2003) Eur J Org Chem 3913
153. Saint-Aman E, Ménage S, Pierre JL, Defrancq E, Gellon G (1998) New J Chem 393
154. Wang Y, DuBois JL, Hedman B, Hodgson KO, Stack TDP (1998) Science 279:537
155. Chaudhuri P, Hess M, Weyhermüller T, Wieghardt K (1999) Angew Chem Int Ed 38:1095
156. Chaudhuri P, Wieghardt K, Weyhermüller T, Paine TK, Mukherjee S, Mukherjee C (2005) Biol Chem 386:1023
157. Paine TK, Weyhermüller T, Wieghardt K, Chaudhuri P (2004) Dalton Trans, p 2092
158. Chaudhuri P, Hess M, Flörke U, Wieghardt K (1998) Angew Chem Int Ed 37:2217
159. Markó IE, Giles PR, Tsukazaki M, Brown SM, Urch CJ (1996) Science 274:2044
160. Chaudhuri P, Hess M, Müller J, Hildenbrand K, Bill E, Weyhermüller T, Wieghardt K (1999) J Am Chem Soc 121:9599
161. Lahtinen P, Korpi H, Haavisto E, Leskelä M, Repo T (2004) J Comb Chem 6:967
162. Berkessel A, Dousset M, Bulat S, Glaubitz K (2005) Biol Chem 386:1035
163. Nairn AK, Archibald SJ, Bhalla R, Gilbert BC, MacLean EJ, Teat SJ, Walton PH (2006) Dalton Trans, p 172
164. Markó IE, Giles PR, Tsukazaki M, Chellé-Regnaut I, Urch CJ, Brown SM (1997) J Am Chem Soc 119:12661
165. Markó IE, Gautier A, Chellé-Regnaut I, Giles PR, Tsukazaki M,Urch CJ, Brown SM J (1998) Org Chem 63:7576
166. Markó IE, Gautier A, Dumeunier R, Doda K, Philippart F, Brown SM, Urch CJ (2004) Angew Chem Int Ed 43:1588
167. Klein Gebbink RJM, Feiters MC, Nolte RJM (1994) J Am Chem Soc 116:5667
168. Klein Gebbink RJM, Martens CF, Feiters MC, Karlin KD, Nolte RJM (1997) Chem Commun, p 389
169. Klein Gebbink RJM, Martens CF, Kenis PJA, Jansen RJ, Nolting HF, Sole VA, Feiters MC, Karlin KD, Nolte RJM (1999) Inorg Chem 38:5755
170. Sprakel VSI, Feiters MC, Meyer-Klaucke W, Klopstra M, Brinksma J, Feringa BL, Karlin KD, Nolte RJM (2005) Dalton Trans, p 3522
171. Zhang CX, Liang HC, Lim E, Gan QF, Tyeklár Z, Lam KC, Rheingold AL, Kaderli S, Zuberbühler AD, Karlin KD (2001) Chem Commun, p 631
172. Mirica LM, Vance M, Rudd DJ, Hedman B, Hodgson KO, Solomon EI, Stack TDP (2002) J Am Chem Soc 124:9332
173. Mirica LM, Rudd DJ, Vance MA, Solomon EI, Hodgson KO, Hedman B, Stack TDP (2006) J Am Chem Soc 128:2654
174. For a related μ-oxo-dicopper(III) species with stoichiometric reactivity towards catechols see: Mahadevan V, DuBois JL, Hedman B, Hodgson KO, Stack TDP (1999) J Am Chem Soc 121:5583
175. Santagostini L, Gullotti M, Monzani E, Casella L, Dillinger R, Tuczek F (2000) Chem Eur J 6:529
176. Battaini G, de Carolis M, Monzani E, Tuczek F, Casella L (2003) Chem Commun, p 726
177. Palavicini S, Granata A, Monzani E, Casella L (2005) J Am Chem Soc 127:18031
178. Itoh S, Kumei H, Taki M, Nagatomo S, Kitagawa T, Fukuzumi S (2001) J Am Chem Soc 123:6708
179. Casella L, Gullotti M, Radaelli R, Di Gennaro P (1991) J Chem Soc Chem Commun, p 1611
180. Casella L, Carugo O, Gullotti M, Garofani S, Zanello P (1993) Inorg Chem 32:2056
181. Casella L, Monzani E, Gullotti M, Cavagnino D, Cerina G, Santagostini L, Ugo R (1996) Inorg Chem 35:7516

182. Monzani E, Quinti L, Perotti A, Casella L, Gullotti M, Randaccio L, Geremia S, Nardin G, Faleschini P, Tabbì G (1998) Inorg Chem 37:553
183. Alzuet G, Casella l, Laura Villa M, Carugo O, Gullotti M (1997) J Chem Soc Dalton Trans, p 4789
184. Battaini G, Monzani E, Perotti A, Para C, Casella L, Santagostini L, Gullotti M, Dillinger R, Näther C, Tuczek F (2003) J Am Chem Soc 125:4185
185. Karlin KD, Gultneh Y, Hayes JC, Cruse RW, McKown JW, Hutchinson JP, Zubieta J (1984) J Am Chem Soc 106:2121
186. Nasir MS, Cohen BI, Karlin KD (1992) J Am Chem Soc 114:2482
187. Karlin KD, Nasir MS, Cohen BI, Cruse RW, Kaderli S, Zuberbühler AD (1994) J Am Chem Soc 116:1324
188. Mahapatra S, Kaderli S, Llobet A, Neuhold YM, Palanchè T, Halfen JA, Young VG Jr, Kaden TA, Que L Jr, Zuberbühler AD, Tolman WB (1997) Inorg Chem 36:6343
189. Matsumoto T, Furutachi H, Kobino M, Tomii M, Nagatomo S, Tosha T, Osako T, Fujinami S, Itoh S, Kitagawa T, Suzuki M (2006) J Am Chem Soc 128:3874
190. Mirica LM, Vance M, Rudd DJ, Hedman B, Hodgson KO, Solomon EI, Stack TDP (2005) Science 308:1890
191. Reinaud O, Capdevielle P, Maumy M (1990) Synthesis, p 612
192. Reinaud O, Capdevielle P, Maumy M (1990) J Chem Soc Chem Commun, p 566
193. Buijs W, Comba P, Corneli D, Pritzkow H (2002) J Organomet Chem 641:71
194. Mukherjee R (2004) Proc Indian Natl Sci Acad 70:329
195. Koval IA, Selmeczi K, Belle C, Philouze C, Saint-Aman E, Gautier-Luneau I, Schuitema AM, van Vliet M, Gamez P, Roubeau O, Lüken M, Krebs B, Lutz M, Spek AL, Pierre JL, Reedijk J (2006) Chem Eur J 12:6138
196. Karlin KD, Guiltneh Y, Nicholson T, Zubieta J (1985) Inorg Chem 24:3725
197. Börzel H, Comba P, Pritzkow H (2001) Chem Commun, p 97
198. Monzani E, Battaini G, Perotti A, Casella L, Gullotti M, Santagostini L, Nardin G, Randaccio L, Geremia S, Zanello P, Opromolla G (1999) Inorg Chem 38:5359
199. Selmeczi K, Réglier M, Giorgi M, Speier G (2003) Coord Chem Rev 245:191
200. Kaizer J, Csonka R, Speier G, Giorgi M, Réglier M (2005) J Mol Catal A: Chem 235:81
201. Selmeczi K, Réglier M, Speier G, Peintler G (2004) React Kinet Catal Lett 81:143
202. Granata A, Monzani E, Casella L (2004) J Biol Inorg Chem 9:903
203. Koval IA, Belle C, Selmeczi K, Philouze C, Saint-Aman E, Schuitema AM, Gamez P, Pierre JL, Reedijk J (2005) J Biol Inorg Chem 10:739
204. Malachowski MR (1989) Inorg Chim Acta 162:199
205. Oishi N, Nishida Y, Ida K, Kida S (1980) Bull Chem Soc Jpn 53:2847
206. Mukherjee J, Mukherjee R (2002) Inorg Chim Acta 337:429
207. Kao CH, Wei HH, Liu YH, Lee GH, Wang Y, Lee CJ (2001) J Inorg Biochem 84:171
208. Torelli S, Belle C, Gautier-Luneau I, Pierre JL, Saint-Aman E, Latour JM, Le Pape L, Luneau D (2000) Inorg Chem 39:3526
209. Belle C, Beguin C, Gautier-Luneau I, Hamman S, Philouze C, Pierre JL, Thomas F, Torelli S, Saint-Aman E, Bonin M (2002) Inorg Chem 41:479
210. Reim J, Krebs B (1997) J Chem Soc Dalton Trans, p 3793
211. Anekwe J, Hammerschmidt A, Rompel A, Krebs B (2006) Z Anorg Allg Chem 632: 1057
212. Neves A, Rossi LM, Bortoluzzi AJ, Szpoganicz B, Wiezbicki C, Schwingel E, Haase W, Ostrovsky S (2002) Inorg Chem 41:1788
213. Koval IA, Huisman M, Stassen AF, Gamez P, Roubeau O, Belle C, Pierre JL, Saint-Aman E, Luken M, Krebs B, Lutz M, Spek AL, Reedijk J (2004) Eur J Inorg Chem, p 4036

214. Merkel M, Möller N, Piacenza M, Grimme S, Rompel A, Krebs B (2005) Chem Eur J 11:1201
215. Thirumavalavan M, Akilan P, Kandaswamy M, Chinnakali K, Senthil Kumar G, Fun HK (2003) Inorg Chem 42:3308
216. Fernandes C, Neves A, Bortoluzzi AJ, Mangrich AS, Rentschler E, Szpoganicz B, Schwingel E (2001) Inorg Chim Acta 320:12
217. Torelli S, Belle C, Hamman S, Pierre JL, Saint-Aman E (2002) Inorg Chem 41:3983
218. Monzani E, Quinti L, Perotti A, Casella L, Gulotti M, Randaccio L, Geremia S, Nardin G, Faleschini P, Tabbi G (1998) Inorg Chem 37:553
219. Battaini G, Casella L, Gullotti M, Monzani E, Nardin G, Perotti A, Randaccio L, Santagostini L, Heinemann FW, Schindler S (2003) Eur J Inorg Chem, p 1197
220. Sreenivasulu B, Zhao F, Gao S, Vittal JJ (2006) Eur J Inorg Chem, p 2656
221. Jocher C, Pape T, Seidel WW, Gamez P, Reedijk J, Hahn FE (2005) Eur J Inorg Chem, p 4914
222. Wegner R, Gottschaldt M, Görls H, Jäger EG, Klemm D (2001) Chem Eur J 7:2143
223. Wegner R, Gottschaldt M, Poppitz W, Jäger EG, Klemm D (2003) J Mol Catal A: Chem 201:93
224. Taki M, Teramae S, Nagatomo S, Tachi Y, Kitagawa T, Itoh S, Fukuzumi S (2002) J Am Chem Soc 124:6367
225. El-Sayed MA, Abdel Salam AH, El-Zayat TA, El-Dissouky A, Ismail KZ (2004) Inorg Chim Acta 357:4057
226. Mimmi MC, Gullotti M, Santagostini L, Battaini G, Monzani E, Pagliarin R, Zoppellaro G, Casella L (2004) Dalton Trans, p 2192
227. Gullotti M, Santagostini L, Pagliarin R, Granata A, Casella L (2005) J Mol Catal A: Chem 235:271
228. Santagostini L, Gullotti M, Pagliarin R, Monzani E, Casella L (2003) Chem Commun, p 2186
229. Brenner W (1972) to Hoffman-La Roche DE Patent 2 221 624
230. Bockstiegel B, Hoercher U, Laas H, Jessel B, Grafen P (1992) to BASF AG, EU Patent 475 272
231. Isshiki T, Yui T, Uno H, Abe M (1984) Mitsubishi Gas Chemical Co, EU Patent 127 888
232. Shimizu M, Watanabe Y, Orita H, Hayakawa T, Takehira K (1992) Bull Chem Soc Jpn 65:1522
233. Baiker A, Bodnar Z, Mallat T (1996) J Mol Catal A: Chem 110:55
234. Sun H, Harms K, Sundermeyer J (2004) J Am Chem Soc 126:9550
235. Zhu J, Griogroriadis NP, Lee JP, Porco JA Jr (2005) J Am Chem Soc 127:9342
236. Velusamy S, Kumar AV, Saini R, Punniyamurthy T (2005) Tetrahedron Lett 46:3819
237. Fujii T, Naito A, Yamaguchi S, Wada A, Funahashi Y, Jitsukawa, Nagatomo S, Kitagawa T, Masuda H (2003) Chem Commun, p 2700
238. Baesjou PJ, Driessen WL, Challa G, Reedijk J (1996) J Mol Catal A: Chem 110:195
239. Viersen FJ (1988) PhD thesis, University of Groningen
240. Chen W (1991) PhD thesis, University of Groningen
241. Gamez P, Simons C, Steensma R, Driessen WL, Challa G, Reedijk J (2001) Eur Polym J 37:1293
242. Gamez P, Simons C, Aromí G, Driessen WL, Challa G, Reedijk (2001) J Appl Catal A: Gen 214:187
243. Baesjou PJ, Driessen WJ, Challa G, Reedijk J (1997) J Am Chem Soc 119:12590
244. Baesjou PJ, Driessen WJ, Challa G, Reedijk J (1999) Macromolecules 32:270
245. Gao J, Reibenspies JH, Martell AE (2002) Inorg Chim Acta 338:157
246. Gao J, Zhong SH, Zingaro RA (2004) J Mol Catal A: Chem 207:15

247. Hay AS, Stafford HS, Endres GF, Eustance JW (1959) J Am Chem Soc 81:6335
248. Guieu SJA, Lanfredi AMM, Massera C, Pachón LD, Gamez P, Reedijk J (2004) Catal Today 96:259
249. Gamez P, van Dijk JAPP, Driessen WL, Challa G, Reedijk J (2002) Adv Synth Catal 344:890
250. Schuitema AM, Aubel PG, Koval IA, Engelen M, Driessen WL, Reedijk J, Lutz M, Spek AL (2003) Inorg Chim Acta 355:374
251. Higashimura H, Fujisawa K, Namekawa S, Kubota M, Shiga A, Moro-oka Y, Uyama H, Kobayashi S (2000) J Polym Sci A: Polym Chem 38:4792
252. Saito K, Tago T, Masuyama T, Nishide H (2004) Angew Chem Int Ed 43:730
253. Oyaizu, Kumaki Y, Saito K, Tsuchida E (2000) Macromolecules 33:5766
254. Mulrooney CA, Li X, DiVirgilio ES, Kozlowski MC (2003) J Am Chem Soc 125:6856
255. Tsubaki K, Miura M, Morikawa H, Tanaka H, Kawabata T, Furuta T, Tanaka K, Fuji K (2003) J Am Chem Soc 125:16200
256. Gupta R, Mukherjee R (2000) Tetrahedron Lett 41:7763
257. Kodera M, Shimakoshi H, Tachi Y, Katayama K, Kano K (1998) Chem Lett, p 441
258. Gao J, Reibenspies JH, Martell AE (2003) Angew Chem Int Ed 42:6008
259. Sharma VB, Jain SL, Sain B (2004) J Mol Cat A: Chem 219:61
260. Temma T, Habaue S (2005) Tetrahedron Lett 46:5655
261. Habaue S, Muraoka R, Aikawa A, Murakami S, Higashimura H (2005) J Polym Sci A: Polym Chem 43:1635
262. Temma T, Habaue S (2005) J Polym Sci A: Polym Chem 43:5872
263. Temma T, Hatano B, Habaue S (2006) Polymer 47:1845
264. Diaconu D, Hu Z, Gorun SM (2002) J Am Chem Soc 124:1564
265. Hay AS (1962) J Org Chem 27:3320
266. Sonogashira K (1991) In: Trost BM, Fleming I (eds) Comprehensive Organic Synthesis. Pergamon Press, Oxford
267. Rossi R, Carpita A, Bellina F (1995) Org Prep Proc 27:127
268. Siemsen P, Livingston RC, Diederich F (2000) Angew Chem Int Ed 39:2632
269. Amatore C, Jutand A (2000) Acc Chem Res 33:314
270. Sayre LM, Nadkarni DV (1994) J Am Chem Soc 116:3157

Author Index Volumes 1–22

The volume numbers are printed in italics

Subject Index